Reconstructing subglacial meltwater dynamics from the spatial and temporal variation in the form and pattern of eskers

STORRAR, ROBERT,DAVID

Reconstructing subglacial meltwater dynamics from the spatial and temporal variation in the form and pattern of eskers

Robert David Storrar

Abstract

Meltwater drainage beneath glaciers and ice sheets is intimately linked to their dynamics. Meltwater may increase ice velocity if it acts to lubricate the bed; conversely, an efficient subglacial meltwater drainage system may preclude meltwater induced ice acceleration by limiting the amount of water available to facilitate sliding. Thus, understanding the nature of meltwater flow beneath ice masses is crucial for predicting how ice sheets and glaciers will react to increased meltwater input. However, direct observation of subglacial meltwater drainage systems is extremely difficult, meaning that indirect methods such as remote sensing, numerical modelling, dye tracing and geophysical survey are the only way to observe this environment. These methods often suffer from excessive uncertainty and poor spatial and, particularly, temporal resolution.

This thesis presents the results of an alternative approach, using the geomorphological record of eskers to understand the former behaviour of meltwater beneath the Laurentide Ice Sheet (LIS) in Canada, and at Breiðamerkurjökull in Iceland. Eskers are elongate, sinuous ridges of glaciofluvial sand and gravel deposited in glacial drainage channels. Despite a large body of research on eskers, no systematic analysis of the large-scale properties of eskers, or the implications this may have for understanding subglacial meltwater, has yet been undertaken. Eskers are mapped at the ice sheet (continental) scale in Canada from 678 Landsat ETM+ images and at high resolution (~30 cm) from 407 aerial photographs of the Breiðamerkurjökull foreland, in order to address three outstanding questions: (i) What controls the pattern and morphology of eskers? (ii) How did subglacial drainage systems evolve during ice sheet deglaciation? (iii) How can eskers be used to further our understanding of subglacial hydrology?

Over 20,000 eskers are mapped in Canada, revealing that esker systems are up to 760 km long, and are surprisingly straight. The spacing between eskers is relatively uniform and they exhibit little change in elevation from one end to another. As the LIS deglaciated between 13 cal ka and 7 cal ka, eskers increased in frequency, which is interpreted to represent an increase in meltwater drainage in channelized, rather than distributed, systems. Eskers are abundant over the resistant rocks of the Canadian Shield and also show a strong preference for formation in areas covered with till. Esker length, sinuosity and spacing appear to be unrelated to the underlying geology. Finally, two types of complex esker systems are proposed: *esker fan complexes* and *topographically constrained esker complexes*. The formation of esker complexes is dependent on sediment and meltwater supply and the pre-existing topography controls the overall shape of the esker systems.

Reconstructing subglacial meltwater dynamics from the spatial and temporal variation in the form and pattern of eskers

Robert David Storrar

A thesis submitted in partial fulfilment of the requirements of the University of Durham for the degree of Doctor of Philosophy

December 2013

Department of Geography

Durham University

Contents

Chapter 1 Introduction 1

1.1 Rationale 1

1.2 Aim, research questions and objectives 3

1.2.1 What controls the pattern and morphology of eskers? 3

1.2.2 How did subglacial drainage systems evolve during ice sheet deglaciation? 4

1.2.3 How can eskers be used to further our understanding of subglacial hydrology? 4

1.2.4 Objectives 5

1.3 Study areas 5

1.3.1 Canada 5

1.3.2 Breiðamerkurjökull 9

1.4 Thesis structure and results 10

1.4.1 Chapter 2 11

1.4.2 Chapter 3 12

1.4.3 Chapter 4 12

1.4.4 Chapter 5 13

1.4.5 Chapter 6 14

1.4.6 Chapter 7 14

1.5 References 15

Chapter 2 Eskers: forms, processes and implications for ice-sheet meltwater drainage 21

2.1 Introduction 21

2.2 Meltwater drainage: theory, significance and consequences 23

2.2.1 Distributed drainage systems 23

2.2.2 Channelized drainage systems 28

2.2.3 Glaciofluvial landforms indicative of meltwater flow 29

2.3 Eskers: types and classifications 31

2.3.1 Types of esker 31

2.3.2 Classification of eskers 37
2.4 Esker sedimentology 39
2.4.1 Esker composition 39
2.4.2 Sedimentary structures and facies in eskers 40
2.4.3 Sedimentological insights into esker processes 42
2.5 Esker geomorphology 47
2.5.1 Morphometry and spatial patterns of eskers 50
2.5.2 Spatial patterns of eskers 56
2.5.3 Landform associations 59
2.5.4 Patterns of ice margin retreat 61
2.6 Controls on esker patterns 62
2.6.1 Ice thickness 63
2.6.2 Outburst floods 66
2.6.3 Substrate resistance 67
2.6.4 Interlobate deposition 69
2.6.5 Groundwater flux 72
2.6.6 Summary 73
2.7 Future research directions 76
2.7.1 Morphometry and large-scale patterns of eskers 76
2.7.2 Channelized and distributed drainage systems at the ice-sheet scale 77
2.7.3 Using eskers to reconstruct drainage of subglacial lakes 77
2.7.4 Using eskers to test numerical models of meltwater drainage 78
2.8 Summary 78
2.9 References 80
Chapter 3 A map of large Canadian eskers from Landsat satellite imagery 95
3.1 Introduction 95
3.2 Previous mapping and purpose of the map 96
3.2.1 Previous mapping 96
3.2.2 Purpose of the map 97
3.3 Methods 100

3.3.1 Data sources, mapping and map production 100
3.3.2 Errors and completeness 103
3.4 Results 105
3.4.1 Esker distribution and patterns 107
3.5 Conclusions and implications 110
3.6 References 112
Chapter 4 Morphometry and pattern of a large sample (>20,000) of Canadian eskers: new insights regarding subglacial drainage beneath ice sheets 118
4.1 Introduction 119
4.2 Methods 120
4.2.1 Datasets 120
4.2.2 Length (l_e) 120
4.2.3 Sinuosity (S) 121
4.2.4 Lateral spacing 123
4.2.5 Tributary ordering 124
4.2.6 Elevation change 125
4.3 Results 126
4.3.1 Pattern and distribution 126
4.3.2 Length and fragmentation 126
4.3.3 Sinuosity 126
4.3.4 Lateral spacing 127
4.3.5 Tributary ordering 130
4.3.6 Elevation change 132
4.4 Discussion 133
4.4.1 Pattern and distribution 133
4.4.2 Length and sinuosity 135
4.4.3 Lateral spacing 137
4.4.4 Elevation change 137
4.5 Conclusions 138
4.6 References 139

Chapter 5 Increased channelization of subglacial drainage during deglaciation of the Laurentide Ice Sheet 146
5.1 Introduction 146
5.2 Methods 147
5.3 Results 150
5.4 Discussion 152
5.5 Conclusions 156
5.6 References 157
Chapter 6 An assessment of lithological controls on esker distribution and morphometry in Canada 160
6.1 Introduction 160
6.2 Background and methods 161
6.2.1 Lithological controls on esker distribution and morphometry 161
6.2.2 Groundwater controls on esker spacing 165
6.3 Results 168
6.3.1 Bedrock geology 168
6.3.2 Surficial geology 170
6.3.3 Sediment thickness 171
6.3.4 Hydraulic conductivity 171
6.4 Discussion 171
6.4.1 Bedrock and surficial geology 171
6.4.2 Hydraulic conductivity 179
6.5 Conclusions 181
6.6 References 182
Chapter 7 Controls on the formation of complex esker systems at decadal timescales, Breiðamerkurjökull, SE Iceland 185
7.1 Introduction 185
7.2 Study area and a brief summary of previous work 187
7.3 Methods 189
7.4 Results 191
7.4.1 Overview of esker systems at Breiðamerkurjökull 191

7.4.2 Major esker system 1 (MES1) 192
7.4.3 Major esker system 2 (MES2) 196
7.4.4 Major esker system 3 (MES3) 198
7.4.5 Chronology of esker emergence 200
7.5 Discussion 200
7.5.1 A depositional model for MES1 201
7.5.2 A deposition model for MES2 202
7.5.3 A deposition model for MES3 203
7.5.4 Are the esker patterns compatible with groundwater controlled hydraulic spacing of esker tunnels? 204
7.5.5 What controls the morphology of simple and complex esker systems? 205
7.5.6 How long do eskers take to form? 206
7.5.7 How does esker morphology evolve through time? 207
7.6 Conclusions 209
7.7 References 209
Chapter 8 Discussion 214
8.1 What controls the pattern and morphology of eskers? 214
8.1.1 Length 214
8.1.2 Sinuosity 215
8.1.3 Spacing 217
8.1.4 Sediment supply 218
8.2 How did subglacial drainage systems evolve during ice sheet deglaciation? 219
8.3 How can eskers be used to further our understanding of subglacial hydrology? 219
8.4 Limitations 220
8.5 Future research directions 221
8.5.1 Time-transgressive or synchronous deposition? 222
8.5.2 Channelized and distributed drainage systems at the ice sheet scale 222
8.5.3 Using eskers to test numerical models of meltwater drainage 223
8.5.4 Quantification of channelized meltwater drainage beneath deglaciating ice sheets 223
8.6 References 224

Chapter 9 Conclusions and implications 230

Appendix..... 233

List of Figures

Figure 1.1 The location of 379 Antarctic subglacial lakes (from Wright & Siegert, 2012). Black triangles refer to lakes detected by radio-echo sounding; yellow triangles refer to lakes detected by seismic sounding; green triangles refer to lakes detected by gravitational field mapping; red circles refer to lakes detected by surface height change measurements; red squares refer to lakes identified from ice surface features. 2
Figure 1.2. The extent of the NAISC (white) at 21.4 cal ka BP (from Dyke *et al.*, 2003), with eskers (not to scale) from Prest *et al.* (1968) shown in red. 6
Figure 1.3. Elevation of Canada from the GTOPO30 database. 7
Figure 1.4. Bedrock geology of Canada from Wheeler *et al.* (1996). 8
Figure 1.5. Surficial geology of Canada from Fulton (1995). 9
Figure 1.6. Location map. A) Location of the Vatnajökull Ice Cap in Iceland. The red box indicates the location of B. B) Location of Breiðamerkurjökull within Vatnajökull. The red box indicates the location of C. C) 1999 Landsat image of Breiðamerkurjökull with margin positions from 1890 to 2012. Note that some margins have gaps relating to the absence of aerial photograph coverage and the 2012 data are points measured by handheld GPS in the field. Breiðamerkurjökull was confluent with Fjallsjökull (to the southwest) until some point between 1945 and 1954. The 1890 margin is from Price (1980) and the 1903 margin is from Price (1982). 10
Figure 1.7. Similar esker morphologies formed beneath the Cordilleran Ice Sheet (A) and Breiðamerkurjökull (B). 11
Figure 2.1. Map showing the locations of Figures used in Chapter 2 in Canada and Iceland (inset). 22
Figure 2.2. Channelized (3 and 4) and distributed (1,2,5,6 and 7) drainage systems. (1) Bulk movement within the deforming skeleton; (2) Darcian porewater flow; (3) Pipe flow; (4) Dendritic channel network; (5) Linked cavity system; (6) Braided canal network; (7) Thin film at the ice-rock interface. From Benn & Evans (1996). 26
Figure 2.3. Idealised subglacial drainage channels: A) N-channel; B) R-channel; C) H-channel. Not to scale. 29
Figure 2.4. Development of a dendritic network of R-channels. A shows an oblique representation of the forces acting to maintain a channel: ice creep is balanced by melting of the conduit by friction. B shows a plan view of a hypothetical arrangement of different sized channels and demonstrates how a dendritic network may be initiated, as smaller (high pressure) channels are subsumed by larger (low pressure) channels. The resultant dendritic network is shown in C. Ice flow direction in B and C is from the top of the page. Not to scale. 30

Figure 2.5. Examples of eskers: a) Oblique aerial photograph of a beaded esker in Manitoba, Canada (a bead is indicated by the arrow). Geological Survey of Canada (Photo 2001-083) by Lynda Dredge; b) Ground photograph of a Beaded esker at Breiðamerkurjökull, Iceland; c) Landsat ETM+ band 8 image of an 'esker-in-the-lake' in Manitoba, Canada; d) Ground photograph of a subglacially engorged esker at the Burroughs Glacier, Alaska, USA. From Syverson *et al.* (1994); e) Crevasse squeeze ridges (demarcated by white arrows) at Brúarjökull, Iceland. From Rea & Evans (2011); f) Aerial photograph extract of a Zig-zag (concertina) esker at Brúarjökull, Iceland. 33
Figure 2.6. Clast roundness (x-axis) plotted against Krumbein's sphericity (y-axis) for three different facies sampled from Midre Lovénbreen and Pedersbreen, Svalbard. Each sample contains 50 clasts and point densities are contoured at 1, 3, 5 and 7% per 1% area. After Bennett *et al.* (1997). 40
Figure 2.7. An example of a 'sliding bed' facies in the Guelph esker, Ontario, Canada, composed of poorly sorted sand and gravel. Trowel is 42 cm long. From Saunderson (1977).. 41
Figure 2.8. Sediment logs from four exposed sections of an esker bead 120-150 m wide in Ontario, Canada (from Gorrell & Shaw, 1991). Note the pronounced downstream fining and rapid changes in facies from predominantly massive, clast supported gravels at the proximal end, to mainly bedded sands at the distal side of the bead. 43
Figure 2.9. Examples of sediments in eskers in Ontario, Canada (after Brennand, 1994). (a) Poorly delineated lenses of bimodal clast-supported, polymodal and openwork gravel, Campellford esker. (b) Vaguely delineated lenticular structure and cluster imbrications of larger clasts, Norwood esker. (c) Massive, imbricate, clast-supported gravel alternating with sand, Tweed esker. (d) Imbricate, polymodal matrix-rich gravel within an in-phase wave structure, Norwood esker. (e) Horizontally bedded gravel, Campbellford esker. (f) Trough cross-bedded gravel in the Campbellford esker. (g) Rhythmically graded foresets of tabular cross-bedded gravel in the Tweed esker. 45
Figure 2.10. Distribution of eskers in Fennoscandia from Boulton (2006). 48
Figure 2.11. Distribution of eskers (A) in Canada (after Prest *et al.*, 1968), (B) in the UK (after Clark *et al.*, 2004) and (C) on the Kola Peninsula, Russia (after Hättestrand & Clark, 2006). .. 49
Figure 2.12. Total number and density of eskers mapped in Canada, the UK and the Kola Peninsula. 50
Figure 2.13. Esker length distribution plotted in 1 km bins for the UK, Kola Peninsula and Canada. 51
Figure 2.14. Box and whisker diagrams showing A) esker length data and B) esker sinuosity data for the UK (n = 857) and Kola Peninsula, Russia (n = 817). Whiskers denote the range of values, points denote means and the boxes span the range of the 25 – 75% percentiles, with the median as a vertical bar. Data were extracted from shapefiles published in Clark *et al.* (2004) and Hättestrand & Clark (2006). 52

Figure 2.15. Landsat ETM+ image (left) and interpretation (right) of fragmented eskers (solid lines) in Northwest Territories, Canada. Note gaps between eskers and inferred channel route (dashed lines). 53
Figure 2.16. Esker sinuosity distribution (0.01 bins) for the UK, Kola Peninsula and Canada.. 55
Figure 2.17. Channel morphology and associated esker cross-sections. (A) low, wide channel forming flat-topped esker; (B) high, narrow channel forming sharp-crested esker; (C) quasi-circular channel forming sharp-crested esker; and (D) keyhole shaped channel forming flat-topped esker. From Price (1973). 55
Figure 2.18. Radiating esker patterns around the Keewatin Ice Divide (A) and in Quebec-Labrador (B) (after Prest *et al.*, 1968). Note the absence of eskers at ice divides (dashed lines). 56
Figure 2.19. Esker tributaries and associated Strahler numbers in the Rennie Lake esker system, Northwest Territories, Canada, showing up to fourth order tributaries (after Shilts *et al.*, 1987). 57
Figure 2.20. Aerial photograph extract showing anastomosing esker ridges. From Menzies & Shilts (1996). 57
Figure 2.21. Quasi-uniform esker spacing in Northwest Territories, Canada. Eskers digitised from Landsat ETM+ image. 58
Figure 2.22. Examples of esker/subglacial channel spacing from the literature. Bars represent stated maxima and minima and points represent stated means. Bold fonts indicate numerical model outputs and regular fonts indicate measurements. LIS = Laurentide Ice Sheet. 59
Figure 2.23. Esker superimposed on a drumlin field. Note that esker crosses drumlins almost perpendicularly indicating that it was deposited under different ice dynamic conditions. Portion of NAPL aerial photograph A14302-17, from Aylsworth & Shilts (1989). 60
Figure 2.24. Extract of Landsat ETM+ image (4,3,2) showing an esker superimposed on ribbed moraine in Labrador, Canada. 61
Figure 2.25. Association of eskers and Glaciofluvial Corridors in Keewatin, Canada (from Utting *et al.*, 2009). 62
Figure 2.26. Conceptual model of synchronous (A) and time-transgressive (B) esker formation and implications for reconstructing ice margin retreat. Arrows indicate the ice margin retreat direction gleaned from the inferred mode of formation and T1-4 shows the chronological position of inferred ice margins. If synchronous deposition is assumed, only the initial ice margin is known, whereas if deposition is assumed to be time-transgressive, esker beads indicate the positions of a receding margin. The features are exaggerated and are not drawn to scale. 63
Figure 2.27. Vertically exaggerated hypothetical movement of water through equipotential surfaces (redrawn from Shreve, 1985a). Hydraulic potential drives water through equipotential

surfaces (from darker to lighter shades of red) which dip up-glacier by approximately 11 times the surface slope..... 64
Figure 2.28. Subglacial hydraulic head maps of the southeastern Burroughs Glacier, Alaska, USA for (A) 1945, (B) 1960 and (C) 1970. From Syverson *et al.* (1994). 65
Figure 2.29. Photographs of the esker formed during the 1996 Skeiðarárhlaup and grids indicating where GPR surveys were undertaken. From Burke *et al.* (2008). 67
Figure 2.30. Esker distribution in Canada compared with hard shield substrate (shaded) and deformable substrate (unshaded). Modified from Clark & Walder (1994)..... 69
Figure 2.31. Conceptual diagram of two interlobate depositional models. Thick black dotted lines represent suture zones where stress is high. Black arrows indicate ice flow. Left hand model shows conditions for synchronous deposition in a persistent conduit, maintained between two lobes. Right hand model shows time-transgressive deposition in two retreating lobes. Red arrows indicate ice retreat and blue dotted lines indicate margin positions. Esker forms in the terminal section of the conduit and extends back up-ice as the ice front recedes. Not to scale.. 70
Figure 2.32. Geological units of the Oak Ridges Moraine, Ontario, Canada. From Sharp *et al.* (2007)..... 71
Figure 2.33. Conceptual geological model of the Oak Ridges Moraine showing the five major stratigraphic units. Note the tunnel valley in the lowermost unit superimposed by the drumlinised Newmarket till and channel sediment. The Oak Ridges Moraine sediment forms the cap of the sequence. From Sharp *et al.* (2007)..... 72
Figure 2.34. Esker spacing in Finland, with ice streams indicated by blue shading. From Boulton *et al.*, (2009). 74
Figure 2.35. Esker spacing plotted as a function of transmissivity and melt rate from Boulton *et al.* (2009). Diagonal lines are contours of esker spacing in metres. Blue lines indicate the minimum and maximum esker spacing observed. Red box indicates the field produced by modelled melt rates and measured transmissivity. Note that the observed esker spacing fits well in the predicted field. 75
Figure 3.1 Eskers mapped in the GMoC and in the this paper. A) Examples of eskers mapped in this paper but not mapped in the GMoC are indicated by arrows. The box indicates the area enlarged in B. See Figure 3.5 for location. B) Landsat image (4,3,2) showing the cartographic simplification of eskers in the GMoC. Note that the gaps in the eskers are not represented in the GMoC and the locations of the esker ridges are relatively imprecise..... 98
Figure 3.2. Map showing coverage of Landsat ETM+ Landsat TM imagery. Each image covers an area of approximately 125 km × 125 km. 101
Figure 3.3. Flow chart showing the two stages of map development: digitisation and production of the final map. 102
Figure 3.4. Two prominent eskers in Northwest Territories (also mapped as eskers by Brown *et al.*, 2011). Note that these features were not included in the Glacial Map of Canada, in which

the area was broadly defined as ‘hummocky terrain’ (Prest *et al.*, 1968). See Figure 3.5 for location..... 103
Figure 3.5. Locations of Figure 3.1, Figure 3.4, Figure 3.9, Figure 3.10 and Figure 3.11 (yellow) and areas mapped from aerial photographs (red boxes, white circles). Inset is an enlargement of the area indicated by the white box..... 104
Figure 3.6. Total length of eskers from both Landsat and aerial photograph analysis in each study area, plotted against the observed detection rate. The red marker indicates the study area in southern Alberta (area 2: Figure 3.5), where the detection rate is significantly lower due to large-scale human activity. The red trendline takes this point into account, whereas the black trendline corresponds to the other 6 areas only. Areas containing a high proportion of eskers tend to result in the most reliable mapping. 105
Figure 3.7. Eskers mapped from Landsat ETM+ imagery and aerial photographs in the McCann Lake area, Northwest Territories. See Figure 3.5 (area 6) for location..... 106
Figure 3.8. Histogram (0.5 km bins) of the length of eskers detected in aerial photographs but not in Landsat imagery (Missed) and the length of the eskers mapped from Landsat imagery (Mapped). Note that more of the ‘missed’ eskers are < 2 km long compared with the ‘mapped’ eskers and, conversely, that more of the ‘mapped’ eskers are > 2 km long compared with the ‘missed’ eskers..... 107
Figure 3.9. Landsat ETM+ image (band 8) of an esker in Nunavut. Note the very well defined shape of the esker and the high continuity along its length. See Figure 3.5 for location..... 110
Figure 3.10. Landsat ETM+ image (3,2,1 in A; 4,3,2 in B) of discontinuous, ‘patchy’ eskers in Nunavut. Note poorly defined edges and presence of hummocky topography surrounding the eskers. See Figure 3.5 for location..... 111
Figure 3.11. Digitised eskers in Northwest Territories exhibiting regular spacing (typically around 15 km). See Figure 3.5 for location. 112
Figure 4.1. A) Eskers in band 8 Landsat image (15 m resolution); B) Eskers in 7,5,2 (R,G,B) Landsat image (30 m resolution); C) Eskers digitised from A) and B). Note fragmentary nature of esker ridges, mostly due to lakes. D) DEM and lakes (blue) with digitised esker ridges (red) and ‘interpolated’ eskers (yellow), which join breaks in esker ridges. Location of A, B and C is shown by the black box..... 121
Figure 4.2. Eskers mapped from Landsat imagery of Canada. Also shown are the areas used to calculate spacing and frequency around the final locations of the Keewatin (west) and Ungava (east) ice divides, the areas used to calculate esker spacing in high density locations (see section 4.2.4), and the area used to measure elevation changes. The Precambrian Shield is shown in yellow (from Wheeler *et al.*, 1996)..... 122
Figure 4.3. The different methods used to calculate the six parameters in this chapter. A) Length: each shaded colour represents possible length measurements. Where tributaries coalesce, the longest measurement was extracted. B) Sinuosity: the length of the esker ridge was

divided by the length of a straight line between the start and end points. C) Lateral spacing: Points were calculated where eskers intersect equidistant transects and lateral spacing was calculated from the distance between these points. D) Stream ordering: the Strahler number for each esker was calculated, based on the number and order of tributaries entering each esker. E) Elevation change: elevation values were extracted at the beginning and end points of each esker from a digital elevation model (CDED). 123
Figure 4.4. The effect of esker length on sinuosity measurements. A) Illustration of how fragmenting an esker can result in a smaller overall sinuosity (S in the second diagram represents the mean of the five smaller ridges). B) Number of measurements sampled for each minimum esker length. C) Mean and median sinuosity for each length. D) Standard deviation. Dashed lines indicate the value calculated from the whole *mapped* eskers dataset. 124
Figure 4.5. Example of the transects used for calculation of *interpolated* esker spacing in the Saskatchewan study area (lower left green box in Figure 4.2). 125
Figure 4.6. Esker patterns. A) Integrated dendritic network with multiple tributaries, typical of the eskers around the final location of the Keewatin Ice Divide. B) and C) Chaotically arranged eskers typical of the Canadian Arctic and far north-west. 127
Figure 4.7. Esker length statistics. A) Histogram of *mapped* esker length (n = 20,186, 1 km bins). B) *Mapped* esker length plotted on $\log_{10}$ x-axis (1 km bins). Log-normal distribution with the same mean and standard deviation shown by dashed line. C) Histogram of *interpolated* esker length (n = 5,932, 1 km bins)). D) *Interpolated* esker length plotted on $\log_{10}$ x-axis (1 km bins). Log-normal distribution with the same mean and standard deviation shown by dashed line. E) Box and whisker plot comparing *mapped* and *interpolated* esker length measurements. Whiskers denote the range of values, points denote means and the boxes span the range of the 25 – 75% percentiles, with the median as a vertical bar. Note $\log_{10}$ x-axis. 128
Figure 4.8. Map of *interpolated* eskers classified by length. Note the radial pattern of long esker systems radiating from the final locations of the Keewatin and Ungava Ice Divides and the relatively even spacing of the largest eskers. 129
Figure 4.9. Histograms of esker sinuosity for (A) *mapped* eskers (n = 20,186, 0.01 bins) and (B) *interpolated* eskers (n = 5,932, 0.01 bins). C) Box and whisker plot comparing the two distributions. Whiskers denote the range of values, points denote means and the boxes span the range of the 25 – 75% percentiles, with the median as a vertical bar. 130
Figure 4.10. Histograms of esker spacing (1 km bins) for the three test areas (see Figure 4.2). Dashed lines are normal distributions with the same mean and standard deviation as the data. A) *Mapped* eskers (n = 347). B) *Interpolated* eskers (n = 632). 131
Figure 4.11. Strahler numbers calculated for *interpolated* eskers around the final location of the Keewatin (shaded). Note that fourth-order tributaries are developed in two locations. 132
Figure 4.12. A) Topography and esker distribution in the Keewatin study area (n = 6,671). B) Topography and esker distribution in the Ungava study area (n = 4,889). C) Histogram of

elevation change values (1 m bins) for eskers in both areas (n = 11,560). Positive values denote eskers trending uphill and negative values indicate a downhill trend. 133
Figure 4.13. Deglaciation of the Laurentide Ice Sheet (smaller ice caps not contiguous with the Laurentide Ice Sheet not shown) from 14.70 to 6.83 kyr B.P. (after Dyke *et al.,* 2003). 134
Figure 4.14. Mean (red line) *interpolated* esker spacing with standard deviation indicated by the shaded area, compared with spacing values obtained from the literature (see caption of Figure 2.22 for further details). 138
Figure 5.1. (A) Ice sheet margin positions and chronology (modified from Dyke *et al.*, 2003) are shown superimposed on mapped eskers (yellow) which reflect the configuration of meltwater channels emanating from the major ice divides in Keewatin (west of Hudson Bay) and Ungava (east of Hudson Bay). (B) shows a close-up of the white box in Keewatin. 148
Figure 5.2. Climate and ice margin retreat rate plotted against the number of eskers and number of esker tributaries during deglaciation in Keewatin (A) and Ungava (B) (see Figure 5.1 for location). The number of eskers per 100 km at the ice margin includes error bars to indicate interpolated ice margin positions. Note $\log_{10}$ y-axis in for the number of tributaries per 100 km of eskers in (A). The NGRIP $\delta^{18}O$ record is from Rasmussen *et al.* (2006) and Vinther *et al.* (2006) and is plotted as a grey line with a 100 year moving average in red. The mean retreat rate of the Laurentide Ice Sheet includes error bars of one standard deviation of each measurement [n = 20]. Continued overleaf. 149
Figure 5.3. Histograms for each margin showing the distribution of the number of eskers observed in each 100 km section (black bars) alongside the mean value (red). 151
Figure 5.4. Esker frequency per 100 km of margin around the Keewatin (A and B) and Ungava (C and D) Ice Divides, derived from (A and C) *mapped* eskers; and (B and D) *interpolated eskers*. Continued overleaf. 154
Figure 5.5. Number of eskers per 100 km of ice margin plotted against margin retreat rate for the Keewatin (A) and Ungava (B) study areas..... 156
Figure 5.6. Schematic illustration of observed changes in eskers through time (not to scale). Black lines are hypothetical margin positions. Blue dashed lines indicate approximate areas of the bed drained by channels (later filled by eskers: red), which increases during deglaciation. Areas of the bed drained by distributed systems, which decrease during deglaciation, are shown as solid blue..... 156
Figure 6.1. Schematic illustration of the methods used to measure esker properties on different substrates. Eskers were split and classified according to the underlying substrate, as illustrated by the different shades. Length and sinuosity values were then calculated for each ridge. 162
Figure 6.2. Bedrock geology classified by lithological type (after Wheeler *et al.*, 1996), overlain with mapped eskers. Inset boxes show close ups of the boxes indicated by the colours in the main map. The top left box shows eskers forming over sedimentary, metamorphic and intrusive rocks relatively evenly. In contrast, the top right box shows a strong preference for eskers to

form over volcanic, intrusive and metamorphic rocks, whilst they do not form over sedimentary rocks. 163
Figure 6.3. Bedrock geology classified by geological era (after Wheeler *et al.*, 1996), overlain with mapped eskers. Note the abundance of eskers on the Precambrian Shield (red). 164
Figure 6.4. Surficial materials of Canada (after Fulton, 1995) overlain with the mapped eskers. The inset box shows eskers located preferentially over thick (typically > 2 m) till blankets (dark green) rather than thinner veneers of till (typically < 2 m) (lighter green). Also note the eskers located in the corridor of glaciofluvial material (brown). 165
Figure 6.5. Sediment thickness and esker distribution in central and southern Alberta. Eskers are digitised from Shetsen (1987;1990) and sediment thickness is derived from Atkinson & Lyster (2011). 167
Figure 6.6. Basis for testing Boulton's (2009) hypothesis. A) Plotting hydraulic conductivity against esker spacing produces a prediction for basal melt rates, which are proportional to both parameters. Whilst hydraulic conductivity is difficult to quantify, an estimate should allow the identification of a positive (B) or negative (C) correlation. A positive correlation would support the hypothesis because it would imply a realistic (small) range of basal melt rates. Conversely, a negative correlation would imply that the range of basal melt rates produced is unrealistic.... 169
Figure 6.7. Spacing measurements taken in the Keewatin study area. Geological units are represented by the shaded areas and spacing measurements by the corresponding coloured line. Spacing measurements were taken where the ice margin crossed only one geological unit between two eskers. 170
Figure 6.8. A) Percentage of total esker (blue) and gap (red) length overlying different rock types. B) Deviation of values in A from the percentage of esker length *expected* over each rock type, when weighted by area. C) Percentage of total esker length overlying rocks of different eras. D) Deviation of values in C from the percentage of esker length *expected* over each rock era, when weighted by area. 173
Figure 6.9. A) Mean esker length and associated 1σ error bars for each bedrock type. B) Regression plot of maximum esker length (for rock types) against sample size. C) Mean esker length and associated 1σ error bars for each bedrock era. D) Regression plot of maximum esker length (for eras) against sample size. E) Mean esker sinuosity and associated 1σ error bars for each bedrock type. F) Regression plot of maximum esker sinuosity (for rock types) against sample size. G) Mean esker sinuosity and associated 1σ error bars for each bedrock era. H) Regression plot of maximum esker sinuosity (for eras) against sample size. Continued overleaf. 174
Figure 6.10. A) Percentage of total esker length overlying different surficial geological facies. B) Deviation of values in A from the percentage of esker length *expected* over each facies, when weighted by area. 176

Figure 6.11. A) Mean esker length and associated 1σ error bars for each facies. B) Regression plot of maximum esker length against sample size. C) Mean esker sinuosity and associated 1σ error bars for each facies. D) Regression plot of maximum esker sinuosity against sample size. 177
Figure 6.12. Comparison of esker distribution and length with substrate thickness in south and central Alberta. A) Distribution of eskers over different sediment thicknesses. B) The deviation from the expected percentage of eskers overlying different sediment thicknesses (1 m bins), based on the percentage of total area covered by sediment of each thickness. C) Sediment thickness at esker centroid plotted against esker length for all 691 eskers. 178
Figure 6.13. Esker spacing (1 km bins) over different (A) geological units and (B) till blankets and till veneers. Shades of red indicate the largest bin in each unit. Spacing measurements of >40 km were recorded but are not shown here for display purposes (no values in this range were >1%)..... 179
Figure 6.14. Mean, median and modal (1 km bins) esker spacing measurements plotted against estimates of hydraulic conductivity for different substrata. The coloured isolines show the basal melt rates predicted by Boulton's (2009) theory..... 180
Figure 6.15. LGM subglacial melt rates beneath the north American Ice Sheet Complex (ice elevations shown by black contours) from Lemieux *et al.* (2008)..... 181
Figure 7.1 Landsat images of different esker morphologies in Canada. A) Complex esker morphology in northern British Columbia, down-ice of the Cassiar Mountains (see Margold *et al.*, 2013). B) Simple, single ridge esker morphology in Nunavut. 188
Figure 7.2. Location map. A) Location of the Vatnajökull Ice Cap in Iceland. The red box indicates the location of B. B) Location of Breiðamerkurjökull within Vatnajökull. The red box indicates the location of C. C) 1999 Landsat image of Breiðamerkurjökull with margin positions from 1890 (neoglacial maximum) to 2012. Note that some margins have gaps relating to the absence of aerial photograph coverage, and the 2012 data are points measured by handheld GPS in the field. Breiðamerkurjökull was confluent with Fjallsjökull (to the southwest) until some point between 1945 and 1954. The 1890 margin is from Price (1980) and the 1903 margin is from Price (1982). 190
Figure 7.3. Example of the resolution of the aerial photographs from 2007, showing a main esker ridge ~30 m wide in the bottom right corner (yellow arrow) and smaller ridges, discernible at just 2 m wide (red arrow) in the centre of the image. Note the complex morphology of the eskers at this location. Copyright NERC ARSF aerial photograph 2007. 191
Figure 7.4. Location map showing eskers digitized from 2007/9 aerial photographs and locations mentioned in the text. Historic ice margin positions are from previous maps (Price 1980; 1982) and aerial photograph mapping and point measurements taken by GPS in 2012. Note that some margins have gaps relating to the absence of aerial photograph coverage. Breiðamerkurjökull was confluent with Fjallsjökull (to the southwest) until some point between

1945 and 1954. The parallel white lines indicate the meltwater drainage axes proposed by Boulton *et al.* (2007a). NN refers to Nygrædnakvis. Areas shown in Figure 7.5 are indicated by black boxes. The area shown in Figure 7.6 corresponds to the black box labelled MES1&2. . 193
Figure 7.5. Detailed topography (in 2007) and ice margin positions (dashed lines) in MES1,2 and 3 (see Figure 7.4 for locations). Locations referred to in the text are given by letters. The location of Figure 7.3 corresponds to C. 194
Figure 7.6. Eskers of MES1 (left) and 2 (right) digitised from 2007 photographs and overlain on 1945 photograph. Note that the esker systems appear to have originated from beneath and from either side of the medial moraine (Mavabyggdarond). See Figure 7.4 for location. 195
Figure 7.7. A) A 'zig-zag' esker west of Stemmulon. B) View to the south-east, of eskers at the distal end of MES1, diverted by the large outwash fan (to the right of the image). Note the preponderance of tributaries branching from the main ridge in the foreground and in the distance. C) Complex morphology of eskers in MES2. D) An esker on the glacier surface, close the eastern snout margin. 196
Figure 7.8. 3-D visualisation of MES1 and 2 in 1965 and 2007 (not to scale). Part of MES1 is melting out of the western section of the medial moraine Mavabyggdarond in the 1965 image (yellow arrow). Note that this esker appears to have decreased in size relative to the more distal eskers (red arrows) by 2007. 197
Figure 7.9. Eskers comprising the fan of MES2 mapped from aerial photographs from 1945, 1955, 1965 and 2007. Note the gradual evolution of the eskers from a flat fan with a few eskers in 1945 to a complex fan of prominent esker ridges in 2007. 199
Figure 7.10. Depositional model for a *topographically constrained esker complex.* A) Englacial stream feeds the development of an ice contact fan. B) As the glacier surface lowers during retreat, drainage is impeded by the fan and meltwater is diverted along the apex of the fan. Eskers form where the channels clog with sediment. Not to scale. 203
Figure 7.11. Depositional model for an *esker fan complex*. A) An englacial stream emerges on the glacier surface and water drains in supraglacial ice walled channels, which form a fan shape because they are at atmospheric pressure and unimpeded by topography. The channels then become choked with sediment. B) An outwash fan subsequently aggrades over the ice-walled channels, burying the channels and ice. The network of eskers preserved in the channel system is gradually lowered onto the bed and emerges as the ice melts out. Not to scale..... 205
Figure 7.12. Conceptual diagram showing the effect of conduit size and sediment supply on esker size and morphology. Dashed lines indicates that eskers do not form until sufficient sediment is available in a sufficiently sized conduit. Examples of different esker morphologies are given from the 2007 photographs and their relative position in the diagram indicated. 208
Figure 8.1. Illustration of fans punctuating a time-transgressive esker. From Brennand (2000). 222

List of Tables

Table 2.1. Parameters used in this paper. 25
Table 2.2. Nomenclature associated with eskers and esker systems from a review of the literature. Note overlapping and similar categories and that various terms may be applied to the same esker. 34
Table 2.3. Bannerjee & McDonald's (1975) classification of eskers. 37
Table 2.4. Warren & Ashley's (1994) classification of eskers. 38
Table 2.5. Brennand's (2000) classification of eskers. 38
Table 2.6. Examples of esker height from the literature. 52
Table 2.7. Suggested diagnostic criteria for outburst flood eskers after Burke *et al.* (2010)..... 68
Table 3.1. Locations used to compare mapping from Landsat ETM+ imagery with mapping from high resolution aerial photographs. Esker detection rates in the Landsat ETM+ imagery, compared with the aerial photographs, is estimated and given as a percentage of total length. Locations are numbered in correspondence with Figure 3.5. 108
Table 4.1. Spacing statistics for each study area. Figures in italics indicate data calculated for eskers with interpolated gaps – note the lower associated standard deviation in each case. 131
Table 4.2. Total length of first- to fourth-order tributary eskers. 132
Table 6.1. Estimates of hydraulic conductivity for different bedrock and surficial geological units, based on Bear (1972). 168
Table 7.1. Aerial photograph properties. 192

Declaration and Statement of Copyright

I confirm that no part of the material presented in this thesis has previously been submitted by me or any other person for a degree in this or any other university. In all cases, where is relevant, material from the work of others has been acknowledged.

Robert David Storrar

Department of Geography

Durham University

December 2013

Acknowledgements

I am indebted to my supervisors, Chris Stokes and Dave Evans, whose patient guidance and insightful comments contributed greatly to this thesis. Despite bombarding them almost weekly, for three years, with different versions of manuscripts (reminiscent of 'PhD comic' 1531), they still managed to provide prompt and informative feedback, for which I am very grateful. I also thank the various members of staff in the Department of Geography who helped to make things run as smoothly as possible. This thesis would not have been possible without funding through a NERC studentship.

My family have provided me with a great deal of support and encouragement over the years and have helped to make my extended stay at University as stress-free as possible. I am especially grateful to my wife, Alysia Zapaśnik, for all that she has been through in order for me to get to this stage. Moving to 'The North' within five days of getting married was a big enough sacrifice in itself, not to mention spending the last two years looking after our wonderful daughter, Connie, whilst I was working and travelling (or, alternatively, gallivanting). Thanks also to my in-laws, Pam and Zed, who graciously entertained Alysia and Connie whilst I was abroad.

Spending the last three years in Durham has been a pleasure, to which the postgraduate community in the Department has contributed immeasurably. Thanks go to my comrades in the GIS lab and coffee room, whose sympathetic ears helped to make the more stressful moments (marking undergraduate essays, for example) all the more bearable.

Finally, my gratitude is also extended to two anonymous members of the public who: (1) alerted me to the fact that my bag was wide open whilst walking to the office in heavy rain, and (2) told me that they had found, and placed in view, my hard drive (containing the up-to-date version of this thesis), which had fallen out of the aforementioned bag about ½ mile up the hill.

For Alysia

Chapter 1 Introduction

1.1 Rationale

Subglacial meltwater is an area of intensive investigation in glaciology because of its important role in governing ice dynamics (e.g. Fricker *et al.*, 2007; Das *et al.*, 2008; Joughin *et al.*, 2008; Stearns *et al.*, 2008; Schoof, 2010; Sundal *et al.*, 2011; Wright *et al.*, 2012). In particular, the form, distribution, and evolution of meltwater drainage systems has been the subject of considerable research, but there are still important gaps in understanding (e.g. Parizek *et al.*, 2002; Alley *et al.*, 2005; Banwell *et al.*, 2010; Catania & Neumann, 2010; Parizek *et al.*, 2010; Bell *et al.*, 2011; Chandler *et al.*, 2013). For example, some studies have identified meltwater-driven increases in ice velocity (Zwally *et al.*, 2002; Joughin *et al.*, 2008; Bartholomew *et al.*, 2010). However, whilst the sudden input of surface meltwater may result in the acceleration of glacier flow (Das *et al.*, 2008), the evolving configuration of the drainage network is highly complex and continued input of meltwater has also been shown to reduce ice velocities (Schoof, 2010; Sundal *et al.*, 2011). The nature of the subglacial drainage system also controls the mechanical behaviour of subglacial sediments, determining how they deform, which in turn has major implications for ice flow (Boulton *et al.*, 2001).

In addition to meltwater drainage, the importance of meltwater storage has also been highlighted recently, with at least 379 subglacial lakes documented beneath the Antarctic ice sheets (Wright & Siegert, 2012; Figure 1.1). Moreover, it has also been shown that these lakes undergo episodic drainage events (Evatt *et al.*, 2006; Wingham *et al.*, 2006; Fricker *et al.*, 2007; Stearns *et al.*, 2008; Carter *et al.*, 2009a; Carter *et al.*, 2009b; Fricker *et al.*, 2010), but the processes occurring during these events are poorly understood. It is not known, for example, whether water drains between lakes in distinct channels or in shallow sheets (Bell *et al.*, 2007; Wright *et al.*, 2008; Le Brocq *et al.*, 2009; Wright *et al.*, 2012), nor whether they necessarily influence ice dynamics (e.g. Pattyn *et al.*, 2004; Bell *et al.*, 2007).

Thus, whilst it is clear that subglacial meltwater is important, there are a number of issues impeding progress. Direct observation of the subglacial hydrological network is problematic and, in most cases, impossible. This means that indirect methods are commonly utilised, such as dye tracing (e.g. Nienow *et al.*, 1996; Schuler & Fischer, 2009; Werder *et al.*, 2009; Willis *et al.*, 2009), remote sensing (e.g. Fricker *et al.*, 2010), numerical modelling (e.g. Lewis & Smith, 2009; Hewitt, 2013) and geophysical surveys (e.g. Carter *et al.*, 2009a).

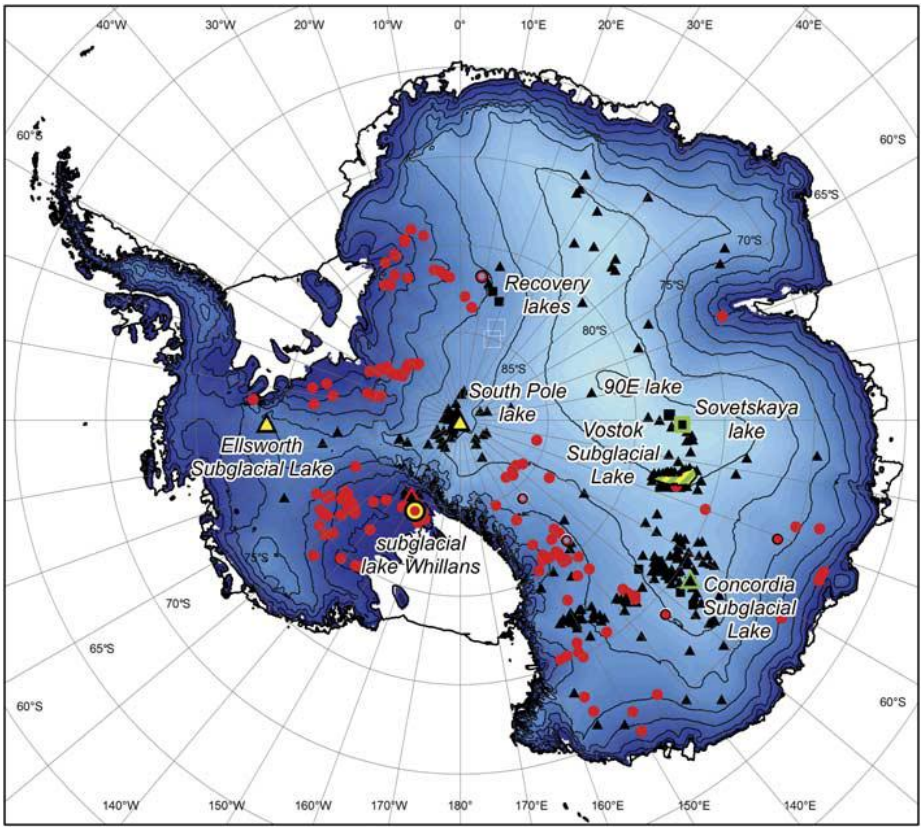

Figure 1.1 The location of 379 Antarctic subglacial lakes (from Wright & Siegert, 2012). Black triangles refer to lakes detected by radio-echo sounding; yellow triangles refer to lakes detected by seismic sounding; green triangles refer to lakes detected by gravitational field mapping; red circles refer to lakes detected by surface height change measurements; red squares refer to lakes identified from ice surface features.

The limited spatial resolution of these techniques often means that more subtle features such as channelization are difficult to detect. Temporal resolution poses a similar problem because drainage systems evolve and are often ephemeral (Bartholomew *et al.*, 2010). Observations are typically made over, at most, a few years (e.g. Nienow *et al.*, 1998; Zwally *et al.*, 2002; Joughin *et al.*, 2008; Fricker *et al.*, 2010; Sundal *et al.*, 2011; Bartholomew *et al.*, 2012), meaning that longer-term trends are difficult to identify. Remote sensing and numerical modelling also have constraints in that assumptions have to be made about complex 'sub-grid' processes. For example, a recent hydrological model of the Greenland Ice Sheet (Lewis & Smith, 2009) assumes that water does not flow in conduits beneath the ice surface and does not take into account moulins - necessary assumptions in order to undertake the modelling but neglecting some important processes.

At a time when polar warming is increasing (Rignot *et al.*, 2011), it is likely that meltwater will play a significant role in future ice-sheet dynamics (Bartholomew *et al.*, 2010; Schoof, 2010). It is, therefore, imperative to better understand how subglacial drainage networks operate because of their profound influence on ice-sheet mass balance and ice flow (Bell, 2008). Such knowledge also provides an important constraint for the development of numerical modelling of

ice sheets which, as noted above, often treat meltwater in a simplistic manner (Le Brocq *et al.*, 2009). However, none of the existing techniques described above have delivered a comprehensive impression of how ice-sheet wide meltwater drainage systems operate and evolve. In particular, the question of where meltwater is configured in a distributed drainage system (inefficient drainage, associated with faster ice flow) and where it is channelized (efficient drainage, associated with slower ice flow) under different regions of the ice sheet remains largely unknown.

One alternative, inverse approach to addressing this question and assessing ice sheet-wide drainage patterns is the use of glacial geomorphology in areas of formerly glaciated terrain. In particular, eskers (elongate ridges composed of glaciofluvial sand and gravel that represent the infillings of former meltwater channels) may prove to be a useful resource. Eskers are well-preserved on palaeo-ice sheet beds (e.g. Prest *et al.*, 1968; Boulton, 2006) and they reflect some of the large-scale patterns present in the subglacial hydrological system at the time of their deposition (e.g. Clark & Walder, 1994). Achieving a robust understanding of the large-scale distribution and patterns of eskers, as well as how they are formed, could therefore lead to important insights regarding meltwater drainage processes. Such an understanding would be a useful proxy for contemporary ice-sheet meltwater drainage and could be used to test the output of models, as well as providing a framework for interpreting data obtained by remote sensing and geophysics.

1.2 Aim, research questions and objectives

In light of the above, the overarching aim of this thesis is to use the spatial and temporal variation in the form and pattern of eskers to gain insight into the subglacial meltwater dynamics which operate beneath ice masses, in both modern and ancient systems. This aim is broken down into three key research questions, which are outlined below.

1.2.1 What controls the pattern and morphology of eskers?

Unlike other glacial landforms, such as drumlins and ribbed moraine (e.g. Hättestrand, 1997; Dunlop & Clark, 2006; Clark *et al.*, 2009; Spagnolo *et al.*, 2010; Spagnolo *et al.*, 2011; Spagnolo *et al.*, 2012), there has been no systematic quantification of esker pattern and morphometry at the continental scale. The absence of such a survey is a significant barrier to understanding what controls where and how eskers form. Several different hypotheses (which are discussed in more detail in Section 2.6) have been developed to explain the prevalence of eskers in certain areas (e.g. Shreve, 1985; Aylsworth & Shilts, 1989; Mäkinen, 2003; Boulton *et al.*, 2009; Burke *et al.*, 2010), but no large scale test of these hypotheses has been undertaken, resulting in uncertainty surrounding the origins of many esker systems. Moreover, recent numerical models (e.g. Boulton *et al.*, 2009; Schuler & Fischer, 2009; Hewitt, 2011) have begun

to make predictions about parameters such as the spacing and sinuosity of subglacial channels, without a robust dataset against which to test the predictions. As well as a large scale analysis of ancient eskers, modern analogues can also be used to assess the controls on esker pattern and morphology and have the advantage that parameters such as timing of ice margin retreat and location are known within small bounds, whereas there is uncertainty over the configuration and timing of deglaciation of palaeo-ice sheets (e.g. Dyke *et al.*, 2002). Thus, a combined approach of using a large dataset of both modern and ancient eskers is used in this thesis to determine the factors which control the pattern and morphology of eskers at different spatial and temporal scales.

1.2.2 How did subglacial drainage systems evolve during ice sheet deglaciation?

Observations from alpine glaciers (e.g. Iken & Truffer, 1997; Nienow *et al.*, 1998) and Greenlandic outlet glaciers (e.g. Bartholomew *et al.*, 2010; Chandler *et al.*, 2013; Shannon *et al.*, 2013) have demonstrated that the subglacial meltwater drainage network is capable of evolving from a distributed to a channelized system over the course of a season, in response to increased meltwater supply in summer months. As mentioned above, no such observations have yet been made at the ice sheet scale, or over longer timescales than a few years. Using mapped esker positions and a published ice margin chronology for the LIS, it is possible, for the first time, to test whether meltwater drainage systems of ice sheets are capable of evolving during deglaciation in a similar manner to alpine glaciers, or whether they behave differently at larger spatial and temporal scales. This has important implications for understanding the stability of deglaciating ice sheets as well as for understanding the role of meltwater at the continental scale.

1.2.3 How can eskers be used to further our understanding of subglacial hydrology?

Eskers have enormous potential to reveal significant insights into subglacial hydrological processes, if we have a robust understanding of how they formed and what controlled where they formed (Brennand, 2000). There are, however, limitations as to how much information eskers can give us. For example, they can inform us only about channelized drainage and (usually) only about the deglaciation or recession of ice masses, because this is when they are revealed. Before using eskers to reconstruct subglacial hydrology, it is essential to develop a rigorous framework for understanding what information they may be able to provide, as well as the limitations that are inherent in using subsets of larger systems to reconstruct those systems.

1.2.4 Objectives

In order to achieve the aim of this thesis and address the three research questions outlined above, the following five specific objectives have been developed:

1. Compile a map and GIS database of Canadian eskers from a consistent data source (Landsat ETM+ imagery). This is presented in Chapter 3.
2. Conduct a morphometric analysis of the mapped Canadian eskers in order to assess the large scale morphometry and pattern of eskers (Chapter 4).
3. Use the map and morphometric dataset of Canadian eskers to assess the evolution of esker systems beneath the LIS through deglaciation (Chapter 5).
4. Produce a time series of esker maps from aerial photographs of Breiðamerkurjökull (Chapter 7).
5. Use the datasets of Canadian and Icelandic eskers to assess the controls on esker morphometry and pattern (Chapters 5, 6 and 7).

1.3 Study areas

Two study areas are used in this thesis to provide a large dataset of eskers at the continental scale (Canada) and to provide a modern analogue of esker formation (Breiðamerkurjökull). This section briefly outlines the context for each area.

1.3.1 Canada

Canada was selected because it contains a large area and number of well-preserved eskers, most of which formed beneath the LIS during the early Holocene and some of which formed beneath the Cordilleran and Innuitian Ice Sheets (Prest *et al.*, 1968; Dyke *et al.*, 2002; Dyke *et al.*, 2003). The eskers which formed beneath the LIS comprise the largest array of eskers related to a single ice mass in the world and, as such, are the most suitable for a large-scale study of esker pattern and morphometry. The extent of the 'North-American Ice Sheet Complex' (NAISC) at the Last Glacial Maximum (LGM), along with the distribution of previously mapped Canadian eskers is shown in Figure 1.2.

Topographically, Canada is broadly characterised by large, relatively flat relief across the Precambrian Shield and prairies, with monadnocks providing notable local exceptions. Mountainous areas include the Rocky mountains in the west and several prominent mountainous regions in the Arctic Archipelago and east coast (Figure 1.3).

The Precambrian volcanic and metamorphic rocks of the Canadian Shield (Wheeler *et al.*, 1996), sedimentary rocks of the Western Canadian Sedimentary Basin (Mossop & Shetsen, 1994) and igneous rocks of the Rocky Mountains (Figure 1.4) comprise the dominant bedrock

characteristics of the country. Surficial geological units reflect the extensive Quaternary glacial history of Canada (Fulton, 1995), with vast tracts of till and glaciolacustrine deposits related to the former presence of ice sheets and proglacial and/or subglacial lakes (Figure 1.5).

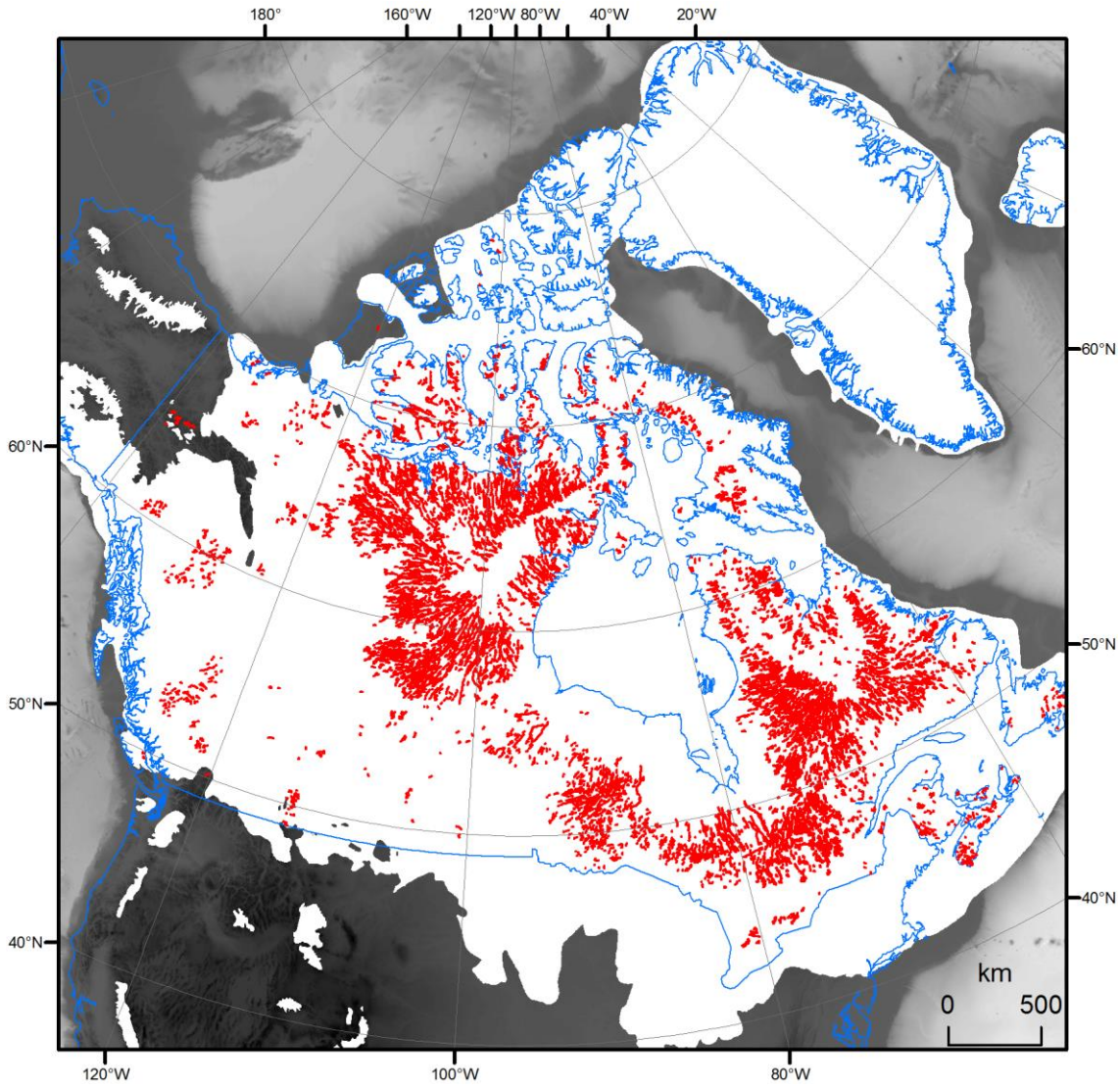

Figure 1.2. The extent of the NAISC (white) at 21.4 cal ka BP (from Dyke *et al.*, 2003), with eskers (not to scale) from Prest *et al.* (1968) shown in red.

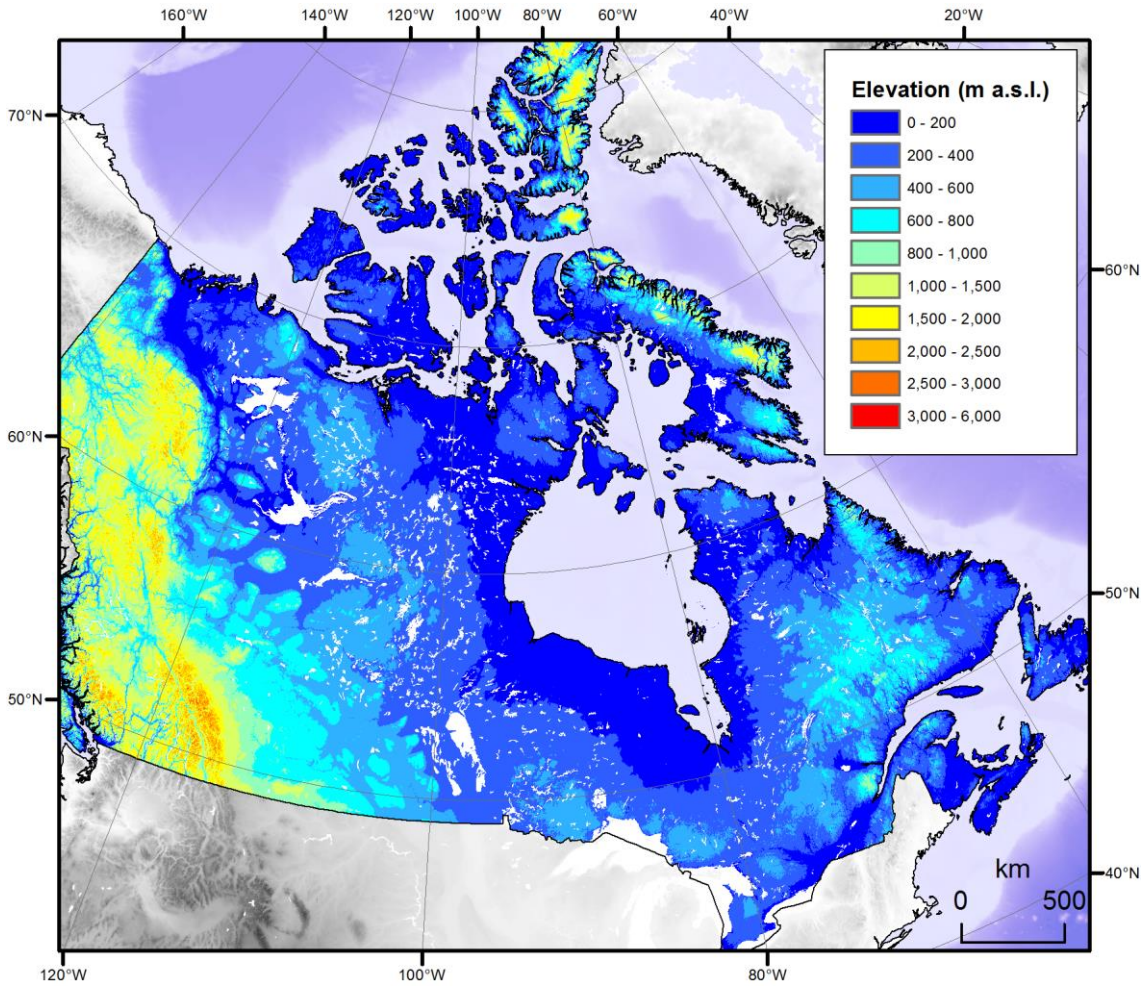

Figure 1.3. Elevation of Canada from the GTOPO30 database.

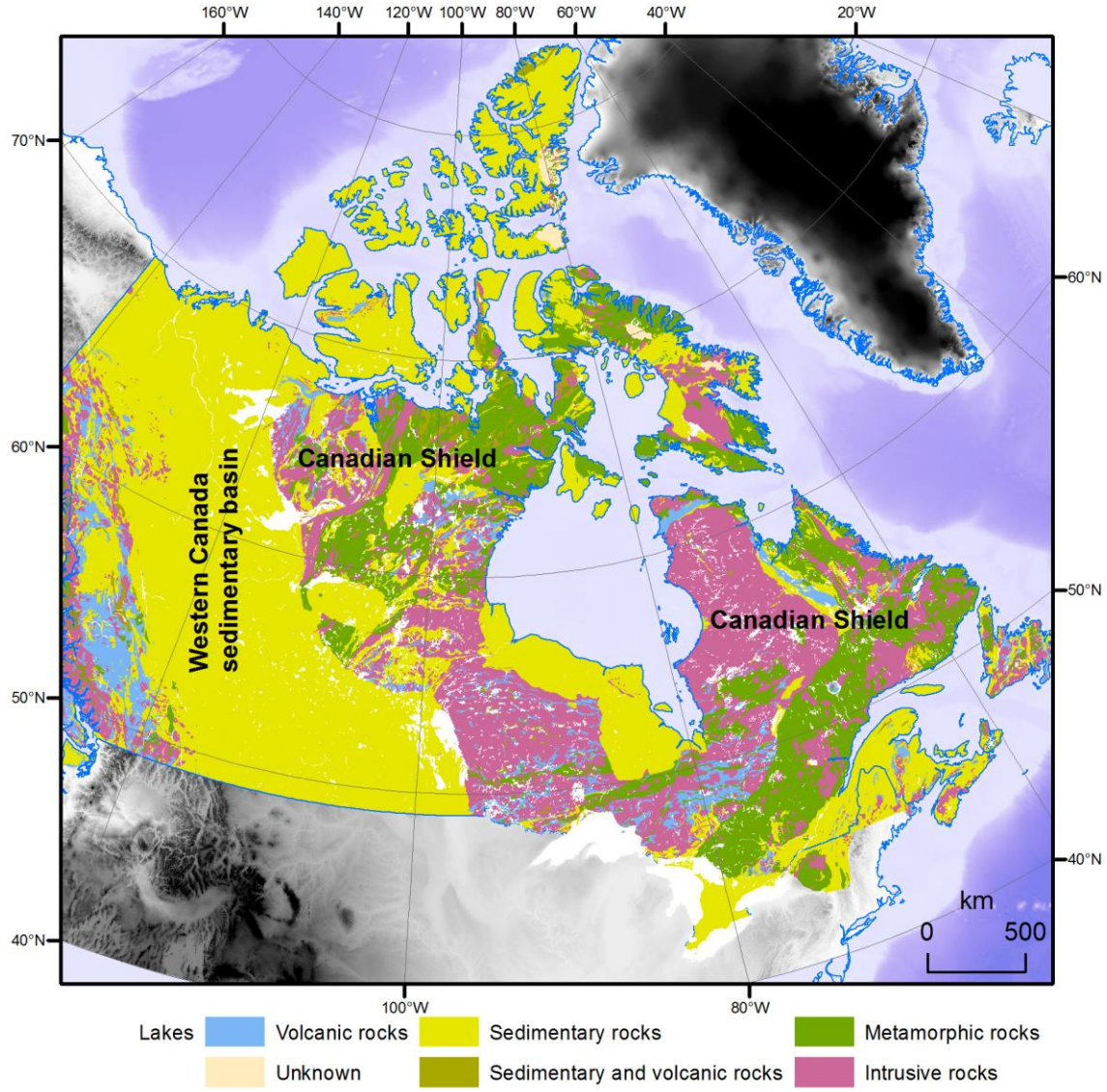

Figure 1.4. Bedrock geology of Canada from Wheeler *et al.* (1996).

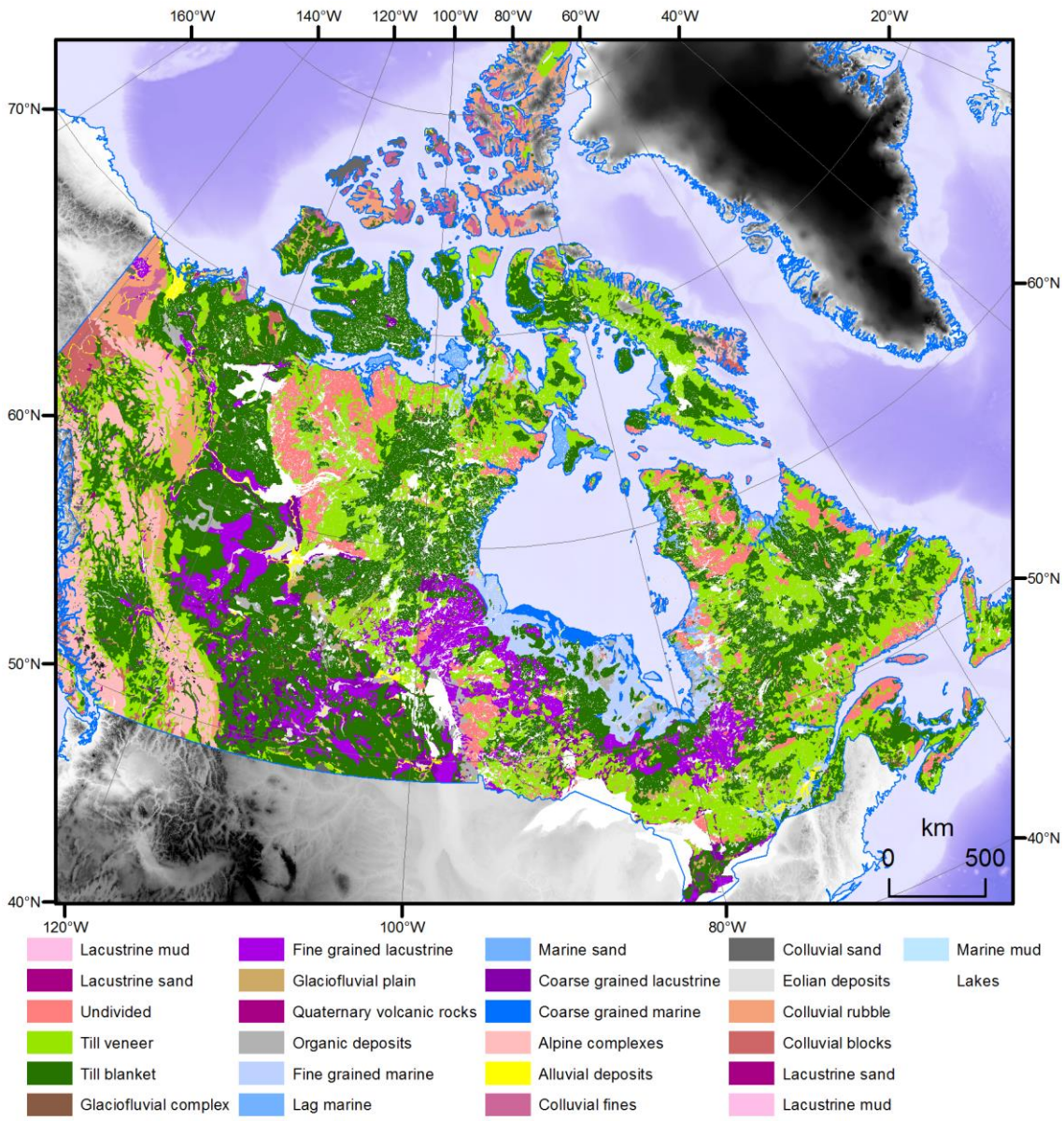

Figure 1.5. Surficial geology of Canada from Fulton (1995).

1.3.2 Breiðamerkurjökull

Breiðamerkurjökull is a large (~13.5 km wide) composite glacier comprising four lobes which are separated by three medial moraines. It drains part of the Vatnajökull ice cap in south-east Iceland and has retreated approximately 5 km from its Neoglacial maximum position in 1890 (Figure 1.6). A large foreland has been revealed containing a diverse and abundant record of glacial geomorphology, including many prominent eskers (Evans & Twigg, 2000;2002). Breiðamerkurjökull was selected as a modern analogue for esker formation because many large (up to ~30 m wide, ~20 m tall) eskers are present there which appear similar in morphology to eskers formed beneath the Laurentide and Cordilleran Ice Sheets (Figure 1.7). Moreover, the glaciological conditions at Breiðamerkurjökull are more similar to sections of the LIS than many other glaciers where eskers are presently forming, because it is relatively wide and large

parts of it are not topographically constrained (Evans & Twigg, 2002; Boulton *et al.*, 2007). The substrate consists predominantly of unlithified sediment at least 120 m thick (Boulton *et al.*, 1982). Surficial sediments often comprise overridden outwash fans which tend to have steep ice-contact faces and dip away from the glacier, producing inset overdeepenings (Evans & Twigg, 2002).

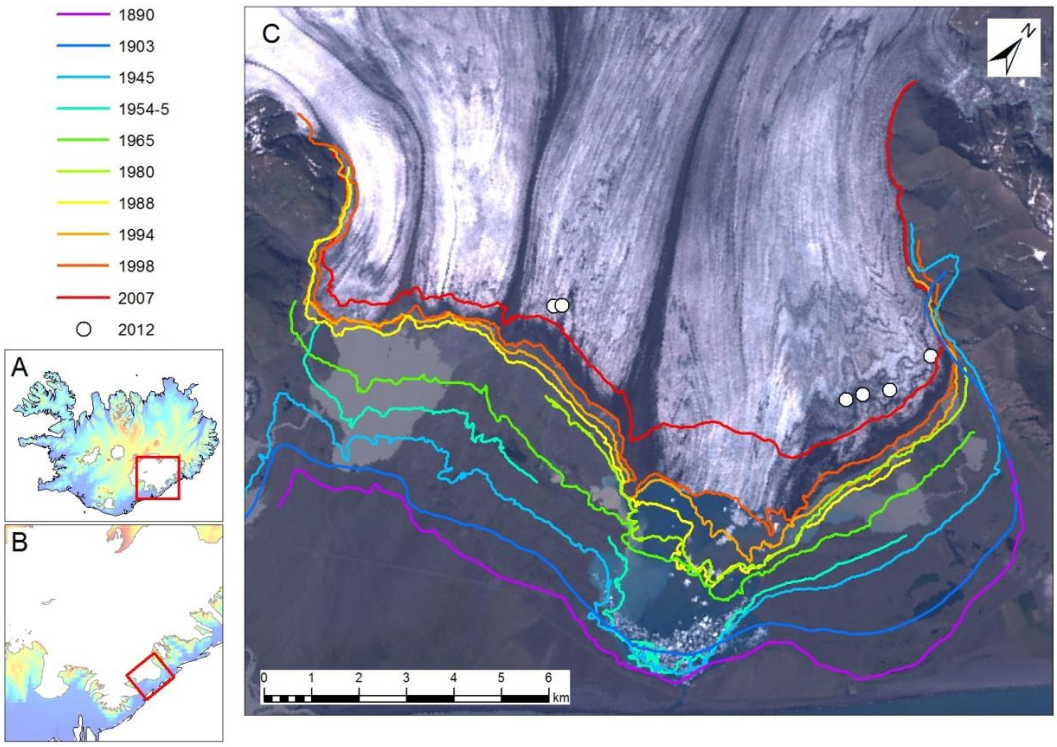

Figure 1.6. Location map. A) Location of the Vatnajökull Ice Cap in Iceland. The red box indicates the location of B. B) Location of Breiðamerkurjökull within Vatnajökull. The red box indicates the location of C. C) 1999 Landsat image of Breiðamerkurjökull with margin positions from 1890 to 2012. Note that some margins have gaps relating to the absence of aerial photograph coverage and the 2012 data are points measured by handheld GPS in the field. Breiðamerkurjökull was confluent with Fjallsjökull (to the southwest) until some point between 1945 and 1954. The 1890 margin is from Price (1980) and the 1903 margin is from Price (1982).

1.4 Thesis structure and results

Chapters 2-7 are given as research papers which will be (or have been) submitted for publication in relevant journals. The papers have been edited in order to ensure consistency throughout the thesis. A detailed review of the literature on eskers is presented in Chapter 2, which provides an overview of previous research on eskers, in the context of ice sheet meltwater drainage patterns, and expands on the above rationale for this thesis. Chapters 3-7 present the results of four different branches of research, aimed at addressing the research questions and objectives presented above. The methods used in each chapter are different and require

explanation in the context of the chapter; thus, the methods are presented at the beginning of each results chapter, rather than comprising a separate chapter. Each chapter also contains a discussion of its findings. An overview of Chapters 2-7 is given below. Chapter 8 draws together the results and discusses the findings in the context of the overall aim of the thesis and the research questions set out above. Finally, the main conclusions of the thesis are drawn together in Chapter 9.

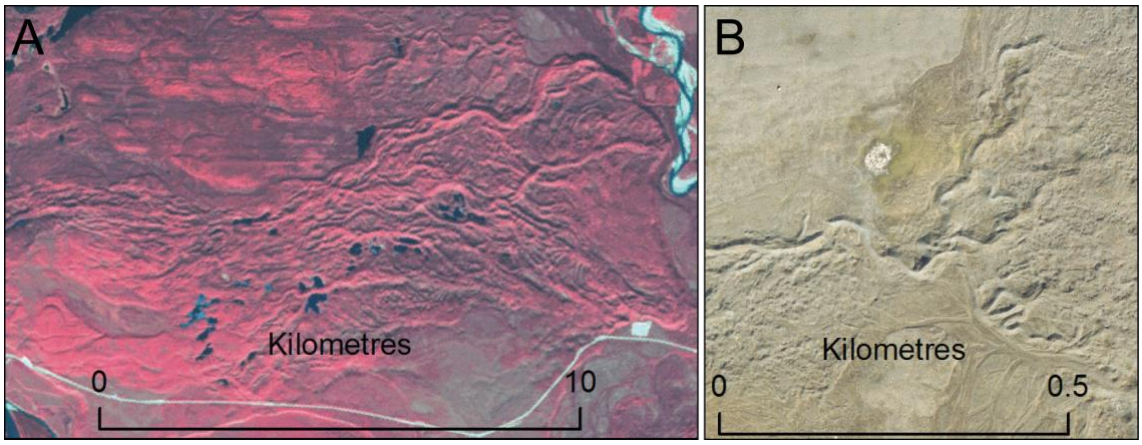

Figure 1.7. Similar esker morphologies formed beneath the Cordilleran Ice Sheet (A) and Breiðamerkurjökull (B).

1.4.1 Chapter 2

Storrar, R.D., Evans, D.J.A. & Stokes, C.R. (in prep) Eskers: forms, processes and implications for ice-sheet meltwater drainage. *Earth Science Reviews.*

This paper reviews the substantial literature on eskers, focusing on their use as indicators of former ice sheet meltwater drainage conditions. The different modes of subglacial drainage (e.g. channelized and distributed systems) and the landforms that they produce are described before focusing on eskers. A review of the terminology used to describe eskers reveals that there is disagreement as to how to define them, with at least 26 different esker types identified, many of which overlap. The literature on esker sedimentology is then briefly reviewed, revealing that eskers contain a diverse range of sedimentary structures related to different conditions of formation. Sediments contained within eskers have the potential to provide a detailed record of the conditions under which individual eskers formed and can be used, for example, to determine whether deposition was synchronous or time-transgressive, or whether sedimentation occurred in a supraglacial, englacial or subglacial environment. Esker geomorphology is then reviewed, including a synthesis of previous work on the morphometry and patterns of eskers (which are the subjects of Chapters 3-7). The next section deals with several hypotheses which have been put forward to account for the distribution and formation of eskers, including ice thickness, outburst floods, substrate resistance, interlobate deposition and groundwater flux. Finally, some

areas for further research are highlighted, some of which are addressed in later chapters. These include the morphometry and large scale pattern of eskers (Chapters 3 and 4), channelized and distributed drainage systems at the ice sheet scale (Chapter 5), using eskers to reconstruct the drainage of subglacial lakes and using eskers to test numerical models of meltwater drainage (Chapters 6 and 7).

In this paper I wrote the text and drew the figures. All authors contributed ideas and edited the text. The paper will be submitted for publication in *Earth Science Reviews.*

1.4.2 Chapter 3

Storrar, R.D., Stokes, C.R. & Evans, D.J.A. (2013) A map of large Canadian eskers from Landsat satellite imagery. *Journal of Maps,* 9, 456-473.

This paper describes the methods and results of mapping eskers from Landsat satellite imagery of Canada, and presents a map of over 20,000 eskers (see appendix). As such, it provides the foundation for the morphometric analysis of eskers presented in Chapter 4, the analysis of temporal changes in eskers during the deglaciation of the LIS presented in Chapter 5 and the analysis of geological controls on esker distribution presented in Chapter 6. The eskers mapped from Landsat imagery are compared with eskers mapped from over 2,000 aerial photographs from seven study areas, in order to check the detection rate of eskers in Landsat imagery against the higher-resolution aerial photographs. It is found that, overall, approximately 75% of eskers are detected using the satellite imagery and that those undetected are likely to be less than 2 km long. This suggests that the resultant map is a robust resource for further work on understanding the large scale characteristics of eskers at the ice sheet scale.

In this paper I conducted the image processing, mapping, writing, and figure drawing. All authors contributed ideas and edited the text. The paper published in *Journal of Maps* has been edited to ensure consistency throughout the thesis.

1.4.3 Chapter 4

Storrar, R.D., Stokes, C.R. & Evans, D.J.A. (in prep) Morphometry and pattern of a large sample (>20,000) of Canadian eskers: new insights regarding subglacial drainage beneath ice sheets. *Quaternary Science Reviews.*

This paper uses the map of eskers presented in Chapter 3 to provide the first systematic large-scale morphometric analysis of eskers. Variations in esker pattern and distribution are analysed and data on esker morphometry including length, fragmentation, sinuosity, lateral spacing, tributary ordering and elevation changes are presented and discussed. Canadian eskers are found

to be absent beneath former ice divides. Around the ice divides, they radiate outwards in dendritic networks with up to fourth-order tributaries, which are quasi-uniformly spaced at approximately 12 km apart. Away from the Canadian Shield, eskers are more scarce and do not conform to integrated patterns. Individual eskers are up to 97.5 km long and systems of eskers, punctuated by small gaps, can be traced for up to 760 km. Eskers are, surprisingly, very straight, with a mean sinuosity of 1.05. Analysis of esker height reveals that eskers show no preference for up- or down-slope trends and that the majority of eskers differ in elevation by no more than 10 m from end to end. The findings of this paper have implications for the formation of eskers, as well as for our understanding of the dimensions of subglacial meltwater channels beneath ice sheets. The data presented here and in Chapter 3 are ideally suited to testing recent numerical models which predict esker spacing. This is explored further in Chapter 6.

In this paper I conducted the analysis, wrote the text and drew the figures. All authors contributed ideas and edited the text. The paper will be submitted for publication in *Quaternary Science Reviews.*

1.4.4 Chapter 5

Storrar, R.D., Stokes, C.R. & Evans, D.J.A. (in press) Increased channelization of subglacial drainage during the deglaciation of the Laurentide Ice Sheet. *Geology.*

This paper uses the eskers mapped in Chapter 3 and data presented in Chapter 4, alongside a published ice margin chronology for the deglaciation on the LIS (Dyke *et al.*, 2003) to determine changes in esker frequency during deglaciation. It tests the hypothesis that the meltwater drainage systems beneath ice sheets are capable of evolving in response to the increased supply of meltwater, as has been observed on seasonal scales beneath alpine and Greenlandic outlet glaciers. It is revealed that, as the climate warmed at the end of the Younger Dryas and surface meltwater production increased, eskers increased in frequency at the ice sheet margin. This is suggested to reflect an increase in the channelized drainage of the Laurentide Ice Sheet during deglaciation and is the first observation of drainage system evolution over millennial and continental scales.

In this paper I conducted the analysis, wrote the text and drew the figures. All authors contributed ideas and edited the text. Chapter 5 is an edited version of the manuscript accepted for publication (pending minor corrections) by *Geology*. It contains additional detail on the analysis and has been edited to ensure consistency throughout the thesis.

1.4.5 Chapter 6

Storrar, R.D., Stokes, C.R. & Evans, D.J.A. (in prep) An assessment of lithological controls on esker distribution and morphometry in Canada. *Sedimentary Geology.*

This paper presents the results of an analysis of the effect of lithology on the distribution and morphometry of Canadian eskers. It uses the map presented in Chapter 3, morphometric data generated in Chapter 4, and published geological data (Fulton, 1995; Wheeler *et al.*, 1996; Atkinson & Lyster, 2011), to quantitatively test the influence of different bedrock and surficial geology on esker length, sinuosity and spacing. It is found that eskers are concentrated preferentially over the resistant rocks of the Precambrian Shield, as predicted by theory (Clark & Walder, 1994). Eskers are typically located in association with blankets of till, though the specific thickness of sediment is found to exert little influence on esker location. Esker length, sinuosity and spacing are found to be independent of the underlying substrate. This result is surprising because esker spacing has been suggested to be controlled by the basal melt rate and hydrogeological properties of the substrate (Boulton *et al.*, 2009).

In this paper I conducted the analysis, wrote the text and drew the figures. All authors contributed ideas and edited the text. The paper will be submitted for publication in *Sedimentary Geology.*

1.4.6 Chapter 7

Storrar, R.D., Evans, D.J.A. & Stokes, C.R. (in review) Controls on the formation of complex esker systems at decadal timescales, Breiðamerkurjökull, SE Iceland. *Earth Surface Processes and Landforms.*

The varying morphology of eskers formed beneath ancient ice sheets (Chapters 2,3 and 4) gives rise to uncertainty regarding the processes responsible for esker formation. Understanding what controls the morphology of different eskers is important when using eskers to reconstruct the drainage of meltwater beneath palaeo-ice sheets (Chapter 2). Modern analogues are therefore an essential tool for understanding some of the processes responsible for esker formation. This paper uses a modern analogue for esker formation at Breiðamerkurjökull, Iceland to evaluate the controls on the formation of complex esker systems, over a period of 62 years. The eskers formed beneath Breiðamerkurjökull are reminiscent of eskers formed beneath the NAISC and this paper uses a time series of aerial photographs from 1945 to 2007 to identify changes in esker systems over this period and, in particular, focuses on what controls the formation of complex esker systems. Two types of esker *complex* are identified and defined, *topographically constrained* and *esker fan*. Esker complexes are suggested to form when sediment is abundant and chokes conduits, leading to the formation of multiple distributary ridges. The complexity of the system is dependent on the balance between sediment supply and meltwater supply.

Topographically constrained esker complexes form where topography impedes drainage, precluding the formation of an *esker fan complex*, which forms where drainage is unimpeded. Boulton *et al.* (2007) suggested that the spacing of the Breiðamerkurjökull eskers is dictated by groundwater-channel coupling, but our mapping reveals that the large esker systems are typically associated with an increased sediment and meltwater supply from large medial moraines, which suggests that other processes also contribute to esker spacing.

In this paper I conducted the analysis, wrote the text and drew the figures. All authors contributed ideas and edited the text. The paper submitted to *Earth Surface Processes and Landforms* has been edited to ensure consistency throughout the thesis.

1.5 References

Alley, R. B., Dupont, T. K., Parizek, B. R. & Anandakrishnan, S. (2005) Access of surface meltwater to beds of sub-freezing glaciers: preliminary insights. *Annals of Glaciology*, 40, 8-14.

Atkinson, N. & Lyster, S. (2011) Thickness and Distribution of Quaternary and Neogene Sediment in Alberta, Canada. *Alberta Geological Survey*, Digital Data, 2010-0036.

Aylsworth, J. M. & Shilts, W. W. (1989) Bedforms of the Keewatin Ice-Sheet, Canada. *Sedimentary Geology*, 62, 407-428.

Banwell, A., Willis, I., Arnold, N. & Ahlstrom, A. (2010) Subglacial Meltwater Drainage at Paakitsoq, West Greenland: Insights from a Distributed, Physically Based Numerical Model. *EGU General assembly 2010*. 12.

Bartholomew, I., Nienow, P., Mair, D., Hubbard, A., King, M. A. & Sole, A. (2010) Seasonal evolution of subglacial drainage and acceleration in a Greenland outlet glacier. *Nature Geoscience*, 3, 408-411.

Bartholomew, I., Nienow, P., Sole, A., Mair, D., Cowton, T. & King, M. A. (2012) Short-term variability in Greenland Ice Sheet motion forced by time-varying meltwater drainage: Implications for the relationship between subglacial drainage system behavior and ice velocity. *J. Geophys. Res.*, 117, F03002.

Bell, R. E. (2008) The role of subglacial water in ice-sheet mass balance. *Nature Geoscience*, 1, 297-304.

Bell, R. E., Ferraccioli, F., Creyts, T. T., Braaten, D., Corr, H., Das, I., Damaske, D., Frearson, N., Jordan, T. & Rose, K. (2011) Widespread Persistent Thickening of the East Antarctic Ice Sheet by Freezing from the Base. *Science*, 25, 1524-1525.

Bell, R. E., Studinger, M., Shuman, C. A., Fahnestock, M. A. & Joughin, I. (2007) Large subglacial lakes in East Antarctica at the onset of fast-flowing ice streams. *Nature*, 445, 904-907.

Boulton, G. S. (2006) Glaciers and their coupling with hydraulic and sedimentary processes. In P. G. Knight, *Glacier Science and Environmental Change*. Oxford, Blackwell, 3-23.

Boulton, G. S., Dobbie, K. E. & Zatsepin, S. (2001) Sediment deformation beneath glaciers and its coupling to the subglacial hydraulic system. *Quaternary International*, 86, 3-28.

Boulton, G. S., Hagdorn, M., Maillot, P. B. & Zatsepin, S. (2009) Drainage beneath ice sheets: groundwater-channel coupling, and the origin of esker systems from former ice sheets. *Quaternary Science Reviews*, 28, 621-638.

Boulton, G. S., Harris, P. W. V. & Jarvis, J. (1982) Stratigraphy and structure of a coastal sediment wedge of glacial origin inferred from Sparker measurements in glacial lake Jokulsarlon in southeast Iceland. *Jokull*, 32, 37-47.

Boulton, G. S., Lunn, R., Vidstrand, P. & Zatsepin, S. (2007) Subglacial drainage by groundwater-channel coupling, and the origin of esker systems: Part I-glaciological observations. *Quaternary Science Reviews*, 26, 1067-1090.

Brennand, T. A. (2000) Deglacial meltwater drainage and glaciodynamics: inferences from Laurentide eskers, Canada. *Geomorphology*, 32, 263-293.

Burke, M. J., Woodward, J., Russell, A. J., Fleisher, P. J. & Bailey, P. K. (2010) The sedimentary architecture of outburst flood eskers: A comparison of ground-penetrating radar data from Bering Glacier, Alaska and Skeiðarárjökull, Iceland. *Bulletin of the Geological Society of America*, 122, 1637-1645.

Carter, S. P., Blankenship, D. D., Young, D. A. & Holt, J. W. (2009a) Using radar-sounding data to identify the distribution and sources of subglacial water: application to Dome C, East Antarctica. *Journal of Glaciology*, 55, 1025-1040.

Carter, S. P., Blankenship, D. D., Young, D. A., Peters, M. E., Holt, J. W. & Siegert, M. J. (2009b) Dynamic distributed drainage implied by the flow evolution of the 1996-1998 Adventure Trench subglacial lake discharge. *Earth and Planetary Science Letters*, 283, 24-37.

Catania, G. A. & Neumann, T. A. (2010) Persistent englacial drainage features in the Greenland Ice Sheet. *Geophysical Research Letters*, 37, L02501.

Chandler, D. M., Wadham, J. L., Lis, G. P., Cowton, T., Sole, A., Bartholomew, I., Telling, J., Nienow, P., Bagshaw, E. B., Mair, D., Vinen, S. & Hubbard, A. (2013) Evolution of the subglacial drainage system beneath the Greenland Ice Sheet revealed by tracers. *Nature Geosci*, 6, 195-198.

Clark, C. D., Hughes, A. L. C., Greenwood, S. L., Spagnolo, M. & Ng, F. S. L. (2009) Size and shape characteristics of drumlins, derived from a large sample, and associated scaling laws. *Quaternary Science Reviews*, 28, 677-692.

Clark, P. U. & Walder, J. S. (1994) Subglacial drainage, eskers, and deforming beds beneath the Laurentide and Eurasian ice sheets. *Bulletin of the Geological Society of America*, 106, 304-314.

Das, S. B., Joughin, I., Behn, M. D., Howat, I. M., King, M. A., Lizarralde, D. & Bhatia, M. P. (2008) Fracture Propagation to the Base of the Greenland Ice Sheet During Supraglacial Lake Drainage. *Science*, 320, 778-781.

Dunlop, P. & Clark, C. D. (2006) The morphological characteristics of ribbed moraine. *Quaternary Science Reviews*, 25, 1668-1691.

Dyke, A., Andrews, J., Clark, P., England, J., Miller, G., Shaw, J. & Veillette, J. (2002) The Laurentide and Innuitian ice sheets during the last glacial maximum. *Quaternary Science Reviews*, 21, 9-31.

Dyke, A. S., Moore, A. & Robertson, L. (2003) Deglaciation of North America. *Geological Survey of Canada, Open File*, 1574.

Evans, D. J. A. & Twigg, D. R. (2000) Breiðamerkurjökull 1998. 1: 30,000 Scale Map. University of Glasgow and Loughborough University.

Evans, D. J. A. & Twigg, D. R. (2002) The active temperate glacial landsystem: a model based on Breiðamerkurjökull and Fjallsjökull, Iceland. *Quaternary Science Reviews*, 21, 2143-2177.

Evatt, G. W., Fowler, A. C., Clark, C. D. & Hulton, N. R. J. (2006) Subglacial floods beneath ice sheets. *Philosophical Transactions of the Royal Society A: Mathematical, Physical and Engineering Sciences*, 364, 1769-1794.

Fricker, H. A., Scambos, T., Bindschadler, R. & Padman, L. (2007) An active subglacial water system in West Antarctica mapped from space. *Science*, 315, 1544-1548.

Fricker, H. A., Scambos, T., Carter, S., Davis, C., Haran, T. & Joughin, I. (2010) Synthesizing multiple remote-sensing techniques for subglacial hydrologic mapping: application to a lake system beneath MacAyeal Ice Stream, West Antarctica. *Journal of Glaciology*, 56, 187-199.

Fulton, R. J. (1995) Surficial materials of Canada *Geological Survey of Canada, "A" Series Map 1880A*. 1:5,000,000

Hättestrand, C. (1997) Ribbed moraines in Sweden — distribution pattern and palaeoglaciological implications. *Sedimentary Geology*, 111, 41-56.

Hewitt, I. J. (2011) Modelling distributed and channelized subglacial drainage: the spacing of channels. *Journal of Glaciology*, 57, 302-314.

Hewitt, I. J. (2013) Seasonal changes in ice sheet motion due to melt water lubrication. *Earth and Planetary Science Letters*, 371–372, 16-25.

Iken, A. & Truffer, M. (1997) The relationship between subglacial water pressure and velocity of Findelengletscher, Switzerland, during its advance and retreat. *Journal of Glaciology*, 43, 328-338.

Joughin, I., Das, S. B., King, M. A., Smith, B. E., Howat, I. M. & Moon, T. (2008) Seasonal Speedup Along the Western Flank of the Greenland Ice Sheet. *Science*, 320, 781-783.

Le Brocq, A. M., Payne, A., Siegert, M. & Alley, R. (2009) A subglacial water-flow model for West Antarctica. *Journal of Glaciology*, 55, 879-888.

Lewis, S. M. & Smith, L. (2009) Hydrologic drainage of the Greenland Ice Sheet. *Hydrological Processes*, 23, 2004-2011.

Mäkinen, J. (2003) Time-transgressive deposits of repeated depositional sequences within interlobate glaciofluvial (esker) sediments in Koylio, SW Finland. *Sedimentology*, 50, 327-360.

Mossop, G. D. & Shetsen, I. (1994) *Geological atlas of the Western Canada Sedimentary Basin*, Canadian Society of Petroleum Geologists and Alberta Research Council.

Nienow, P., Sharp, M. & Willis, I. (1998) Seasonal changes in the morphology of the subglacial drainage system, Haut Glacier d'Arolla, Switzerland. *Earth Surface Processes and Landforms*, 23, 825-843.

Nienow, P. W., Sharp, M. & Willis, I. C. (1996) Velocity-discharge relationships derived from dye tracer experiments in glacial meltwaters: implications for subglacial flow conditions. *Hydrological Processes*, 10, 1411-1426.

Parizek, B. R., Alley, R. B., Anandakrishnan, S. & Conway, H. (2002) Sub-catchment melt and long-term stability of ice stream D, West Antarctica. *Geophysical Research Letters*, 29, 1214.

Parizek, B. R., Alley, R. B., Dupont, T. K., Walker, R. T. & Anandakrishnan, S. (2010) Effect of orbital-scale climate cycling and meltwater drainage on ice sheet grounding line migration. *J. Geophys. Res.*, 115, F01011.

Pattyn, F., de Smedt, B. & Souchez, R. (2004) Influence of subglacial Vostok lake on the regional ice dynamics of the Antarctic ice sheet: a model study. *Journal of Glaciology*, 50, 583-589.

Prest, V. K., Grant, D. R. & Rampton, V. N. (1968) Glacial map of Canada. Geological Survey of Canada, Map 1253A. 1:5,000,000

Price, R. J. (1980) Rates of geomorphological changes in proglacial areas. In R. A. Cullingford, D. A. Davidson and J. Lewin, *Timescales in geomorophology*. Chichester, Wiley, 79-93.

Price, R. J. (1982) Changes in the proglacial area of Breiðamerkurjökull , southeastern Iceland: 1890-1980. *Jökull*, 29-35.

Rignot, E., Velicogna, I., van den Broeke, M. R., Monaghan, A. & Lenaerts, J. (2011) Acceleration of the contribution of the Greenland and Antarctic ice sheets to sea level rise. *Geophys. Res. Lett.*, 38, L05503.

Schoof, C. (2010) Ice-sheet acceleration driven by melt supply variability. *Nature*, 468, 803-806.

Schuler, T. V. & Fischer, U. H. (2009) Modeling the diurnal variation of tracer transit velocity through a subglacial channel. *Journal of Geophysical Research*, 114, F04017.

Shannon, S. R., Payne, A. J., Bartholomew, I. D., van den Broeke, M. R., Edwards, T. L., Fettweis, X., Gagliardini, O., Gillet-Chaulet, F., Goelzer, H., Hoffman, M. J., Huybrechts, P., Mair, D. W. F., Nienow, P. W., Perego, M., Price, S. F., Smeets, C. J. P. P., Sole, A. J., van de Wal, R. S. W. & Zwinger, T. (2013) Enhanced basal lubrication and the contribution of the Greenland ice sheet to future sea-level rise. *Proceedings of the National Academy of Sciences*, 110, 14156-14161.

Shreve, R. L. (1985) Esker characteristics in terms of glacier physics, Katahdin esker system, Maine. *Bulletin of the Geological Society of America*, 96, 639-646.

Spagnolo, M., Clark, C. D. & Hughes, A. L. C. (2012) Drumlin relief. *Geomorphology*, 153–154, 179-191.

Spagnolo, M., Clark, C. D., Hughes, A. L. C. & Dunlop, P. (2011) The topography of drumlins; assessing their long profile shape. *Earth Surface Processes and Landforms*, 36, 790-804.

Spagnolo, M., Clark, C. D., Hughes, A. L. C., Dunlop, P. & Stokes, C. R. (2010) The planar shape of drumlins. *Sedimentary Geology*, 232, 119-129.

Stearns, L. A., Smith, B. E. & Hamilton, G. S. (2008) Increased flow speed on a large East Antarctic outlet glacier caused by subglacial floods. *Nature Geoscience*, 1, 827-831.

Storrar, R.D., Stokes, C.R. & Evans, D.J.A. (2013) A map of large Canadian eskers from Lansat satellite imagery. *Journal of Maps*, 9, 456-473.

Storrar, R.D., Stokes, C.R. & Evans, D.J.A. (in press) Increased channelization of subglacial drainage during the deglaciation of the Laurentide Ice Sheet. *Geology.*

Storrar, R.D., Evans, D.J.A. & Stokes, C.R. (in review) Controls on the formation of complex esker systems at decadal timescales, Breiðamerkurjökull, SE Iceland. *Earth Surface Processes and Landforms.*

Storrar, R.D., Evans, D.J.A. & Stokes, C.R. (in prep) Eskers: forms, processes and implications for ice-sheet meltwater drainage. *Earth Science Reviews.*

Storrar, R.D., Stokes, C.R. & Evans, D.J.A. (in prep) Morphometry and pattern of a large sample (>20,000) of Canadian eskers: new insights regarding subglacial drainage beneath ice sheets. *Quaternary Science Reviews.*

Storrar, R.D., Stokes, C.R. & Evans, D.J.A. (in prep) An assessment of lithological controls on esker distribution and morphometry in Canada. *Sedimentary Geology.*

Werder, M. A., Loye, A. & Funk, M. (2009) Dye tracing a jokulhlaup: I. Subglacial water transit speed and water-storage mechanism. *Journal of Glaciology*, 55, 889-898.

Wheeler, J. O., Hoffman, P. F., Card, K. D., Davidson, A., Sanford, B. V., Okulitch, A. V. & Roest, W. R. (1996) Geological map of Canada. *Geological Survey of canada, map 1860A.*

Willis, I., Lawson, W., Owens, I., Jacobel, B. & Autridge, J. (2009) Subglacial drainage system structure and morphology of Brewster Glacier, New Zealand. *Hydrological Processes*, 23, 384-396.

Wingham, D. J., Siegert, M. J., Shepherd, A. & Muir, A. S. (2006) Rapid discharge connects Antarctic subglacial lakes. *Nature*, 440, 1033-1036.

Wright, A. & Siegert, M. (2012) A fourth inventory of Antarctic subglacial lakes. *Antarctic Science*, 24, 659-664.

Wright, A., Siegert, M., Le Brocq, A. & Gore, D. (2008) High sensitivity of subglacial hydrological pathways in Antarctica to small ice-sheet changes. *Geophysical Research Letters*, 35, L17504.

Wright, A. P., Young, D. A., Roberts, J. L., Schroeder, D. M., Bamber, J. L., Dowdeswell, J. A., Young, N. W., Le Brocq, A. M., Warner, R. C., Payne, A. J., Blankenship, D. D., van Ommen, T. D. & Siegert, M. J. (2012) Evidence of a hydrological connection between the ice divide and ice sheet margin in the Aurora Subglacial Basin, East Antarctica. *J. Geophys. Res.*, 117, F01033.

Zwally, H. J., Abdalati, W., Herring, T., Larson, K., Saba, J. & Steffen, K. (2002) Surface melt-induced acceleration of Greenland ice-sheet flow. *Science*, 297, 218-222.

Chapter 2 Eskers: forms, processes and implications for ice-sheet meltwater drainage

Storrar, R.D., Evans, D.J.A. & Stokes, C.R. (in prep) Eskers: forms, processes and implications for ice-sheet meltwater drainage. *Earth Science Reviews.*

Abstract

Eskers may be used to further our understanding of how meltwater behaves beneath ice-sheets – a subject which is crucial for ice dynamics, but difficult to observe beneath contemporary ice-sheets. Before this can be done, the literature on eskers needs to be addressed in order to ascertain how they vary, what processes are responsible for their formation and to what extent they may be used for reconstructions of sub-ice-sheet meltwater drainage systems. This paper provides a review of the literature relating to eskers, in terms of their sedimentology, geomorphology and the processes invoked to explain their distribution. It is demonstrated that at least 26 different types of esker have been identified in the literature, some of which have some similar characteristics and hence occupy positions on a morphological continuum. Esker sediments vary enormously and echo the complexities surrounding esker deposition. Nevertheless, key sedimentological investigations are highlighted which have progressed our understanding of how eskers are formed. Hypotheses concerning esker location and distribution are reviewed and include: ice thickness; outburst floods; substrate resistance; interlobate deposition and groundwater flux. No single hypothesis has yet been demonstrated to be responsible for esker distributions and it seems likely that several processes may be responsible for observed esker patterns. In light of this review, four key areas of future research are outlined, which will help to understand what controls the distribution and formation of eskers and, when this is sufficiently understood, how eskers can be used to further our understanding of subglacial meltwater drainage at the ice sheet scale: i) quantifying the morphometry and large-scale pattern of eskers; ii) using esker patterns to reconstruct channelized meltwater drainage beneath ice sheets; iii) the potential use of esker patterns to reconstruct the drainage of subglacial lakes; and iv) using eskers to test numerical models of meltwater drainage.

2.1 Introduction

A large literature exists in relation to eskers and the processes surrounding their formation and this paper provides a detailed review of our understanding of eskers, including their sedimentology, geomorphology, and the controls on esker formation and pattern. The aim of this paper is to provide an accessible synthesis of current understanding of eskers but with an

over-arching objective of assessing their use as proxies for ice sheet-wide meltwater drainage (see Chapter 1). As such, large-scale processes and patterns are emphasised. Key questions regarding the use of eskers to reconstruct ice-sheet meltwater processes are addressed.

By way of introduction, Section 2.2 deals with the underlying concepts of meltwater drainage beneath ice, as well as some of the landforms that result from glaciofluvial erosion and deposition. Various definitions and classifications of eskers are reviewed in Section 2.3, and Sections 2.4, 2.5 and 2.6 deal with esker sedimentology, geomorphology and their spatial controls, respectively. The areas of future research most relevant to ice-sheet meltwater drainage and esker systems are set out in Section 2.7. Section 2.8 provides a summary. Table 2.1 defines the glaciological parameters used throughout the paper. Locations of Figures used are shown in Figure 2.1.

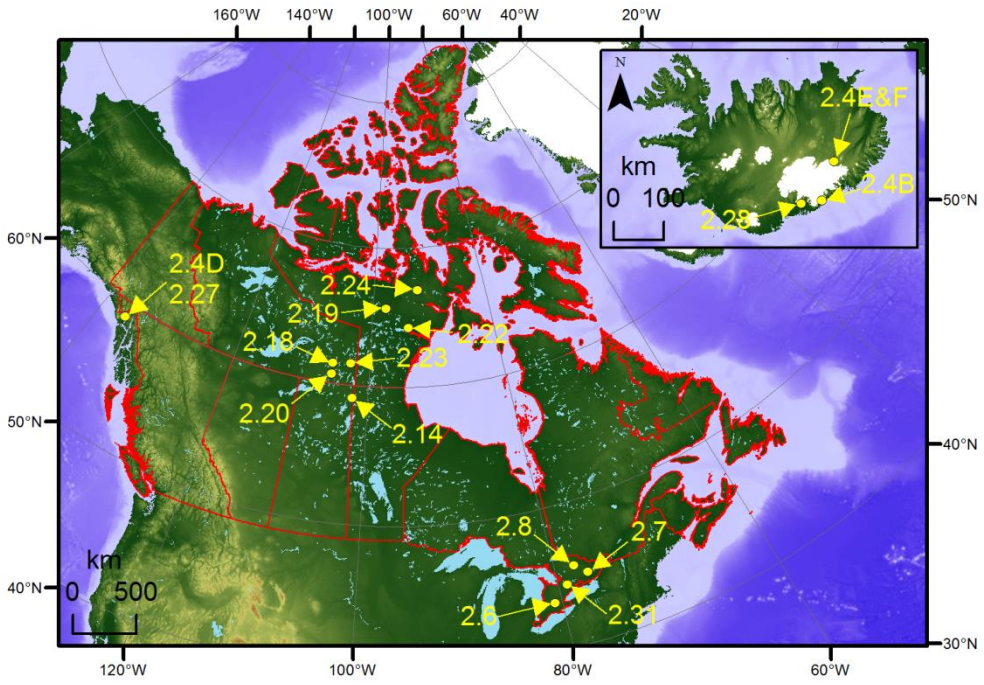

Figure 2.1. Map showing the locations of Figures used in Chapter 2 in Canada and Iceland (inset).

Before discussing eskers, it is important to briefly summarise the production and movement of meltwater, which can enter and be routed through the glacier system by various means. The most prominent factors controlling supraglacial meltwater production are insolation and a warm and moist atmosphere (Cuffey & Paterson, 2010). Englacial meltwater can be produced by friction as a result of ice creep, a process which also occurs at the glacier bed (Benn & Evans, 2010). Additionally, subglacial meltwater may be produced if ice is at the pressure melting point and the geothermal heat is sufficient to melt ice. Water can also enter glacier systems as rain, runoff or groundwater (Benn & Evans, 2010).

2.2 Meltwater drainage: theory, significance and consequences

Once in the glacial drainage system, meltwater is transferred by several different mechanisms, but which can be broadly categorised as 'distributed' or 'channelized' systems (Figure 2.2). Distributed systems occur where water is not organised into discrete channels. As such, these systems are usually less efficient than channelized systems at transporting water and are typically associated with higher ice velocities (Fountain & Walder, 1998). In contrast, where water is efficiently removed through a channelized system, ice velocities tend to be slower. It is for this reason that Fountain and Walder (1998) termed these two different modes as 'fast' (channelized) and 'slow' (distributed) meltwater drainage systems. Both systems can be further subdivided into discrete types of drainage system, which are described in an extensive literature. For this reason, they are only introduced briefly below and the reader is directed to the references and wider literature for further information. It is important to note that distributed and channelized systems vary spatially and temporally and that there are often transitional zones between them (Fountain & Walder, 1998). There is also evidence to suggest that they can exist simultaneously (Mernild, 2006; Willis *et al.*, 2012). Various landforms are produced by these different drainage systems, though eskers are only produced by channelized systems.

2.2.1 Distributed drainage systems

Several mechanisms of water transport in distributed systems have been described, including linked-cavity flow, water films, groundwater flow, englacial fractures, and canals.

2.2.1.1 Linked-cavity flow

Linked-cavity flow was first described by Lliboutry (1969) and describes the movement of water in a system where water-filled cavities and orifices (narrow channels between cavities) occur at the bed (Figure 2.2). Cavities form where P_i is locally low, typically in the lee of bedrock bumps (Benn & Evans, 2010). Areas of rough bedrock topography are therefore the most likely to develop linked-cavity drainage because there are many cavities in close proximity. Cavities are maintained by ice sliding (Nye, 1970) and also where $P_w > P_i$ (Benn & Evans, 2010). Linked-cavity systems may be relatively stable where water moves between persistent cavities (such as topographic depressions) to maintain pressure equilibrium.

Direct evidence of linked cavities was observed by Vivian & Bocquet (1973) beneath the Glacier d'Argentière, France. They found a series of cavities on the order of a few 10s of m in length. The observation of air currents between cavities suggested that they were connected and Vivian & Bocquet (1973) also noted that the linked-cavity system occurred in association with a large ice fall. Geomorphological evidence of linked cavity systems in deglaciated areas has also been identified by several authors (e.g. Walder & Hallet, 1979; Hallet & Anderson, 1980; Sharp

et al., 1989), where 'fossilised' cavities and orifices are preserved in limestone bedrock. Walder & Hallet (1979) concluded that at least 20% of the bed of the Blackfoot Glacier, USA was drained by linked-cavity drainage, though the temporal evolution of this system is unclear.

2.2.1.2 Water films

Weertman (1964) speculated that meltwater beneath a glacier with an impermeable bed would be drained by a thin water film, because basal melting by geothermal heat and friction would outweigh the ability of the ice to dissipate heat by conduction. Water films are suggested to be very thin: Weertman (1969) calculated that water films beneath most glaciers would be between 1-10 mm. Subsequently, Alley (1989) calculated film thickness also varying between 1-10 mm for Ice Stream B, Antarctica. Water films are purported to exist alongside linked-cavity drainage systems and measurements of siltskin (calcite cemented lithic grains inferred to have been transported and deposited in water films) thickness by Carter *et al.* (2003) suggests that water films are thinner (0.5-2.0 mm) on the stoss-side and thicker (2-20 mm) on the lee-side of cavity-forming bumps at the Mendenhall Glacier, USA. Water is often thought to be transferred by water films from areas of pressure melting to areas of regelation under glaciers (Benn & Evans, 2010).

The major assumption in water film calculations is that glaciers exist on impermeable beds (Weertman, 1972). In reality, glacier beds tend to interact with the underlying substrate and, therefore, groundwater flow can, in some circumstances, be an important factor controlling the behaviour of subglacial meltwater. Glacial drainage systems underlain by permeable aquifers are intimately linked with the underlying groundwater (Boulton & Hindmarsh, 1987). In these systems, water can move both through the aquifer and also in the subglacial drainage system, either in the till or in channels.

Table 2.1. Parameters used in this paper.

Symbol	Definition (units)
ϕ	Hydraulic potential (dimensionless)
ρ_w	Density of water (1,005 kg m^{-3})
ρ_i	Density of ice (km m^{-3})
g	Acceleration due to gravity (9.81 m s^{-2})
Z	Elevation (m)
h_b	Bed elevation (m)
P_w	Water pressure (Pa)
P_i	Ice pressure (Pa)
P_o	Atmospheric pressure (Pa)
P_e	Effective pressure (Pa)
$\dot{m}$	Tunnel expansion rate (m a^{-1})
$\dot{r}$	Tunnel closure rate (m a^{-1})
h_i	Ice surface elevation (m)
Ts	Tunnel spacing (m)
T	Bed transmissivity (m^2 a^{-1})
m	Basal melt rate (m a^{-1})
S	Sinuosity (dimensionless)
l_s	Esker length (m)
W	Esker width (m)

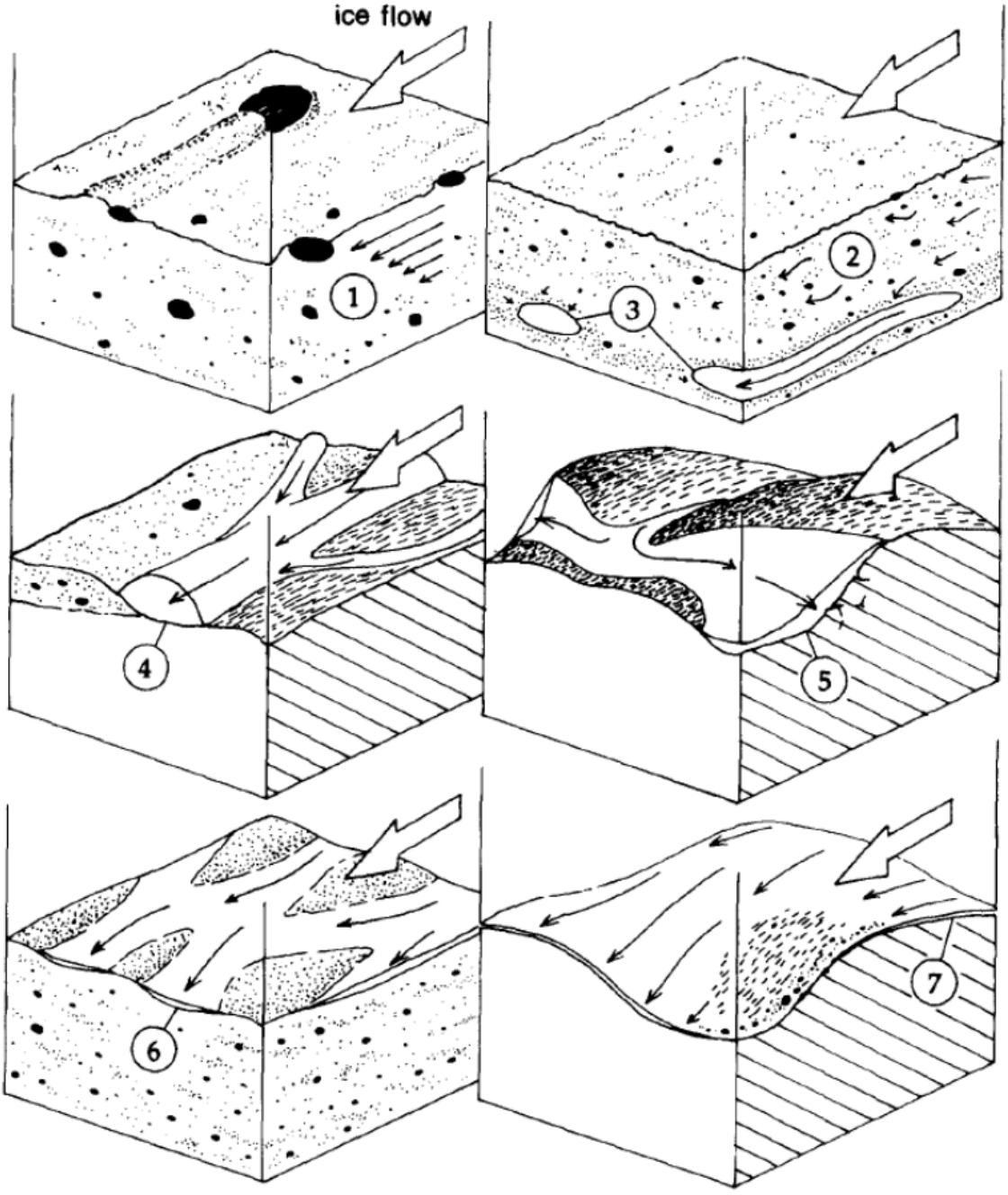

Figure 2.2. Channelized (3 and 4) and distributed (1,2,5,6 and 7) drainage systems. (1) Bulk movement within the deforming skeleton; (2) Darcian porewater flow; (3) Pipe flow; (4) Dendritic channel network; (5) Linked cavity system; (6) Braided canal network; (7) Thin film at the ice-rock interface. From Benn & Evans (1996).

2.2.1.3 Groundwater flow

In order to investigate the relationship between groundwater flow and subglacial drainage, Boulton *et al.* (2001) inserted a series of pressure transducers into the till and sub-till aquifer in front of eastern Breiðamerkurjökull, Iceland, prior to a surge. Water pressure was initially higher in the sub-till aquifer than the till. However, as the glacier advanced, the pressure became higher in the till, indicating that water moves between the subglacial system and the

groundwater system, depending on the pressure acting on it. Boulton *et al.* (2001) suggested that meltwater initially moves downwards through the till, before entering the more permeable aquifer. Closer to the margin, the water upwells as the pressure in the till decreases. This process is highly variable, both spatially and temporally, indicating that it is a complex system dependent on subtle changes in pressure and meltwater supply. The importance of groundwater flow in the development of eskers is discussed in more detail in section 2.6.5.

2.2.1.4 Englacial fractures

Meltwater may be transported in englacial fractures, where supraglacial water enters existing crevasses to form moulins. If there is sufficient water, the fracture will remain open. Though they exist as distributed systems and do not usually tend to be channelized, englacial fractures are often assumed to operate in conjunction with widely spaced channels (Fountain & Walder, 1998; Fountain *et al.*, 2005b; Cuffey & Paterson, 2010) and may therefore occupy an intermediate position between distributed and channelized drainage systems. One mechanism that has been shown to develop a fractured englacial drainage system is the drainage of supraglacial lakes (Das *et al.*, 2008; Catania & Neumann, 2010) because the supply of water can be sufficient to connect and maintain a moulin to the glacier bed (e.g. Boon & Sharp, 2003). Moreover, some moulins have been demonstrated to be stable over several years (Catania & Neumann, 2010). Evidence of englacial fractures exists in the form of borehole observations (Fountain *et al.*, 2005a) as well as glacio-speliological exploration (e.g. Gulley *et al.*, 2009).

2.2.1.5 Canals

Walder & Fowler's (1994) theoretical work predicted the occurrence of 'canal' type drainage whereby wide, shallow canals are incised into saturated, deformable sediment. Under these circumstances, water is unable to escape through the bed because the sediment is saturated. P_e is inversely related to discharge in canals (Ng, 2000) and where P_e is low, Walder & Fowler (1994) suggest that canal drainage occurs because water incises the sediment to open channels, which are subject to closure by subsequent creep of the sediment. Channel closure is balanced by fluvial erosion which results in a network of canals. Canal drainage networks tend to be anastomosing, rather than dendritic because large and small canals do not necessarily exist at different pressures, precluding the formation of an integrated network (unlike R-channels; see Section 2.2.2).

2.2.2 Channelized drainage systems

In the 1970s, significant advances were made in the field of subglacial drainage (e.g. Röthlisberger, 1972; Shreve, 1972; Weertman, 1972; Nye, 1973). In particular, theoretical analyses by several authors advanced our understanding of the channelized systems operating beneath temperate glaciers. Channelized drainage networks are more efficient at removing water from the glacier system than distributed networks because they are relatively better connected and the channels are, by definition, larger. Three main types of channels have been described and are illustrated in Figure 2.3: R-channels (Röthlisberger, 1972); N-channels (Nye, 1973) and H-channels (Hooke, 1984).

2.2.2.1 R-channels

R-channels are conduits completely filled with water. Thus, they exist under pressure and are maintained by a balance between conduit closure by viscous ice creep and conduit expansion by melting of the walls by the friction induced by water flowing through the conduit (Röthlisberger, 1972; Shreve, 1972). Water pressure is close to ice overburden pressure, but can be less in larger R-channels because the high discharge increases the expansion of the conduit by melting (Röthlisberger, 1972). A consequence of lower water pressure in the larger channels is that water is preferentially drawn in to them due to the resultant pressure gradient. This results in the development of a dendritic network, as illustrated in Figure 2.4.

2.2.2.2. N-channels

N-channels are similar to R-channels in that they form coherent subglacial networks and exist under pressure. They differ from R-channels in that they are incised into the substrate (see Figure 2.3B). N-channels can exist in dendritic or anastomosing networks (Booth & Hallet, 1993). Though superficially similar to canals, N-channels may be incised into bedrock, rather than just sediment, and are conducive to forming integrated networks because of the presence of a pressure gradient.

2.2.2.3 H-channels

Following the seminal papers of Röthlisberger (1972) and Shreve (1972), Hooke (1984) suggested that R-channels may be less prevalent than previously thought. Hooke (1984) reasoned that conduits may not always be full of water and that air gaps may exist. The premise for this is that larger discharges and steeper bed slopes would provide sufficient energy for meltwater to melt conduit walls, without the need to invoke pressurised water (Hooke, 1984).

Steeper bed slopes and higher discharges would increase the energy available for melting of the conduit wall, resulting in open channels. Thus, where excess melting exists, it is possible for H-channels to trend horizontally across glacier flow, in contravention of the Shreve model (see Section 2.6.1). Hooke's work implies that R-channels and H-channels form part of a continuum, whereby spatial and/or temporal variations may cause drainage to occur in either state. As such, it may often be impracticable to differentiate between them, especially where direct observations have not been made.

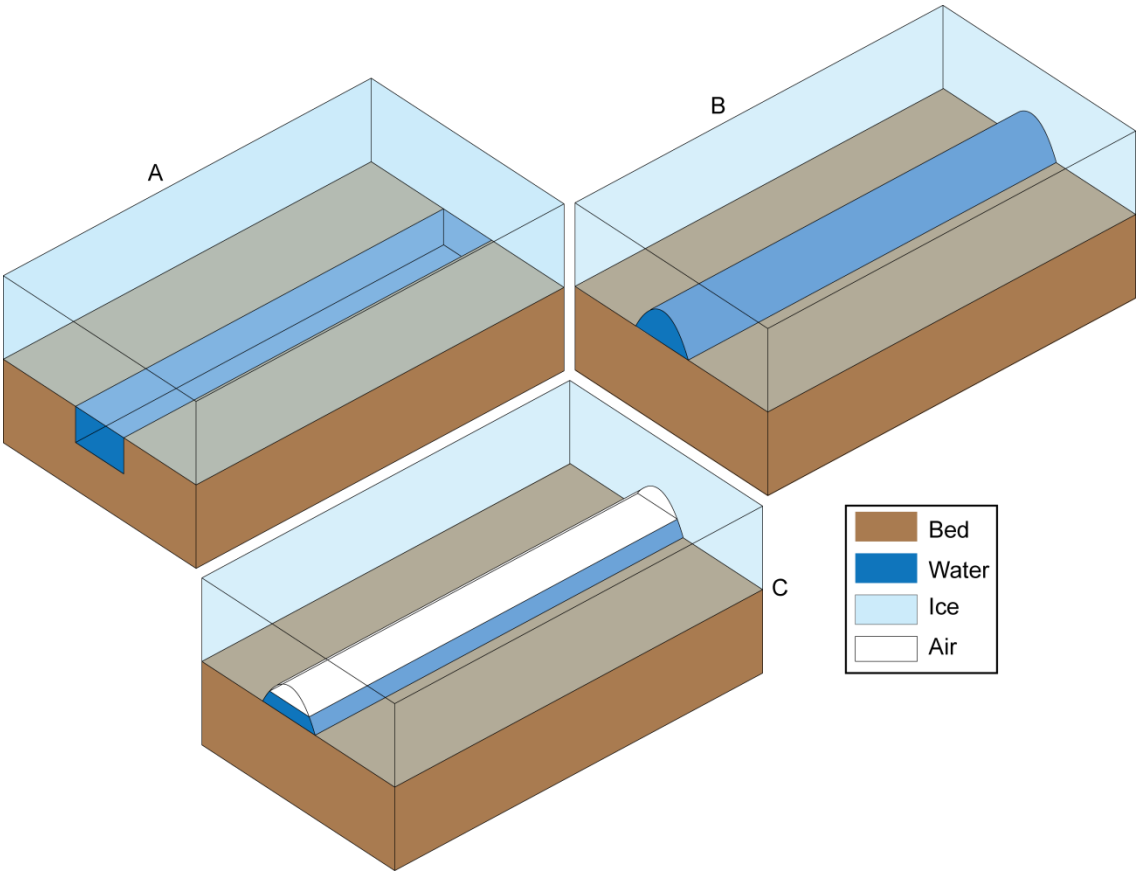

Figure 2.3. Idealised subglacial drainage channels: A) N-channel; B) R-channel; C) H-channel. Not to scale.

2.2.3 Glaciofluvial landforms indicative of meltwater flow

Meltwater draining from palaeo-ice sheets, in the various forms described previously, has produced an extensive range of glaciofluvial landforms, all of which record the nature of meltwater flow (i.e. the direction and magnitude). Before reviewing eskers in more detail, it is necessary to briefly mention other related landforms in order to provide a broader context of the landform associations created by meltwater drainage networks.

Lateral, marginal, submarginal or subglacial meltwater channels are formed by erosion of the substrate by meltwater (often in the form of N-channels). Meltwater channels are often

prevalent where there are relatively few eskers, suggesting that they form under different conditions. Indeed, Dyke (1993) suggests that meltwater channels in parts of Arctic Canada were formed around the margins of cold-based ice, because meltwater would not be able to penetrate the frozen surface layer. Similarly, eskers were not able to form under cold-based ice for the same reason. The Shaler Mountains of north-west Victoria Island provide a good example of a landscape dominated by meltwater channels where eskers are relatively sparse (Prest *et al.*, 1968; Storrar & Stokes, 2007). Whilst some areas show distinct zones of either eskers or meltwater channels, other areas contain both landforms (e.g. Labrador: Jansson, 2005), sometimes with meltwater channels merging into eskers (or *vice versa*).

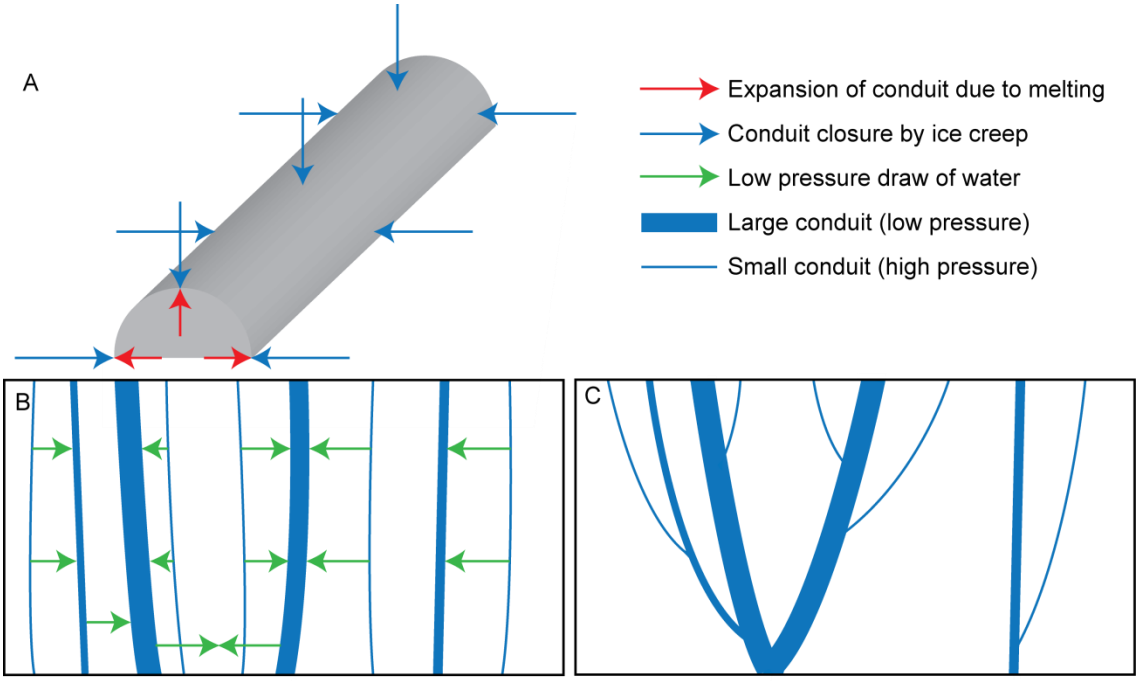

Figure 2.4. Development of a dendritic network of R-channels. A shows an oblique representation of the forces acting to maintain a channel: ice creep is balanced by melting of the conduit by friction. B shows a plan view of a hypothetical arrangement of different sized channels and demonstrates how a dendritic network may be initiated, as smaller (high pressure) channels are subsumed by larger (low pressure) channels. The resultant dendritic network is shown in C. Ice flow direction in B and C is from the top of the page. Not to scale.

On a larger scale than meltwater channels, tunnel valleys (or channels) are large, overdeepened, elongate depressions in bedrock or till (Ó Cofaigh, 1996). They are common in glaciated areas and can reflect coherent patterns of anastomosing and anabranching networks (Beaney, 2002). Tunnel valleys can reach several hundred km in length and several km in width (Ó Cofaigh, 1996). Tunnel valleys often contain eskers (Brennand *et al.*, 2007), indicating that their origin is related to subglacial meltwater flow. The mechanism(s) by which they are formed are, however, debated (Ó Cofaigh, 1996; Kehew *et al.*, 2012). Suggested mechanisms for tunnel valley

formation are: erosion by pressurised subglacial meltwater in N-channels (Clayton *et al.*, 1999); catastrophic meltwater flows (e.g. Brennand & Shaw, 1994); and the progressive removal of deforming sediment by a subglacial conduit (Boulton & Hindmarsh, 1987).

Glaciofluvial corridors (GFCs; St-Onge, 1984) are wide, elongate tracts of water scoured terrain containing discrete glaciofluvial landforms. They are common in more northerly parts of the Canadian shield, such as Keewatin (Aylsworth & Shilts, 1989; Utting *et al.*, 2009) and have also been observed elsewhere (e.g. Iceland: Evans, 2011). Eskers are frequently superimposed on GFCs (Hebrand & Åmark, 1989; Brennand, 1994) and are therefore likely to be closely linked to their formation. GFCs in the District of Mackenzie are regularly spaced every 12-15 km and occur in a quasi-dendritic pattern (St-Onge, 1984). Relatively little attention has been paid to these features in the literature, but their origin is suggested to be related to deposition in high-discharge subglacial streams (St-Onge, 1984; Rampton, 2000; Utting *et al.*, 2009). Utting *et al.* (2009) used Ground Penetrating Radar (GPR) to observe sedimentary structures in a GFC hummock and speculated that the sediments reflect either sliding bed facies (cf. Saunderson, 1977; Ringrose, 1982) or hyperconcentrated flow (cf. Brennand, 1994) deposits. Others (e.g. Shilts, 1984) have suggested that GFCs are the remnants of outwash deposited on thin ice. The apparent correlation between GFCs and eskers suggests that similar meltwater processes may be responsible for their creation and detailed analysis of this relationship could yield important insights, both into the genesis of GFCs and into ice-sheet meltwater drainage processes.

Eskers form predominantly by sedimentation in R-channels, though different types of esker can also form in proglacial and supraglacial positions as well as in re-entrants. The different forms of eskers are discussed in more detail in the next section.

2.3 Eskers: types and classifications

2.3.1 Types of esker

Eskers may be broadly defined as straight-to-sinuous, elongate ridges composed of glaciofluvial sand and gravel (e.g. Banerjee & McDonald, 1975; Warren & Ashley, 1994; Brennand, 2000). Eskers form by deposition of sediment in subglacial streams (though some eskers also form in englacial or supraglacial positions) and become exposed when the surrounding ice melts away. Despite this simple description of eskers, there are many different forms and the main types are now described below.

Bird (1967) described *Embankment eskers* (also termed '*long, dendritic eskers'* by Brennand, 2000) which are the most common type of esker, abundant across large portions of palaeo-ice sheet beds. These eskers are characterised by their great length and the dendritic systems in which they typically occur. Ridges tend to be sharp crested and do not typically anastomose or

contain multiple crests. Embankment eskers are suggested to form in R-channels which terminate either subaqueously or subaerially (Brennand, 2000).

Beaded eskers are esker ridges containing a series of intermittent large beads (Figure 2.5A; B), which may occur throughout the length of the esker. They have been studied in detail (e.g. Banerjee & McDonald, 1975; Thomas, 1984; Hebrand & Åmark, 1989; Gorrell & Shaw, 1991; Brennand, 1994; Warren & Ashley, 1994; Mäkinen, 2003; Hooke & Fastook, 2007) and are generally thought to have been formed by sedimentation in stages as the ice margin retreats. Beads are produced where the ice margin is temporarily stable and sediment is deposited subaqueously. Alternatively, beads may form in R-channels where the cross-section temporarily widens, permitting sedimentation because of the resultant decrease in flow energy (McCabe, 2008). Subsets of beaded eskers are described by Warren & Ashley (1994) who distinguish between long beads formed in subglacial tunnels and short beads formed as subaqueous fans. Hooke & Fastook (2007) suggested that beads may be 'tadpole' shape in planform, reflecting increased sedimentation in the down-ice direction.

Subglacially engorged eskers or '*valley eskers'* (Mannerfelt, 1945; Figure 2.5D) are typically smaller and shorter-lived than beaded eskers. As the name suggests, they are formed subglacially where water flows back into a valley glacier after flowing between the ice margin and the valley wall. They are suggested to form under thin, stagnating ice (Syverson *et al.*, 1994) and are commonly seen emerging from glaciers. This makes them a useful indicator of how eskers evolve during ice margin retreat (e.g. Price, 1965), but they are small and transitory features which typically disappear quickly after formation (Price, 1973) and may operate almost entirely independently of larger scale subglacial drainage networks.

Concertina or '*zig-zag*' eskers portray a planform as indicated by the name and are often associated with deposition during glacier surges. A surge at Brúarjökull in Iceland in 1964 is thought to have produced the esker shown in Figure 2.5F, either by modification of a pre-existing esker (Knudsen, 1995) or, perhaps more likely, by deposition of the entire esker in a large crevasse network associated with the surge (Evans & Rea, 2003). *Crevasse-squeeze ridges* (or crevasse fillings) are closely related to concertina/zig-zag eskers and are formed by similar mechanisms, where pressurised sediment is squeezed into crevasses. Crevasse squeeze ridges are also often associated with enhanced crevassing and abundant meltwater during glacier surges (Sharp, 1985; Rea & Evans, 2011).

Esker fans are systems where discrete esker ridges appear to merge into a fan-shaped complex of anabranching esker ridges (e.g. Spooner & Dalrymple, 1993; Margold *et al.*, 2013a). Often esker fans are the product of a system in which outwash fans evolve (as ice melts) into esker ridges. The mechanisms controlling this process are discussed further in Chapter 7.

In addition to the main types of eskers summarised above, a large number of names have been suggested in the literature and are given here in Table 2.2.

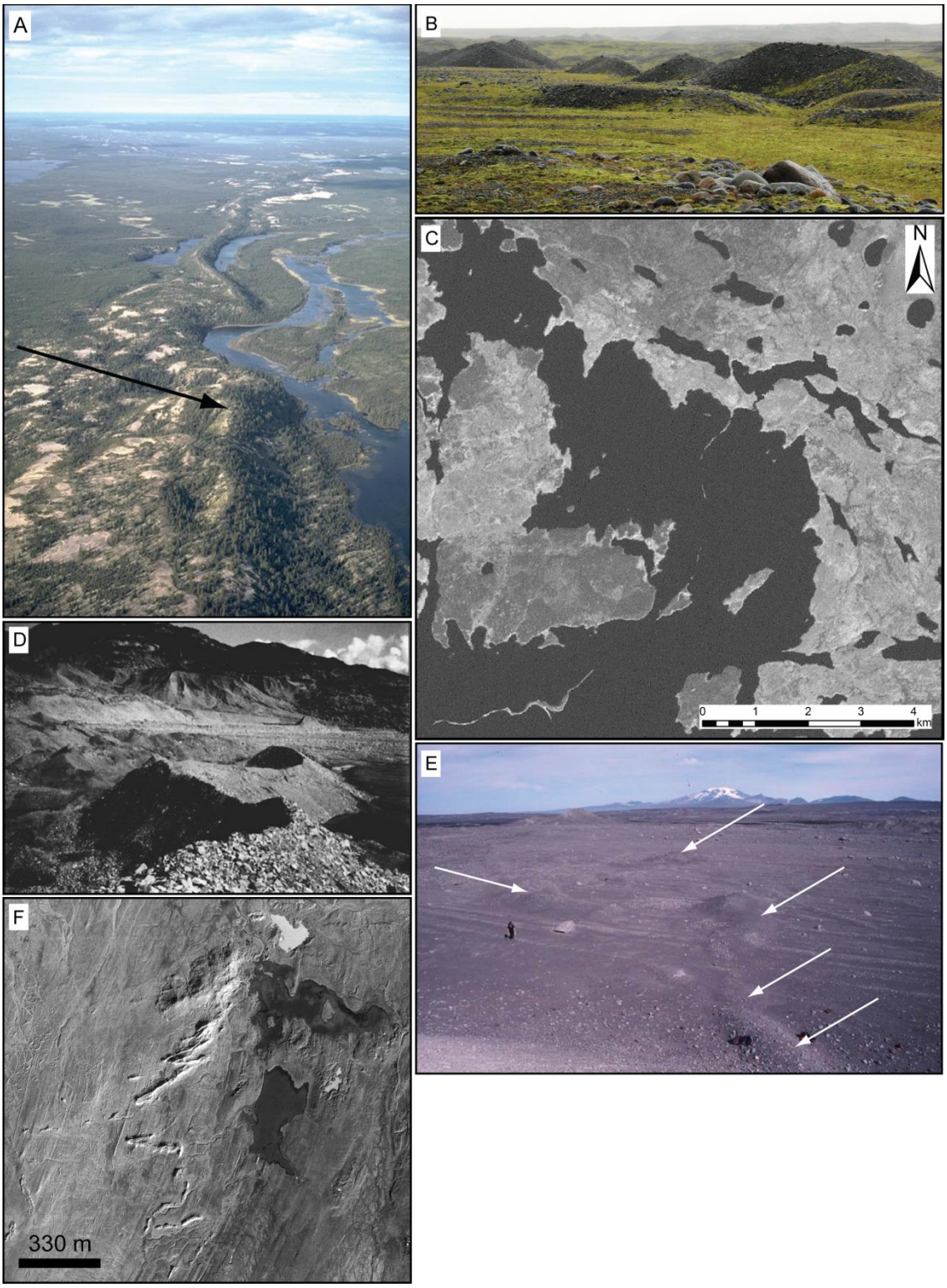

Figure 2.5. Examples of eskers: a) Oblique aerial photograph of a beaded esker in Manitoba, Canada (a bead is indicated by the arrow). Geological Survey of Canada (Photo 2001-083) by Lynda Dredge; b) Ground photograph of a Beaded esker at Breiðamerkurjökull, Iceland; c) Landsat ETM+ band 8 image of an 'esker-in-the-lake' in Manitoba, Canada; d) Ground photograph of a subglacially engorged esker at the Burroughs Glacier, Alaska, USA. From Syverson *et al.* (1994); e) Crevasse squeeze ridges (demarcated by white arrows) at Brúarjökull, Iceland. From Rea & Evans (2011); f) Aerial photograph extract of a Zig-zag (concertina) esker at Brúarjökull, Iceland.

Table 2.2. Nomenclature associated with eskers and esker systems from a review of the literature. Note overlapping and similar categories and that various terms may be applied to the same esker.

Name	Description	Reference(s)
Beaded eskers	Ridges punctuated by fans. Formed subaqueously at a retreating ice margin.	Bannerjee & McDonald (1975) Figure 2.5A;B
Bottom eskers	Eskers formed in ice tunnels on the valley floor, under dead ice. Similar to valley eskers	Embleton & King (1975)
Concertina eskers	Eskers displaying a zig-zag appearance in plan view. Formed by surging glaciers and related to compression of englacial tunnel fills.	Knudsen (1995)
Crevasse fillings **Crevasse-fill ridges** **Crevasse-Squeeze Ridges**	Ridges deposited subaerially in crevasses.	Menzies & Shilts (1996) Sharp (1985) Rea & Evans (2011) Figure Figure 2.5E
De Geer eskers	Consisting of a series of hillocks and deposited subaqueously at a retreating margin. Similar to beaded eskers.	Embleton & King (1975)
Embankment eskers	Similar to long, dendritic eskers	Bird (1967)
Esker chains	Suites of long eskers.	Menzies & Shilts (1996)
Esker enlargements	Sections of eskers much larger and wider than the main ridge. Similar to esker beads.	Lindström (1993)
Esker fans	Complex system of esker ridges making up a fan system.	Spooner & Dalrymple (1993)
Esker-in-the-lake	Eskers located in depressions, commonly in the form of lakes.	Lindström (1993) Figure 2.5C

Esker nets	Anastomosing eskers where individual ridges bifurcate and re-join parent ridges.	Hooke (2005) Stone (1899)
Esker ribs	Low eskers superimposed on a main esker ridge, descending in the direction of flow.	Lindström (1993)
Esker trains	Series of short eskers, kames and other glaciofluvial deposits.	Lundqvist (1997)
Fluvial-ice-channel-fill eskers	Continuous ridge formed in an H-channel or supraglacial stream.	Warren & Ashley (1994)
Long, dendritic eskers	Formed synchronously in large networks.	Brennand (2000)
Short, deranged eskers	Formed in subaerially terminating H-channels.	Brennand (2000)
Short, sub-parallel eskers	Formed in short, subaqueously terminating R-channels.	Brennand (2000)
Slope eskers	Infillings of subglacial chutes on valley sides (akin to valley eskers).	Embleton & King (1975)
Squeeze-up eskers	Ridges formed by subglacial sediment that is squeezed up into a low pressure conduit.	Menzies & Shilts (1996)
Subaqueous eskers	Similar to beaded eskers.	Menzies & Shilts (1996)
Subaqueous-fan eskers	Similar morphologically to beaded eskers. Consisting of short beads that are formed subaqueously.	(Warren & Ashley, 1994)
Subglacially engorged eskers	Ridges deposited in subglacial channels cut by water draining back into a glacier margin.	Mannerfelt (1945)
Subglacial-tunnel-fill eskers	Similar morphologically to beaded eskers. Formed in subglacial tunnels and forming large beads.	Warren & Ashley (1994)
Supraglacial eskers	Eskers formed on cold ice sheets ice in the ice marginal area. Relatively rare and not usually preserved because they are unlikely to survive deglaciation.	Fitzsimons (1991)
Till eskers	Sinuous till ridges associated with flutings and created by the squeezing of till into R-	Christofferson et al. (2005)

	channels	Evans et al. (2010)
Valley eskers	Same as subglacially engorged eskers, forming in accordance with topography.	Bird (1967)
Zig-zag eskers	Term to describe concertina eskers without the genetic inference but also interpreted as crevasse fills, not compressed englacial tunnel fills.	Evans *et al.* (2007) Figure 2.5F

2.3.2 Classification of eskers

In light of the widely varying types of eskers given in Table 2.2 and discussed above, several authors have attempted to classify eskers based on morphology, sedimentology and/or implied mode or formation. Banerjee & McDonald (1975) classified eskers according to their morphological variations (Table 2.3), noting differences between ridge morphology (single, broad, multiple crested or beaded), as well as by the association of other sediments, leading to a genetic interpretation of each esker type. This classification provided a useful distinction between different esker morphologies but does not capture the variety of processes responsible for the deposition of eskers. For example, it would not be possible to differentiate between single-ridge eskers deposited in pressurized subglacial conduits and single-ridge eskers deposited englacially.

Table 2.3. Bannerjee & McDonald's (1975) classification of eskers.

Basic morphology	Characteristics of esker complex	Deglaciation environment
Continuous single ridge; flanking outwash	Central esker ridge is highest element of complex; flanked progressively outward on each side by elongate marginal kettles, outwash terraces, and scalloped till plain; abrupt topographic discontinuities.	No standing water at glacier terminus.
Continuous single ridge; no flanking outwash	Ridge subdued by subsequent wave action commonly resulting in beach development on esker ridge; flanked by till.	Deposited within glacier but below level of standing water body at glacier terminus.
Broad ridge with multiple crests	May or may not be flanked by outwash; commonly multiple ridges form reticulate pattern.	Where broader than 200 to 300 m. Probably in part subaerial and some may be part of interlobate moraine complex; narrower varieties flanked by outwash indicate no standing water at glacier terminus.
Beaded	Pronounced isolated beads are regularly spaced and flanked by till.	Deposited where esker stream entered standing water at glacier terminus.

Warren & Ashley (1994) also favoured a genetic classification, modifying the Banerjee & McDonald (1975) classification to differentiate between continuous and segmented ridges and whether deposition took place sub- or supra-glacially (Table 2.4). This classification is more useful in differentiating between eskers formed in subglacial or supraglacial/englacial tunnels and provides a distinction between beaded and continuous eskers. Again, not all types of esker shown in Table 2.2 would fit into the classification. For example, eskers formed by squeezing of till into R-channels (Christoffersen *et al.*, 2005; Evans *et al.*, 2010) would be classified the same as 'embankment eskers', which may form by a different process.

Table 2.4. Warren & Ashley's (1994) classification of eskers.

Esker type	Description
Continuous ridge - Subglacial tunnel fill	Continuous ridge formed in a subglacial conduit.
Continuous ridge - Fluvial ice-channel fill	Continuous ridge formed in a supraglacial channel in stagnating ice.
Segmented ridge - Subglacial tunnel fill (long beads)	Segmented ridge formed in subglacial conduits in a retreating margin.
Segmented ridge - Subaqueous fans (short beads)	Short segmented ridges formed in supraglacial channels in retreating ice.

A morphological classification was adopted by Brennand (2000), who proposed three different types of eskers (Table 2.5) which may form in different conditions. The morphological classes provide a useful way to distinguish different eskers, though the genetic inference made for each class is broad, stipulating only whether eskers were formed in R-channels or re-entrants and whether deposition took place in standing water, subaerially or subaqueously. Once again, not all esker types would fit into this classification.

Table 2.5. Brennand's (2000) classification of eskers.

Esker type	Description
Long dendritic eskers	Formed either in standing water or subaerially terminating R-channels.
Short, subparallel eskers	Formed in R-channels or re-entrants that terminated subaqueously or subaerially.
Short, deranged eskers	Formed in R-channels that terminated in standing water.

Esker classifications to date have relied upon various morphological and sedimentological observations of a small sample of eskers. This means that while several important differences have been observed and categorised, there are always exceptions because of the range of different esker types and methods of deposition described in the literature. For these reasons, a unifying classification scheme for eskers has remained a potentially useful, yet elusive resource. In order to resolve this, and to see whether different processes are responsible for the formation of different eskers, some have looked at the sedimentology of eskers, which is discussed in the next section.

2.4 Esker sedimentology

Eskers are complex depositional landforms and, as such, their sedimentology is fundamental to understanding their genesis. It is no surprise therefore that a huge literature exists on esker sedimentology, addressing a wide range of questions surrounding the processes responsible for esker sedimentation. A comprehensive review of esker sedimentology is beyond the scope of this thesis. Nevertheless, some key insights into esker genesis have been attained through sedimentological investigations and this section therefore aims to provide a brief synopsis of this field of research.

2.4.1 Esker composition

Eskers are generally described as being composed of glaciofluvial sand and gravel (e.g. Warren & Ashley, 1994). Bolduc (1992) examined the detailed lithological composition of eskers in Labrador, Canada, and found that esker lithology closely resembled local till lithology, indicating that esker materials are locally derived. More specifically, material at the base of eskers was found to most closely resemble the local till, whereas material higher up in esker stratigraphic exposures lithologically resembled tills several km up-esker. Esker 'dispersal trains' (long, narrow belts of glacial debris which can be traced back to source) tend to be similar in length to surrounding till dispersal trains, but shifted downstream (Cummings *et al.*, 2011b), further indicating that material carried by eskers is locally derived. Esker dispersal trains are not necessarily related to esker length (Cummings *et al.*, 2011b), suggesting that esker forming streams are not particularly efficient at removing material.

Finer material such as clay and silt is not usually found in eskers because still water is rare in esker-forming channels, unless tunnels become flooded due to ice marginal flotation at lake or marine termini (e.g. Gorrell & Shaw, 1991). Larger material up to boulder size is sometimes observed in eskers (e.g. Brennand, 1994; Warren & Ashley, 1994), although very large boulders are less common because they are only likely to be transported by low frequency catastrophic

discharges, such as those that formed the ice-walled channel fill esker at Skeiðarárjökull in Iceland in 1996 (Russell *et al.*, 2001).

Clasts in esker sediments are often rounded to well rounded, reflecting the glaciofluvial nature of their deposition (e.g. King & Buckley, 1968). Indeed, Mills (1977) noted that outwash could be distinguished from subglacial diamictons on the basis of high values of roundness. King & Buckley (1968) were able to use high roundness values as a diagnostic criterion for eskers on Baffin Island, Canada. Clast shape data from various High-Arctic glacial sediments in Svalbard were analysed by Bennett *et al.* (1997) who, conversely, found that glaciofluvial facies were difficult to distinguish from basal diamictons, though they may be slightly more rounded (Figure 2.6). 'Egg' gravels, which are sometimes observed in eskers (e.g. Huddart *et al.*, 1999), however, were unique in having very high roundness and sphericity values in comparison with all other facies (Figure 2.6).

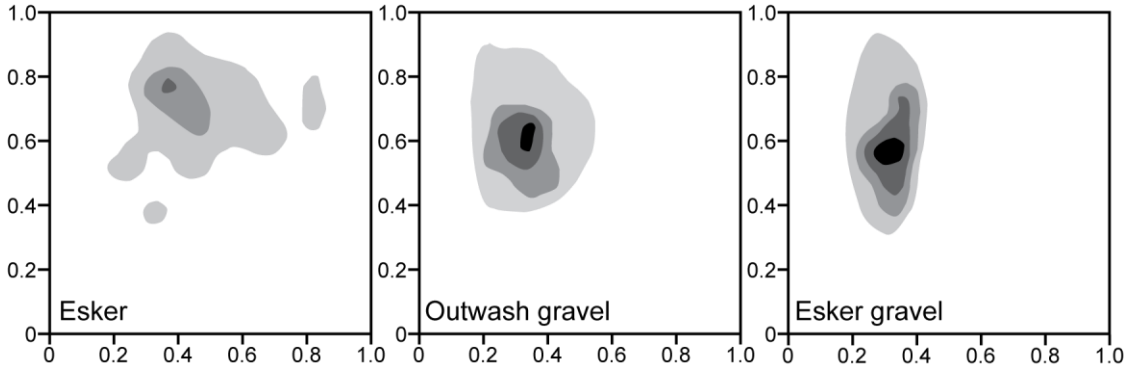

Figure 2.6. Clast roundness (x-axis) plotted against Krumbein's sphericity (y-axis) for three different facies sampled from Midre Lovénbreen and Pedersbreen, Svalbard. Each sample contains 50 clasts and point densities are contoured at 1, 3, 5 and 7% per 1% area. After Bennett *et al.* (1997).

2.4.2 Sedimentary structures and facies in eskers

Eskers exhibit a wide range of sedimentary structures, reflecting the various dynamic conditions under which they are formed. This is often seen in individual eskers which commonly contain different structures indicative of changes in flow regime (e.g. Banerjee & McDonald, 1975; Huddart *et al.*, 1999). In broad terms, eskers contain all the sedimentary structures found in normal fluvial deposits (Price, 1973). Menzies & Shilts (1996) argue that, as a result of the large variability in source debris as well as the complex processes responsible for esker formation, eskers may not be identified by sedimentology alone.

Typically found in eskers are 'sliding bed' facies (Saunderson, 1977), which consist of massive, matrix supported deposits of sand and gravel (e.g. Figure 2.7) and are interpreted to represent flow in full pipe (R-channel) conditions, where all of the sediment moved *en masse.* Sliding bed

facies, however, may not necessarily be diagnostic of full pipe flow, as it has been demonstrated by Todd (1989) that similar facies can form subaerially as 'traction carpets', which are highly concentrated deposits formed by turbulent flows (Sohn, 1997).

Figure 2.7. An example of a 'sliding bed' facies in the Guelph esker, Ontario, Canada, composed of poorly sorted sand and gravel. Trowel is 42 cm long. From Saunderson (1977).

Palaeocurrent indicators are common in eskers. Clasts within esker sediments often tend to be oriented with the *a*-axis horizontal and transverse to flow and with *b*-axes plunging upstream, commonly resulting in imbrication (Gorrell & Shaw, 1991). Delaney (2001) suggested that imbricate pebble and cobble facies in the Rooskagh esker, Ireland, indicate high dispersive pressure when the sediment was deposited. Alternatively, clast *ab*-planes may be aligned parallel to the esker ridge, indicating the direction of the flow in which the clasts were deposited. Cross-beds and cross-laminations may also be used to deduce palaeocurrent direction, though the results tend to be more variable because of the more subtle processes responsible for their deposition (e.g. Brennand, 1994).

Whilst many eskers display a range of sedimentary structures, others often appear to be structureless or display heavily distorted structures. These may be interpreted as englacially or supraglacially produced features, whereby any primary depositional structure is lost or deformed as the underlying ice wastes and the esker is deposited (Price, 1973; Huddart *et al.*, 1999; Benn & Evans, 2010). Subglacially engorged and ice-cored eskers have been related to this process (Syverson *et al.*, 1994; Boulton *et al.*, 1999; Huddart *et al.*, 1999; Evans *et al.*,

2007; Schomacker & Kjær, 2008) but questions remain about the precise mechanisms by which many such eskers are formed.

In beaded eskers, striking decreases in grain size are often observed in individual beads (e.g. Banerjee & McDonald, 1975; Gorrell & Shaw, 1991) and may be interpreted to indicate rapid deceleration of flow as the stream entered either a body of standing water, or an aggrading fan (Gorrell & Shaw, 1991). Figure 2.8 shows an example of pronounced downstream fining observed in an esker bead in Ontario, Canada.

As an example of the variety of facies found in eskers, Figure **2.9** illustrates the major facies observed in four long, dendritic eskers in Ontario, Canada, which were examined in detail by Brennand (1994). In addition to rhythmically alternating sand and gravel units, the principal facies present in the eskers were: heterogeneous, unstratified gravel (Figure 2.9A;B); massive, imbricate, clast-supported gravel (Figure 2.9c); imbricate, polymodal matrix rich gravel (Figure 2.9D); horizontally bedded gravel (Figure 2.9E); and cross-bedded gravel (Figure 2.9F;G) (Brennand, 1994). Three 'macroforms' were also identified: composite macroforms, consisting of a number of different sand and gravel facies; pseudoanticlinal macroforms, consisting of arched bedding on roughly the same scale as the eskers; and oblique accretion avalanche bed macroforms, where steep avalanche beds consisting of pebbles predominate (Brennand, 1994). This example highlights the variety and complexity of esker sediments, as well as the detail that may be gleaned from their close examination.

2.4.3 Sedimentological insights into esker processes

In light of the wide variety of sediments recorded in different eskers, the majority of sedimentological investigations have concentrated on what insights can be gleaned from individual eskers from their constituents. These techniques have addressed some key questions, although contrasting answers are provided by different authors based on their chosen eskers. It is important, therefore, that sedimentological investigation of eskers continues until the sample size is large enough for clear trends to emerge. Thus, some aspects of esker sedimentology are rigorously constrained whereas others are based on few examples and await further testing. This section reviews some of the key sedimentological questions which have been addressed to some extent by different authors: (2.4.3.1) Was deposition synchronous or time-transgressive?; (2.4.3.2) Was deposition subglacial, englacial or supraglacial?; (2.4.3.3) Was deposition in a pressurised or open channel?; and (2.4.4.4) Was the discharge high, low or variable?

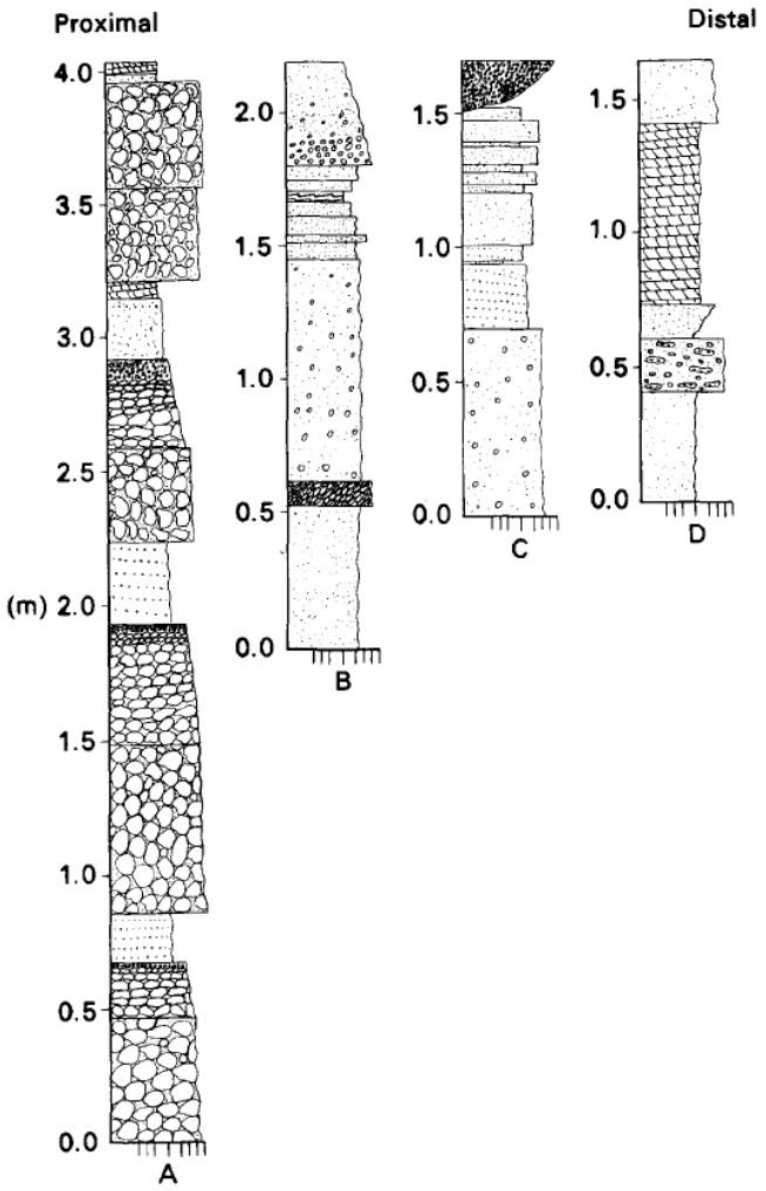

Figure 2.8. Sediment logs from four exposed sections of an esker bead 120-150 m wide in Ontario, Canada (from Gorrell & Shaw, 1991). Note the pronounced downstream fining and rapid changes in facies from predominantly massive, clast supported gravels at the proximal end, to mainly bedded sands at the distal side of the bead.

2.4.3.1 Was deposition synchronous or time-transgressive?

Large-scale facies analysis of eskers may indicate whether they were formed in a continuous conduit or in a series of segments. Eskers consisting of a series of beads or morphosequences have been interpreted to have been deposited time-transgressively (e.g. Hebrand & Åmark, 1989) because each segment would relate to a depositional episode. Eskers consisting of large, single, continuous facies are more likely to be interpreted as being deposited synchronously because it is unlikely that several separate depositional episodes would contribute to one continuous unit (Brennand, 1994). The juxtaposition of esker beads may form a continuous ridge in some instances, but beaded eskers can usually be differentiated from continuous eskers

because the ridges of non-beaded eskers tend to display more regular sedimentation, with individual units persisting for 10s of m (Gorrell & Shaw, 1991).

Other lines of sedimentological evidence indicative of synchronous deposition are strong palaeocurrent indicators and the absence of fine-grained sediments in the sequence (Brennand, 1994). This suggests that discharge was high and that the sediment was deposited in one flow, consistent with deposition across an entire conduit. Brennand (2000) proposed that synchronous sedimentation throughout a large R-channel would be manifested by coarse ridges with terminal or superimposed fans containing fines, low palaeoflow variability (except in the fans) and a regional, as opposed to segmental, trend in clast lithology and roundness. Conversely, time-transgressive deposition would be invoked if sediments displaying segmental trends in sediment texture, structure and clast roundness were observed, as well as more variable palaeoflow indicators.

Whilst the majority of studies infer time-transgressive deposition (e.g. Banerjee & McDonald, 1975; Gorrell & Shaw, 1991; Boulton *et al.*, 2009), synchronous deposition has also been invoked in some places (Brennand, 1994; Brennand & Shaw, 1996) and some authors indicate that different eskers may be formed either synchronously or time-transgressively (Brennand, 2000) depending on glaciological conditions. There remains no definitive answer as to whether one form of deposition predominates in nature.

2.4.3.2 Was deposition subglacial, englacial or supraglacial?

Evidence for whether esker sedimentation occurred subglacially, englacially or supraglacially has been presented by several authors. Banerjee & McDonald (1975) suggested three sedimentological criteria which could be used to suggest where an esker was formed. Firstly, they suggest that an absence of till beneath an esker implies that deposition occurred subglacially. This assumes, however, that the esker was not deposited on bedrock, which in many places is incorrect (see Clark & Walder, 1994). Secondly, where till overlies esker sediments, englacial or subglacial deposition may be invoked because ice must have been present above the esker to deposit the till. Finally, esker sediments containing evidence of deformation may suggest that the esker has been lowered after initial deposition, indicating that it has a supraglacial or englacial origin. Normal and reverse faults in esker sediments and anticlinal bedding (with the axis of the anticline parallel to the ridge of the esker) are suggested to relate to the collapse of supporting ice walls (e.g. McDonald & Shilts, 1975; Cheel, 1982; Brennand, 1994). Banerjee & McDonald (1975) also noted the intrusion of vertically laminated diapirs in two eskers in Quebec, Canada, and suggested that this indicated that the glacier had overridden varved lake sediments. This was taken as evidence that the esker forming stream had flowed directly over these sediments and thus provided further support for a subglacial origin.

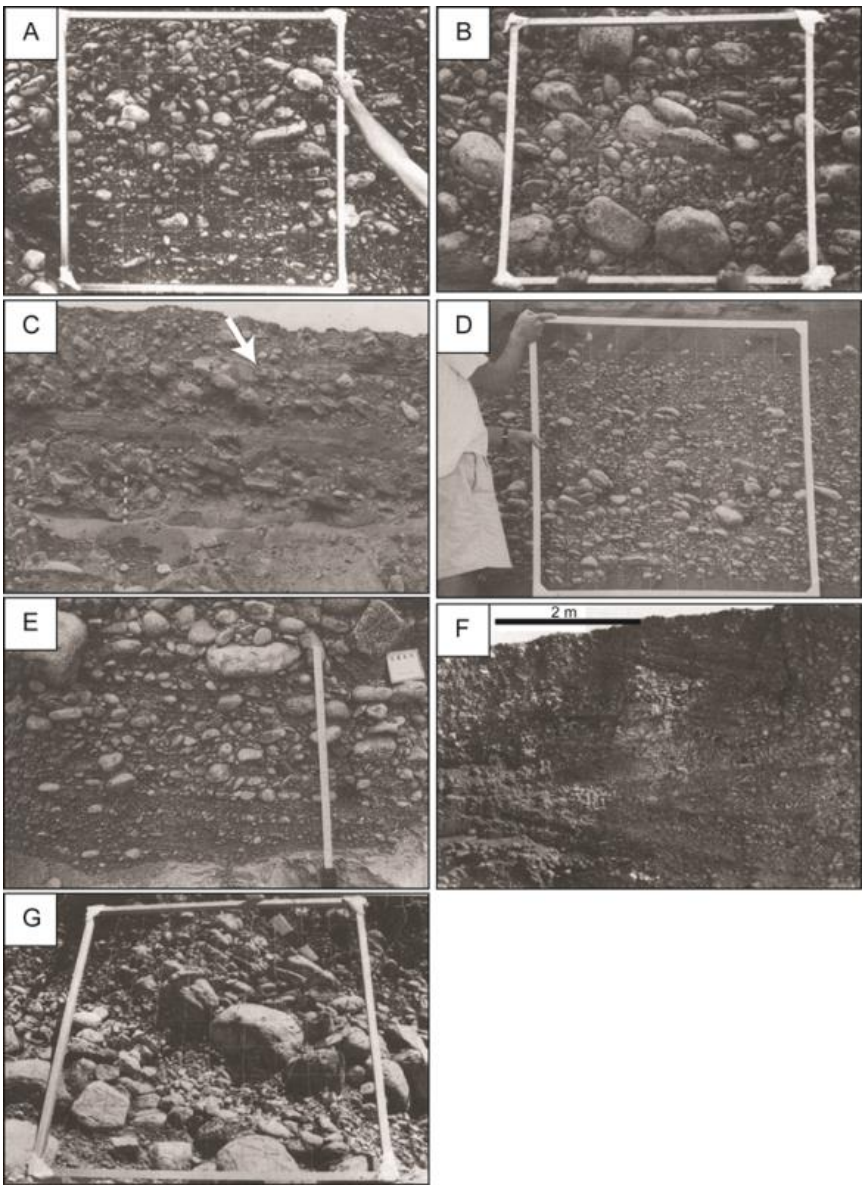

Figure 2.9. Examples of sediments in eskers in Ontario, Canada (after Brennand, 1994). (a) Poorly delineated lenses of bimodal clast-supported, polymodal and openwork gravel, Campellford esker. (b) Vaguely delineated lenticular structure and cluster imbrications of larger clasts, Norwood esker. (c) Massive, imbricate, clast-supported gravel alternating with sand, Tweed esker. (d) Imbricate, polymodal matrix-rich gravel within an in-phase wave structure, Norwood esker. (e) Horizontally bedded gravel, Campbellford esker. (f) Trough cross-bedded gravel in the Campbellford esker. (g) Rhythmically graded foresets of tabular cross-bedded gravel in the Tweed esker.

Some recently formed eskers contain ice-cores, which indicate englacial or supraglacial deposition and subsequent lowering as the ice-core melts out (e.g. Petrie & Price, 1966; Price, 1969). The occurrence of some of these examples emerging from downwasting ice-cored outwash on the Breiðamerkurjökull foreland, where Boulton *et al.* (2007a;b) made a convincing argument for a groundwater-coupled subglacial system, raises some important questions about drainage tunnel evolution, with convincing evidence for subglacial and englacial esker formation. Clearly, the Breiðamerkurjökull eskers have evolved as complex networks

characterized by subglacial, englacial and supraglacial deposition. Chapter 7 presents the results of new mapping of these eskers and addresses this problem in more detail.

Zig-zag eskers on recently deglaciated forelands contain significant ice cores (Evans & Rea, 1999; 2003), consistent with their deposition in crevasse networks during surging (Rea & Evans, 2011). Gorrell & Shaw (1991) suggested that deformation structures observed in eskers in Ontario, Canada may relate to sediment lowering following the melting of an ice-core. In contrast, the presence of normal faults and large-scale folds in some esker beads in the same landform complex was interpreted by Gorrell & Shaw (1991) to imply that the beads were formed subglacially. Specifically, the faults were produced when the ice tunnel walls collapsed and the large-scale folds were created by ice that settled on, and deformed, the bed.

The majority of the literature focuses on eskers which were deposited subglacially. For example, a rudimentary meta-analysis of the literature, using a *Web of Science* search (6th November 2013), produces 114 results for 'subglacial esker', 22 results for 'supraglacial esker' and 13 results for 'englacial esker'. This suggests either that subglacial deposition is the dominant process, or that for some reason workers have concentrated more on eskers formed in subglacial positions or have assumed subglacial deposition. Supraglacial or englacial deposition is most usually invoked for eskers emerging from valley-scale glaciers (e.g. Price, 1966; Howarth, 1971; Burke *et al.*, 2008; Benn *et al.*, 2009a), rather than the more numerous eskers associated with ice-sheets and so the former suggestion, that most eskers form subglacially, may be preferred.

2.4.3.3 Was deposition in a pressurised or open channel?

Backset antidunes in eskers were taken by Banerjee & McDonald (1975) to suggest that surface waves were present in the channel while the sediment was deposited, implying that deposition took place in a conduit where the water surface was in contact with air, thus ruling out the possibility of deposition in an R-channel. Others have argued that antidunes are able to form under a range of conditions (Brennand, 2000) and that they are not necessarily indicative of open channel sedimentation. Low palaeocurrent variability has also been taken to indicate pressurised flow (e.g. Shaw, 1972; Gorrell & Shaw, 1991) because the flow is more likely to be constant under pressurised conditions. As mentioned in Section 2.4.2, Saunderson (1977) suggested that sliding bed facies are diagnostic of sedimentation in R-channels, though this may not always be the case.

Many authors have supported the notion that eskers associated with palaeo-ice sheets most likely formed in pressurised R-channels (e.g. Clark & Walder, 1994; Brennand, 2000; Boulton *et al.*, 2009; Cummings *et al.*, 2011a). As noted in the previous section, smaller eskers associated with valley glaciers may be more likely to form in open channels because they often

emerge englacially or supraglacially (e.g. Howarth, 1971), though pressurised R-channels have also been invoked for some eskers deposited under valley glaciers (Boulton *et al.*, 2009).

2.4.3.4 Was the discharge high, low or variable?

The nature of the flow that results in esker sedimentation may be preserved in the sedimentary record. Contrasting flow regimes result in contrasting bedforms (Ashley, 1990) and thus some information can be gleaned from structures contained within eskers. An absence of fine-grained sediment is indicative of a high discharge depositional environment (Banerjee & McDonald, 1975), though some eskers thought to have formed in high discharge flows have been found to contain fine grained material, which is assumed to have been deposited during flow cessation or decrease in winter (Hebrand & Åmark, 1989; Gorrell & Shaw, 1991). Huge grain size variability occurs in esker networks created during high magnitude, low frequency events such as the Skeiðarárjökull jökulhlaup in Iceland in 1996 (Russell *et al.*, 2001; Burke *et al.*, 2008).

Variations in flow are often recorded in sedimentary sequences in eskers. Cyclic sequences of sand and gravel are frequently observed in eskers (Banerjee & McDonald, 1975; Ringrose, 1982; Benn & Evans, 2010) and relate to varying discharge and sediment availability. Fining upwards sequences indicate decreasing flow discharge, whereas coarsening upwards sequences represent increasing discharge. Estimates of how quickly discharge changes are represented in cyclic esker sediments vary from a number of hours (Allen, 1971) to a year (Banerjee & McDonald, 1975).

There is no clear answer to whether eskers typically represent high or low discharge regimes, though many eskers contain clasts on the order of metres in diameter, indicating very high discharge at some point during their formation (e.g. Fard, 2001). The literature contains many examples of eskers formed under complex and dynamic discharge regimes (e.g. Fard & Gruszka, 2007; Hooke & Fastook, 2007; Cummings *et al.*, 2011a) and the difficulty in answering this question may be, in part, due to a paucity of sedimentological descriptions (for the good reason that this is difficult, expensive and time-consuming) of very large eskers such as those of the Canadian Shield and Fennoscandia.

2.5 Esker geomorphology

It has been shown that eskers contain a diverse array of sediments and this complexity is echoed in the geomorphology of eskers. Throughout this section, three case studies of esker morphology in Canada, the UK and the Kola Peninsula, Russia, are used to illustrate various points. Shapefiles included in the publications of eskers mapped in Prest *et al.* (1968), Clark *et al.* (2004) and Hättestrand & Clark (2006), respectively, were used to derive esker length and sinuosity data. These sources were selected because they are published and data is freely

available. Furthermore, these areas portray different conditions in terms of former ice dynamics, geology and scale, and so are representative of the variety of conditions under which eskers may form. Note that these publications do not necessarily represent *all* the eskers in these locations: improved methods and data sources over time and simplification for cartographic purposes means that the eskers published are likely a sample of those present in nature. A large number of well-developed eskers exist in Fennoscandia (Figure 2.10) which would ideally have also been incorporated in this section. Unfortunately, however, the authors have not been able to locate any digitised data for these eskers, prohibiting calculation of their morphometric properties.

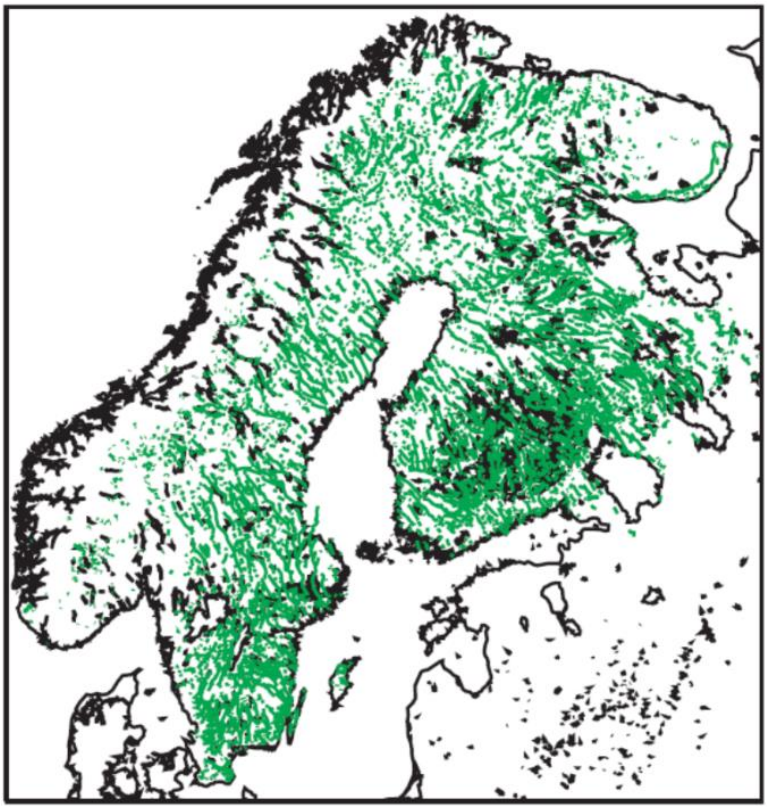

Figure 2.10. Distribution of eskers in Fennoscandia from Boulton (2006).

In addition to the eskers of Fennoscandia depicted in Figure 2.10, the distribution of eskers in Canada, the UK and the Kola Peninsula (Russia) are shown in Figure 2.11. By far the largest population of eskers is in Canada, on the bed of the Laurentide Ice Sheet (Figure 2.12). The UK and Kola Peninsula have far fewer eskers than Canada in total, though eskers are more densely distributed in these two areas overall (Figure 2.12). It must be noted, of course, that esker density varies spatially and it can be seen in Figure 2.11 that some parts of Canada portray very high esker density, whereas other do not.

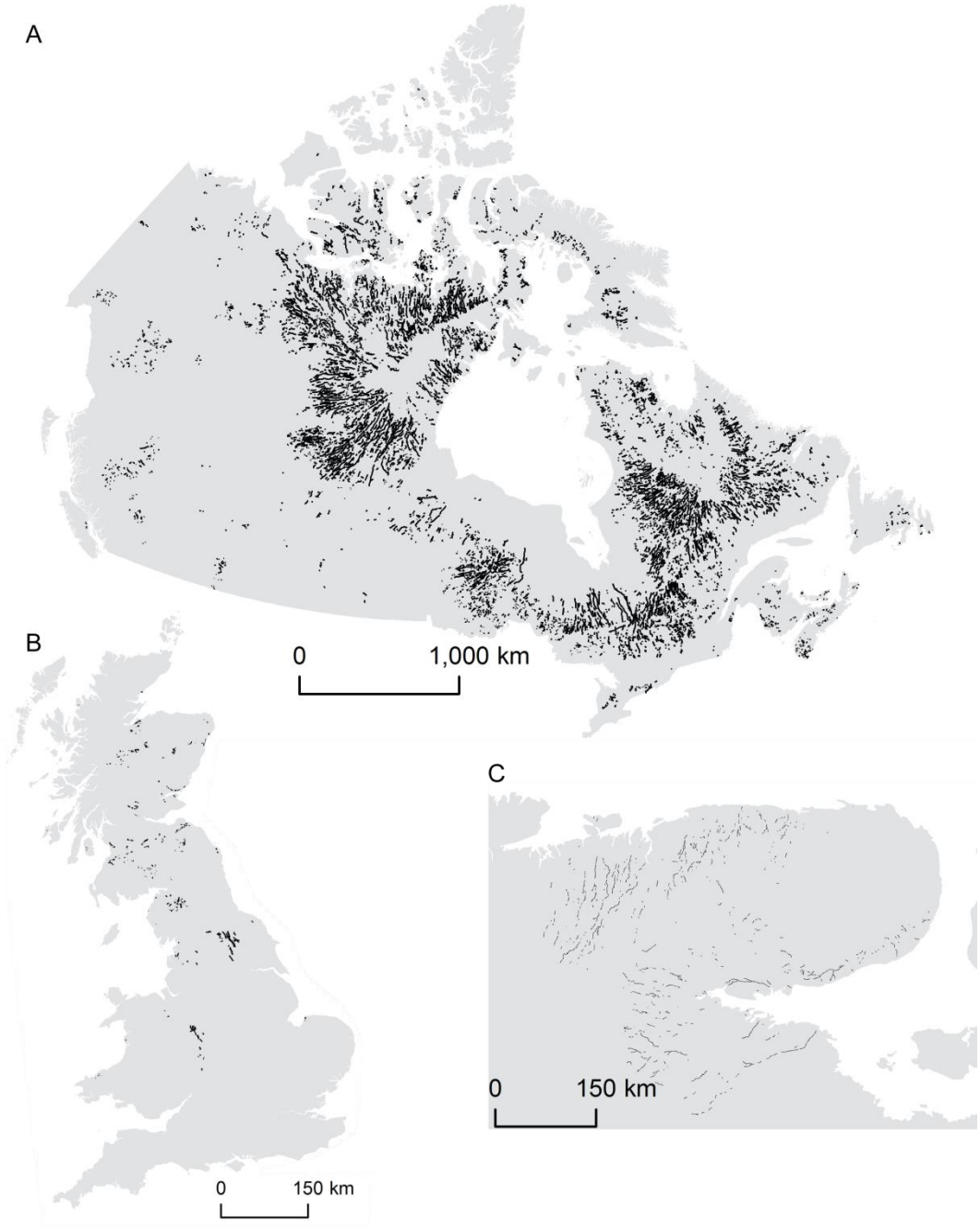

Figure 2.11. Distribution of eskers (A) in Canada (after Prest *et al.*, 1968), (B) in the UK (after Clark *et al.*, 2004) and (C) on the Kola Peninsula, Russia (after Hättestrand & Clark, 2006).

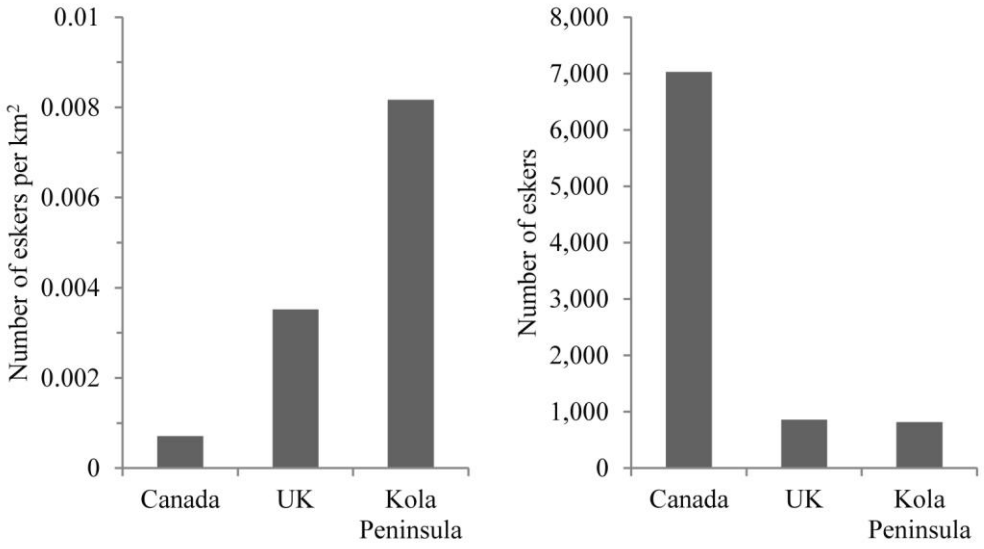

Figure 2.12. Total number and density of eskers mapped in Canada, the UK and the Kola Peninsula.

2.5.1 Morphometry and spatial patterns of eskers

2.5.1.1 Dimensions

Eskers cover a broad range of lengths, as displayed in Figure 2.13 and Figure 2.14A. Eskers typically tend to occur in fragments: distribution of esker length is strongly positively skewed (skewness is 4.29 for Canada, 5.10 for the UK and 1.07 for the Kola Peninsula). The longest contiguous esker in these datasets was mapped by Prest *et al.* (1968) and is 331 km long, though measurements of esker length vary from author to author depending on the mapping convention used. For example, some authors may simplify eskers with small gaps to one continuous feature, whereas others may be more meticulous and map several shorter eskers. Eskers may extend to over 800 km if gaps are ignored (Banerjee & McDonald, 1975) and systems of eskers consisting of fragmentary ridges are frequently observed to stretch for several hundreds of kilometres (Shilts *et al.*, 1987). Particularly long eskers exist around the Keewatin Ice Divide, Canada (Aylsworth & Shilts, 1989) and the longest eskers are in Canada, where there are 65 eskers greater than 100 km in length (Prest *et al.*, 1968).

Data on esker height have been compiled in Table 2.6 and reveal that, in general, eskers are typically between 5 and 50 m tall, with a large degree of variation. The ambiguity of esker height data may be due to the absence of a large-scale survey of esker height (this is more difficult to measure remotely than esker length, for example). Thus, the majority of esker height descriptions relate to specific examples or areas.

Measurements of esker width cover a larger range than measurements of esker height, with some eskers purportedly being up to 7 km wide (Banerjee & McDonald, 1975). Measurement of esker width depends on the subjective interpretation of the individual and, as such, varies

depending on what each author actually *defines* as an esker (see Section 2.3.1). Eskers occasionally merge into other landforms (see Section 2.5.3) and some authors may group several ridges as one esker. Thus, it is difficult to effectively set out the general characteristics of eskers when they are open to different interpretations. Nevertheless, Banerjee and McDonald (1975) suggested that esker ridges are usually less than 150 m wide, which seems reasonable from an analysis of the wider literature. Observations of the height and length of a small sample of eskers led Price (1973) to speculate that esker height and width may be a function of length. Price (1973) suggested that eskers up to 200 m long tend to be 3-10 m high and that eskers > 1 km long may be 10-100 m high, though no further research has tested this to date.

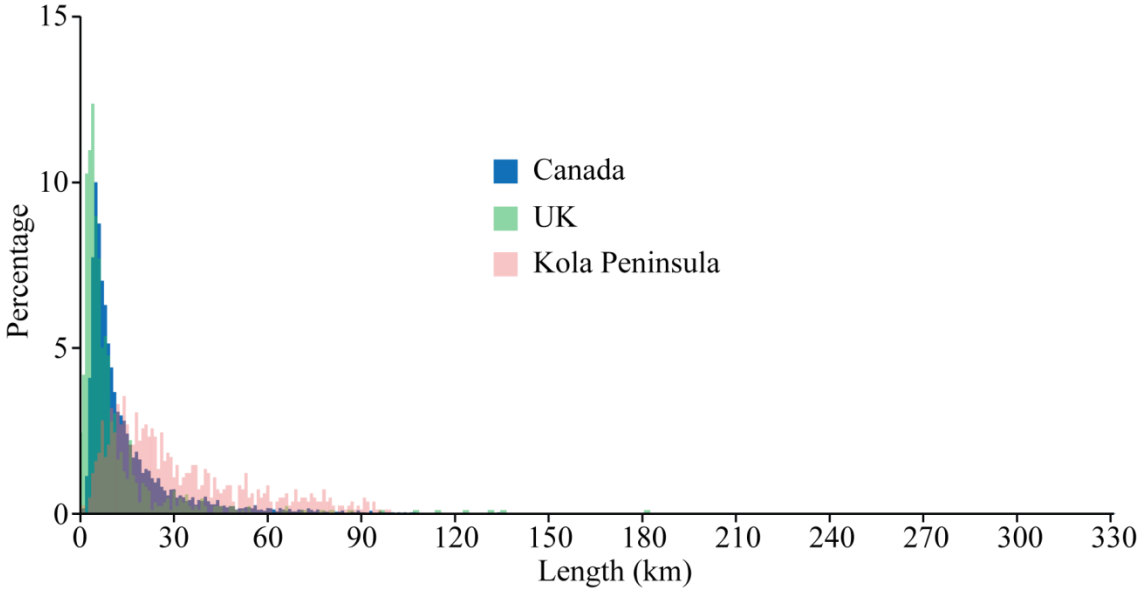

Figure 2.13. Esker length distribution plotted in 1 km bins for the UK, Kola Peninsula and Canada.

2.5.1.2 Fragmentation

Gaps are frequently observed in eskers (e.g. Goldthwait, 1939; Saunderson, 1977; Shreve, 1985a; Shilts *et al.*, 1987; Metzger, 1992; Figure 2.32). For example, Metzger (1992) calculated that esker ridges in New York State, USA, demonstrate between 28% and 100% continuity (i.e. gaps occupy 0-72% of esker lengths). No eskers greater than 18 km in length were more than 67% continuous (Metzger, 1992), indicating that fragmentation is a pervasive phenomenon. Shilts *et al.* (1987) noted that esker ridges in Canada can be traced for up to 600 km when gaps are taken into consideration, whereas unbroken esker ridges rarely exceed 75 km. If eskers are to be used to reconstruct ice-sheet drainage characteristics, the origin of gaps is an important factor to consider because this could have implications for the processes depositing eskers, as well as for whether separate ridges form part of a single, contiguous system.

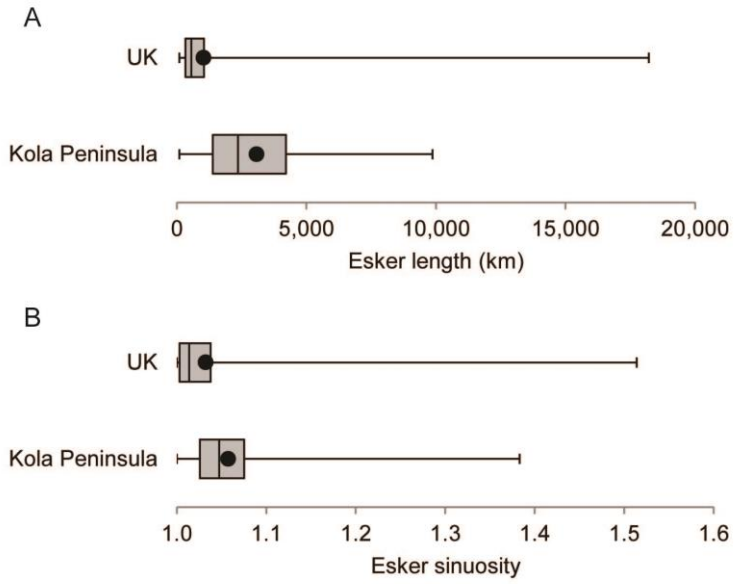

Figure 2.14. Box and whisker diagrams showing A) esker length data and B) esker sinuosity data for the UK (n = 857) and Kola Peninsula, Russia (n = 817). Whiskers denote the range of values, points denote means and the boxes span the range of the 25 – 75% percentiles, with the median as a vertical bar. Data were extracted from shapefiles published in Clark *et al.* (2004) and Hättestrand & Clark (2006).

Table 2.6. Examples of esker height from the literature.

Height	**Reference**
May be more than 200 m	Flint (1971)
Occasionally more than 30 m	Aylsworth and Shilts (1989)
Occasionally more than 50 m	Banerjee and Mcdonald (1975)
Up to 80 m	Donner (1965)
Can be more than 50 m	Benn & Evans (2010)
Can be more than 50 m	Menzies and Shilts (1996)
Frequently 30-35 m; occasionally up to 75 m	Bird (1967)

Several authors have suggested mechanisms which could lead to gaps in esker systems. Cessation of sediment supply was suggested by Aylsworth & Shilts (1989) as the most likely explanation for the paucity of eskers in the area between Great Bear and Great Slave Lakes, Canada. Aylsworth & Shilts (1989) argued that whilst the requisite esker-forming drainage conditions may have existed, a lack of sediment availability from the local substrate would mean that eskers would not be able to develop. Banerjee & McDonald (1975) suggested that

where esker sedimentation occurs in standing water, eskers are more likely to be preserved than where they are deposited in flowing water, because in the latter environment there is more energy available for subsequent erosion. The close association of gaps and sliding bed facies (see Section 2.4.2) in the Guelph esker, Ontario, Canada, was suggested by Saunderson (1977) to indicate that the gaps were formed at relatively low shear intensities, contemporaneous with deposition of the sliding bed facies. Hooke & Fastook (2007) suggest that eskers form in segments, which would naturally facilitate the punctuating of larger esker portions with smaller sections or gaps. Where gaps are small compared with ridge length, or post depositional erosion is clearly responsible for gaps (for example where a stream has dissected an esker), it is parsimonious to assume that the ridges form part of the same system (e.g. McCabe, 2008). Thus, counter-intuitively, understanding why esker systems contain gaps may be able to help us to understand what processes control the formation of the eskers themselves.

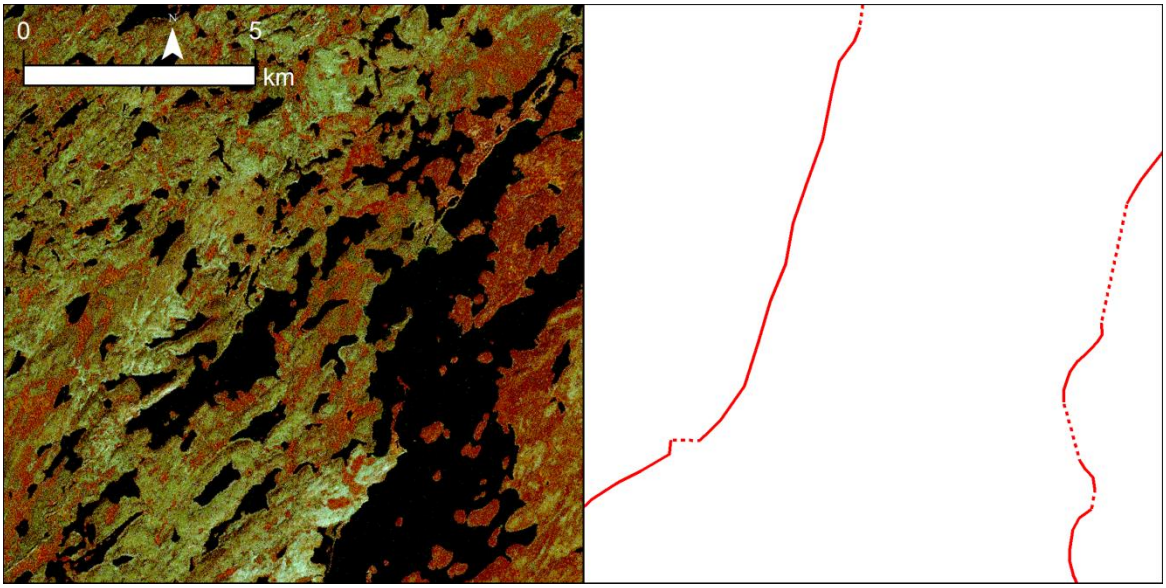

Figure 2.15. Landsat ETM+ image (left) and interpretation (right) of fragmented eskers (solid lines) in Northwest Territories, Canada. Note gaps between eskers and inferred channel route (dashed lines).

2.5.1.3 Sinuosity

'Sinuous' is a term frequently used in descriptions of eskers (e.g. Price, 1973; Sugden & John, 1976; Russell *et al.*, 2006; Benn & Evans, 2010). Sinuosity is expressed as the ratio between the length of the esker (l_e) and the length of a straight line between the beginning and end points of the esker (l_s):

$$S = \frac{l_e}{l_s} \tag{2.1}$$

Sinuosity is important because it is related to the discharge within the channel (cf. Makaske, 2001) and to the width-depth ratio and sediment load of the channel (cf. Schumm, 1963). Moreover, sinuosity is an important parameter for models and tracer experiments in subglacial channels (e.g. Schuler & Fischer, 2009). Eskers are often described as sinuous (e.g. Clark & Walder, 1994; Syverson *et al.*, 1994; Warren & Ashley, 1994), although there are few reports or quantification of esker sinuosity. Flint (1971) suggested that eskers are nearly as sinuous as subaerial streams and Warren & Ashley (1994) highlighted the potential for comparing esker morphology with river meander morphology. Bolduc (1992) measured the sinuosity of eskers in Labrador and found that sinuosity varied between 1.00 and 1.32. A recent study of the Chasm esker, British Columbia, Canada (Burke *et al.*, 2012), noted a sinuosity value of 1.07. Extraction of sinuosity values for the eskers mapped in the UK and Kola Peninsula by Clark *et al.* (2004) and Hättestrand & Clark (2006) indicate a mean esker sinuosity of 1.032 and 1.057, respectively (Figure 2.14B).

Figure 2.16 shows esker sinuosity, calculated from three published geomorphological maps and indicates that eskers are much less sinuous than previously thought. The values may reflect, to some extent, the mapping convention of each author. For example, sinuosity will equal one if a straight line is drawn to represent an esker, which may produce an overall underestimate of esker sinuosity. This phenomenon is apparent in the data obtained from Prest *et al.* (1968), wherein 3,230 eskers are straight lines. Those lines could either be artificially straight, for cartographic reasons, or used to indicate *almost* straight eskers, which would not significantly bias the results. The values obtained indicate that the vast majority of eskers have a sinuosity value of less than 1.2.

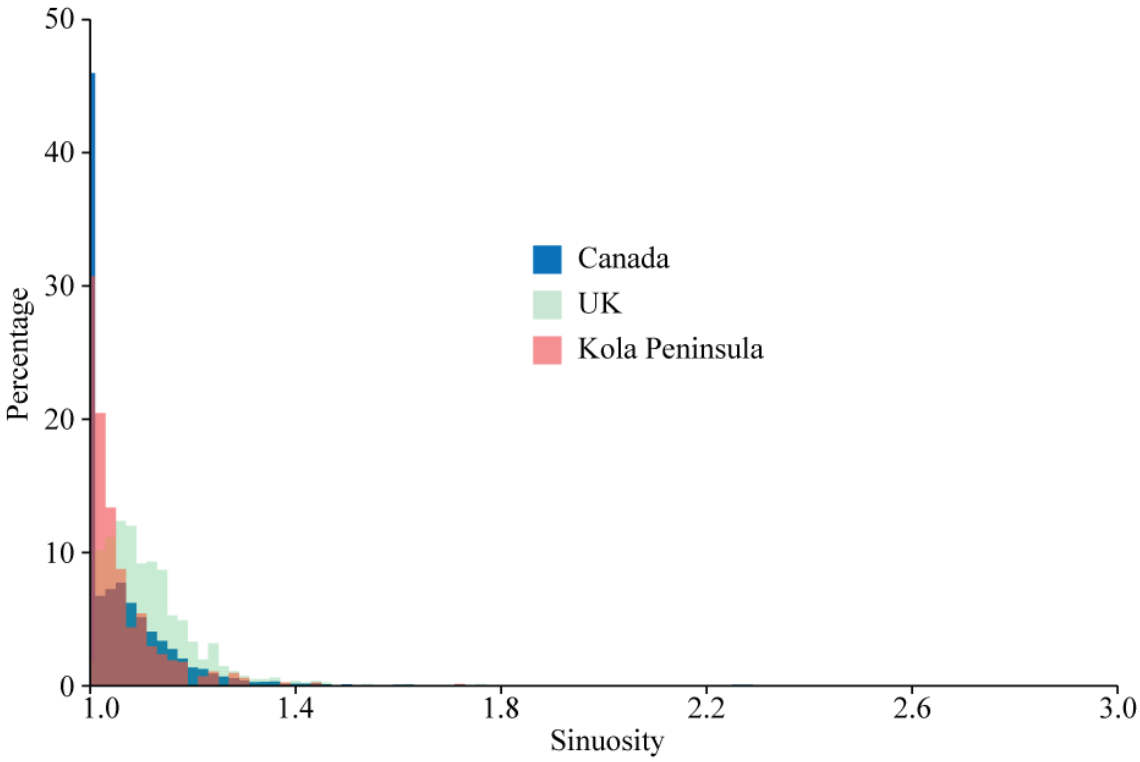

Figure 2.16. Esker sinuosity distribution (0.01 bins) for the UK, Kola Peninsula and Canada.

2.5.1.4 Cross-sectional shape

In cross-section, eskers may be sharp-crested, multiple-crested or broad-crested (Benn & Evans, 2010). Cross-sectional geometry of the esker forming channel is important and the ridge morphology is attained when the supporting ice has melted away (Price, 1973). Price (1973) envisaged four channel morphologies and associated esker cross-sections (Figure 2.17): low, wide channels which form flat-topped eskers; high, narrow channels forming sharp-crested eskers; quasi-circular channels which form sharp-crested eskers; and keyhole-shaped channels forming flat-topped eskers.

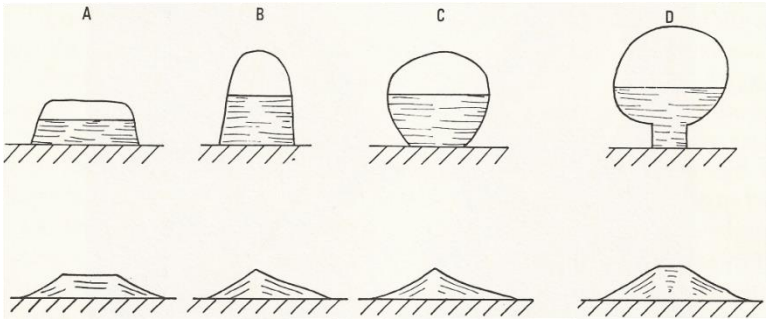

Figure 2.17. Channel morphology and associated esker cross-sections. (A) low, wide channel forming flat-topped esker; (B) high, narrow channel forming sharp-crested esker; (C) quasi-circular channel forming sharp-crested esker; and (D) keyhole shaped channel forming flat-topped esker. From Price (1973).

2.5.2 Spatial patterns of eskers

Groups of eskers sometimes display distinctive spatial patterns at a variety of scales. These may be related to large-scale controls such as ice divides (cf. Clark, 1993; McMartin & Henderson, 2004), or smaller-scale processes such as bifurcation of individual ridges (e.g. Aylsworth & Shilts, 1989). In general, the literature reveals that four major spatial patterns predominate and operate at different scales.

At the largest scale, eskers radiate away from former ice divides. Striking examples of this are seen in Keewatin (Aylsworth & Shilts, 1989) and Labrador (Clark *et al.*, 2000; Jansson *et al.*, 2002) where the ice divide locations are clearly demarcated by the sudden absence of eskers (Figure 2.18).

Operating at a smaller scale, esker systems often display integrated dendritic networks, analogous to Hortonian river systems. An example from the Rennie Lake esker system in Keewatin (Shilts *et al.*, 1987) is shown in Figure 2.19, which highlights the development of up to fourth order tributaries. Though analogous in morphology to Hortonian river systems, McCabe (2008) noted that because eskers do not typically increase in size through these networks, dendritic esker networks may not be related to increasing discharge downstream, as would a river system. Shilts *et al.* (1987) noted that esker tributaries in the Keewatin sector of the Laurentide Ice Sheet typically (but not exclusively) join trunk eskers from the left. From this they envisaged that the esker network reflects the configuration of surface streams draining over a large, flat ice sheet, the absence of significant topography resulting in drainage being strongly influenced by the Coriolis Effect.

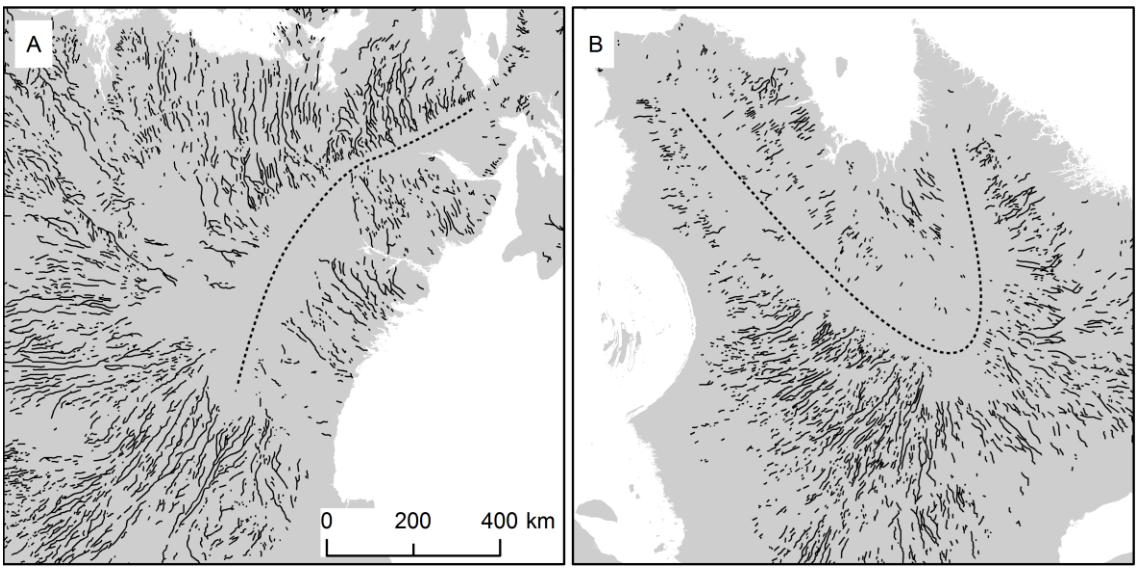

Figure 2.18. Radiating esker patterns around the Keewatin Ice Divide (A) and in Quebec-Labrador (B) (after Prest *et al.*, 1968). Note the absence of eskers at ice divides (dashed lines).

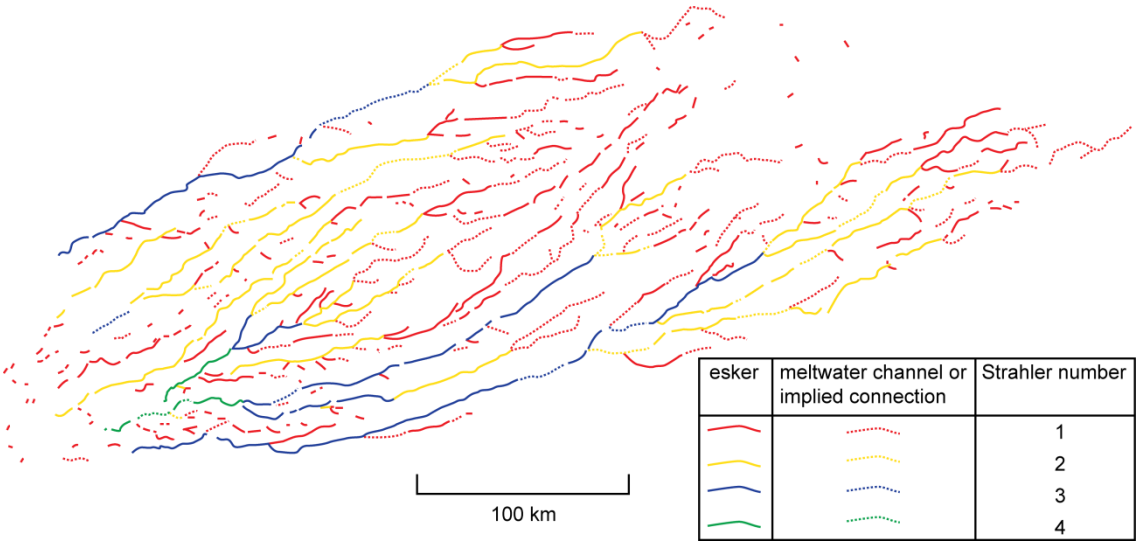

Figure 2.19. Esker tributaries and associated Strahler numbers in the Rennie Lake esker system, Northwest Territories, Canada, showing up to fourth order tributaries (after Shilts *et al.*, 1987).

On the scale of individual to multiple esker ridges, eskers may be anastomosing and contain numerous tributaries (e.g. Figure 2.20). Anastomosing eskers are not predominant and are restricted to certain regions. They may form under specific conditions, such as where a channel is clogged with sediment, leading to the formation of a separate channel (Menzies & Shilts, 1996). Channels may reconnect down-ice as they would likely follow the same hydraulic pathways.

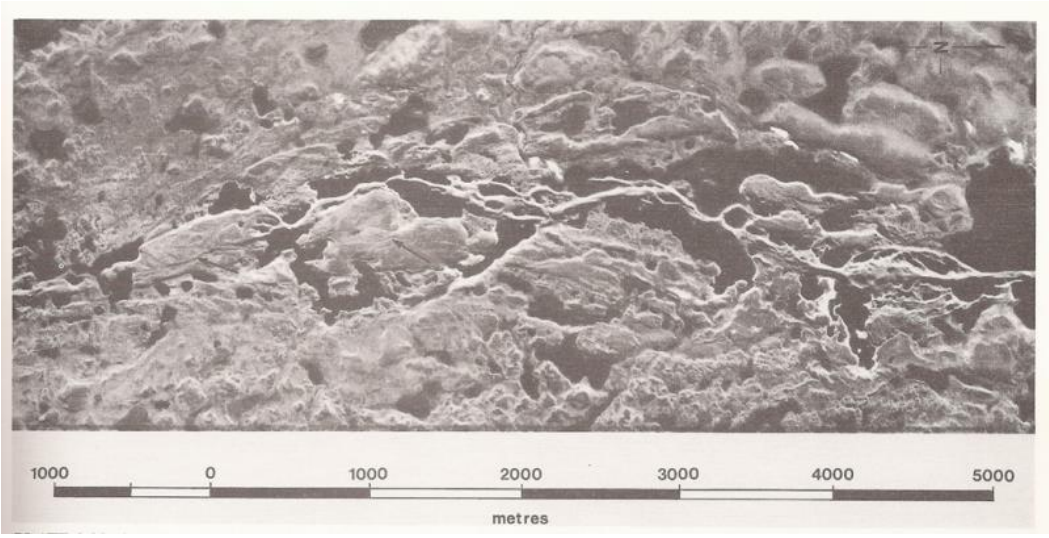

Figure 2.20. Aerial photograph extract showing anastomosing esker ridges. From Menzies & Shilts (1996).

In some areas, eskers are spaced quasi-uniformly (e.g. Figure 2.21). Boulton *et al.* (2009) note that eskers in Fennoscandia are spaced between 8 and 25 km apart and that spacing decreases

toward the ice sheet margin. Shilts *et al.* (1987) recorded spacing of 13 km in the area surrounding the Keewatin ice divide. Esker spacing was also noted by Boulton *et al.* (2009) to decrease in zones of ice streaming. Several papers have reported measurements or model predictions of the spacing of eskers or subglacial channels, which are summarised in Figure 2.22. The values vary between 0 and 35 km, but the values reported for different parts of the LIS appear to indicate that spacing between channels of 12-15 km is common (Banerjee & McDonald, 1975; St-Onge, 1984; Shilts *et al.*, 1987; Bolduc, 1992). To date, the only application of esker spacing measurements to test these models is provided by Boulton *et al.* (2009) who measured esker spacing in Finland, noting that measured esker spacing was generally consistent with their model predictions, which ranged from 2.5 km to 50 km. Esker spacing has been linked with bed geology and groundwater conditions (e.g. Boulton *et al.*, 2009; Hewitt, 2011), which is discussed in more detail in Section 2.6.5.

In Europe and Canada, eskers are abundant in hard, Shield zones but much less prevalent in soft-bedded areas (Clark & Walder, 1994). Similarly, eskers are absent on the marine based palaeo-ice stream beds of Antarctica (Livingstone *et al.*, 2012). Their observations led Clark & Walder (1994) to theorise that bed rigidity is responsible for esker location, which is discussed further in Section 2.6.3.

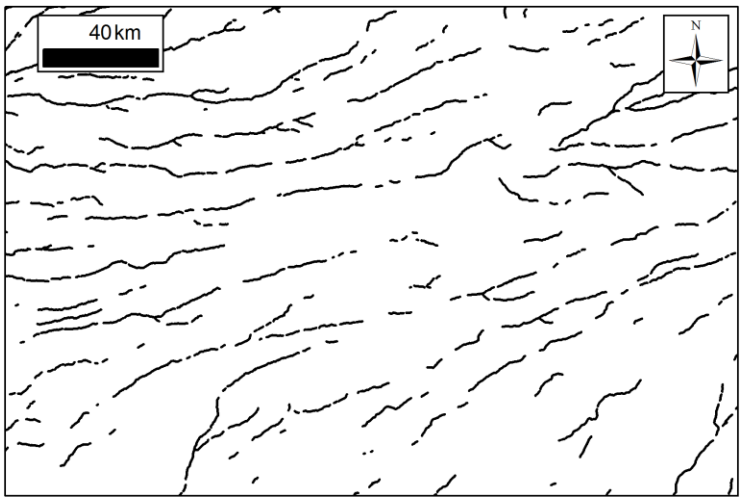

Figure 2.21. Quasi-uniform esker spacing in Northwest Territories, Canada. Eskers digitised from Landsat ETM+ image.

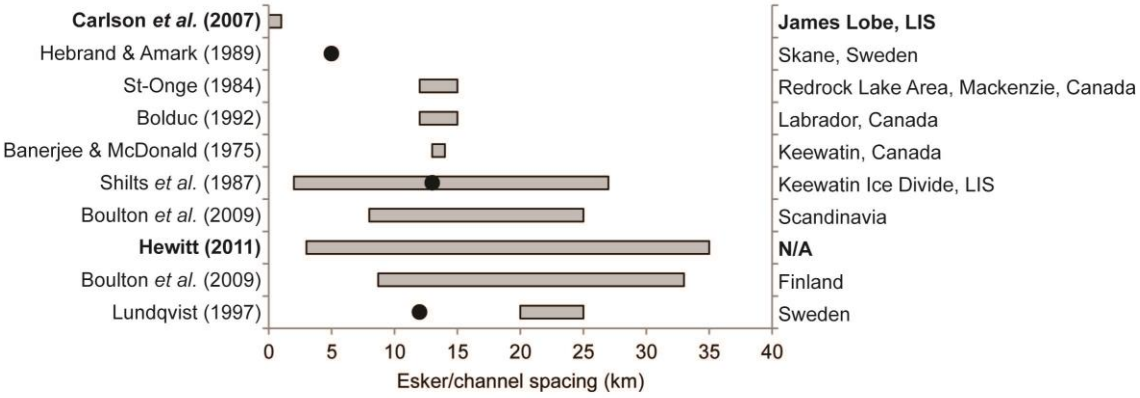

Figure 2.22. Examples of esker/subglacial channel spacing from the literature. Bars represent stated maxima and minima and points represent stated means. Bold fonts indicate numerical model outputs and regular fonts indicate measurements. LIS = Laurentide Ice Sheet.

Differences in elevation between the beginning and end of eskers are important because theoretically, eskers will follow the hydraulic gradient, which is determined by the ice surface slope and bed topography (Shreve, 1972), meaning that they can sometimes climb 'uphill' (e.g. Sissons, 1958; Price, 1969; Shreve, 1985a; Brennand, 1994). There are several reports of esker crestline profiles in the literature (e.g. Price, 1969; Howarth, 1971; Shreve, 1985a; Brennand, 1994; Brennand & Shaw, 1996), although these are not systematic. Profiles often reveal undulating elevations, frequently reflecting esker beads (e.g. Price, 1969; Gorrell & Shaw, 1991), thought to reflect sedimentation in stages and resulting in elevated sections of eskers at semi-regular intervals.

2.5.3 Landform associations

Eskers are frequently observed to be superimposed on drumlins (Figure 2.23) and ribbed moraine (Figure 2.24) (Shilts *et al.*, 1987; e.g. Menzies & Shilts, 1996; Knight & McCabe, 1997; Hättestrand & Kleman, 1999). This has been taken as evidence that ice was thin and slow moving at the time of esker deposition because it was not able to modify the pre-existing landforms. This may suggest that any relationship between eskers and the groundwater system is more complex than previously thought, because the hydrogeology of the substrate will be influenced by these pre-existing landforms. According to Hättestrand and Kleman (1999), no observations have been made of ribbed moraines superimposed on eskers. They suggested that this is because ribbed moraine formation preceded the production of abundant, esker forming subglacial meltwater.

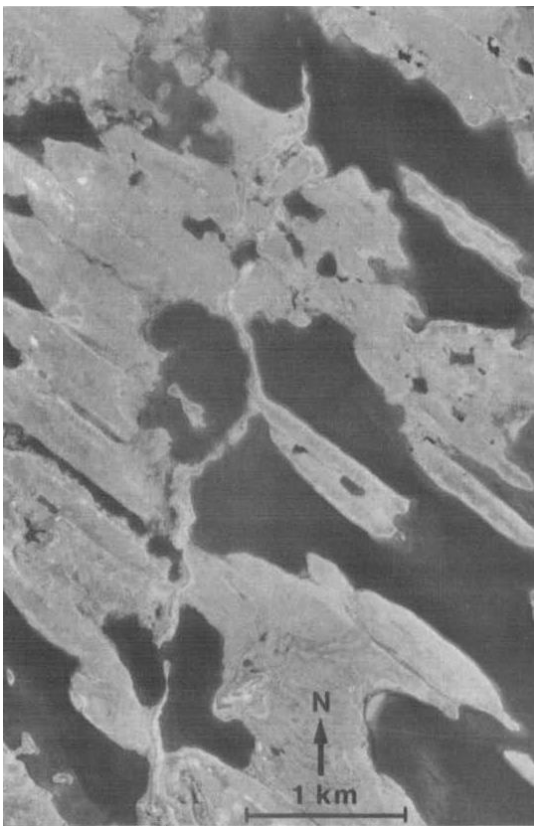

Figure 2.23. Esker superimposed on a drumlin field. Note that esker crosses drumlins almost perpendicularly indicating that it was deposited under different ice dynamic conditions. Portion of NAPL aerial photograph A14302-17, from Aylsworth & Shilts (1989).

In some areas, particularly the southern margins of the Larentide Ice Sheet, eskers are enclosed by terminal moraines, indicating that they were formed near to the ice margin (Shilts *et al.*, 1987). Eskers are often located in tunnel valleys (Hooke & Jennings, 2006; Brennand *et al.*, 2007) and GFCs (St-Onge, 1984; Utting *et al.*, 2009; Figure 2.24) and are commonly associated with meltwater channels, occasionally gradually merging into them (e.g. Livingstone *et al.*, 2010).

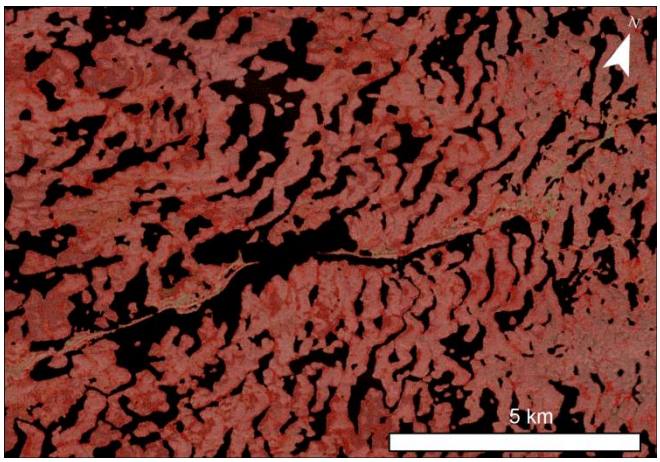

Figure 2.24. Extract of Landsat ETM+ image (4,3,2) showing an esker superimposed on ribbed moraine in Nunavut, Canada.

2.5.4 Patterns of ice margin retreat

It is possible to reconcile glacial geomorphology and geochronology in some areas to develop an accurate reconstruction of ice margin retreat. Eskers are central to this process and have been used by several authors to identify ice margin retreat patterns (e.g. Sugden, 1970; Clapperton, 1971; Lauriol & Gray, 1987; Kleman, 1992; Stokes *et al.*, 2009; Clark *et al.*, 2012; Margold *et al.*, 2013a; Margold *et al.*, 2013b). Assuming that eskers are formed during deglaciation and are chronologically constrained, it is possible to trace how, where, and how fast deglaciation took place.

An important implication for using eskers to reconstruct ice margin retreat is how they are formed, particularly whether they were formed synchronously (e.g. Brennand, 1994; Brennand & Shaw, 1996), or time-transgressively at a retreating margin (e.g. Banerjee & McDonald, 1975; Dyke & Dredge, 1989). Both of these interpretations have a very different result in terms of ice margin stability and timing of retreat. In each case, the ice margin is interpreted as being perpendicular to the esker ridge (Shreve, 1985a). If eskers are assumed to form synchronously, the ice margin position at the time of formation is known (where the esker terminates), but its subsequent retreat is not documented by the esker position. Conversely, if time-transgressive sedimentation is assumed, the position of the esker provides the location of the ice margin throughout retreat. Esker beads, if present, provide snapshots of the ice margin location because the ice margin is inferred to have been stationary in order for the beads to accumulate (Figure 2.25). Resolving the synchronous vs. time-transgressive argument is of fundamental importance to understanding how eskers are formed and is particularly relevant to large esker systems of Canada and Fennoscandia, whose precise origin remains elusive.

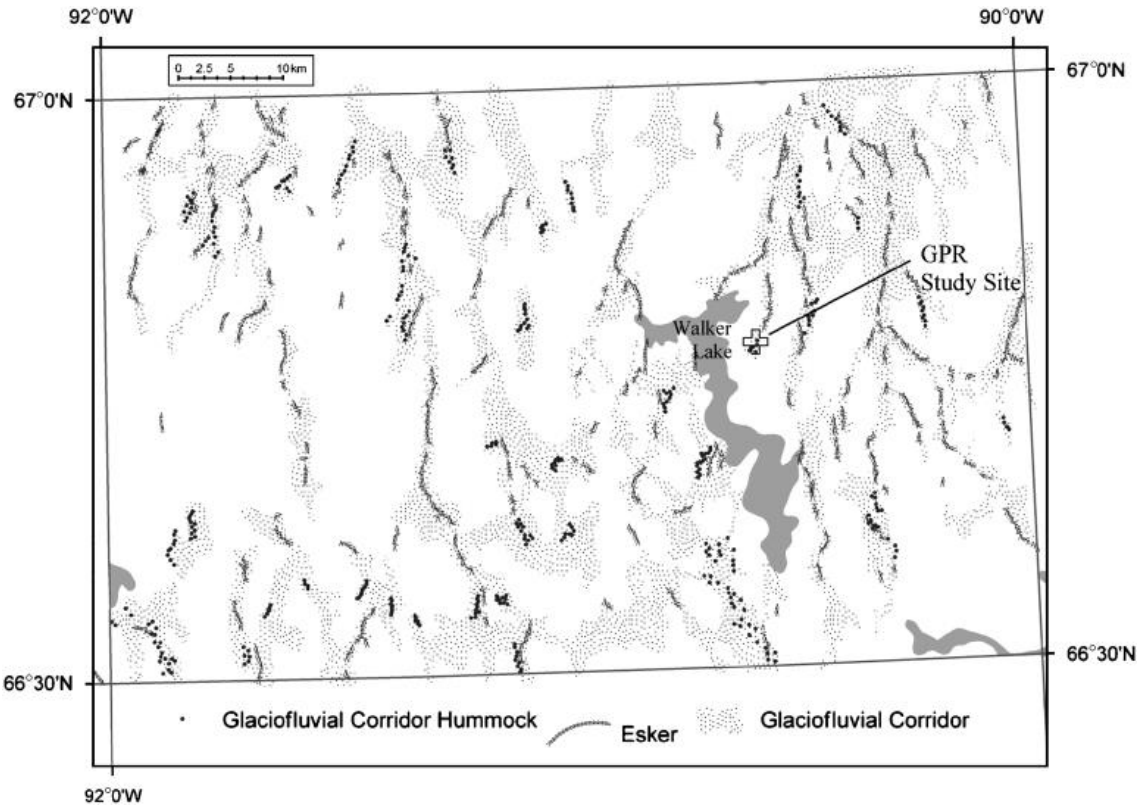

Figure 2.25. Association of eskers and Glaciofluvial Corridors in Keewatin, Canada (from Utting *et al.*, 2009).

2.6 Controls on esker patterns

It was shown in Section 2.3 that multiple terms have been used to describe similar eskers, and that no consensus has been reached on how to classify them. This may relate, in part, to the similar lack of consensus over what controls the distribution of eskers. For example, if we know the conditions under which different eskers formed, we might want to classify and define them. This section reviews the main hypotheses regarding controls on esker patterns. Note that it is likely that more than one mechanism is responsible for the variation in eskers observable in the geomorphological record because eskers form under a range of different conditions (cf. Price, 1969; Aylsworth & Shilts, 1989; Fitzsimons, 1991; Lundqvist, 1999). Each hypothesis is illustrated with a case study.

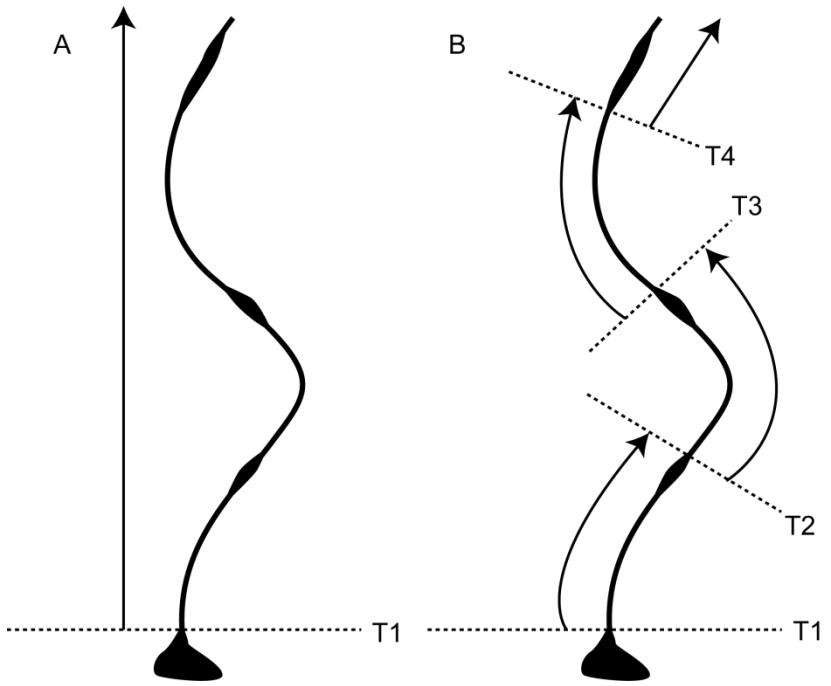

Figure 2.26. Conceptual model of synchronous (A) and time-transgressive (B) esker formation and implications for reconstructing ice margin retreat. Arrows indicate the ice margin retreat direction gleaned from the inferred mode of formation and T1-4 shows the chronological position of inferred ice margins. If synchronous deposition is assumed, only the initial ice margin is known, whereas if deposition is assumed to be time-transgressive, esker beads indicate the positions of a receding margin. The features are exaggerated and are not drawn to scale.

2.6.1 Ice thickness

The theoretical framework for channelized subglacial drainage developed in the 1970s (Section 2.2.2) led to the development of a model for predicting where eskers would form, based on the conditions necessary to maintain R-channels (Shreve, 1972;1985a;b). Fundamentally, such a model is dependent on ice thickness. Shreve (1972) envisaged equipotential surfaces in glaciers where the pressure of meltwater balances the weight of the overlying ice. Thus, water descends normal to equipotential surfaces (Figure 2.27), following the hydraulic potential given by:

$$\Phi = \rho_w g h_b + \rho_i g(h_i - z) \qquad (2.2)$$

A consequence of this system is that water may not necessarily follow the slope of the bed, therefore providing one explanation of how eskers can deviate across valleys or up slopes (Shreve, 1972).

This model for englacial and subglacial water routing was then taken by Shreve (1985a) and used to predict the location of major subglacial R-channels (and hence esker locations) in Maine. Shreve (1985a) demonstrated that esker positions closely reflect the reconstructed hydraulic potential gradients, a result that has been repeated by others in some (but not all - see for example Syverson *et al.*, 1994) areas. The Shreve model has also been applied to

contemporary ice masses, often in accordance with other techniques such as dye tracing, to predict their basal hydrology (e.g. Björnsson, 1986; Sharp *et al.*, 1993; Hagen *et al.*, 2000; Björnsson, 2003; Vaughan *et al.*, 2008).

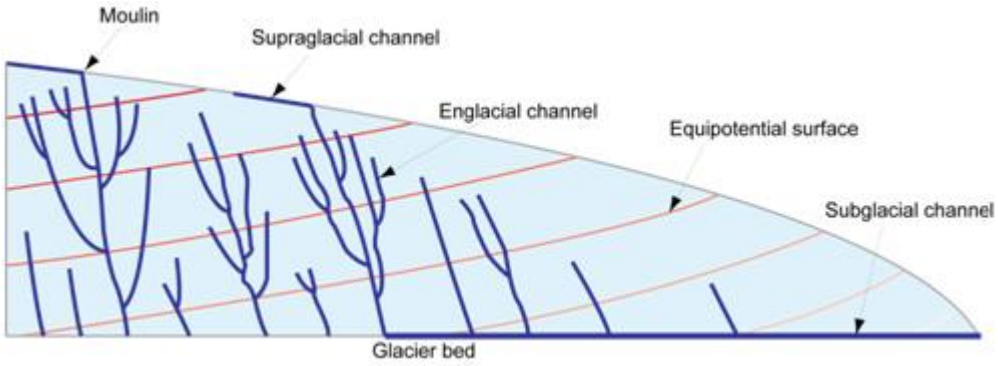

Figure 2.27. Vertically exaggerated hypothetical movement of water through equipotential surfaces (redrawn from Shreve, 1985a). Hydraulic potential drives water through equipotential surfaces (from darker to lighter shades of red) which dip up-glacier by approximately 11 times the surface slope.

2.6.1.1 The Burroughs Glacier, USA case study

The Shreve model for predicting esker location was used by Syverson *et al.* (1994) to investigate the relationship between esker morphology and former ice-surface topography of the Burroughs Glacier, Alaska. Rather than using eskers to predict the former hydraulic head, rapid retreat of the glacier allowed Syverson *et al.* (1994) to use topographic maps from 1948 to 1990 to generate subglacial hydraulic head maps of the former ice extent (Figure 2.28). These were then compared with known esker locations, providing empirical constraints on both former ice surface and esker location. Syverson *et al.* (1994) found that, in general, the Shreve model adequately explained the location of most eskers. There were some exceptions, however, as some eskers formed in accordance with bed topography rather than ice surface. All of these eskers formed under ice less than 50 m in thickness and, thus, Syverson *et al.* (1994) concluded that the Shreve model applies only to ice greater than approximately 50 m in thickness, and that bed topography controls esker locations under thinner ice.

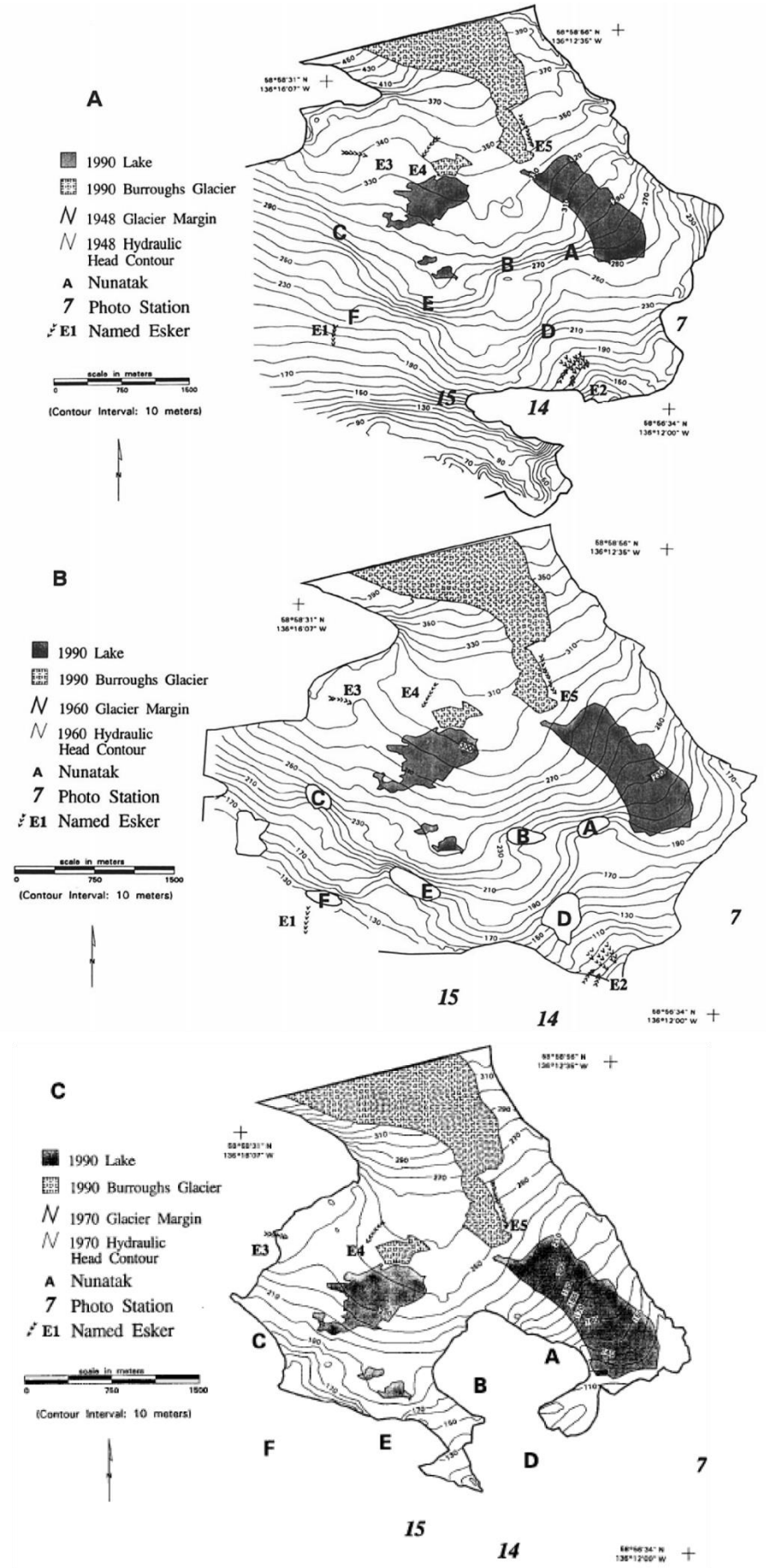

Figure 2.28. Subglacial hydraulic head maps of the southeastern Burroughs Glacier, Alaska, USA for (A) 1945, (B) 1960 and (C) 1970. From Syverson *et al.* (1994).

2.6.2 Outburst floods

Outburst floods have been suggested to form eskers (e.g. Brennand, 1994; Brennand & Shaw, 1996; Russell *et al.*, 2001; Fard, 2002; Sutinen *et al.*, 2007; Burke *et al.*, 2010b). Observations have confirmed that relatively small eskers can be formed by outburst floods (jökulhlaups) on a timescale of hours to days (Burke *et al.*, 2008; Burke *et al.*, 2010b). Eskers form where outburst floods are routed through a conduit, depositing sediment at various stages in the flood, often leading to complex sedimentary architecture (Burke *et al.*, 2008). The Harricana Glaciofluvial Complex in Ontario, Canada, was interpreted by Brennand & Shaw (1996) as the product of deposition by the waning stage of a large outburst flood, where elevated discharge in the convergence zone of two lobes and input of supraglacial meltwater from moulins provides the requisite high discharge and material to build a large esker. The evidence for this hypothesis, however, rests on the interpretation of drumlins and striae in the area as having been formed by meltwater – a strongly contested idea (Evans *et al.*, 2006; Ó Cofaigh *et al.*, 2010).

2.6.2.1 Skeiðarárjökull, Iceland case study

On 5th and 6th November 1996, a jökulhlaup from Grímsvötn, Iceland occurred beneath Skeiðarárjökull (Guðmundsson *et al.*, 1997). The 'Skeiðarárhlaup' reached a peak discharge of 45,000 m^3 s^{-1} in 14 hours (Russell *et al.*, 2001) and left behind many sedimentary features (e.g. Russell & Knudsen, 1999; Roberts *et al.*, 2000; Russell *et al.*, 2001; Russell *et al.*, 2006; Russell *et al.*, 2007; Burke *et al.*, 2008; Burke *et al.*, 2009; Burke *et al.*, 2010a). In particular, an esker approximately 700 m long and 30 m high (Figure 2.29) was formed as a direct consequence of the Skeiðarárhlaup (Burke *et al.*, 2008), clearly demonstrating that outburst floods can form eskers. GPR analysis of the esker by Burke *et al.* (2008) revealed a complex sedimentary architecture which varied through the length of the esker. Six major facies reflecting the dynamic sedimentation of the esker were identified: trough cross-strata; upper-stage gravel plane beds; backset accretion associated with large-scale bedform development; foreset accretion associated with macroform progradation; boulder clustering; and buried ice associated with the channel base (Burke *et al.*, 2008). As a result of the high discharge and short timescale (17 to 24 hours) of the jökulhlaup, sedimentation rates were found to be very high. The sedimentary architecture was controlled by conduit geometry, which changed rapidly to accommodate the meltwater and sediment flux (Burke *et al.*, 2008). Based on the work at Skeiðarárjökull and also at the Bering Glacier, Alaska, USA, Burke *et al.* (2010b) suggested that certain sedimentary characteristics may be diagnostic of eskers formed by outburst floods (Table 2.7).

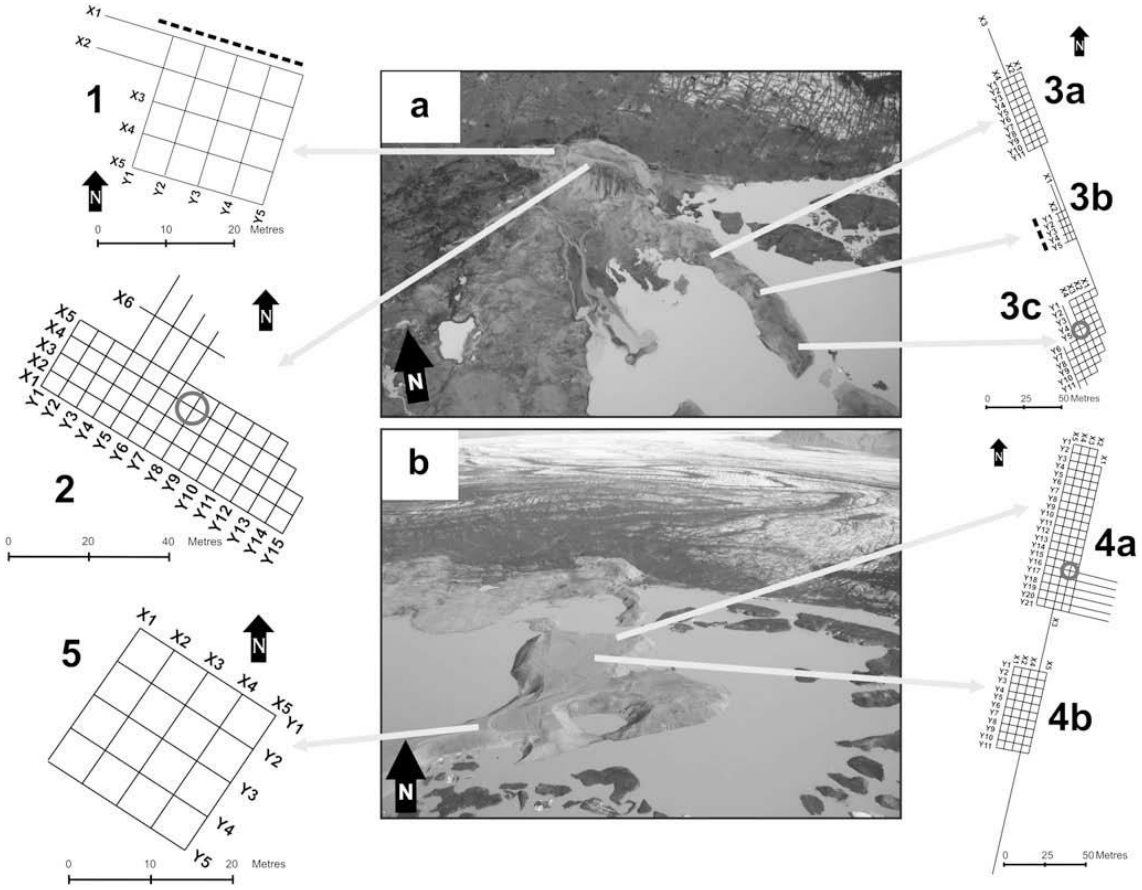

Figure 2.29. Photographs of the esker formed during the 1996 Skeiðarárhlaup and grids indicating where GPR surveys were undertaken. From Burke *et al.* (2008).

2.6.3 Substrate resistance

Esker location was suggested by Clark & Walder (1994) to be controlled by the resistance of the underlying substrate. Clark & Walder (1994) predicted that eskers should be more prevalent on crystalline substrates than on deformable sediments. The 'substrate hypothesis' assumes that eskers are formed in R-channels, which are more likely to be sustained on hard rather than soft beds. Clark & Walder (1994) assumed that R-channels are more likely to form on hard substrates because water at the bed would erode upwards into the (relatively) weaker ice rather than the stiff tills (or exposed bedrock) typically associated with hard beds. Conversely, soft beds would be prone to substrate incision by canals (Section 2.2.1) rather than ice incision by R-channels. This is supported by the presence of eskers on the European and Canadian shields and absence in the areas of softer beds (Clark & Walder, 1994). Furthermore, eskers have not been reported anywhere on the unconsolidated sedimentary substrate of the Antarctic shelf, potentially for the same reason, though this could also be a result of the lack of surface melting in Antarctica (Livingstone *et al.*, 2012).

Table 2.7. Suggested diagnostic criteria for outburst flood eskers after Burke *et al.* (2010).

Criterion	Description
Large-scale antidune cross-strata	High flow velocities and sedimentation rates associated with the outburst floods lead to the initial deposition of large antidune cross-strata
Upper-stage plane beds	Found as the stratigraphically highest deposits of the outburst eskers, plane beds were deposited by high velocity flows and often drape the lower bounding contacts in the narrow down-flow sections of the eskers.
Large grain size	Outburst eskers are largely composed of coarse sands, gravels, and, in places, meter-size boulders.
Composite macroforms	Outburst eskers consist of composite macroforms. During high-magnitude outburst floods the erosive nature of the floodwaters results in rapid conduit enlargement, which create localized reduction in flow velocity and consequently allow the deposition of composite macroforms.
Wide depositional units	Depositional units in the outburst flood eskers often span the width of the landforms, indicating that final esker cross section corresponds directly to outburst flood conduit geometry.

2.6.3.1 Canadian Shield case study

The substrate hypothesis was tested by Clark & Walder (1994) by comparing eskers mapped by Prest *et al.* (1968) and UNESCO (1967-1980) with the bedrock lithology in Canada and Europe, respectively. The results indicate that eskers are more ubiquitous on crystalline bedrock than on deformable sediments, as predicted. Figure 2.30 shows the distribution of eskers in Canada and the delineation of ‘hard’ (Shield) and ‘soft’ (deformable sediment) substrate areas used by Clark & Walder (1994). It can be seen that the majority of eskers do indeed occur in the crystalline bedrock areas of the Canadian Shield (shaded in Figure 2.30) and that far fewer eskers occur over sedimentary bedrock (unshaded).

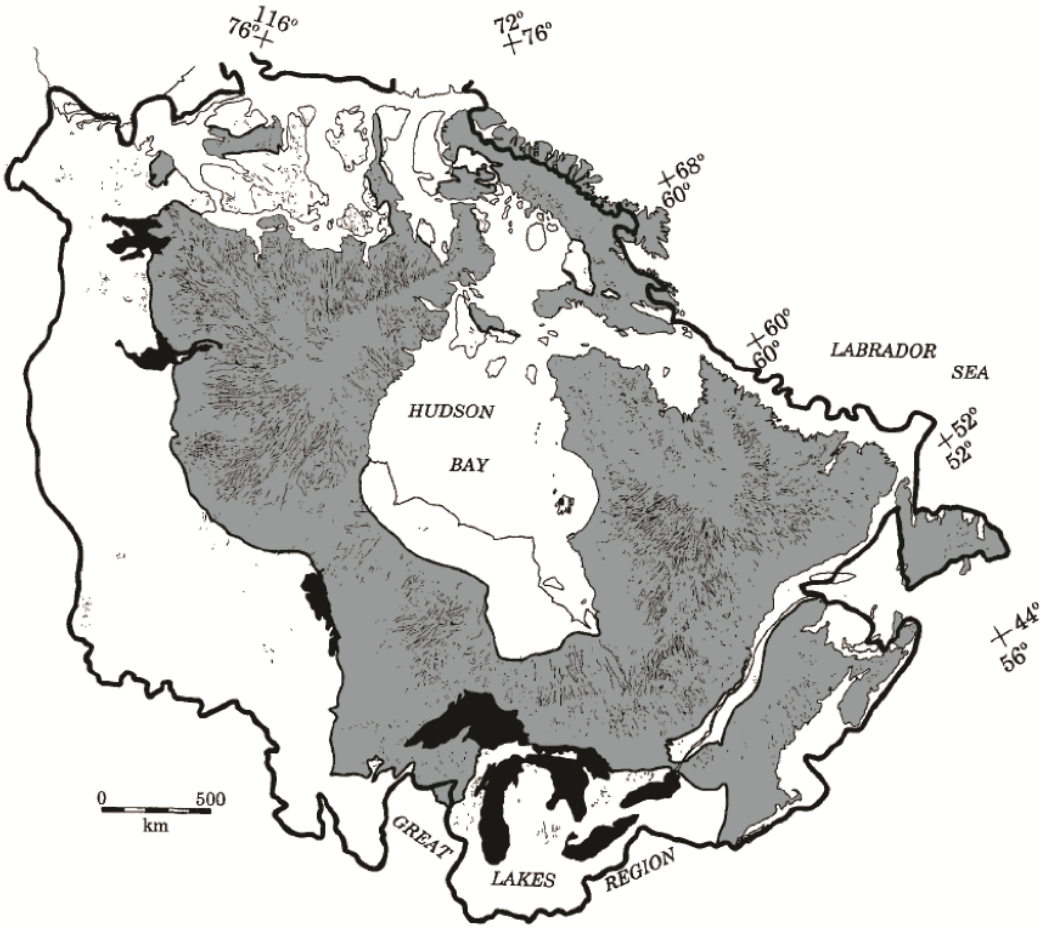

Figure 2.30. Esker distribution in Canada compared with hard shield substrate (shaded) and deformable substrate (unshaded). Modified from Clark & Walder (1994).

2.6.4 Interlobate deposition

Where two lobes of ice coalesce, meltwater is often concentrated because of the ice surface slope (Thome, 1986). This has implications for the development of some eskers. Initially, the term 'interlobate moraine' was introduced to describe glaciofluvial deposits formed under these conditions (Punkari, 1980). Interlobate moraines are often reinterpreted as eskers (e.g. Brennand *et al.*, 1996) because when investigated in more detail, the fluvial origin of the sediments becomes apparent. Subglacial conduits may be maintained in interlobate positions because of the concentration of meltwater in these areas and the differential movement of the two ice masses causing high stresses between the lobes (Punkari, 1997; Benn *et al.*, 2009b). Consequently, eskers have been suggested to develop in these areas, although the precise mechanisms controlling sedimentation are contested (e.g. Brennand & Shaw, 1996; Brennand *et al.*, 1996; Mäkinen, 2003; Figure 26).

Supraglacial drainage has also been suggested to result in eskers forming at confluent ice lobes (e.g. Huddart *et al.*, 1999). Crevasses may form preferentially in interlobate areas because of high shear strain rates that tend to coincide with medial moraines (Boulton *et al.*, 1999).

Crevasses are then exploited by surface drainage which produces complex channel systems, similar to those found in limestone areas (Boulton *et al.*, 1999).

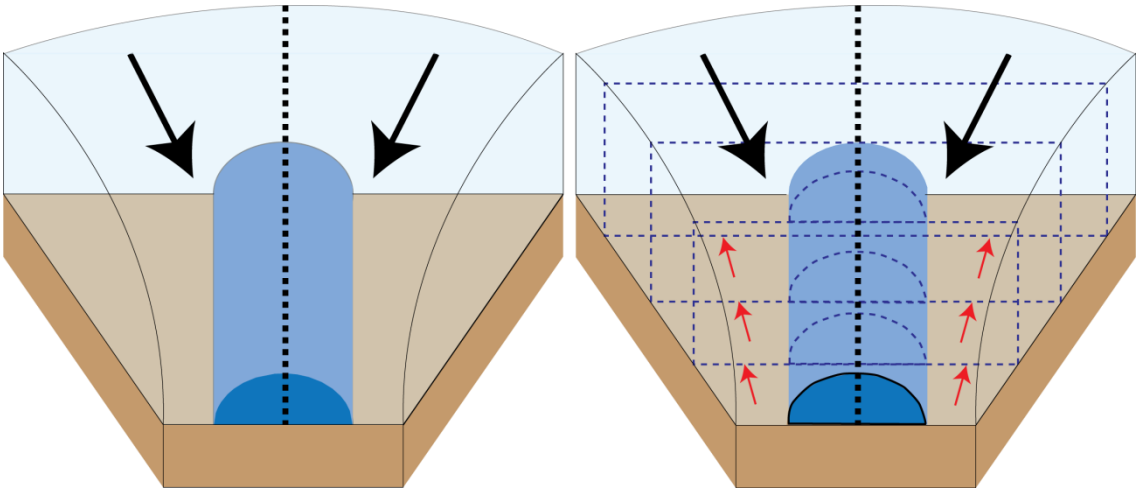

Figure 2.31. Conceptual diagram of two interlobate depositional models. Thick black dotted lines represent suture zones where stress is high. Black arrows indicate ice flow. Left hand model shows conditions for synchronous deposition in a persistent conduit, maintained between two lobes. Right hand model shows time-transgressive deposition in two retreating lobes. Red arrows indicate ice retreat and blue dotted lines indicate margin positions. Esker forms in the terminal section of the conduit and extends back up-ice as the ice front recedes. Not to scale.

2.6.4.1 The Oak Ridges Moraine, Canada case study

The Oak Ridges Moraine (ORM; Figure 2.32) is a large glaciofluvial complex in Ontario, Canada, consisting of sediments up to 200 m thick (Sharpe *et al.*, 2007). It is located in the southern marginal zone of the Laurentide Ice Sheet (Barnett *et al.*, 1998) and occupies an area of 11,000 km^2 (Sharpe *et al.*, 2007). The ORM is largely composed of well-sorted sand and gravel (Russell *et al.*, 1998) which have been interpreted to indicate a glaciofluvial origin (Barnett *et al.*, 1998; Russell *et al.*, 1998; Pugin *et al.*, 1999; Russell & Arnott, 2003; Russell *et al.*, 2003; Sharpe *et al.*, 2007), thus providing an excellent example of the reinterpretation of interlobate moraines as glaciofluvial features. Five primary stratigraphic units were identified in the ORM by Sharpe *et al.* (1997) (Figure 2.33): Palaeozoic bedrock; Lower sediment; Newmarket Till; Oak Ridges Moraine and channel sediment; and Halton Till. The ORM is associated with the Peterborough drumlin field to the north and a series of tunnel valleys to the north and east, some of which contain eskers (Brennand & Shaw, 1994). Seismic profile investigations revealed that the tunnel valleys also occur beneath the ORM (Pugin *et al.*, 1996;1999).

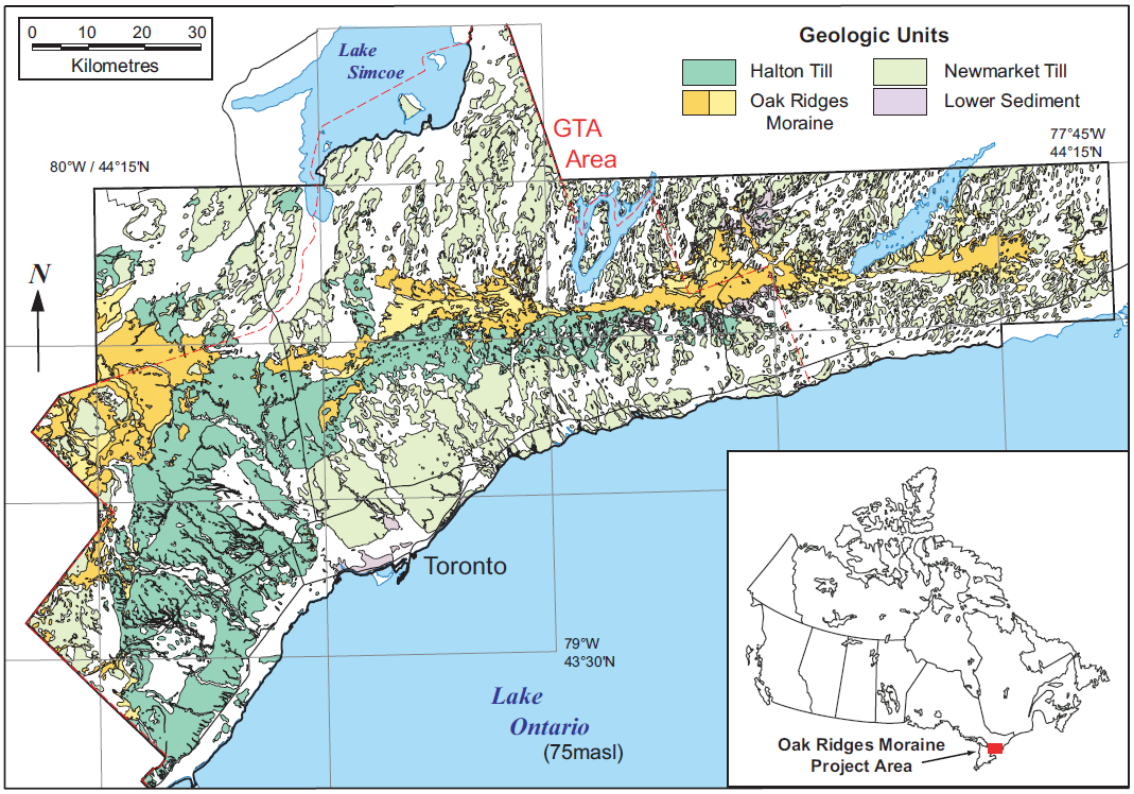

Figure 2.32. Geological units of the Oak Ridges Moraine, Ontario, Canada. From Sharp *et al.* (2007).

Most authors have suggested that the ORM is interlobate in origin (e.g. Gravenor, 1957; Barnett *et al.*, 1998; Russell *et al.*, 2003). Barnett *et al.* (1998) proposed a four-stage depositional model for the ORM based on sedimentation in a widening re-entrant into the ice-sheet margin. This consisted of: (1) high-energy, coarse deposition of a subglacial esker, (2) subaqueous fan sedimentation – high to reduced energy deposition, (3) fan to delta deposition and (4) Ice-marginal fan sedimentation. This mechanism helps to explain the complex nature of interlobate sedimentation and how a relatively simple process can manifest itself in complex sedimentary structures.

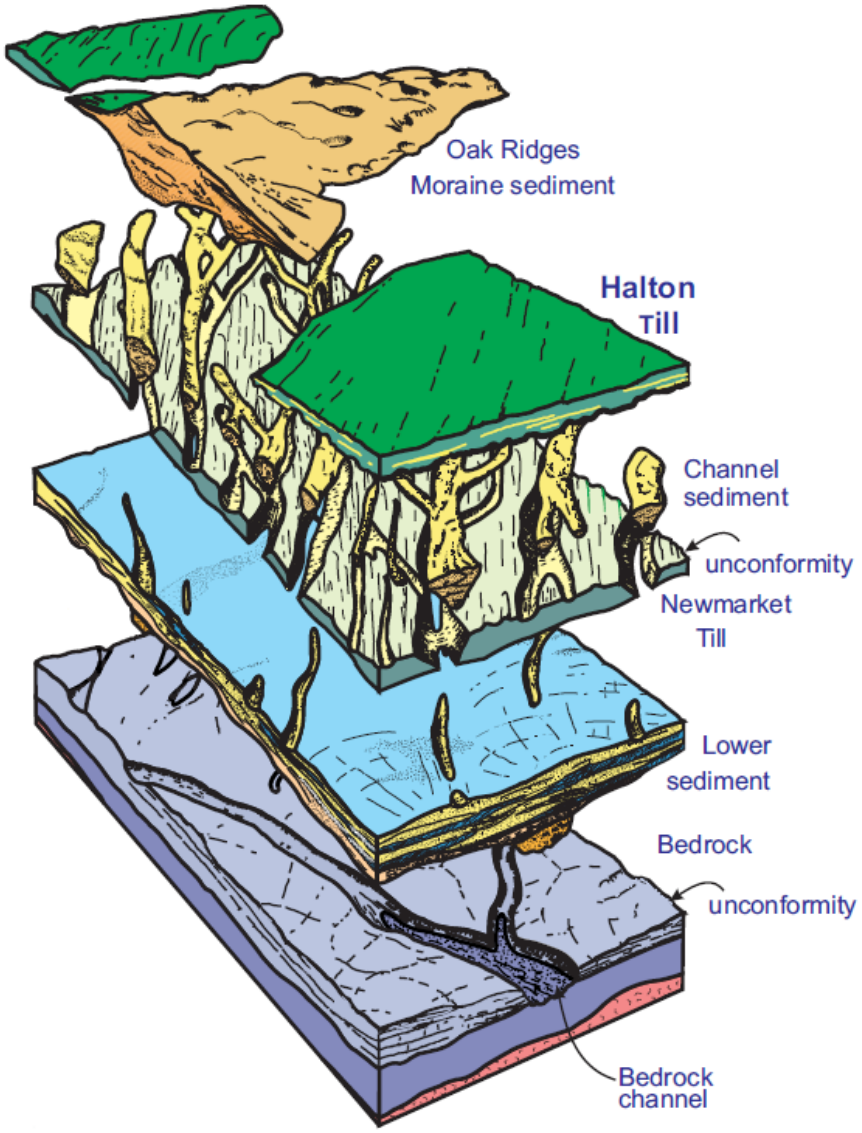

Figure 2.33. Conceptual geological model of the Oak Ridges Moraine showing the five major stratigraphic units. Note the tunnel valley in the lowermost unit superimposed by the drumlinised Newmarket till and channel sediment. The Oak Ridges Moraine sediment forms the cap of the sequence. From Sharp *et al.* (2007).

2.6.5 Groundwater flux

The groundwater hypothesis for esker spacing is based on the interaction of basal meltwater and groundwater at the glacier-bed interface (Boulton & Caban, 1995; Boulton *et al.*, 1995; Piotrowski, 1997; Boulton *et al.*, 2001; Boulton *et al.*, 2007a;b; Boulton *et al.*, 2009; Boulton, 2010). The premise is that groundwater flow is able to transport subglacial meltwater without the need for channelized subglacial drainage, but only until the subglacial aquifer becomes saturated. Any excess water entering the bed will thus form R-channels because the water is only able to erode upwards into the ice due to the underlying sediment being saturated. In these situations, sediment creep may lead to partial or total channel closure. R-channels are able to draw water from surrounding areas (Section 2.2.2) and so the spacing of these R-channels

becomes self-organising, in that channel spacing adjusts in response to the water excess. Where stability is maintained, eskers are formed (Boulton *et al.*, 2007a;b; Boulton *et al.*, 2009). Boulton *et al*. (2009) suggested that the groundwater hypothesis can be simplified to a relationship between esker spacing, basal melt rate and bed transmissivity (Equation 2).

$$\mathrm{Ts} = 77.8 \left(\frac{\mathrm{T}}{\mathrm{m}}\right)^{1/2} \text{ (after Boulton } \textit{et al.}\text{, 2009).} \qquad (2.3)$$

Recent research has focused on numerical modelling of groundwater beneath ice (Boulton *et al.*, 2007a;b; Boulton *et al.*, 2009; Rempel, 2009; Boulton, 2010; Hewitt, 2011) to predict channel spacing and other parameters. Modelling of distributed and channelized subglacial drainage by Hewitt (2011) suggests that more permeable distributed systems result in more widely spaced eskers because larger amounts of water may be drawn into a channel through a more porous medium. This is similar to Boulton's model, but Hewitt (2011) emphasises the need for a threshold discharge value in order to maintain an esker-forming conduit by frictional melting to counteract the closure of the conduit by ice creep.

2.6.5.1 Fennoscandian Shield case study

The groundwater flux hypothesis was tested by Boulton *et al*. (2009), who used the model formulated by Boulton *et al.* (2007a;b), alongside measurements of esker spacing (Figure 2.34) and bed transmissivity from the Fennoscandian Shield to predict former basal melt rate (Equation 2). They then compared the predicted values with values obtained from an ice-sheet model (Boulton & Hagdorn, 2006) to test whether realistic basal melt rate values could be predicted by the groundwater hypothesis. Boulton *et al*. (2009) found that observed esker spacing correlated well with values of basal melt rate deduced from the model and measured values of transmissivity (Figure 2.35).

Boulton *et al.* (2009) also tested the hypothesis against the locations of four palaeo-ice streams in Finland (from Boulton *et al.*, 2003). The model predicts that eskers will be more closely spaced in areas of streaming because of the associated increased basal melt rate. The results supported the hypothesis, indicating that eskers were more densely spaced downstream and in areas of streaming, compared with inter-stream areas.

2.6.6 Summary

The 'Shreve model' for esker location based on ice thickness has been widely used for predicting the locations of subglacial streams (e.g. Björnsson, 1986; Sharp *et al.*, 1993; Hagen *et al.*, 2000; Björnsson, 2003; Vaughan *et al.*, 2008), but it is subject to several assumptions. The most significant assumption is that conduits flow full ($P_w = P_i$). This steady-state is unlikely to be the case all of the time and others have suggested that a more realistic approximation is that

$P_w = 0.5P_i$ (e.g. Flowers & Clarke, 1999; Hagen *et al.*, 2000; Rippin *et al.*, 2003), representing occasions where tunnels are not full (i.e. H-channels rather than R-channels). Experiments on modern temperate glaciers support this notion, indicating that R-channels exist on a diurnal and/or seasonal basis (e.g. Nienow *et al.*, 1996).

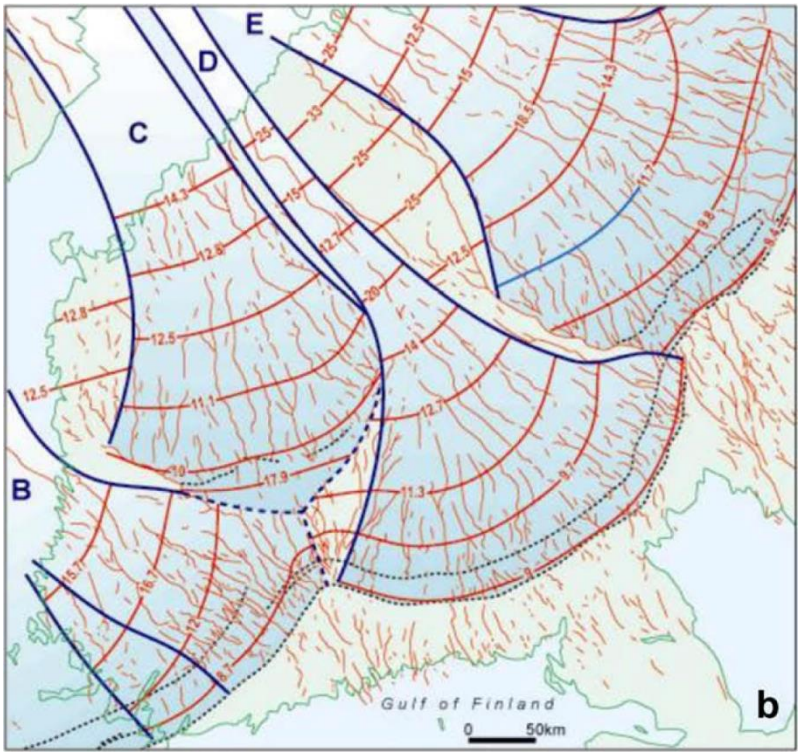

Figure 2.34. Esker spacing in Finland, with ice streams indicated by blue shading. From Boulton *et al.*, (2009).

Burke *et al.* (2010b) speculated that outburst floods may deserve more attention in the context of the larger Quaternary eskers, in light of the similarity between some of the observed sedimentary structures in Quaternary examples and the two jökulhlaup eskers they studied (Table 2.7). However, more work is required in order to determine whether eskers which are at least one order of magnitude larger than those observed by Burke *et al.* (2010b) could have been formed by similar processes, especially given the scarcity of examples. The vast area covered by eskers on the beds of palaeo-ice sheets would make it unlikely that they were *all* formed by floods, though it is possible that this is the case in more localised examples. The application of GPR and similar techniques to the older and larger eskers in Canada and Fennoscandia would undoubtedly provide some important insights to this end.

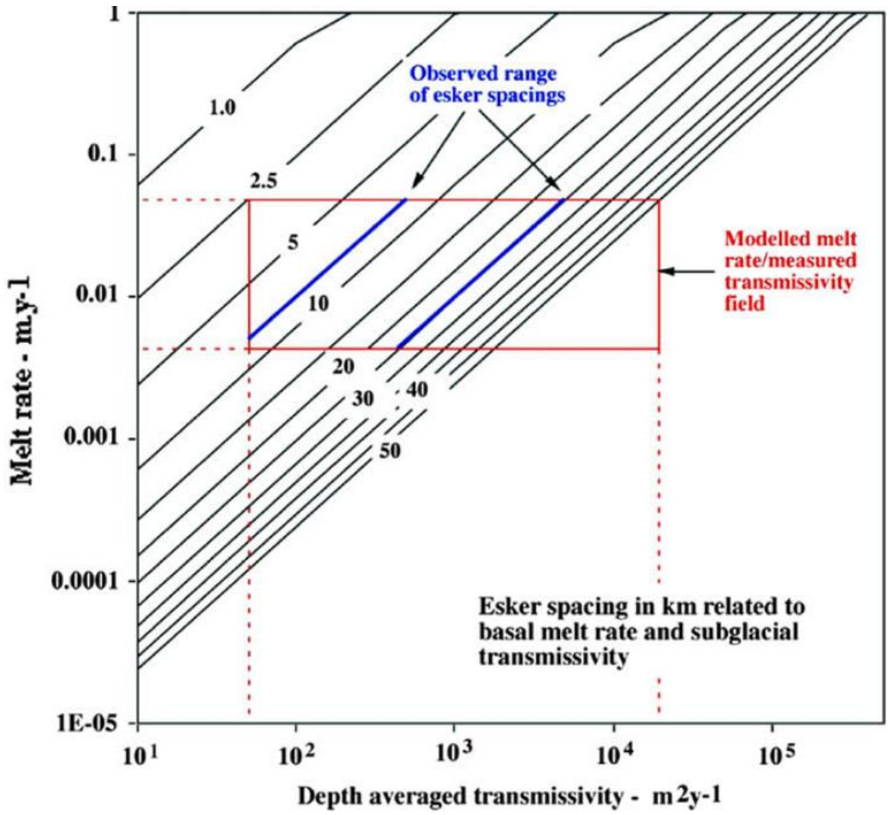

Figure 2.35. Esker spacing plotted as a function of transmissivity and melt rate from Boulton *et al.* (2009). Diagonal lines are contours of esker spacing in metres. Blue lines indicate the minimum and maximum esker spacing observed. Red box indicates the field produced by modelled melt rates and measured transmissivity. Note that the observed esker spacing fits well in the predicted field.

The substrate hypothesis has also received opposition from some authors. Sedimentological (e.g. Fard & Gruszka, 2007) and theoretical work (e.g. Alley, 1992) has demonstrated that subglacial channels can occur on deformable beds. The extent to which this occurs is not well understood and this may cast doubt on the hypothesis, or it may explain the presence of some eskers outside the 'hard bed' zones outlined by Clark & Walder (1994) if channels can operate there under specific conditions. Aylsworth & Shilts (1989) argued that, rather than the rigidity of the bed, sediment supply was the dominant control of Laurentide esker location. They highlighted the distribution of eskers around the Keewatin Ice Divide and noted that eskers radiate away from the divide and become sparser towards the western edge of the shield, disappearing where there is no drift cover. This implies a different mechanism, which may account for similar patterns of esker distribution and demonstrates that the hypothesis must be examined more carefully.

The groundwater hypothesis set out by Boulton and others provides a strong case for the origin of regularly spaced esker systems. Further work is necessary, however, to demonstrate the validity of the idea – especially with reference to the two key parameters used by Boulton *et al.* (2009), namely transmissivity and melt rate. The graph produced by Boulton *et al.* (and

reproduced here in Figure 2.35) shows depth averaged transmissivity of the bed on the x-axis. Note that the values span five orders of magnitude, from 10 m^2y^{-1} to 10^5 m^2y^{-1}. Similarly, estimated melt rates on the y-axis range from 10^{-5} my^{-1} to 1 my^{-1}. This vast range of values does not discount the hypothesis, rather it emphasises that caution should be used when drawing conclusions from the data.

In short, no single control has been demonstrated to apply to all eskers and each control appears to have strengths and weaknesses. This may, in part, be an artefact of the relatively small study areas used to develop and support each idea and the lack of a large-scale dataset against which different hypotheses can be rigorously tested.

2.7 Future research directions

2.7.1 Morphometry and large-scale patterns of eskers

Whilst there are some useful data available in the literature, no systematic quantitative analysis of large-scale esker morphometry (i.e. quantification of esker measurements such as length, width, height, sinuosity, long profiles) has hitherto been conducted. This contrasts markedly with the literature on other glacial landforms such as drumlins, mega-scale glacial lineations and ribbed moraine (e.g. Dunlop & Clark, 2006; Clark *et al.*, 2009; Stokes *et al.*, 2013); analyses of very large samples have provided a wealth of information relating to their characteristics, distribution and modes of formation (e.g. Clark *et al.*, 2009; Spagnolo *et al.*, 2010; Spagnolo *et al.*, 2011; Spagnolo *et al.*, 2012; Hillier *et al.*, 2013; Stokes *et al.*, 2013). A similar study of eskers is required in order to develop a robust understanding of how they vary, as well as to provide a means of testing hypotheses such as those outlined in Section 2.6. Constraining parameters such as esker length, continuity (e.g. Metzger, 1992) and sinuosity, for large sample sizes, will provide a foundation for analysing hypotheses concerning esker distribution. For example, longer, more continuous eskers may be spatially related to more resistant substrates (cf. Clark & Walder, 1994) which, if true, would add weight to the substrate hypothesis for esker distribution.

Very few of the hypotheses reviewed in section 2.6 have been rigorously tested using large sample sizes of esker characteristics. The Shreve model (Section 2.6.1) for esker distribution has been directly tested by Syverson *et al.* (1994) who demonstrated that it largely calculated esker distribution effectively. Other hypotheses, such as the outburst flood hypothesis, have yet to be tested and are related to just two observations (Burke *et al.*, 2010b). Testing and refining the hypotheses for controls on esker distribution is imperative because understanding what controls the location of eskers is the key to deciphering what controls the location of subglacial meltwater channels. Future work should focus on determining the controls of esker location to

meet this end. This may necessitate the creation of new hypotheses to be evaluated but is a process that is fundamental to understanding eskers on a large-scale.

2.7.2 Channelized and distributed drainage systems at the ice-sheet scale

Crucial to understanding the more complex phenomena associated with ice-sheet hydrology is determining the extent and type of channelized and distributed drainage systems operating under ice-sheets at different points in time. Numerous papers on glacier hydrology at the small, mountain glacier and outlet glacier scales have profoundly influenced our understanding of how meltwater is integrated into the drainage systems of temperate glaciers, revealing complex networks of R-channels that evolve on diurnal and seasonal scales (e.g. Sharp *et al.*, 1993; Nienow *et al.*, 1996; Iken & Truffer, 1997; Bartholomew *et al.*, 2010) from less efficient distributed systems. Current techniques are not able to discern in detail the nature of the continental-scale drainage systems of Greenland and Antarctica and whilst these techniques are improving, we must turn to the palaeo-record for proxies. The use of eskers to reconstruct major R-channel networks under Pleistocene ice-sheets could, therefore, provide a vital analogue for contemporary drainage processes. If the timing of esker formation is known, for example by matching esker locations with ice margin chronologies (e.g. Saarnisto & Saarinen, 2001; Dyke *et al.*, 2003; Nygard *et al.*, 2004; Clark *et al.*, 2012; Tarasov *et al.*, 2012), a snapshot of the subglacial channelized drainage network is available. A relationship between the configuration of the ice-sheet and the drainage network may then be used as a transfer function to predict the likely configuration of present day sub-ice-sheet drainage.

2.7.3 Using eskers to reconstruct drainage of subglacial lakes

Interest in subglacial lakes is increasing, especially given the recent attempts to sample them for the first time (e.g. Inman, 2005; Siegert *et al.*, 2007; Siegert *et al.*, 2012), and understanding the interactions of subglacial lakes and meltwater drainage is becoming increasingly significant because they can discharge very large quantities of water in relatively short periods (McMillan *et al.*, 2013). The inferred presence of subglacial lakes beneath the Laurentide Ice Sheet (e.g. Munro-Stasiuk, 1999; Munro-Stasiuk, 2003; (but see Evans *et al.*, 2006); Evatt *et al.*, 2006; Christoffersen *et al.*, 2008; Livingstone *et al.*, 2013) hints that the geomorphological and sedimentary records, as well as numerical modelling, may be able to indicate where subglacial lakes existed in the past. Eskers and other landforms indicative of meltwater flow could then potentially be used to reconstruct drainage pathways and modes of drainage associated with these lakes. These reconstructions could then be used as analogues for the drainage of present-day subglacial lakes, such as those in Antarctica. This is, of course, rather speculative and relies

on demonstrating that the lakes existed at the time that the meltwater landforms formed. Nevertheless, this presents an interesting area for future research.

2.7.4 Using eskers to test numerical models of meltwater drainage

Numerical models of subglacial meltwater drainage have attempted to encapsulate the behaviour of glacial meltwater in both channelized (e.g. Shreve, 1972) and distributed (e.g. Flowers *et al.*, 2003) systems. Model outcomes are often compared with measured data such as tracer velocities (Schuler & Fischer, 2009) or digital elevation models (e.g. Hagen *et al.*, 2000), to provide a 'real-world' constraint on model parameters. Often, however, important parameters are difficult to measure in subglacial drainage systems and thus are estimated. Sinuosity is one such parameter and is discussed here as an example of how measurement of eskers may be able to support model assumptions. Schuler & Fischer (2009; pp.7) use two arbitrary values for channel sinuosity (S = 2 and S = 3) in their model of diurnal velocity variations in subglacial channels. Sinuosity is important because it is closely related to channel length, width, cross-section, water pressure and discharge (e.g. Leopold *et al.*, 1960; Schuler & Fischer, 2009). For example, Schuler & Fischer (2009) find that modelling higher values of sinuosity in R-channels leads to higher outputs of water pressure. Their model predicts a tentative 'realistic' value of 1.6 for R-channel sinuosity, which they concede is associated with large margins of error and is based on unrealistic assumptions. Preliminary calculations indicate that this may be an over-estimate (see Section 2.5.1.3) as measurements of esker sinuosity suggest values much closer to 1. Further measurements of esker sinuosity could provide a significant contribution to such models as a proxy for meltwater channel sinuosity.

Conversely, some models have been used to *predict* esker spacing (e.g. Boulton *et al.*, 2007a;b; Boulton *et al.*, 2009; Boulton, 2010; Hewitt, 2011). Evidently, accurate mapping of esker locations is the only way that such models could be tested. Esker locations in Fennoscandia have been used to test Boulton's model for esker spacing, the results appearing to support the hypothesis (Boulton *et al.*, 2009). Further analysis of esker spacing from different areas, such as the Laurentide Ice Sheet, where esker spacing has not yet been used to test models, will supplement the work already published and may be used to test Boulton's conclusions.

2.8 Summary

This paper has reviewed the literature on eskers, including their sedimentology, geomorphology, controls on esker patterns and how eskers might be useful as a tool for understanding ice-sheet meltwater drainage. Five main conclusions drawn from the paper are summarised below:

1. Meltwater is an important component of ice-sheet systems and has significant implications for ice dynamics. The difficulty in accessing contemporary ice-sheet beds means that we do not yet fully understand the processes controlling the distribution and movement of meltwater under ice-sheets. Glacial geomorphology has traditionally been used to account for processes that operated in the past but which are difficult to discern in contemporary systems. Thus, because they represent the configuration of the drainage networks of past ice-sheets as they deglaciated, eskers may be able to address problems surrounding ice-sheet meltwater drainage such as how the drainage system operates through deglaciation, how long individual subglacial channels may be, how straight/sinuous they are or to what extent they adhere to bed or surface topography.

2. There is a lack of consensus over a specific definition of the term esker, which at present is poorly defined in the literature. At least 26 different terms for eskers have been described, some of which relate to the same, or overlapping, categories. This makes it difficult to classify eskers, which is a useful goal if an understanding of the large-scale variations in eskers is to be linked to ice-sheet meltwater drainage as well as the controls on the formation and distribution of eskers.

3. Sedimentological and geomorphological investigation of eskers has revealed a wealth of information. Eskers contain a wide variety of sediments which have been used, in some cases, to elucidate specific processes and environments of deposition. The variety of sediments contained in eskers points to complex evolution of different eskers, which is also echoed in the geomorphology of eskers, which take several different forms and exist at a range of scales (from several m to 340 km in length). Few large scale studies of esker patterns have been conducted, though four patterns are apparent in the literature, operating at different scales: eskers radiating away from ice divides; dendritic networks of eskers; anastomosing branches of individual eskers and regularly spaced networks of eskers.

4. Five main controls have been put forward to account for the variations in esker patterns: ice thickness; outburst floods; substrate resistance; interlobate deposition and groundwater flux. No consensus has yet been reached and it is likely that all these controls exert an influence to some extent. Refining and testing these ideas is an important step towards achieving an understanding of what controls large-scale subglacial meltwater processes.

5. Future research directions should include: analysis of the morphometry and large-scale patterns of eskers; further research into what controls the distribution of eskers; research into the extent to which channelized and distributed drainage systems operate at the ice-sheet scale; using eskers to reconstruct drainage between subglacial lakes; using eskers to test numerical models of esker distribution and also to refine subglacial channel parameters currently being used in ice-sheet models.

Section 2.7 identified four areas of potential future research, and this thesis will specifically address three of them, alongside the research questions set out in Chapter 1. Chapters 3 and 4

present the results of large-scale mapping and morphometric analysis of Canadian eskers, addressing the need for such data as described in Section 2.7.1. The data are then used in Chapter 5 to assess the evolution of channelized meltwater drainage systems beneath the Laurentide Ice Sheet as it deglaciated, providing key insights into the role of channelized meltwater drainage at the ice sheet scale (as described in Section2.7.2). Chapters 6 and 7 deal with the controls on esker pattern and morphometry and present the results of work aimed at testing different hypotheses for esker formation, and also numerical models of groundwater controlled esker spacing (Section 2.7.4).

2.9 References

Allen, J. R. L. (1971) A theoretical and experimental study of climbing-ripple cross-lamination, with a field application to the Uppsala esker. *Geografiska Annaler Series A-Physical Geography*, 53, 157-187.

Alley, R. B. (1992) How can low-pressure channels and deforming tills coexist subglacially? *Journal of Glaciology*, 38, 200-207.

Alley, R. B., Blankenship, D. D., Rooney, S. T. & Bentley, C. R. (1989) Water-Pressure Coupling of Sliding and Bed Deformation: III Application to Ice Stream B, Antarctica. *Journal of Glaciology*, 35, 130-139.

Ashley, G. M. (1990) Classification of large-scale subaqueous bedforms: a new look at an old problem. *Journal of Sedimentary Petrology*, 60, 160-172.

Aylsworth, J. M. & Shilts, W. W. (1989) Bedforms of the Keewatin Ice-Sheet, Canada. *Sedimentary Geology*, 62, 407-428.

Banerjee, I. & McDonald, B. C. (1975) Nature of esker sedimentation. In A. V. Jopling and B. C. McDonald, *Glaciofluvial and Glacilacustrine Sedimentation*. Oklahoma, SEPM, 304-320.

Barnett, P., Sharpe, D., Russell, H., Brennand, T., Gorrell, G., Kenny, F. & Pugin, A. (1998) On the origin of the Oak Ridges Moraine. *Canadian Journal of Earth Sciences*, 35, 1152-1167.

Bartholomew, I., Nienow, P., Mair, D., Hubbard, A., King, M. A. & Sole, A. (2010) Seasonal evolution of subglacial drainage and acceleration in a Greenland outlet glacier. *Nature Geoscience*, 3, 408-411.

Beaney, C. L. (2002) Tunnel channels in southeast Alberta, Canada: evidence for catastrophic channelized drainage. *Quaternary International*, 90, 67-74.

Benn, D. I. & Evans, D. J. A. (1996) The interpretation and classification of subglacially-deformed materials. *Quaternary Science Reviews*, 15, 23-52.

Benn, D. I. & Evans, D. J. A. (2010) *Glaciers & glaciation*. London, Hodder Arnold.

Benn, D. I., Gulley, J., Luckman, A., Adamek, A. & Glowacki, P. S. (2009a) Englacial drainage systems formed by hydrologically driven crevasse propagation. *Journal of Glaciology*, 55, 513-523.

Benn, D. I., Kristensen, L. & Gulley, J. D. (2009b) Surge propagation constrained by a persistent subglacial conduit, Bakaninbreen-Paulabreen, Svalbard. *Annals of Glaciology*, 50, 81-86.

Bennett, M. R., Hambrey, M. J. & Huddart, D. (1997) Modification of clast shape in high-Arctic glacial environments. *Journal of Sedimentary Research*, 67, 550-559.

Bird, J. B. (1967) *The physiography of arctic Canada*. Baltimore, Johns Hopkins Press

Björnsson, H. (1986) Delineation of glacier drainage basins on western Vatnajökull. *Annals of Glaciology*, 8, 19–21.

Björnsson, H. (2003) Subglacial lakes and jökulhlaups in Iceland. *Global and Planetary Change*, 35, 255-271.

Bolduc, A. M. (1992) The formation of eskers based on their morphology, stratigraphy and lithologic composition, Labrador, Canada. *Unpublished Ph.D. thesis, Lehigh University*.

Boon, S. & Sharp, M. (2003) The role of hydrologically-driven ice fracture in drainage system evolution on an Arctic glacier. *Geophysical Research Letters*, 30, 1916-1919.

Booth, D. B. & Hallet, B. (1993) Channel networks carved by subglacial water: Observations and reconstruction in the eastern Puget Lowland of Washington. *Bulletin of the Geological Society of America*, 105, 671-683.

Boulton, G. S. (2006) Glaciers and their coupling with hydraulic and sedimentary processes. In P. G. Knight, *Glacier Science and Environmental Change*. Oxford, Blackwell, 3-23.

Boulton, G. S. (2010) Drainage pathways beneath ice sheets and their implications for ice sheet form and flow: the example of the British Ice Sheet during the Last Glacial Maximum. *Journal of Quaternary Science*, 25, 483-500.

Boulton, G. S. & Caban, P. E. (1995) Groundwater flow beneath ice sheets: Part II--Its impact on glacier tectonic structures and moraine formation. *Quaternary Science Reviews*, 14, 563-587.

Boulton, G. S., Caban, P. E. & Van Gijssel, K. (1995) Groundwater flow beneath ice sheets: part I--large scale patterns. *Quaternary Science Reviews*, 14, 545-562.

Boulton, G. S., Dobbie, K. E. & Zatsepin, S. (2001) Sediment deformation beneath glaciers and its coupling to the subglacial hydraulic system. *Quaternary International*, 86, 3-28.

Boulton, G. S. & Hagdorn, M. (2006) Glaciology of the British Isles Ice Sheet during the last glacial cycle: form, flow, streams and lobes. *Quaternary Science Reviews*, 25, 3359-3390.

Boulton, G. S., Hagdorn, M. & Hulton, N. R. J. (2003) Streaming flow in an ice sheet through a glacial cycle. *Annals of Glaciology*, 36, 117-128.

Boulton, G. S., Hagdorn, M., Maillot, P. B. & Zatsepin, S. (2009) Drainage beneath ice sheets: groundwater-channel coupling, and the origin of esker systems from former ice sheets. *Quaternary Science Reviews*, 28, 621-638.

Boulton, G. S. & Hindmarsh, R. C. A. (1987) Sediment deformation beneath glaciers: rheology and geological consequences. *Journal of Geophysical Research*, 92, 9059-9082.

Boulton, G. S., Lunn, R., Vidstrand, P. & Zatsepin, S. (2007a) Subglacial drainage by groundwater-channel coupling, and the origin of esker systems: Part I-glaciological observations. *Quaternary Science Reviews*, 26, 1067-1090.

Boulton, G. S., Lunn, R., Vidstrand, P. & Zatsepin, S. (2007b) Subglacial drainage by groundwater-channel coupling, and the origin of esker systems: part II-theory and simulation of a modern system. *Quaternary Science Reviews*, 26, 1091-1105.

Boulton, G. S., Van der Meer, J. J. M., Beets, D. J., Hart, J. K. & Ruegg, G. H. J. (1999) The sedimentary and structural evolution of a recent push moraine complex: Holmstrømbreen, Spitsbergen. *Quaternary Science Reviews*, 18, 339-371.

Brennand, T. A. (1994) Macroforms, large bedforms and rhythmic sedimentary sequences in subglacial eskers, south-central Ontario - implications for esker genesis and meltwater regime. *Sedimentary Geology*, 91, 9-55.

Brennand, T. A. (2000) Deglacial meltwater drainage and glaciodynamics: inferences from Laurentide eskers, Canada. *Geomorphology*, 32, 263-293.

Brennand, T. A., Russell, H. A. J. & Sharpe, D. R. (2007) Tunnel Channel Character and Evolution in Central Southern Ontario. In P. G. Knight, *Glacier Science and Environmental Change*. Malden, M.A., Blackwell Publishing, 37-39.

Brennand, T. A. & Shaw, J. (1994) Tunnel channels and associated landforms, south-central Ontario: their implications for ice-sheet hydrology. *Canadian Journal of Earth Sciences*, 31, 505-522.

Brennand, T. A. & Shaw, J. (1996) The Harricana glaciofluvial complex, Abitibi region, Quebec: its genesis and implications for meltwater regime and ice-sheet dynamics. *Sedimentary Geology*, 102, 221-262.

Brennand, T. A., Shaw, J. & Sharpe, D. R. (1996) Regional-scale meltwater erosion and deposition patterns, northern Quebec, Canada. *Annals of Glaciology*, 22, 85-92.

Burke, M. J., Brennand, T. A. & Perkins, A. J. (2012) Transient subglacial hydrology of a thin ice sheet: insights from the Chasm esker, British Columbia, Canada. *Quaternary Science Reviews*, 58, 30-55.

Burke, M. J., Woodward, J. & Russell, A. J. (2010a) Sedimentary architecture of large-scale, jökulhlaup-generated, ice-block obstacle marks: Examples from Skeiðarársandur, SE Iceland. *Sedimentary Geology*, 227, 1-10.

Burke, M. J., Woodward, J., Russell, A. J. & Fleisher, P. J. (2009) Structural controls on englacial esker sedimentation: Skeiðarárjökull, Iceland. *Annals of Glaciology*, 50, 85-92.

Burke, M. J., Woodward, J., Russell, A. J., Fleisher, P. J. & Bailey, P. K. (2008) Controls on the sedimentary architecture of a single event englacial esker: Skeiðarárjökull, Iceland. *Quaternary Science Reviews*, 27, 1829-1847.

Burke, M. J., Woodward, J., Russell, A. J., Fleisher, P. J. & Bailey, P. K. (2010b) The sedimentary architecture of outburst flood eskers: A comparison of ground-penetrating radar data from Bering Glacier, Alaska and Skeiðarárjökull, Iceland. *Bulletin of the Geological Society of America*, 122, 1637-1645.

Carter, C. L., Dethier, D. P. & Newton, R. L. (2003) Subglacial environment inferred from bedrock-coating siltskins, Mendenhall Glacier, Alaska, USA. *Journal of Glaciology*, 49, 568-576.

Catania, G. A. & Neumann, T. A. (2010) Persistent englacial drainage features in the Greenland Ice Sheet. *Geophysical Research Letters*, 37, L02501.

Cheel, R. (1982) The depositional history of an esker near Ottawa, Canada. *Canadian Journal of Earth Sciences*, 19, 1417-1427.

Christoffersen, P., Piotrowski, J. A. & Larsen, N. K. (2005) Basal processes beneath an Arctic glacier and their geomorphic imprint after a surge, Elisebreen, Svalbard. *Quaternary Research*, 64, 125-137.

Christoffersen, P., Tulaczyk, S., Wattrus, N. J., Peterson, J., Quintana-Krupinski, N., Clark, C. D. & Sjunneskog, C. (2008) Large subglacial lake beneath the Laurentide Ice Sheet inferred from sedimentary sequences. *Geology*, 36, 563-566.

Clapperton, C. M. (1971) The Pattern of Deglaciation in Part of North Northumberland. *Transactions of the Institute of British Geographers*, 53, 67-78.

Clark, C. D. (1993) Mega-scale glacial lineations and cross-cutting ice-flow landforms. *Earth Surface Processes and Landforms*, 18, 1-29.

Clark, C. D., Evans, D. J. A., Khatwa, A., Bradwell, T., Jordan, C., Marsh, S., Mitchell, W. & Bateman, M. (2004) Map and GIS database of glacial landforms and features related to the last British Ice Sheet. *Boreas*, 33, 359-375.

Clark, C. D., Hughes, A. L. C., Greenwood, S. L., Jordan, C. & Sejrup, H. P. (2012) Pattern and timing of retreat of the last British-Irish Ice Sheet. *Quaternary Science Reviews*, 44, 112-146.

Clark, C. D., Hughes, A. L. C., Greenwood, S. L., Spagnolo, M. & Ng, F. S. L. (2009) Size and shape characteristics of drumlins, derived from a large sample, and associated scaling laws. *Quaternary Science Reviews*, 28, 677-692.

Clark, C. D., Knight, J. K. & T Gray, J. (2000) Geomorphological reconstruction of the Labrador sector of the Laurentide Ice Sheet. *Quaternary Science Reviews*, 19, 1343-1366.

Clark, P. U. & Walder, J. S. (1994) Subglacial drainage, eskers, and deforming beds beneath the Laurentide and Eurasian ice sheets. *Bulletin of the Geological Society of America*, 106, 304-314.

Clayton, L., Attig, J. W. & Mickelson, D. M. (1999) Tunnel channels formed in Wisconsin during the last glaciation. *Geological Society of America Special Papers*, 337, 69-82.

Cuffey, K. M. & Paterson, W. S. B. (2010) *The physics of glaciers*. Amsterdam ; London, Butterworth-Heinemann.

Cummings, D. I., Gorrell, G., Guilbault, J.-P., Hunter, J. A., Logan, C., Ponomarenko, D., André, J.-M. P., Pullan, S. E., Russell, H. A. J. & Sharpe, D. R. (2011a) Sequence stratigraphy of a glaciated basin fill, with a focus on esker sedimentation. *Geological Society of America Bulletin*, 123, 1478-1496.

Cummings, D. I., Kjarsgaard, B. A., Russell, H. A. J. & Sharpe, D. R. (2011b) Eskers as mineral exploration tools. *Earth-Science Reviews*, 109, 32-43.

Das, S. B., Joughin, I., Behn, M. D., Howat, I. M., King, M. A., Lizarralde, D. & Bhatia, M. P. (2008) Fracture Propagation to the Base of the Greenland Ice Sheet During Supraglacial Lake Drainage. *Science*, 320, 778-781.

Delaney, C. (2001) Esker formation and the nature of deglaciation: the Ballymahon esker, Central Ireland. *North West Geography*, 1, 23-33.

Donner, J. J. (1965) The Quaternary of Finland. In K. Rankama, *The Quaternary*. New York, Interscience, 199-272.

Dunlop, P. & Clark, C. D. (2006) The morphological characteristics of ribbed moraine. *Quaternary Science Reviews*, 25, 1668-1691.

Dyke, A. S. (1993) Landscapes of cold-centred Late Wisconsinan ice caps, Arctic Canada. *Progress in Physical Geography*, 17, 223-247.

Dyke, A. S. & Dredge, L. A. (1989) Quaternary geology of the northwestern Canadian Shield. In R. J. Fulton, *Quaternary geology of Canada and Greenland*. Ottawa, Geological Survey of Canada, 189-214.

Dyke, A. S., Moore, A. & Robertson, L. (2003) Deglaciation of North America. *Geological Survey of Canada, Open File*, 1574.

Embleton, C. & King, C. A. M. (1975) *Glacial geomorphology*. London, Edward Arnold.

Evans, D. J. A. (2011) Glacial landsystems of Satujökull, Iceland: A modern analogue for glacial landsystem overprinting by mountain icecaps. *Geomorphology*, 129, 225-237.

Evans, D. J. A., Nelson, C. D. & Webb, C. (2010) An assessment of fluting and "till esker" formation on the foreland of Sandfellsjokull, Iceland. *Geomorphology*, 114, 453-465.

Evans, D. J. A. & Rea, B. R. (1999) Geomorphology and sedimentology of surging glaciers: a land-systems approach. *Annals of Glaciology*, 28, 75-82.

Evans, D. J. A. & Rea, B. R. (2003) Surging Glacier Landsystem. In D. J. A. Evans, *Glacial Landsystems*. London, Hodder Arnold, 259-288.

Evans, D. J. A., Rea, B. R., Hiemstra, J. F. & Ó Cofaigh, C. (2006) A critical assessment of subglacial mega-floods: a case study of glacial sediments and landforms in south-central Alberta, Canada. *Quaternary Science Reviews*, 25, 1638-1667.

Evans, D. J. A., Twigg, D. R., Rea, B. R. & Shand, M. (2007) Surficial geology and geomorphology of the Brúarjökull surging glacier landsystem. *Journal of Maps*, 2007, 349-367.

Evatt, G. W., Fowler, A. C., Clark, C. D. & Hulton, N. R. J. (2006) Subglacial floods beneath ice sheets. *Philosophical Transactions of the Royal Society A: Mathematical, Physical and Engineering Sciences*, 364, 1769-1794.

Fard, A. M. (2001) Morphology of subglacial conduit deposits: control by bedrock topography, discharge flow variation, or both? A cautionary case study: Axelsberg, Nynäshamn, south central Sweden. *Global and Planetary Change*, 28, 145-161.

Fard, A. M. (2002) Large dead-ice depressions in flat-topped eskers: evidence of a Preboreal jökulhlaup in the Stockholm area, Sweden. *Global and Planetary Change*, 35, 273-295.

Fard, A. M. & Gruszka, B. (2007) Subglacial conditions in a branching Saalian esker in north-central Poland. *Sedimentary Geology*, 193, 33-46.

Fitzsimons, S. J. (1991) Supraglacial eskers in Antarctica. *Geomorphology*, 4, 293-299.

Flint, R. F. (1971) *Glacial and Quaternary geology*. New York, Wiley.

Flowers, G. E., Bjornsson, H. & Palsson, F. (2003) New insights into the subglacial and periglacial hydrology of Vatnajokull, Iceland, from a distributed physical model. *Journal of Glaciology*, 49, 257-270.

Flowers, G. E. & Clarke, G. K. C. (1999) Surface and bed topography of Trapridge Glacier, Yukon Territory, Canada: digital elevation models and derived hydraulic geometry. *Journal of Glaciology*, 45, 165-174.

Fountain, A. G., Jacobel, R. W., Schlichting, R. & Jansson, P. (2005a) Fractures as the main pathways of water flow in temperate glaciers. *Nature*, 433, 618-621.

Fountain, A. G., Schlichting, R. B., Jansson, P. & Jacobel, R. W. (2005b) Observations of englacial water passages: a fracture-dominated system. *Annals of Glaciology*, 40, 25-30.

Fountain, A. G. & Walder, J. S. (1998) Water flow through temperate glaciers. *Reviews of Geophysics*, 36, 299-328.

Goldthwait, L. (1939) Esker chains of the Attleboro, Massachusetts, district. *American Journal of Science*, 237, 110-115.

Gorrell, G. & Shaw, J. (1991) Deposition in an esker, bead and fan complex, Lanark, Ontario, Canada. *Sedimentary Geology*, 72, 285-314.

Gravenor, C. P. (1957) *Surficial Geology of the Lindsay-Peterborough Area, Ontario, Victoria, Peterborough, Durham, and Northumberland Counties, Ontario*, E. Cloutier.

Guðmundsson, M. T., Sigmundsson, F. & Björnsson, H. (1997) Ice-volcano interaction of the 1996 Gjálp subglacial eruption, Vatnajökull, Iceland. *Nature*, 389, 954-957.

Gulley, J. D., Benn, D. I., Screaton, E. & Martin, J. (2009) Mechanisms of englacial conduit formation and their implications for subglacial recharge. *Quaternary Science Reviews*, 28, 1984-1999.

Hagen, J. O., Etzelmuller, B. & Nuttall, A. M. (2000) Runoff and drainage pattern derived from digital elevation models, Finsterwalderbreen, Svalbard. *Annals of Glaciology*, 31, 147-152.

Hallet, B. & Anderson, R. (1980) Detailed glacial geomorphology of a proglacial bedrock area at Castleguard Glacier, Alberta, Canada. *Zeitschrift für Gletscherkunde und Glazialgeologie*, 16, 171-184.

Hättestrand, C. & Clark, C. D. (2006) The glacial geomorphology of Kola Peninsula and adjacent areas in the Murmansk Region, Russia. *Journal of Maps*, 30, 30-42.

Hättestrand, C. & Kleman, J. (1999) Ribbed moraine formation. *Quaternary Science Reviews*, 18, 43-61.

Hebrand, M. & Åmark, M. (1989) Esker formation and glacier dynamics in eastern Skane and adjacent areas, southern Sweden. *Boreas*, 18, 67-81.

Hewitt, I. J. (2011) Modelling distributed and channelized subglacial drainage: the spacing of channels. *Journal of Glaciology*, 57, 302-314.

Hillier, J. K., Smith, M. J., Clark, C. D., Stokes, C. R. & Spagnolo, M. (2013) Subglacial bedforms reveal an exponential size-frequence distribution. *Geomorphology*, 190, 82-91.

Hooke, R. L. (1984) On the role of mechanical energy in maintaining subglacial water conduits at atmospheric pressure. *Journal of Glaciology*, 30, 180-187.

Hooke, R. L. & Fastook, J. (2007) Thermal conditions at the bed of the Laurentide ice sheet in Maine during deglaciation: implications for esker formation. *Journal of Glaciology*, 53, 646-658.

Hooke, R. L. & Jennings, C. E. (2006) On the formation of the tunnel valleys of the southern Laurentide ice sheet. *Quaternary Science Reviews*, 25, 1364-1372.

Hooke, R. L. B. (2005) *Principles of glacier mechanics*. Cambridge, Cambridge Univ Pr.

Howarth, P. J. (1971) Investigations of two eskers at eastern Breiðamerkurjökull, Iceland. *Arctic and Alpine Research*, 3, 305-318.

Huddart, D., Bennett, M. R. & Glasser, N. F. (1999) Morphology and sedimentology of a high-arctic esker system: Vegbreen, Svalbard. *Boreas*, 28, 253-273.

Iken, A. & Truffer, M. (1997) The relationship between subglacial water pressure and velocity of Findelengletscher, Switzerland, during its advance and retreat. *Journal of Glaciology*, 43, 328-338.

Inman, M. (2005) The plan to unlock Lake Vostok. *Science*, 310, 611-612.

Jansson, K. N. (2005) Map of the glacial geomorphology of north-central Québec-Labrador, Canada. *Journal of Maps*, 2005, 46-55.

Jansson, K. N., Kleman, J. & Marchant, D. R. (2002) The succession of ice-flow patterns in north-central Québec-Labrador, Canada. *Quaternary Science Reviews*, 21, 503-523.

Kehew, A. E., Piotrowski, J. A. & Jørgensen, F. (2012) Tunnel valleys: Concepts and controversies — A review. *Earth-Science Reviews*, 113, 33-58.

King, C. A. M. & Buckley, J. T. (1968) The analysis of stone size amd shape in Arctic environments. *Journal of Sedimentary Petrology*, 38, 200-214.

Kleman, J. (1992) The Palimpsest Glacial Landscape in Northwestern Sweden. Late Weichselian Deglaciation Landforms and Traces of Older West-Centered Ice Sheets. *Geografiska Annaler. Series A, Physical Geography*, 74, 305-325.

Knight, J. & McCabe, A. M. (1997) Identification and significance of ice flow transverse subglacial ridges (Rogen moraines) in northern central Ireland. *Journal of Quaternary Science*, 12, 519-524.

Knudsen, Ó. (1995) Concertina eskers, Brúarjökull, Iceland: An indicator of surge-type glacier behaviour. *Quaternary Science Reviews*, 14, 487-493.

Lauriol, B. & Gray, J. T. (1987) The decay and disappearance of the late Wisconsin ice sheet in the Ungava peninsula, northern Quebec, Canada. *Arctic and Alpine Research*, 19, 109-126.

Leopold, L. B., Bagnold, R. A., Wolman, M. G. & Brush, L. M. J. (1960) Flow resistance in sinuous or irregular channels. *U.S. Geological Survey Professional Paper*, 282-D, 111-134.

Lindström, E. (1993) Esker enlargements in northern Sweden. *Geografiska Annaler Series A - Physical Geography*, 75, 95-110.

Livingstone, S. J., Clark, C. D. & Tarasov, L. (2013) Modelling North American palaeo-subglacial lakes and their meltwater drainage pathways. *Earth and Planetary Science Letters*, 375, 13-33.

Livingstone, S. J., Evans, D. J. A., Ó Cofaigh, C. & Hopkins, J. (2010) The Brampton kame belt and Pennine escarpment meltwater channel system (Cumbria, UK): Morphology, sedimentology and formation. *Proceedings of the Geologists' Association*, 121, 423-443.

Livingstone, S. J., Ó Cofaigh, C., Stokes, C. R., Hillenbrand, C.-D., Vieli, A. & Jamieson, S. S. R. (2012) Antarctic palaeo-ice streams. *Earth-Science Reviews*, 111, 90-128.

Lliboutry, L. A. (1969) Contribution à la théorie des ondes glaciaires. *Canadian Journal of Earth Sciences*, 6, 943-956.

Lundqvist, J. (1999) Scandinavian eskers, global climatic relationships, and solar forcing. *Geological Quarterly*, 43, 149-152.

Lundqvist, J. A. N. (1997) Structure and rhythmic pattern of glaciofluvial deposits north of Lake Vänern, south-central Sweden. *Boreas*, 26, 127-140.

Makaske, B. (2001) Anastomosing rivers: a review of their classification, origin and sedimentary products. *Earth-Science Reviews*, 53, 149-196.

Mäkinen, J. (2003) Time-transgressive deposits of repeated depositional sequences within interlobate glaciofluvial (esker) sediments in Koylio, SW Finland. *Sedimentology*, 50, 327-360.

Mannerfelt, C. M. (1945) Nagra glacialmorfologiska formelement. *Geografiska Annaller*, 27, 1-239.

Margold, M., Jansson, K. N., Kleman, J. & Stroeven, A. P. (2013a) Lateglacial ice dynamics of the Cordilleran Ice Sheet in northern British Columbia and southern Yukon Territory: retreat pattern of the Liard Lobe reconstructed from the glacial landform record. *Journal of Quaternary Science*, 28, 180-188.

Margold, M., Jansson, K. N., Kleman, J., Stroeven, A. P. & Clague, J. J. (2013b) Retreat pattern of the Cordilleran Ice Sheet in central British Columbia at the end of the last glaciation reconstructed from glacial meltwater landforms. *Boreas*, n/a-n/a.

McCabe, A. M. (2008) *Glacial geology and geomorphology*. Edinburgh, Dunedin Academic Press Ltd.

McDonald, B. C. & Shilts, W. W. (1975) Interpretation of faults in glaciofluvial sediments. In A. V. Jopling and B. C. McDonald, *Glaciofluvial and Glacilacustrine sedimentation*. Oklahoma, SEPM, 123-131.

McMartin, I. & Henderson, P. J. (2004) Evidence from Keewatin (central Nunavut) for paleo-ice divide migration. *Géographie physique et Quaternaire*, 58, 163-186.

McMillan, M., Corr, H., Shepherd, A., Ridout, A., Laxon, S. & Cullen, R. (2013) Three-dimensional mapping by CryoSat-2 of subglacial lake volume changes. *Geophysical research letters*, n/a-n/a.

Menzies, J. & Shilts, W. W. (1996) Subglacial environments. In J. Menzies, *Past glacial environments, sediments, forms and techniques*. Oxford, Butterworth/Heinemann. 2, 15-136.

Mernild, S. H. (2006) The internal drainage system of the lower Mittivakkat Glacier, Ammassalik Island, SE Greenland. *Geografisk Tidsskrift, Danish Journal of Geography*, 106, 13-24.

Metzger, S. M. (1992) The eskers of New York state: Formation process implications and esker-like features on the planet Mars. *Abstracts of the Lunar and Planetary Science Conference*, 23, 901.

Mills, H. H. (1977) Differentiation of glacier environments by sediment characteristics; Athabasca Glacier, Alberta, Canada. *Journal of Sedimentary Research*, 47, 728-737.

Munro-Stasiuk, M. J. (1999) Evidence for water storage and drainage at the base of the Laurentide ice sheet, south-central Alberta, Canada. *Annals of Glaciology*, 28, 175-180.

Munro-Stasiuk, M. J. (2003) Subglacial Lake McGregor, south-central Alberta, Canada. *Sedimentary Geology*, 160, 325-350.

Ng, F. S. L. (2000) Canals under sediment-based ice sheets. *Annals of Glaciology*, 30, 146-152.

Nienow, P. W., Sharp, M. & Willis, I. C. (1996) Velocity-discharge relationships derived from dye tracer experiments in glacial meltwaters: implications for subglacial flow conditions. *Hydrological Processes*, 10, 1411-1426.

Nye, J. F. (1970) Glacier Sliding Without Cavitation in a Linear Viscous Approximation. *Proceedings of the Royal Society of London. A. Mathematical and Physical Sciences*, 315, 381-403.

Nye, J. F. (1973) Water at the bed of a glacier. *International Association of Scientific Hydrology Publication*, 95, 189-194.

Nygard, A., Sejrup, H. P., Haflidason, H., Cecchi, M. & Ottesen, D. A. G. (2004) Deglaciation history of the southwestern Fennoscandian Ice Sheet between 15 and 13 14C ka BP. *Boreas*, 33, 1-17.

Ó Cofaigh, C. (1996) Tunnel valley genesis. *Progress in Physical Geography*, 20, 1-19.

Ó Cofaigh, C., Dowdeswell, J. A., King, E. C., Anderson, J. B., Clark, C. D., Evans, D. J. A., Evans, J., Hindmarsh, R. C. A., Larter, R. D. & Stokes, C. R. (2010) Comment on Shaw J., Pugin, A. and Young, R. (2008): "A meltwater origin for Antarctic shelf bedforms with special attention to megalineations", Geomorphology 102, 364-375. *Geomorphology*, 117, 195-198.

Petrie, G. & Price, R. (1966) Photogrammetric measurements of the ice wastage and morphological changes near the Casement glacier, Alaska. *Canadian Journal of Earth Sciences*, 3, 827-840.

Piotrowski, J. A. (1997) Subglacial hydrology in north-western Germany during the last glaciation: groundwater flow, tunnel valleys and hydrological cycles. *Quaternary Science Reviews*, 16, 169-185.

Prest, V. K., Grant, D. R. & Rampton, V. N. (1968) Glacial map of Canada. Geological Survey of Canada, Map 1253A. 1:5,000,000

Price, R. J. (1965) The changing proglacial environment of the Casement Glacier, Glacier Bay, Alaska. *Transactions of the Institute of British Geographers*, 36, 107-116.

Price, R. J. (1966) Eskers near the Casement glacier, Alaska. *Geografiska Annaler. Series A. Physical Geography*, 48, 111-125.

Price, R. J. (1969) Moraines, sandar, kames and eskers near Breiðamerkurjökull , Iceland. *Transactions of the Institute of British Geographers*, 46, 17-43.

Price, R. J. (1973) *Glacial and fluvioglacial landforms*. Edinburgh, Oliver and Boyd.

Pugin, A., Pullan, S. E. & Sharpe, D. R. (1996) Observations of tunnel channels in glacial sediments with shallow land-based seismic reflection. *Annals of Glaciology*, 22, 176-180.

Pugin, A., Pullan, S. E. & Sharpe, D. R. (1999) Seismic facies and regional architecture of the Oak Ridges Moraine area, southern Ontario. *Canadian Journal of Earth Sciences*, 36, 409-432.

Punkari, M. (1980) The ice lobes of the Scandinavian ice sheet during the deglaciation in Finland. *Boreas*, 9, 307-310.

Punkari, M. (1997) Glacial and glaciofluvial deposits in the interlobate areas of the Scandinavian Ice Sheet. *Quaternary Science Reviews*, 16, 741-753.

Rampton, V. (2000) Large-scale effects of subglacial meltwater flow in the southern Slave Province, Northwest Territories, Canada. *Canadian Journal of Earth Sciences*, 37, 81-93.

Rea, B. R. & Evans, D. J. A. (2011) An assessment of surge-induced crevassing and the formation of crevasse squeeze ridges. *Journal of Geophysical Research*, 116, F04005.

Rempel, A. W. (2009) Effective stress profiles and seepage flows beneath glaciers and ice sheets. *Journal of Glaciology*, 55, 431-443.

Ringrose, S. (1982). *Depositional processes in the development of eskers in Manitoba*. Research in Glacial, Glacio-Fluvial and Glacio-Lacustrine Systems., Proceedings of the 6th Guelph Symposium on Geomorphology, 1980.

Rippin, D., Willis, I., Arnold, N., Hodson, A., Moore, J., Kohler, J. & Bjornsson, H. (2003) Changes in geometry and subglacial drainage of Midre Lovenbreen, Svalbard, determined from digital elevation models. *Earth Surface Processes and Landforms*, 28, 273-298.

Roberts, M. J., Russell, A. J., Tweed, F. S. & Knudsen, Ó. (2000) Ice fracturing during jökulhlaups: implications for englacial floodwater routing and outlet development. *Earth Surface Processes and Landforms*, 25, 1429-1446.

Röthlisberger, H. (1972) Water pressure in intra-and subglacial channels. *Journal of Glaciology*, 11, 177-203.

Russell, A. J., Gregory, A. R., Large, A. R. G., Fleisher, P. J. & Harris, T. D. (2007) Tunnel channel formation during the November 1996 jokulhlaup, Skeiðarárjökull, Iceland *Annals of Glaciology*, 45, 95-103.

Russell, A. J. & Knudsen, Ó. (1999) An ice-contact rhythmite (turbidite) succession deposited during the November 1996 catastrophic outburst flood (jökulhlaup), Skei[z.eth]arárjökull, Iceland. *Sedimentary Geology*, 127, 1-10.

Russell, A. J., Knudsen, O., Fay, H., Marren, P. M., Heinz, J. & Tronicke, J. (2001) Morphology and sedimentology of a giant supraglacial, ice-walled, jokulhlaup channel, Skeiðarárjökull, Iceland: implications for esker genesis. *Global and Planetary Change*, 28, 193-216.

Russell, A. J., Roberts, M. J., Fay, H., Marren, P. M., Cassidy, N. J., Tweed, F. S. & Harris, T. (2006) Icelandic jökulhlaup impacts: implications for ice-sheet hydrology, sediment transfer and geomorphology. *Geomorphology*, 75, 33-64.

Russell, H. A. J. & Arnott, R. W. C. (2003) Hydraulic-jump and hyperconcentrated-flow deposits of a glacigenic subaqueous fan: Oak Ridges Moraine, Southern Ontario, Canada. *Journal of Sedimentary Research*, 73, 887-905.

Russell, H. A. J., Arnott, R. W. C. & Sharpe, D. R. (2003) Evidence for rapid sedimentation in a tunnel channel, Oak Ridges Moraine, southern Ontario, Canada. *Sedimentary Geology*, 160, 33-55.

Russell, H. A. J., Sharpe, D. R. & Arnott, R. W. C. (1998) Sedimentology of the Oak Ridges Moraine, Humber River watershed, southern Ontario: a preliminary report. *Geological Survey of Canada*, Current research -1998C, 155-166.

Saarnisto, M. & Saarinen, T. (2001) Deglaciation chronology of the Scandinavian Ice Sheet from the Lake Onega Basin to the Salpausselkä End Moraines. *Global and Planetary Change*, 31, 387-405.

Saunderson, H. C. (1977) Sliding bed facies in esker sands and gravels: a criterion for full-pipe (tunnel) flow? *Sedimentology*, 24, 623-638.

Schomacker, A. & Kjær, K. H. (2008) Quantification of dead ice melting in ice cored moraines at the high Arctic glacier Holmströmbreen, Svalbard. *Boreas*, 37, 211-225.

Schuler, T. V. & Fischer, U. H. (2009) Modeling the diurnal variation of tracer transit velocity through a subglacial channel. *Journal of Geophysical Research*, 114, F04017.

Schumm, S. (1963) Sinuosity of alluvial rivers on the Great Plains. *Geological Society of America Bulletin*, 74, 1089-1100.

Sharp, M. (1985) "Crevasse-Fill" Ridges: A Landform Type Characteristic of Surging Glaciers? *Geografiska Annaler. Series A, Physical Geography*, 67, 213-220.

Sharp, M., Gemmell, J. C. & Tison, J. L. (1989) Structure and stability of the former subglacial drainage system of the Glacier de Tsanfleuron, Switzerland. *Earth Surface Processes and Landforms*, 14, 119-134.

Sharp, M., Richards, K., Willis, I., Arnold, N., Nienow, P., Lawson, W. & Tison, J. L. (1993) Geometry, bed topography and drainage system structure of the Haut Glacier d'Arolla, Switzerland. *Earth Surface Processes and Landforms*, 18, 557-571.

Sharpe, D. R., Barnett, P. J., Brennand, T. A., Finley, D., Gorrell, G., Russell, H. A. J. & Stacey, P. (1997) Surficial geology of the Greater Toronto and Oak Ridges Moraine area, southern Ontario. *Geological Survey of Canada, Open File*, 3062.

Sharpe, D. R., Russell, H. A. J. & Logan, C. (2007) A 3-dimensional geological model of the Oak Ridges Moraine area, Ontario, Canada. *Journal of Maps*, 2007, 239-253.

Shaw, J. (1972) Sedimentation in the ice contact environment, with examples from Shropshire (England). *Sedimentology*, 18, 23-62.

Shilts, W. W. (1984) Esker sedimentation models, Deep Rose Lake map area, District of Keewatin. *Geological Survey of Canada, Paper*, 84-1B, 217-222.

Shilts, W. W., Aylsworth, J. M., Kaszycki, C. A. & Klassen, R. A. (1987) Canadian Shield. In W. L. Graf, *Geomorphic Systems of North America*. Boulder, Colorado, Geological Society of America, Centennial Special Volume. 2, 119-161.

Shreve, R. L. (1972) Movement of water in glaciers. *Journal of Glaciology*, 11, 205-214.

Shreve, R. L. (1985a) Esker characteristics in terms of glacier physics, Katahdin esker system, Maine. *Bulletin of the Geological Society of America*, 96, 639-646.

Shreve, R. L. (1985b) Late Wisconsin ice-surface profile calculated from esker paths and types, Katahdin esker system, Maine. *Quaternary Research*, 23, 27-37.

Siegert, M., Behar, A., Bentley, M., Blake, D., Bowden, S., Christoffersen, P., Cockell, C., Corr, H., Cullen, D. & Edwards, H. (2007) Exploration of Ellsworth Subglacial Lake: a concept paper on the development, organisation and execution of an experiment to explore, measure and sample the environment of a West Antarctic subglacial lake. *Reviews in Environmental Science and Biotechnology*, 6, 161-179.

Siegert, M. J., Clarke, R. J., Mowlem, M., Ross, N., Hill, C. S., Tait, A., Hodgson, D., Parnell, J., Tranter, M. & Pearce, D. (2012) Clean access, measurement, and sampling of Ellsworth Subglacial Lake: A method for exploring deep Antarctic subglacial lake environments. *Reviews of Geophysics*, 50, RG10003.

Sissons, J. B. (1958) Sub-glacial stream erosion in Southern Northumberland. *Scottish Geographical Magazine*, 74, 163-174.

Sohn, Y. K. (1997) On traction-carpet sedimentation. *Journal of Sedimentary Research*, 67, 502-509.

Spagnolo, M., Clark, C. D. & Hughes, A. L. C. (2012) Drumlin relief. *Geomorphology*, 153–154, 179-191.

Spagnolo, M., Clark, C. D., Hughes, A. L. C. & Dunlop, P. (2011) The topography of drumlins; assessing their long profile shape. *Earth Surface Processes and Landforms*, 36, 790-804.

Spagnolo, M., Clark, C. D., Hughes, A. L. C., Dunlop, P. & Stokes, C. R. (2010) The planar shape of drumlins. *Sedimentary Geology*, 232, 119-129.

Spooner, I. & Dalrymple, R. (1993) Sedimentary facies relationships in esker-ridge/esker-fan complexes, southeastern ontario, Canada: Application to the exploration for asphalt blending sand. *Quaternary International*, 20, 81-92.

St-Onge, D. A. (1984) Surficial deposits of the Redrock Lake area, District of Mackenzie. *Current research: part A. Geological Survey of Canada Paper*, 84-01A, 271-278.

Stokes, C. R., Clark, C. D. & Storrar, R. (2009) Major changes in ice stream dynamics during deglaciation of the north-western margin of the Laurentide Ice Sheet. *Quaternary Science Reviews*, 28, 721-738.

Stokes, C. R., Spagnolo, M., Clark, C. D., O'Cofaigh, C., Lian, O. B. & Dunstone, R. B. (2013) Formation of mega-scale glacial lineations on the Dubawnt Lake Ice Stream bed: 1. size, shape and spacing from a large remote sensing dataset. *Quaternary Science Reviews*, 77, 190-209.

Stone, G. H. (1899) *The glacial gravels of Maine and their associated deposits*, US Geological Survey.

Storrar, R. D. & Stokes, C. R. (2007) A Glacial Geomorphological Map of Victoria Island, Canadian Arctic. *Journal of Maps*, 3, 191-210.

Sugden, D. E. (1970) Landforms of deglaciation in the Cairngorm Mountains, Scotland. *Transactions of the Institute of British Geographers*, 51, 201-219.

Sugden, D. E. & John, B. S. (1976) *Glaciers and landscape : a geomorphological approach*. London, Edward Arnold.

Sutinen, R., Jakonen, M., Liwata, P. & Hyvönen, E. (2007) Late Weichselian sheetflow drainage of subglacial Lokka ice lake. *Applied Quaternary research in the central part of glaciated terrain*, 55.

Syverson, K. M., Gaffield, S. J. & Mickelson, D. M. (1994) Comparison of esker morphology and sedimentology with former ice-surface topography, Burroughs Glacier, Alaska. *Geological Society of America Bulletin*, 106, 1130-1142.

Tarasov, L., Dyke, A. S., Neal, R. M. & Peltier, W. R. (2012) A data-calibrated distribution of deglacial chronologies for the North American ice complex from glaciological modeling. *Earth and Planetary Science Letters*, 315–316, 30-40.

Thomas, G. (1984) Sedimentation of a sub-aqueous esker-delta at Strabathie, Aberdeenshire. *Scottish Journal of Geology*, 20, 9.

Thome, K. N. (1986) Melt-water drainage pattern of composite glaciers. *Journal of Glaciology*, 32, 95-100.

Todd, S. P. (1989) Stream driven, high density gravelly traction carpets: possible deposits in the Trabeg Conglomerate Formation, SW Ireland and some theoretical considerations of their origin. *Sedimentology*, 36, 513-530.

UNESCO (1967-1980) International Quaternary map of Europe. 1:2,500,000

Utting, D. J., Ward, B. C. & Little, E. C. (2009) Genesis of hummocks in glaciofluvial corridors near the Keewatin Ice Divide, Canada. *Boreas*, 38, 471-481.

Vaughan, D. G., Corr, H. F. J., Smith, A. M., Pritchard, H. D. & Shepherd, A. (2008) Flow-switching and water piracy between Rutford Ice Stream and Carlson Inlet, West Antarctica. *Journal of Glaciology*, 54, 41-48.

Vivian, R. & Bocquet, G. (1973) Subglacial cavitation phenomena under the glacier d'Argentière, Mont Blanc, France. *Journal of Glaciology*, 12, 439-451.

Walder, J. & Hallet, B. (1979) Geometry of former subglacial water channels and cavities. *Journal of Glaciology*, 23, 335-346.

Walder, J. S. & Fowler, A. (1994) Channelized subglacial drainage over a deformable bed. *Journal of Glaciology*, 40, 3-15.

Warren, W. P. & Ashley, G. M. (1994) Origins of the ice-contact stratified ridges (eskers) of Ireland. *Journal of Sedimentary Research*, 64, 433-499.

Weertman, J. (1964) The theory of glacier sliding. *Journal of Glaciology*, 5, 287-303.

Weertman, J. (1969) Water lubrication mechanism of glacier surges. *Canadian Journal of Earth Sciences*, 6, 929-942.

Weertman, J. (1972) General theory of water flow at the base of a glacier or ice sheet. *Reviews of Geophysics*, 10, 287-333.

Willis, I. C., Fitzsimmons, C. D., Melvold, K., Andreassen, L. M. & Giesen, R. H. (2012) Structure, morphology and water flux of a subglacial drainage system, Midtdalsbreen, Norway. *Hydrological Processes*, 26, 3810-3829.

Chapter 3 A map of large Canadian eskers from Landsat satellite imagery

Storrar, R.D., Stokes, C.R. & Evans, D.J.A. (2013) A map of large Canadian eskers from Landsat satellite imagery. *Journal of Maps,* 9, 456-473.

Abstract

Meltwater drainage systems beneath ice sheets are a poorly understood, yet fundamentally important environment for understanding glacier dynamics, which are strongly influenced by the nature and quantity of meltwater entering the subglacial system. Contemporary sub-ice sheet meltwater drainage systems are notoriously difficult to study, but we can utilise exposed beds of palaeo-ice sheets to further our understanding of subglacial drainage. In particular, eskers record deposition in glacial drainage channels and are widespread on the exposed beds of former ice sheets. This paper presents a 1:5,000,000 scale map of >20,000 large eskers (typically >2 km long) deposited by the Laurentide Ice Sheet (LIS), mapped from Landsat imagery of Canada, in order to establish a dataset suitable for analysis of esker morphometry and drainage patterns at the ice sheet scale. Comparisons between eskers mapped from Landsat imagery and aerial photographs indicate that, in most areas, approximately 75% of eskers are detected using Landsat. The data presented in this map build on and extend previous work in providing a consistent map of an unprecedented sample of eskers for quantitative analysis. It offers an alternative perspective on the problems surrounding ice-sheet meltwater drainage and can be used for: (i) detailed investigations of esker morphometry and distribution from a large sample size; (ii), testing of numerical models of meltwater drainage routing that predict esker characteristics (e.g. channel spacing, sinuosity), (iii) assessment of the factors that control esker location and formation; and (iv), a refined understanding of ice margin configurations during retreat of the LIS.

3.1 Introduction

Subglacial meltwater drainage systems are intimately linked with ice sheet dynamics (e.g. Chapter 1; Chapter 2; Boulton *et al.*, 2001; Stearns *et al.*, 2008; Schoof, 2010). Given the increase in meltwater production as a result of increased warming in polar regions (e.g. Mernild *et al.*, 2011; Rignot *et al.*, 2011), a large amount of research has recently been directed at furthering our understanding of how the routing and arrangement of meltwater interacts with ice flow (e.g. Catania & Neumann, 2010; Parizek *et al.*, 2010; Schoof, 2010; Sundal *et al.*, 2011). However, our current understanding of meltwater drainage systems beneath the Antarctic and

Greenland ice sheets is limited by the difficulty in accessing their subglacial environments. To date, techniques designed to investigate the configuration of subglacial meltwater drainage (e.g. channelized versus distributed systems: see Section 2.2; Walder & Fowler, 1994; Mair *et al.*, 2002) are mostly remote or indirect and include, for example, radar sounding (e.g. Carter *et al.*, 2009), dye-tracing (e.g. Schuler & Fischer, 2009), remote sensing (e.g. Fricker *et al.*, 2007) and/or numerical modelling (e.g. Lewis & Smith, 2009). An alternative approach is to use the geomorphological record of palaeo-ice sheets as an analogue for the meltwater systems of contemporary ice sheets (e.g. Aylsworth & Shilts, 1989a; Punkari, 1997; Delaney, 2001; Mäkinen, 2003; Boulton *et al.*, 2009; Margold & Jansson, 2012). The most prolific landforms recording channelized meltwater activity are eskers: elongate, straight-to-sinuous ridges composed of glaciofluvial sand and gravel, formed by deposition in (predominantly subglacial) drainage conduits (e.g. Price, 1969; Shreve, 1985a; Warren & Ashley, 1994; Brennand, 2000).

The largest assemblage of eskers occurs on the bed of the former North American Ice Sheet complex, which covered most of Canada (Figure 1.2; Section 2.5; Prest *et al.*, 1968; Dyke & Prest, 1987; Dyke *et al.*, 2003). Although there have been numerous investigations of individual esker ridges (e.g. Banerjee & McDonald, 1975; Gorrell & Shaw, 1991; Brennand, 2000; Burke *et al.*, 2012) and/or small regions of eskers from this ice sheet complex (e.g. in the form of surficial geology mapping; Shilts, 1984; Aylsworth & Shilts, 1989a; Aylsworth & Shilts, 1989b; Menzies & Shilts, 1996; Hooke & Fastook, 2007), much less research has focused on larger-scale patterns at the ice sheet scale, although there are notable exceptions (see Section 2.5). It is clear that this approach has much potential to lead to major advances in our understanding of esker formation and meltwater drainage (see Aylsworth & Shilts, 1989a; Clark & Walder, 1994). With this in mind, this paper builds on a significant legacy of previous mapping in Canada (e.g. Armstrong & Tipper, 1948; Prest *et al.*, 1968; Shetsen, 1987; Aylsworth & Shilts, 1989b; Shetsen, 1990; Klassen *et al.*, 1992; Fulton, 1995) to present a new map (see appendix) of unprecedented detail (>20,000 eskers). Our aim is to provide a foundation for future work on the morphometry and spatial characteristics of eskers (similar to drumlins: see e.g. Clark *et al.*, 2009), which is presented in this thesis in Chapter 4, as well as the factors controlling how and where they form in relation to ice margin retreat (see Chapters 5 and 6), with a view to ultimately providing a more robust model of how subglacial meltwater drainage systems operate on a large scale.

3.2 Previous mapping and purpose of the map

3.2.1 Previous mapping

Given that numerous eskers have already been identified and mapped in Canada, it is necessary to briefly outline previous work and explain the purpose of the map presented in this paper. As noted above, eskers have been the focus of detailed mapping for several decades, most notably

in the numerous Geological Survey of Canada (GSC) Surficial and Quaternary Geology maps (e.g. Armstrong & Tipper, 1949; Gravenor, 1959; Henderson, 1977; Veillette, 1987; Aylsworth & Shilts, 1989b; Ward *et al.*, 1997). Many of these maps were created from aerial photograph analysis, often supplemented by fieldwork, and provide a high level of detail. However, this detailed approach necessitates that only relatively small regions can be mapped, although there are some notable exceptions of larger regions (Aylsworth & Shilts, 1989b).

Much of the early work was subsequently compiled on the Glacial Map of Canada (GMoC: Prest *et al.*, 1968). This impressive synthesis and its more recent derivatives (e.g. Fulton, 1995) remains the only map showing the distribution of eskers for all of Canada. It shows a total of 7,026 eskers but the GMoC was printed at a scale of 1:5,000,000 and, as such, eskers were generalised from more detailed mapping, which appears to have necessitated a cartographic simplification of their form (Figure 3.1), e.g. straightening their plan form and exaggerating their continuity (perhaps ignoring small gaps). Thus, although the data are now available electronically (from http://geoscan.ess.nrcan.gc.ca/), extraction of measurements of esker morphometry may be difficult (e.g. sinuousity, which is an important parameter for modelling velocity through subglacial tunnels: Schuler & Fischer, 2009).

It is also the case that recent mapping (e.g. Gravenor, 1959; Shetsen, 1987; Veillette, 1987; Shetsen, 1990; Margold *et al.*, 2011; Mernild *et al.*, 2011) portrays eskers in more detail than the GMoC and has sometimes identified eskers that may have been missed on the GMoC. In theory, these more recent maps could be compiled and added to the GMoC but a potential draw-back is that these maps have been produced by different workers and are unlikely to be consistent in terms of their accuracy, scale or cartographic representation, notwithstanding differences in interpretation and the fact that some regions remain largely unmapped. Thus, our approach is to use these maps as a valuable 'ground-truth' and guide, but we chose to identify and map eskers from a consistent data source, in this case Landsat Satellite imagery (see Methods). As noted, a further advantage of our remote sensing approach is that all the data is ingested directly into a GIS, from which quantitative data can be easily extracted. This is an important advance on previous work and we now briefly outline the purpose of the map.

3.2.2 Purpose of the map

The purpose of the map is to fill a niche between high resolution maps of small areas, which provide a high level of detail but consequently lack the spatial coverage and sample size for assessment of regional/continental scale patterns, and the GMoC, which provides a continental coverage, but which necessitated a degree of cartographic generalisation. The result is a map that portrays >20,000 individual eskers ridges/segments, which is around three times the number on the GMoC. This increased number largely results because we refrain from interpolating gaps between separate esker ridges that are longitudinally aligned, but also

because we identify some eskers that do not appear on the GMoC (Figure 3.1). Thus, it is anticipated that this map has the potential to advance understanding of ice sheet hydrology in four main areas, which are briefly highlighted below:

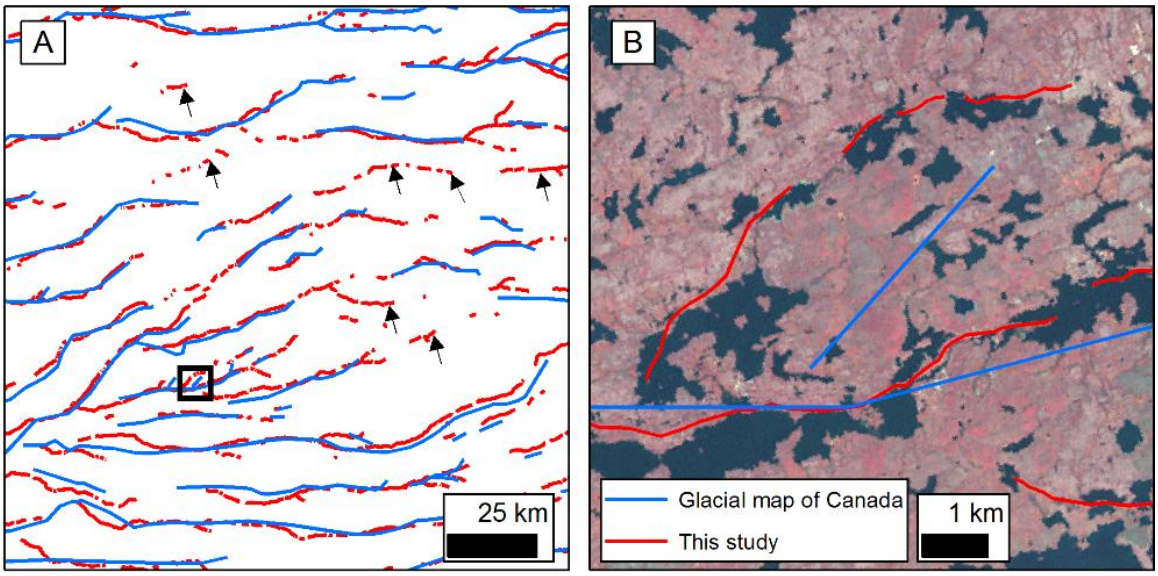

Figure 3.1 Eskers mapped in the GMoC and in the this paper. A) Examples of eskers mapped in this paper but not mapped in the GMoC are indicated by arrows. The box indicates the area enlarged in B. See Figure 3.5 for location. B) Landsat image (4,3,2) showing the cartographic simplification of eskers in the GMoC. Note that the gaps in the eskers are not represented in the GMoC and the locations of the esker ridges are relatively imprecise.

1. ***Detailed investigations of esker morphometry and distribution from a large sample size:***

The burgeoning availability of remotely sensed imagery and digital elevation data has increased capacity to map populations of glacial landforms at hitherto unprecedented sample sizes (Clark *et al.*, 2009; Spagnolo *et al.*, 2010; Spagnolo *et al.*, 2011; Spagnolo *et al.*, 2012). This has generated statistically representative sample sizes of 10s of thousands of landforms (e.g. drumlins, ribbed moraine) which can be used to gain insight into their formation. For example, large sample sizes of drumlin measurements have been used identify potential scales of bedform growth (Clark *et al.*, 2009) and demonstrate that their size-frequency distribution is exponential, which is a potentially powerful constraint on numerical models of drumlin formation (Hillier *et al.*, 2013). A similarly large and statistically robust dataset of esker characteristics is currently not available and the data presented in the map fills this important gap and can be used to address important research questions, such as: what are the statistical distributions of esker length, sinuosity, density and spacing (addressed here in Chapter 4)? How do these characteristics vary on different lithologies (see Chapter 6) or during ice margin retreat (see Chapter 5)? How do esker patterns evolve during deglaciation (see Chapter 5)?

2. ***Rigorous testing of numerical models of meltwater drainage routing:***

The statistically robust data described above can also be used as a powerful constraint for numerical modelling (see Chapter 6). For example, large sample sizes of ribbed moraine measurements have been used to test numerical models of their formation (Dunlop *et al.*, 2008). As noted above, such data has hitherto not been available for eskers and the data presented in this map can be used to test numerical models that, for example, predict esker spacing (see Chapter 6; Boulton *et al.*, 2007a;b; Boulton *et al.*, 2009; Hewitt, 2011) or make assumptions about, and parameterise, channel sinuosity (Schuler & Fischer, 2009). A key advantage of our dataset is that these numerical models can be tested against representative data from over 20,000 eskers, rather than being subject to the vagaries of smaller sample sizes. Indeed, the continental scale of our quantitative data is well suited to testing the subglacial routing of water predicted by large-scale ice sheet models (Tarasov & Peltier, 2006; Le Brocq *et al.*, 2009; Tarasov *et al.*, 2012).

3. ***Assessment of the factors that control esker location and formation:***

Previous work has demonstrated that the large scale pattern of eskers can be used to gain insights into the factors that control where and when they occur under an ice sheet (Section 2.6; Shilts *et al.*, 1987; Aylsworth & Shilts, 1989a; Clark & Walder, 1994; Menzies & Shilts, 1996). Various (and sometimes inter-relating) factors have been suggested as being an important control on the location and formation of eskers (Section 2.6). These include ice thickness (Shreve, 1972;1985a;b); sediment supply (Aylsworth & Shilts, 1989a); underlying geology (Clark & Walder, 1994) and groundwater characteristics (Boulton *et al.*, 2009). Some of these controls have gained support from large-scale mapping on the GMoC (e.g. Aylsworth & Shilts, 1989a; Clark & Walder, 1994), but most are explored using smaller samples of eskers from specific regions of palaeo-ice sheets (Shreve, 1985a; Boulton *et al.*, 2009). Our new data and map will add to this body of work in being able to demonstrate quantitatively how and where the distribution and pattern of eskers changes in relation to the ice sheet or sub-surface properties (see Chapter 6).

4. ***A refined understanding of ice margin configurations during retreat of the Laurentide Ice Sheet:***

Detailed mapping of eskers can be used to reconstruct ice margin retreat patterns (Clark *et al.*, 2012) and the GMoC and its derivatives (e.g. Fulton, 1995) have been used extensively, together with dating constraints, to reconstruct an impressive ice margin chronology for the North American Ice Sheet complex (Dyke *et al.*, 2003). Although it is not the primary purpose of the present map, the increased density of eskers on our map may help to subtly refine aspects of the existing ice margin retreat pattern for North America.

3.3 Methods

Mapping glacial geomorphological features at the ice sheet scale necessitates a compromise in the level of detail which can be mapped because it is not efficient, financially or practically, to map entire ice sheet beds by field survey or analysis of aerial photographs. In this study, the majority of mapping was therefore based on the identification of eskers from Landsat 7 Enhanced Thematic Mapper (ETM)+ imagery. Landsat ETM+ imagery was chosen because it is freely available and has excellent spatial coverage and relatively high resolution (~30 m and ~15 m in the panchromatic band). This makes it an ideal resource for mapping large-scale glacial geomorphology (Clark, 1997).

3.3.1 Data sources, mapping and map production

A total of 678 Landsat images were downloaded from the Global Land Cover Facility (GLCF; www.landcover.org) in orthorectified GeoTIFF format. All images were projected into the relevant Universal Transverse Mercator (UTM) zones, referenced to the World Geodetic Datum (WGS84). The panchromatic band (band 8) provided higher resolution imagery which was used to aid detection and mapping. In some small areas (see Figure 3.2), no Landsat 7 ETM+ data were available and Landsat 5 Thematic Mapper (TM) images (comparable to Landsat 7 ETM+ images, with the exception of the absence of the panchromatic band) were used to fill these gaps. Figure 3.2 shows the individual images used and indicates the areas where only TM data were available.

The workflow involved in the production of the map is outlined in Figure 3.3. Firstly, images were visualised at a variety of scales and using different band combinations, but the most useful were typically a 4, 3, 2 (red, green, blue) or 7, 5, 2 composite. Eskers were then identified according to the criteria set out by Margold & Jansson (2012 pp. 2364) who described their morphology as well-defined sub-linear ridges often accompanied by lakes and kettle holes that are often marked by shadows and/or by a different spectral signature due to the presence of glaciofluvial sediments (sands and gravels) and changes in soil moisture/vegetation cover. Esker crestlines were digitised as polylines in shapefile format in ArcGIS 10. To ensure minimal spatial distortion, they were mapped in separate shapefiles, corresponding to the local UTM zone of the Landsat imagery. The shapefiles were then merged in ArcGIS 10 to produce a single shapefile, projected to the Canadian Lambert Conformal Conical projection, which was used for the final map.

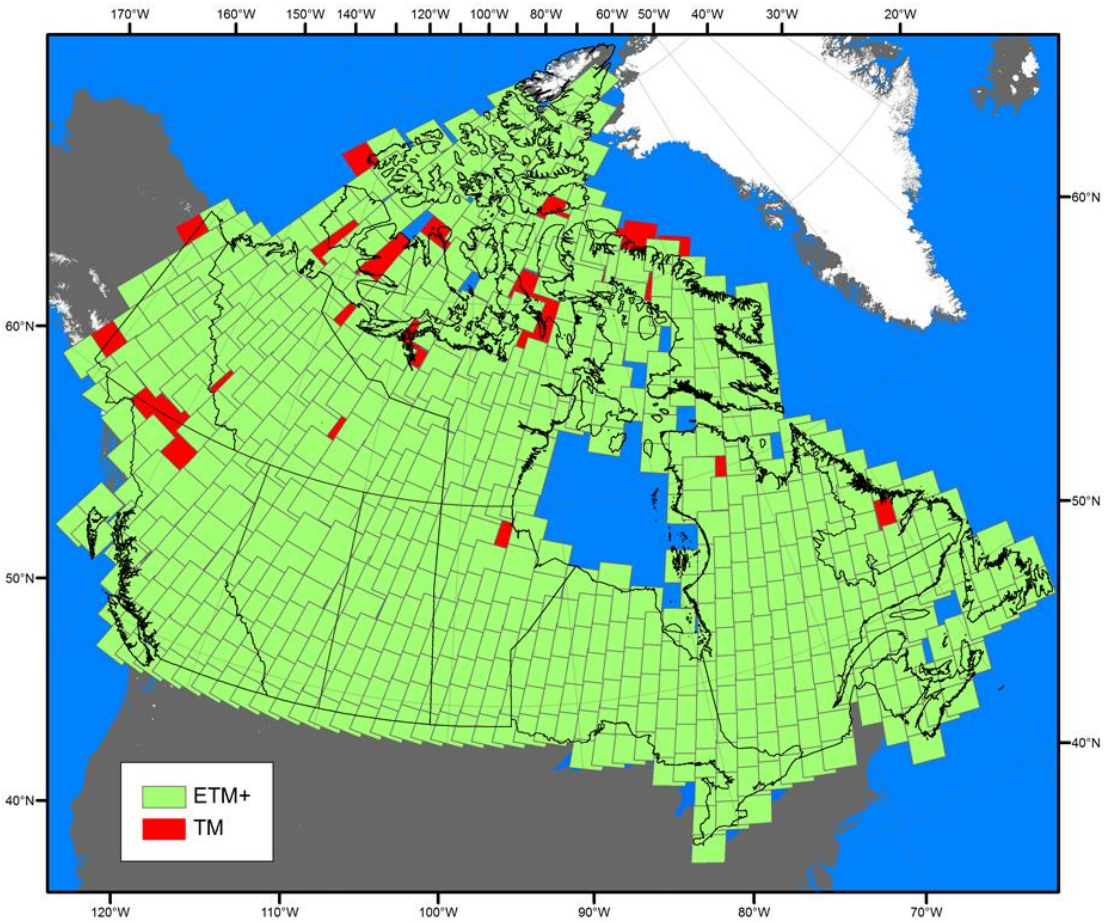

Figure 3.2. Map showing coverage of Landsat ETM+ Landsat TM imagery. Each image covers an area of approximately 125 km × 125 km.

Eskers were identified and mapped at a variety of scales. In the 30 m resolution imagery, eskers were typically identified at 1:80,000 and digitised at 1:40,000, to ensure that crestlines were portrayed as accurately and precisely as possible. In the panchromatic band (15 m resolution), smaller eskers were often identifiable at 1:30,000 scale. In some instances, features such as moraine ridges may be indistinguishable from eskers in remotely sensed images and mapping was therefore checked, where possible, against published geomorphological maps and other sources. In some instances, features have been mapped as eskers by some and moraine ridges by others (see Figure 3.4).

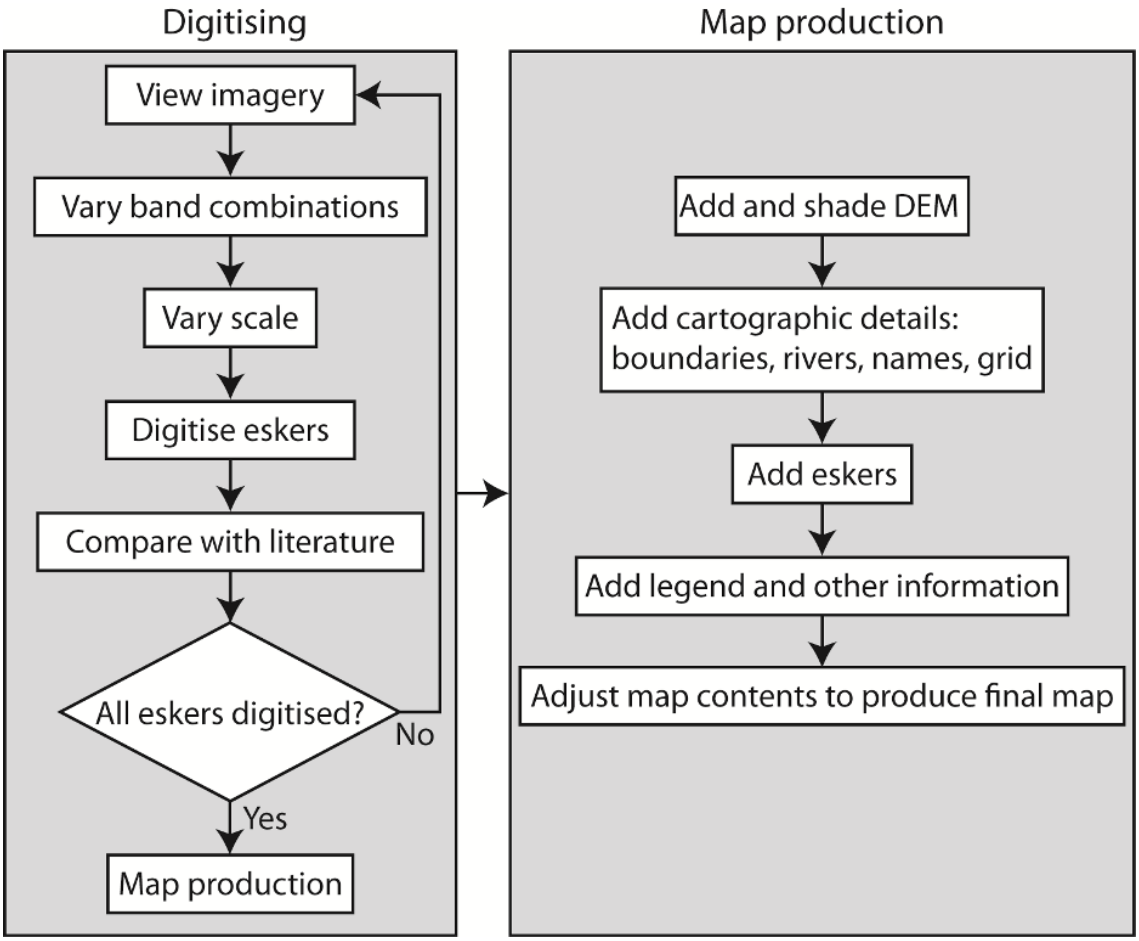

Figure 3.3. Flow chart showing the two stages of map development: digitisation and production of the final map.

The Digital Elevation Model (DEM) used as a background for the map was produced from the GTOPO30 dataset (available from http://eros.usgs.gov), which has a spatial resolution of 30 arc-seconds. Contemporary ice cover data shown on the map were downloaded from the Atlas of the Cryosphere (available from http://nsidc.org/data/atlas/) and the Randolph Glacier Inventory (Arendt *et al.*, 2012). Outlines of major lakes used for illustration were obtained from the North American Atlas (available from http://www.nationalatlas.gov). Coastline data are from the Geological Survey of Canada (http://www.nrcan.gc.ca/earth-sciences).

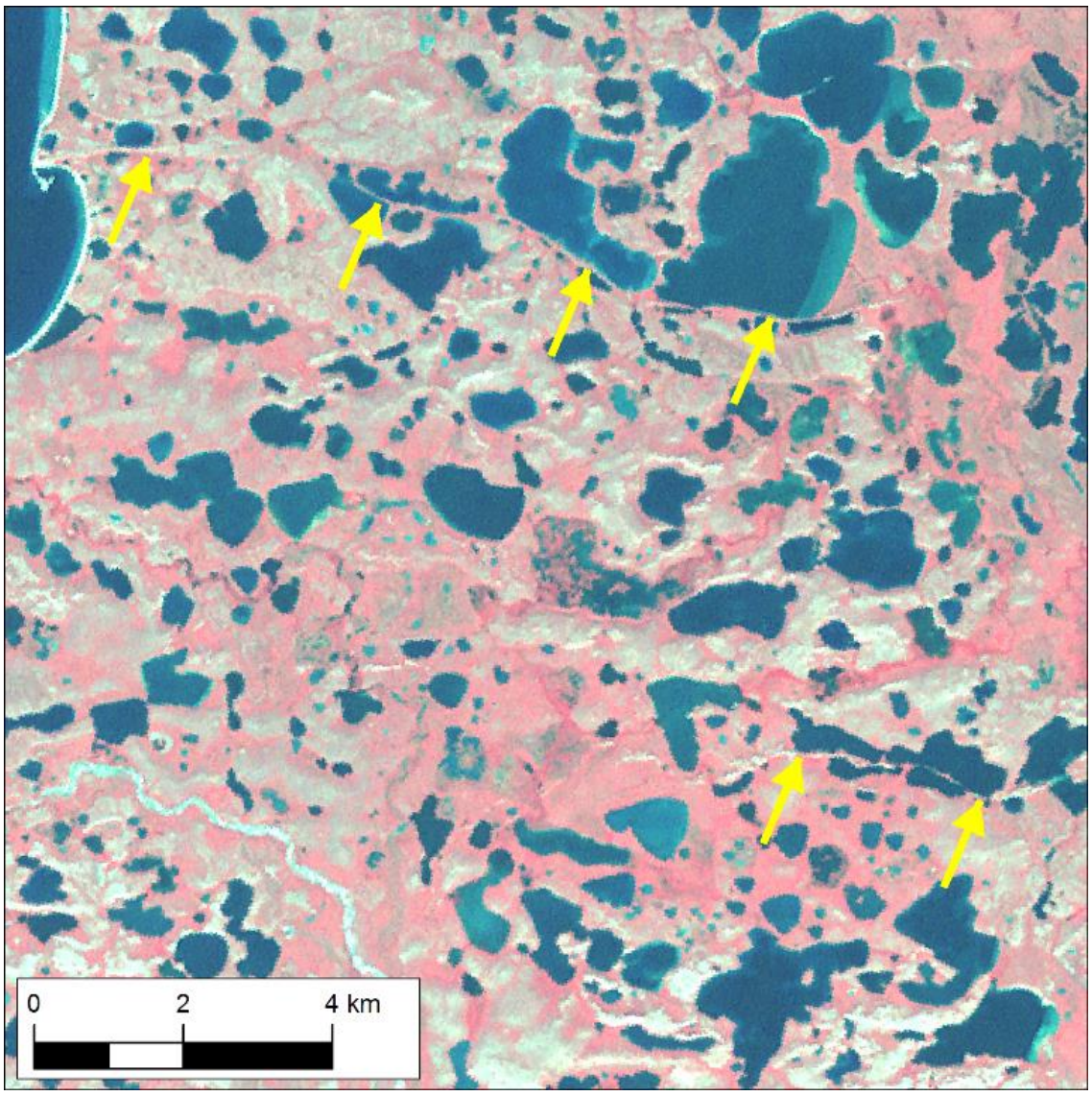

Figure 3.4. Two prominent eskers in Northwest Territories (also mapped as eskers by Brown *et al.*, 2011). Note that these features were not included in the Glacial Map of Canada, in which the area was broadly defined as 'hummocky terrain' (Prest *et al.*, 1968). See Figure 3.5 for location.

3.3.2 Errors and completeness

Despite its advantages, a potential limitation of using satellite imagery is that some small features may go undetected (Smith & Wise, 2007; Smith, 2011; Margold & Jansson, 2012). Thus, in order to quantify this uncertainty and verify the detection of eskers on the Landsat imagery, seven small regions were also mapped from high resolution (~2-3 m) aerial photographs. This included 2,717 aerial photographs (and 30 aerial photomosaics), covering approximately 175,000 km^2 in seven contrasting locations (Figure 3.5). The locations were selected from a variety of situations: shield *versus* non-shield areas; areas significantly altered by human activity; zones of inferred fast *versus* slow palaeo-ice flow; areas of high/low esker density; and areas observed to be problematic when observed in Landsat imagery (Figure 3.5).

The results of the aerial photograph comparison are presented in Table 1 and indicate that areas containing a high density of eskers on aerial photographs are mapped the most completely on the Landsat imagery (see Figure 3.6). For example, detection rates of 86-88% are found for eskers emanating from the former Keewatin Ice Divide (areas 1 and 6: Figure 3.5) and indicate that the mapping from Landsat imagery is likely to be representative and captures most esker systems (Figure 3.7). Where aerial photograph mapping indicates that there are fewer eskers, or in areas affected by human activity such as the St. Lawrence valley (area 3: Figure 3.5) and southern Alberta (area 2: Figure 3.5), the detection rate using Landsat imagery is lower, as would be expected for significantly modified terrain or regions containing less well preserved features. Closer inspection of the eskers that were missed by the Landsat imagery but detected on the aerial photographs (n = 639) shows that the vast majority (81%) are <2 km in length (see Figure 3.8). Thus, the map should be seen as a representation of large eskers (>2 km) that captures the major drainage channels of the ice sheet. Finally, it should be noted that eskers exist in parts of the United States of America formerly occupied by the Laurentide Ice Sheet, but our mapping extends only to the Canadian border, partly because eskers are more difficult to detect in southern Canada and northern USA due to anthropogenic landscape modification. Thus, the map represents a systematic dataset of large (>2 km long) esker patterns at the ice sheet-scale, rather than a map of every esker on the ice sheet bed.

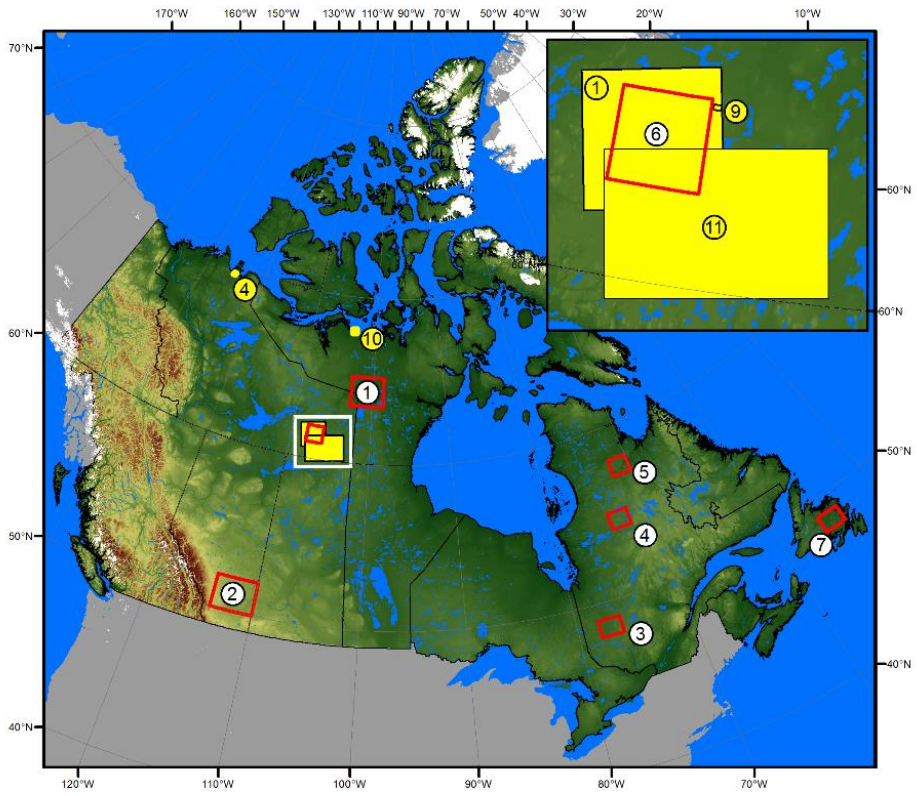

Figure 3.5. Locations of Figure 3.1, Figure 3.4, Figure 3.9, Figure 3.10 and Figure 3.11 (yellow) and areas mapped from aerial photographs (red boxes, white circles). Inset is an enlargement of the area indicated by the white box.

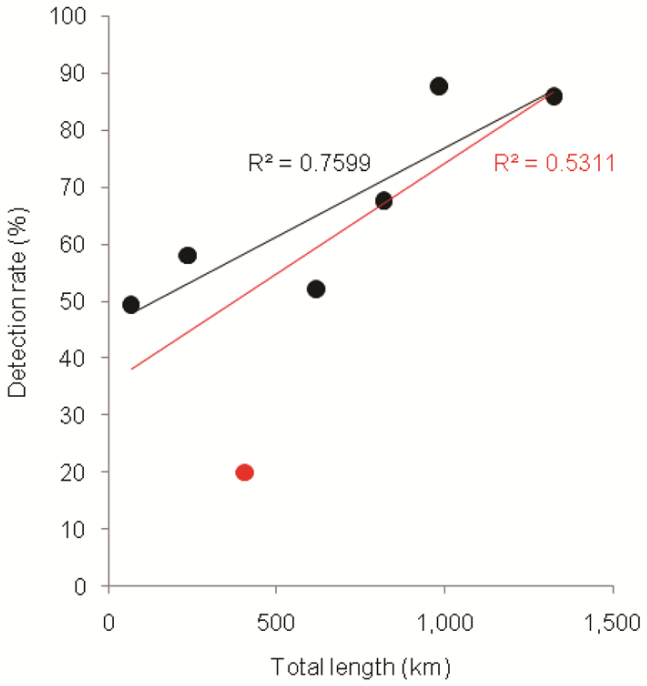

Figure 3.6. Total length of eskers from both Landsat and aerial photograph analysis in each study area, plotted against the observed detection rate. The red marker indicates the study area in southern Alberta (area 2: Figure 3.5), where the detection rate is significantly lower due to large-scale human activity. The red trendline takes this point into account, whereas the black trendline corresponds to the other 6 areas only. Areas containing a high proportion of eskers tend to result in the most reliable mapping.

3.4 Results

A total of 20,186 individual esker ridges were mapped from Landsat ETM+ imagery of Canada, which is almost three times as many as appear on the Glacial Map of Canada (7,026). As noted above, the increased number largely reflects our conservative mapping approach, in that we refrained from drawing separate esker ridges as a single line feature. This is because it was not always possible to deduce whether a gap resulted from post-glacial modification/erosion or whether it represented a genuine lack of deposition within the palaeo-channel. Notwithstanding this, we also identified numerous eskers that were not mapped on the GMoC (see Figure 3.1).

The most common (and the classical) type of esker is a single, well-defined ridge displaying a straight-to-sinuous morphology. The area around the Keewatin Ice Divide provides exemplars of these eskers, where they are pervasive and are very well preserved (Figure 3.9). Some individual esker ridges extend without gaps for several tens of kilometres. The longest continuous ridge is measured at 97.5 km (in Ontario) and some systems can be traced for up to 760 km when gaps are taken into account. Indeed, eskers are usually found in fragments, reflecting either discontinuous formation, or post-depositional modification. This is quantified and addressed further in Chapter 4.

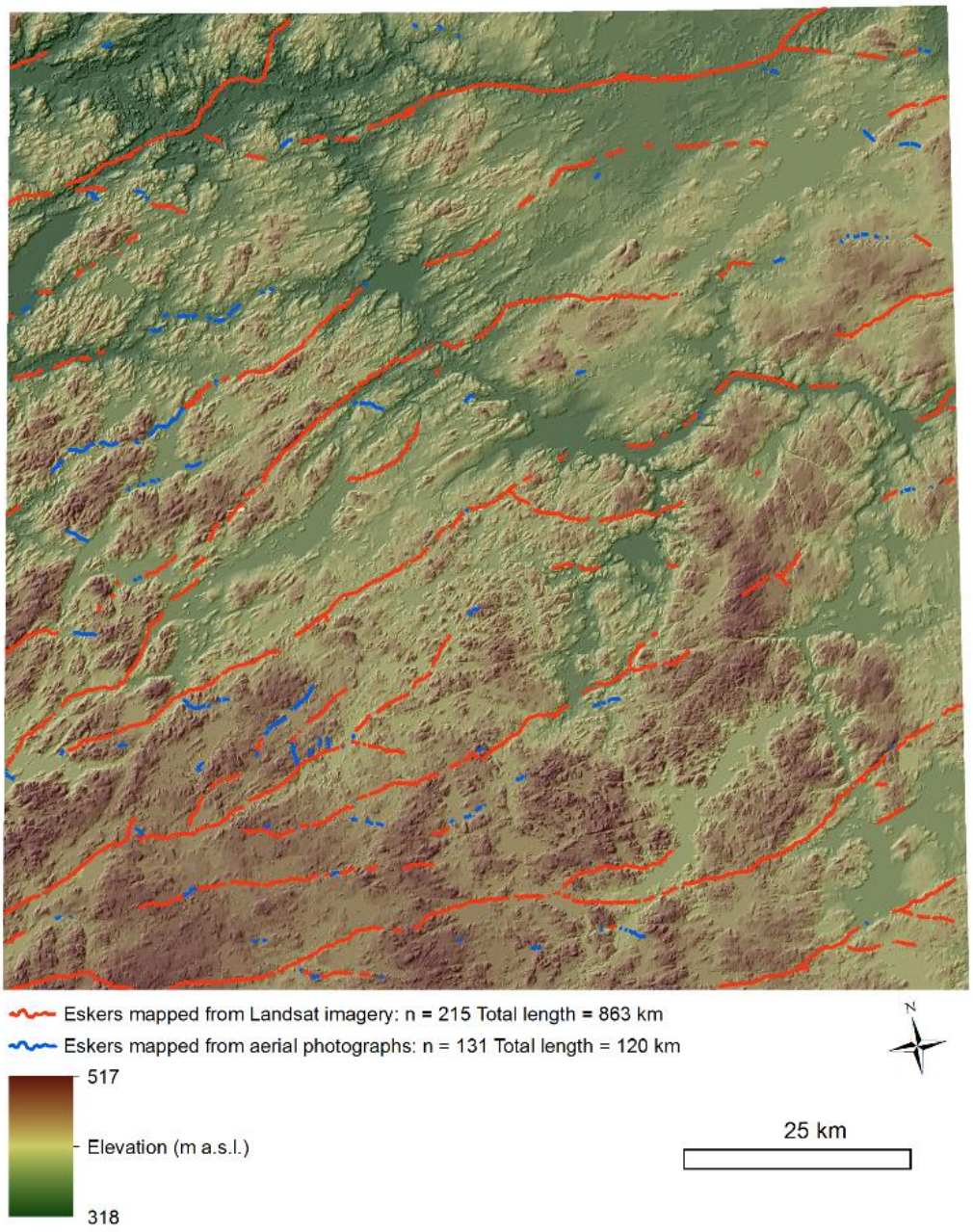

Figure 3.7. Eskers mapped from Landsat ETM+ imagery and aerial photographs in the McCann Lake area, Northwest Territories. See Figure 3.5 (area 6) for location.

Though uncommon, esker ridges appear to be 'patchy' in some areas and do not display a coherent crestline, contrasting markedly with the classic Keewatin examples (Figure 3.10). Others consist of multiple ridges, which anastomose to produce complex patterns, although these eskers are usually confined to a relatively narrow 'swath'. In places, these swathes are marked by broader corridors of glaciofluvial sediment that appear as 'bright' patches on imagery and which some workers have called 'glaciofluvial corridors' (Section 2.3.3; St-Onge, 1984; Utting *et al.*, 2009).

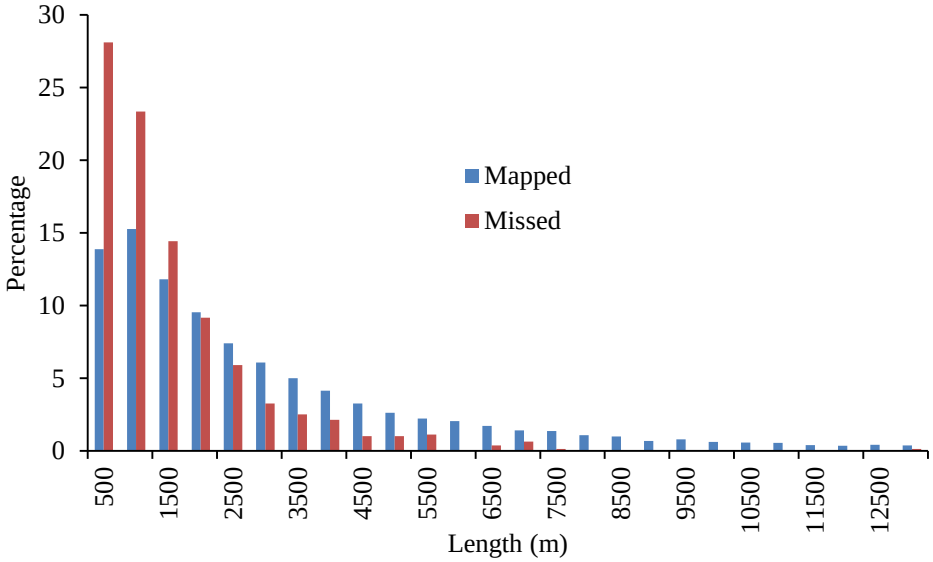

Figure 3.8. Histogram (0.5 km bins) of the length of eskers detected in aerial photographs but not in Landsat imagery (Missed) and the length of the eskers mapped from Landsat imagery (Mapped). Note that more of the 'missed' eskers are < 2 km long compared with the 'mapped' eskers and, conversely, that more of the 'mapped' eskers are > 2 km long compared with the 'missed' eskers.

3.4.1 Esker distribution and patterns

Several spatial patterns, visible at various scales, were recognised in the mapping. In general, the pattern of eskers is similar to that mapped by Prest *et al.* (1968) and clearly shows eskers radiating away from the former location of major ice divides, for example in Keewatin and Ungava (see map in appendix; cf. Dyke & Prest, 1987; Aylsworth & Shilts, 1989a; Aylsworth & Shilts, 1989b; Boulton & Clark, 1990; Menzies & Shilts, 1996). Beneath the former ice divides, however, eskers are conspicuously absent. As others have noted, integrated dendritic networks of eskers exist around the Keewatin Ice Divide (see Aylsworth & Shilts, 1989a), indicative of a well-connected drainage system. This is examined in more detail in Chapter 4.

In contrast, some areas display little or no recognisable pattern and eskers appear rather chaotic. This is particularly apparent off the Canadian Shield and over soft sedimentary rocks, e.g. north of Great Bear Lake in Northwest Territories, as well as on Victoria Island, where complex ice dynamics were recorded during deglaciation (Stokes *et al.*, 2009). More generally, eskers are abundant on the Canadian Shield and are relatively sparse on the surrounding soft-bedded areas, as noted by Clark & Walder (1994), who hypothesised that eskers form preferentially on more resistant substrates (see also Chapter 6).

Table 3.1. Locations used to compare mapping from Landsat ETM+ imagery with mapping from high resolution aerial photographs. Esker detection rates in the Landsat ETM+ imagery, compared with the aerial photographs, is estimated and given as a percentage of total length. Locations are numbered in correspondence with Figure 3.5.

Location	No. and type of images (approximate resolution)	Area covered (km^2)	Number of eskers mapped on ETM+ imagery	Total length of eskers mapped on ETM+ imagery (km)	Number of additional eskers mapped	Total length of additional eskers mapped (km)	Esker detection rate in ETM+ imagery
(1) Dubawnt Lake Area, Nunavut	847 aerial photographs (~2-3 m)	41,287	158	1,138	57	186	85.91%
(2) South and Central Alberta	30 aerial photomosaics (~5 m)	62,142	18	81	221	325	19.95%
(3) Senneterre, Québec	449 aerial photographs (~2-3 m)	16,626	111	322	156	295	52.13%
(4) Lac Aigneu, Québec	230 aerial photographs (~2-3 m)	12,981	46	137	63	99	58.02%
(5) Lac Mistanukaw area, Québec	280 aerial photographs (~2-3 m)	14,131	260	555	206	265	67.61%

(6) McCann Lake area, Northwest Territories	538 aerial photographs (~2-3 m)	11,511	215	863	131	120	87.76%
(7) Gander Lake area, Newfoundland	373 aerial photographs (~2-3 m)	16,585	20	34	26	34	49.59%
Total	2,717 aerial photographs; 193 aerial photomosaics	175,263	810	3,099	639	1,002	75.57%

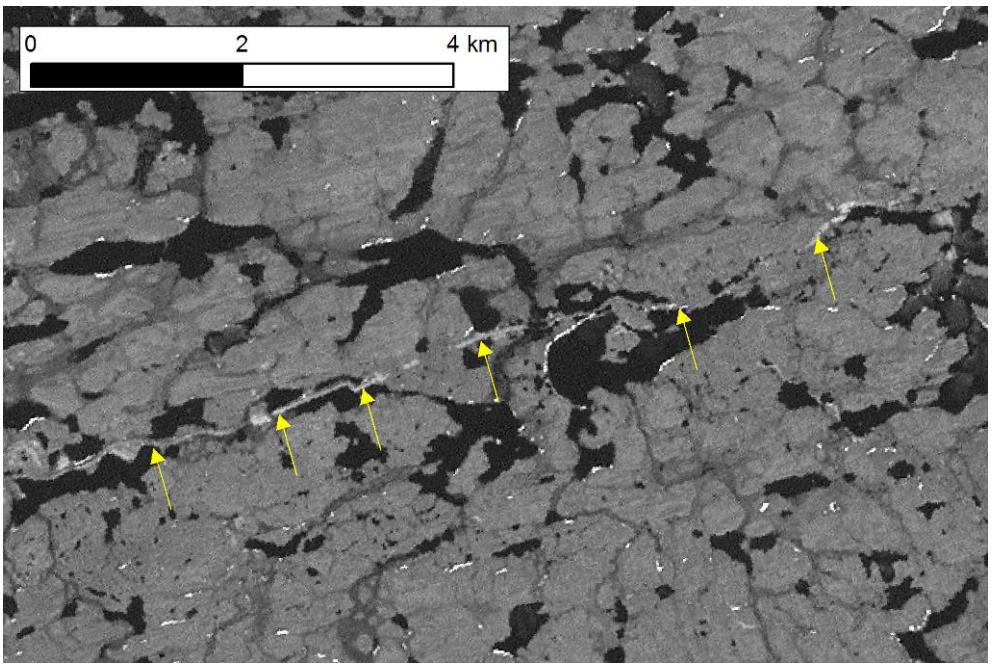

Figure 3.9. Landsat ETM+ image (band 8) of an esker in Nunavut. Note the very well defined shape of the esker and the high continuity along its length. See Figure 3.5 for location.

In many places, eskers are relatively evenly spaced (typically from 10 to 20 km: see Figure 3.11), a phenomenon also observed in Finland and used as the basis of a hypothesis for groundwater control on esker spacing (Section 2.6.5; Boulton *et al.*, 2009). The map presented here is therefore used as the foundation for a more in-depth analysis of esker morphometry in Chapter 4 and to test numerical models that predict esker spacing (e.g. Boulton *et al.*, 2009; Hewitt, 2011) in Chapter 6.

3.5 Conclusions and implications

This paper presents a map of 20,186 large Canadian eskers mapped from Landsat satellite imagery. Analysis of aerial photographs in seven test areas suggests that approximately 75% of all eskers were detected using Landsat imagery alone, with most of those undetected being <2 km long, based on comparison to aerial photograph mapping. The morphology of eskers was found to vary and several distinctive types were observed: classical, well-defined, single-ridge eskers; multiple-ridged and anastomosing eskers; and 'patchy' eskers. Eskers are predominantly preserved in fragments but systems of eskers can be interpolated from the patterns which often extend for several hundred kilometres. Eskers frequently conform to distinctive patterns at different scales, indicating highly organised systems. At the largest scale, eskers are seen to radiate away from former ice divides in Keewatin and Labrador. Within these radial esker systems, integrated networks of eskers can be seen with many tributary eskers. In some areas, eskers are very regularly spaced.

The map of eskers presented in this paper is well suited to a large-scale morphometric analysis of eskers (e.g. similar to that recently undertaken for drumlins: Clark et al., 2009) as well as an ice sheet-wide analysis of esker patterns at various scales, as presented here in Chapter 4. These data could then be used to test numerical models that predict the configuration of meltwater drainage beneath ice sheets, such as in Chapter 6 (e.g. Boulton *et al.*, 2009; Hewitt, 2011) and evaluate various hypotheses that seek to explain where and why eskers form (e.g. subglacial geology, groundwater characteristics, ice surface slope, etc.). Esker patterns can also provide new insights regarding the margin configuration during deglaciation of the former Laurentide Ice Sheet (see Chapter 5), since they typically form perpendicular to ice margins. This has significant implications both for our understanding of eskers and palaeoglaciology, as well as for improving our knowledge of how large subglacial meltwater drainage systems operate under contemporary ice sheets.

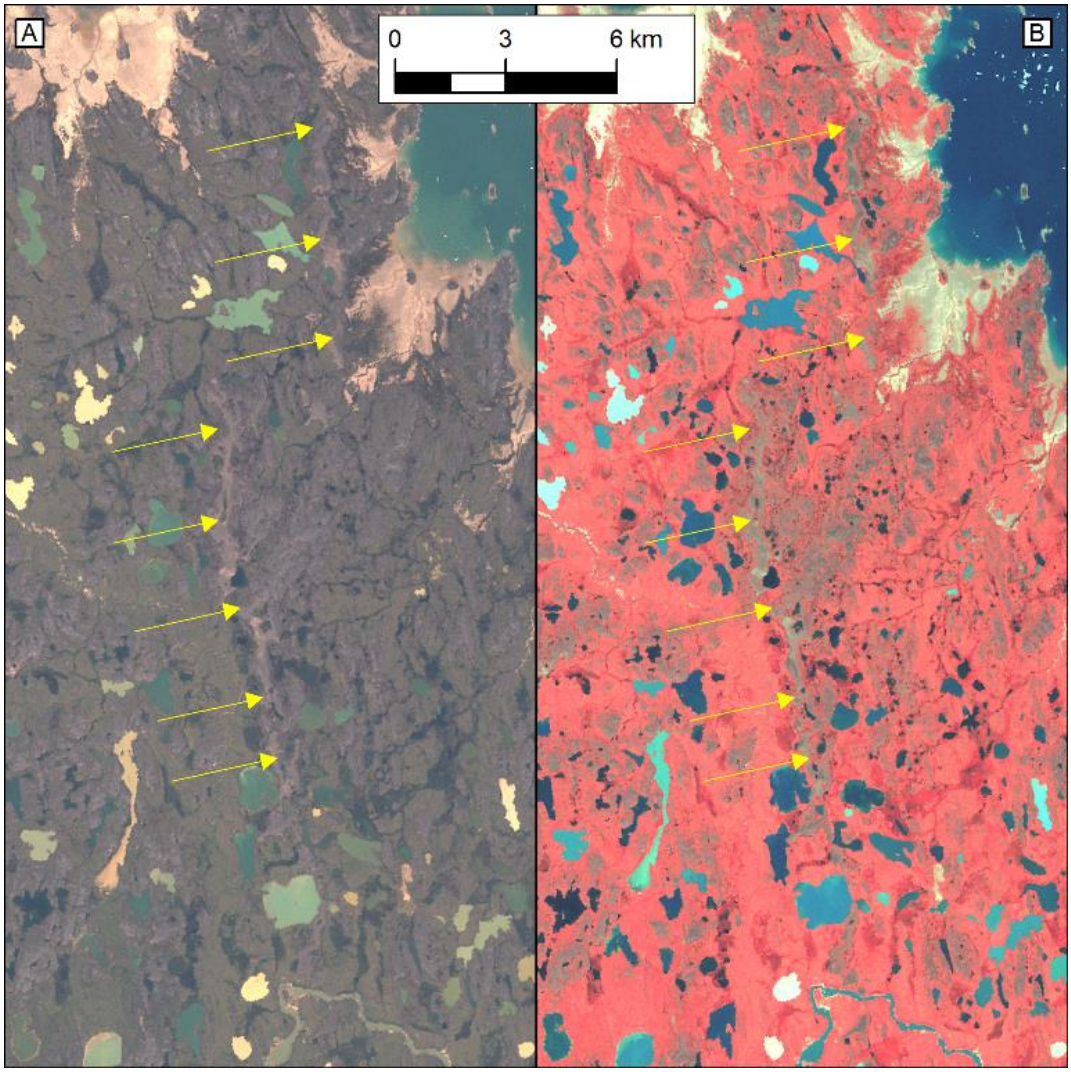

Figure 3.10. Landsat ETM+ image (3,2,1 in A; 4,3,2 in B) of discontinuous, 'patchy' eskers in Nunavut. Note poorly defined edges and presence of hummocky topography surrounding the eskers. See Figure 3.5 for location.

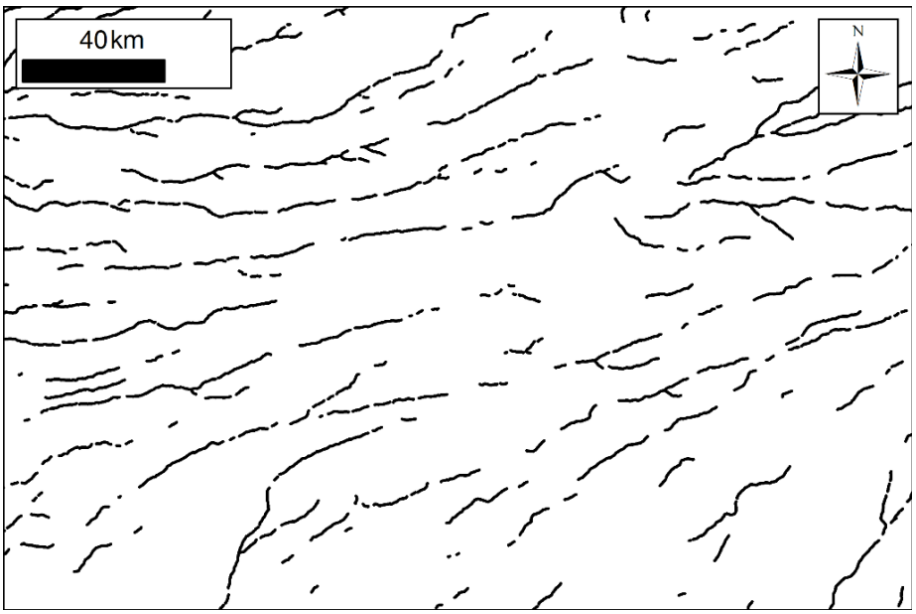

Figure 3.11. Digitised eskers in Northwest Territories exhibiting regular spacing (typically around 15 km). See Figure 3.5 for location.

3.6 References

Arendt, A., Bolch, T., Cogley, J. G., Gardner, A., Hagen, J.-O., Hock, R., Kaser, G., Pfeffer, W. T., Moholdt, G., Paul, F., Radic, V., Andreassen, L., Bajracharya, S., Beedle, M., Berthier, E., Bhambri, R., Bliss, A., Brown, I., Burgess, E., Burgess, D., Cawkwell, F., Chinn, T., Copland, L., Davies, B., De Angelis, H., Dolgova, E., Filbert, K., Forester, R., Fountain, A., Frey, H., Giffen, B., Glasser, N. F., Gurney, S. D., Hagg, W., Hall, D., Haritashya, U. K., Hartmann, G., Helm, C., Herreid, S., Howat, I., Kapustin, G., Khromova, T., Kienholz, C., Koenig, M., Kohler, J., Kriegel, D., Kutuzov, S., Lavrentiev, I., LeBris, R., Lund, J., Manley, W., Mayer, C., Miles, E., Li, X., Menounos, B., Mercer, A., Moelg, N., Mool, P., Nosenko, G., Negrete, A., Nuth, C., Pettersson, R., Racoviteanu, A., Ranzi, R., Rastner, P., Rau, F., Raup, B. H., Rich, J., Rott, H., Schneider, C., Selivertsov, N., Sharp, M., Sigurdson, O., Stokes, C. R., Wheate, R., Winsvold, S., Wolken, G., Wyatt, F. & Zheltyhina, N. (2012) Randolph Glacier Inventory [v2.0]: A Dataset of Global Glacier Outlines. Global Land Ice Measurements from Space, Boulder Colorado, USA. Digital Media.

Armstrong, J. E. & Tipper, H. W. (1948) Glaciation in north-central British Columbia. *American Journal of Science*, 246, 283-310.

Armstrong, J. E. & Tipper, H. W. (1949) Surface Deposits, Carp Lake, Cariboo District, British Columbia. Geological Survey of Canada map 980A. 1:283,440

Aylsworth, J. M. & Shilts, W. W. (1989a) Bedforms of the Keewatin Ice-Sheet, Canada. *Sedimentary Geology*, 62, 407-428.

Aylsworth, J. M. & Shilts, W. W. (1989b) Glacial features around the Keewatin Ice Divide: Districts of Mackenzie and Keewatin. Geological Survey of Canada, Map 24-1987. 1:1,000,000

Banerjee, I. & McDonald, B. C. (1975) Nature of esker sedimentation. In A. V. Jopling and B. C. McDonald, *Glaciofluvial and Glacilacustrine Sedimentation*. Oklahoma, SEPM, 304-320.

Boulton, G. S. & Clark, C. D. (1990) A highly mobile Laurentide ice sheet revealed by satellite images of glacial lineations. *Nature*, 346, 813-817.

Boulton, G. S., Dobbie, K. E. & Zatsepin, S. (2001) Sediment deformation beneath glaciers and its coupling to the subglacial hydraulic system. *Quaternary International*, 86, 3-28.

Boulton, G. S., Hagdorn, M., Maillot, P. B. & Zatsepin, S. (2009) Drainage beneath ice sheets: groundwater-channel coupling, and the origin of esker systems from former ice sheets. *Quaternary Science Reviews*, 28, 621-638.

Boulton, G. S., Lunn, R., Vidstrand, P. & Zatsepin, S. (2007a) Subglacial drainage by groundwater-channel coupling, and the origin of esker systems: Part I-glaciological observations. *Quaternary Science Reviews*, 26, 1067-1090.

Boulton, G. S., Lunn, R., Vidstrand, P. & Zatsepin, S. (2007b) Subglacial drainage by groundwater-channel coupling, and the origin of esker systems: part II-theory and simulation of a modern system. *Quaternary Science Reviews*, 26, 1091-1105.

Brennand, T. A. (2000) Deglacial meltwater drainage and glaciodynamics: inferences from Laurentide eskers, Canada. *Geomorphology*, 32, 263-293.

Burke, M. J., Brennand, T. A. & Perkins, A. J. (2012) Transient subglacial hydrology of a thin ice sheet: insights from the Chasm esker, British Columbia, Canada. *Quaternary Science Reviews*, 58, 30-55.

Carter, S. P., Blankenship, D. D., Young, D. A. & Holt, J. W. (2009) Using radar-sounding data to identify the distribution and sources of subglacial water: application to Dome C, East Antarctica. *Journal of Glaciology*, 55, 1025-1040.

Catania, G. A. & Neumann, T. A. (2010) Persistent englacial drainage features in the Greenland Ice Sheet. *Geophysical Research Letters*, 37, L02501.

Clark, C. D. (1997) Reconstructing the evolutionary dynamics of former ice sheets using multi-temporal evidence, remote sensing and GIS. *Quaternary Science Reviews*, 16, 1067-1092.

Clark, C. D., Hughes, A. L. C., Greenwood, S. L., Jordan, C. & Sejrup, H. P. (2012) Pattern and timing of retreat of the last British-Irish Ice Sheet. *Quaternary Science Reviews*, 44, 112-146.

Clark, C. D., Hughes, A. L. C., Greenwood, S. L., Spagnolo, M. & Ng, F. S. L. (2009) Size and shape characteristics of drumlins, derived from a large sample, and associated scaling laws. *Quaternary Science Reviews*, 28, 677-692.

Clark, P. U. & Walder, J. S. (1994) Subglacial drainage, eskers, and deforming beds beneath the Laurentide and Eurasian ice sheets. *Bulletin of the Geological Society of America*, 106, 304-314.

Delaney, C. (2001) Morphology and Sedimentology of the Rooskagh Esker, Co. Roscommon. *Irish Journal of Earth Sciences*, 19, 5-22.

Dunlop, P., Clark, C. D. & Hindmarsh, R. C. A. (2008) Bed Ribbing Instability Explanation: Testing a numerical model of ribbed moraine formation arising from coupled flow of ice and subglacial sediment. *Journal of Geophysical Research-Earth Surface*, 113, 1-15.

Dyke, A. S., Moore, A. & Robertson, L. (2003) Deglaciation of North America. *Geological Survey of Canada, Open File*, 1574.

Dyke, A. S. & Prest, V. K. (1987) Late Wisconsinan and Holocene history of the Laurentide ice sheet. *Géographie physique et Quaternaire*, 41, 237-263.

Fricker, H. A., Scambos, T., Bindschadler, R. & Padman, L. (2007) An active subglacial water system in West Antarctica mapped from space. *Science*, 315, 1544-1548.

Fulton, R. J. (1995) Surficial materials of Canada *Geological Survey of Canada, "A" Series Map 1880A*. 1:5,000,000

Gorrell, G. & Shaw, J. (1991) Deposition in an esker, bead and fan complex, Lanark, Ontario, Canada. *Sedimentary Geology*, 72, 285-314.

Gravenor, C. P. (1959) Surficial Geology, Lindsay-Peterborough area, Ontario. Geological Survey of Canada, map 1050A. 1:126,720

Henderson, E. P. (1977) Surficial Geology, Avalon Peninsula, Newfoundland. Geological Survey of Canada map 1320A.

Hewitt, I. J. (2011) Modelling distributed and channelized subglacial drainage: the spacing of channels. *Journal of Glaciology*, 57, 302-314.

Hillier, J. K., Smith, M. J., Clark, C. D., Stokes, C. R. & Spagnolo, M. (2013) Subglacial bedforms reveal an exponential size-frequence distribution. *Geomorphology*, 190, 82-91.

Hooke, R. L. & Fastook, J. (2007) Thermal conditions at the bed of the Laurentide ice sheet in Maine during deglaciation: implications for esker formation. *Journal of Glaciology*, 53, 646-658.

Klassen, R. A., Paradis, S., Bolduc, A. M. & Thomas, R. D. (1992) Glacial Landforms and Deposits, Labrador, Newfoundland and eastern Quebec. *Geological Survey of Canada, Map 1814A*. 1:1000000

Le Brocq, A. M., Payne, A., Siegert, M. & Alley, R. (2009) A subglacial water-flow model for West Antarctica. *Journal of Glaciology*, 55, 879-888.

Lewis, S. M. & Smith, L. (2009) Hydrologic drainage of the Greenland Ice Sheet. *Hydrological Processes*, 23, 2004-2011.

Mair, D. W. F., Sharp, M. J. & Willis, I. C. (2002) Evidence for basal cavity opening from analysis of surface uplift during a high-velocity event: Haut Glacier d'Arolla, Switzerland. *Journal of Glaciology*, 48, 208-216.

Mäkinen, J. (2003) Time-transgressive deposits of repeated depositional sequences within interlobate glaciofluvial (esker) sediments in Koylio, SW Finland. *Sedimentology*, 50, 327-360.

Margold, M. & Jansson, K. N. (2012) Evaluation of data sources for mapping glacial meltwater features. *International Journal of Remote Sensing*, 33, 2355-2377.

Margold, M., Jansson, K. N., Kleman, J. & Stroeven, A. P. (2011) Glacial meltwater landforms of central British Columbia. *Journal of Maps*, 2011, 486-506.

Menzies, J. & Shilts, W. W. (1996) Subglacial environments. In J. Menzies, *Past glacial environments, sediments, forms and techniques*. Oxford, Butterworth/Heinemann. 2, 15-136.

Mernild, S. H., Mote, T. L. & Liston, G. E. (2011) Greenland ice sheet surface melt extent and trends: 1960 - 2010. *Journal of Glaciology*, 57, 621-628.

Parizek, B. R., Alley, R. B., Dupont, T. K., Walker, R. T. & Anandakrishnan, S. (2010) Effect of orbital-scale climate cycling and meltwater drainage on ice sheet grounding line migration. *Journal of Geophysical Research*, 115, F01011.

Prest, V. K., Grant, D. R. & Rampton, V. N. (1968) Glacial map of Canada. Geological Survey of Canada, Map 1253A. 1:5,000,000

Price, R. J. (1969) Moraines, sandar, kames and eskers near Breiðamerkurjökull , Iceland. *Transactions of the Institute of British Geographers*, 46, 17-43.

Punkari, M. (1997) Glacial and glaciofluvial deposits in the interlobate areas of the Scandinavian Ice Sheet. *Quaternary Science Reviews*, 16, 741-753.

Rignot, E., Velicogna, I., van den Broeke, M. R., Monaghan, A. & Lenaerts, J. (2011) Acceleration of the contribution of the Greenland and Antarctic ice sheets to sea level rise. *Geophys. Res. Lett.*, 38, L05503.

Schoof, C. (2010) Ice-sheet acceleration driven by melt supply variability. *Nature*, 468, 803-806.

Schuler, T. V. & Fischer, U. H. (2009) Modeling the diurnal variation of tracer transit velocity through a subglacial channel. *Journal of Geophysical Research*, 114, F04017.

Shetsen, I. (1987) Quaternary Geology, Southern Alberta. Alberta Research Council. 1:500,000

Shetsen, I. (1990) Quaternary Geology, Central Alberta. Alberta Research Council. 1:500,000

Shilts, W. W. (1984) Esker sedimentation models, Deep Rose Lake map area, District of Keewatin. *Geological Survey of Canada, Paper*, 84-1B, 217-222.

Shilts, W. W., Aylsworth, J. M., Kaszycki, C. A. & Klassen, R. A. (1987) Canadian Shield. In W. L. Graf, *Geomorphic Systems of North America*. Boulder, Colorado, Geological Society of America, Centennial Special Volume. 2, 119-161.

Shreve, R. L. (1972) Movement of water in glaciers. *Journal of Glaciology*, 11, 205-214.

Shreve, R. L. (1985a) Esker characteristics in terms of glacier physics, Katahdin esker system, Maine. *Bulletin of the Geological Society of America*, 96, 639-646.

Shreve, R. L. (1985b) Late Wisconsin ice-surface profile calculated from esker paths and types, Katahdin esker system, Maine. *Quaternary Research*, 23, 27-37.

Smith, M. J. (2011) Digital Mapping: Visualisation, Interpretation and Quantification of Landforms. In M. J. Smith, P. Paron and J. S. Griffiths, *Geomorphological Mapping*. Oxford, Elsevier. 15, 225-251.

Smith, M. J. & Wise, S. M. (2007) Problems of bias in mapping linear landforms from satellite imagery. *International Journal of Applied Earth Observation*, 9, 65-78.

Spagnolo, M., Clark, C. D. & Hughes, A. L. C. (2012) Drumlin relief. *Geomorphology*, 153–154, 179-191.

Spagnolo, M., Clark, C. D., Hughes, A. L. C. & Dunlop, P. (2011) The topography of drumlins; assessing their long profile shape. *Earth Surface Processes and Landforms*, 36, 790-804.

Spagnolo, M., Clark, C. D., Hughes, A. L. C., Dunlop, P. & Stokes, C. R. (2010) The planar shape of drumlins. *Sedimentary Geology*, 232, 119-129.

St-Onge, D. A. (1984) Surficial deposits of the Redrock Lake area, District of Mackenzie. *Current research: part A. Geological Survey of Canada Paper*, 84-01A, 271-278.

Stearns, L. A., Smith, B. E. & Hamilton, G. S. (2008) Increased flow speed on a large East Antarctic outlet glacier caused by subglacial floods. *Nature Geoscience*, 1, 827-831.

Stokes, C. R., Clark, C. D. & Storrar, R. (2009) Major changes in ice stream dynamics during deglaciation of the north-western margin of the Laurentide Ice Sheet. *Quaternary Science Reviews*, 28, 721-738.

Sundal, A. V., Shepherd, A., Nienow, P., Hanna, E., Palmer, S. & Huybrechts, P. (2011) Melt-induced speed-up of Greenland ice sheet offset by efficient subglacial drainage. *Nature*, 469, 521-524.

Tarasov, L., Dyke, A. S., Neal, R. M. & Peltier, W. R. (2012) A data-calibrated distribution of deglacial chronologies for the North American ice complex from glaciological modeling. *Earth and Planetary Science Letters*, 315–316, 30-40.

Tarasov, L. & Peltier, W. (2006) A calibrated deglacial drainage chronology for the North American continent: evidence of an Arctic trigger for the Younger Dryas. *Quaternary Science Reviews*, 25, 659-688.

Utting, D. J., Ward, B. C. & Little, E. C. (2009) Genesis of hummocks in glaciofluvial corridors near the Keewatin Ice Divide, Canada. *Boreas*, 38, 471-481.

Veillette, J. J. (1987) Surficial Geology, Grand Lake Victoria North, Québec. Geological Survey of Canada, Map 1641A. 1:100,000

Walder, J. S. & Fowler, A. (1994) Channelized subglacial drainage over a deformable bed. *Journal of Glaciology*, 40, 3-15.

Ward, B. C., Dredge, L. A. & Kerr, D. E. (1997) Surficial Geology, Lac de Gras, District of Mackenzie, Northwest Territories. Geological Survey of Canada Map 1870A. 1:125,000

Warren, W. P. & Ashley, G. M. (1994) Origins of the ice-contact stratified ridges (eskers) of Ireland. *Journal of Sedimentary Research*, 64, 433-499.

Chapter 4 Morphometry and pattern of a large sample (>20,000) of Canadian eskers: new insights regarding subglacial drainage beneath ice sheets

Storrar, R.D., Stokes, C.R. & Evans, D.J.A. (in prep) Morphometry and pattern of a large sample (>20,000) of Canadian eskers: new insights regarding subglacial drainage beneath ice sheets. *Quaternary Science Reviews.*

Abstract

Subglacial drainage beneath ice sheets has a profound effect on glacier dynamics, which are strongly influenced by the nature and quantity of meltwater entering the subglacial system. Accessing and monitoring contemporary sub-ice sheet meltwater drainage systems is notoriously difficult, but it is possible to utilise the exposed beds of palaeo-ice sheets. In particular, eskers record deposition in glacial drainage channels and are widespread on the exposed beds of former ice sheets, although they have only rarely been studied in detail at the ice sheet scale. This paper presents new data on the distribution, pattern, and morphometry of a large (>20,000) sample of eskers in Canada, formed under the Laurentide Ice Sheet, including quantification of their length, fragmentation, sinuosity, lateral spacing, number of tributaries and downstream elevation changes. Results indicate that the channels in which eskers formed were typically very long (hundreds of km) and often very straight (mean sinuosity approximates 1), which has implications for our understanding of how eskers form and how subglacial meltwater channels are configured, the major implication being that they seem to be quite stable. In many locations, the lateral distance between neighbouring eskers is remarkably consistent and results indicate a preferred spacing of around 12 km, a figure which can be used alongside recent theoretical work to explore what controls channel spacing. In other locations, typically over soft sediments, esker patterns are more chaotic, as predicted by theory. Integration of esker patterns with an existing ice margin chronology reveals that the meltwater drainage system evolved during deglaciation: eskers became more closely spaced with fewer tributaries as deglaciation progressed, which may relate to increased meltwater supply from surface melt. Eskers show no preference to trend up or down slopes, indicating that ice surface was an important control on their location, as suggested by theory. In addition, the data are particularly suitable for: (i), assessment of the factors that control esker location and formation; (ii), rigorous testing of numerical models of meltwater drainage routing, and (iii), a refined understanding of ice margin configurations during retreat of the Laurentide Ice Sheet.

4.1 Introduction

Eskers are common in formerly warm-based glaciated terrains (e.g. Chapter 3; Prest *et al.*, 1968; Clark *et al.*, 2004), making them a useful indicator of subglacial meltwater drainage pathways. Meltwater drainage beneath ice sheets is of fundamental importance to our understanding of ice dynamics (see Chapters 1 and 2). Unfortunately, direct observation of the subglacial drainage systems of ice sheets is extremely difficult and so indirect methods such as dye tracing (e.g. Nienow *et al.*, 1996), remote sensing (e.g. Fricker *et al.*, 2010), numerical modelling (e.g. Lewis & Smith, 2009; Hewitt, 2013) and geophysical surveys (e.g. Carter *et al.*, 2009) are employed to investigate how they operate. Whilst significant breakthroughs have been made with these techniques (e.g. Richards *et al.*, 1996; Nienow *et al.*, 1998; Wingham *et al.*, 2006; Fricker *et al.*, 2007), they are often limited by their rather coarse spatial and temporal resolution. Furthermore, numerical modelling of subglacial drainage systems is also inhibited because there are few data with which to test model predictions, e.g. channel spacing (Hewitt, 2011) and sinuosity (Schuler & Fischer, 2009). As such, it is difficult to assess how water moves beneath contemporary ice sheets: for example, where and whether it occurs in distributed or channelized systems. The abundance of eskers on palaeo-ice sheet beds provides huge potential to record aspects of subglacial meltwater drainage that are otherwise difficult or impossible to investigate using existing techniques.

Despite their huge potential, there is uncertainty as to exactly how eskers form (see Section 2.6). For example, it has been suggested that eskers may form synchronously or, alternatively, time-transgressively over large portions of their length (e.g. Banerjee & McDonald, 1975; Shilts, 1984; Hebrand & Åmark, 1989; Brennand, 2000; Mäkinen, 2003). This has important implications for whether meltwater conduits maintained a stable location at the margin (i.e. remained open each winter) over significant lengths of time (time-transgressive esker formation), or whether they are potentially more transitory, reflecting sudden deposition in a long conduit (synchronous esker formation). Similarly, several different types of esker have been reported in the literature (e.g. Price, 1969; Warren & Ashley, 1994; Knudsen, 1995; Menzies & Shilts, 1996; Christoffersen *et al.*, 2005; Evans *et al.*, 2007; Evans *et al.*, 2010), which raises questions as to whether different eskers may be formed by different combinations of subglacial processes or even englacial and supraglacial tunnels, fractures, or crevasse filling (see Chapter 2).

These important questions arise from the findings of numerous studies of eskers which are often based on small sample sizes and localised observations (e.g. Gorrell & Shaw, 1991; Brennand, 1994; Burke *et al.*, 2010). To date, no large-scale, systematic quantification of the spatial patterns and morphometry of eskers has been undertaken. The aim of this paper is to address this shortfall by producing the first large-scale quantitative analysis of the patterns and spatial characteristics of eskers across an ice sheet bed, similar to those recently undertaken for ribbed

moraine (Dunlop & Clark, 2006), drumlins (Clark *et al.*, 2009; Spagnolo *et al.*, 2010; Spagnolo *et al.*, 2011; Spagnolo *et al.*, 2012) and mega-scale glacial lineations (Stokes *et al.*, 2013). This is achieved using the GIS dataset of eskers mapped from Landsat 7 ETM+ imagery of the whole of Canada and covering almost 10,000,000 km^2 formerly occupied by the Laurentide Ice Sheet (LIS), presented in Chapter 3. We present data on esker pattern, distribution, length, fragmentation, sinuosity, spacing, tributaries, 'stream' ordering and down-esker elevation changes, thereby providing an important dataset for testing both conceptual and numerical models of esker formation and new insights into channelized meltwater drainage at the ice sheet scale.

4.2 Methods

4.2.1 Datasets

We analyse esker morphometry and pattern from two datasets. The first is an ice sheet-wide map of 20,186 large (mostly > 2 km) eskers digitised from Landsat ETM+ imagery of Canada, recently published in Storrar *et al.* (2013) and presented here in Chapter 3 and as a map in the appendix. For details of the methods employed during the mapping, see Chapter 3.

For further analysis of some metrics, such as the minimum length of esker forming channels and lateral spacing, we also derived a second dataset from the above whereby 'gaps' between esker ridges (that result from non-detection, fragmentary deposition, post-depositional erosion or submergence beneath lakes) were filled by interpolating a straight line between eskers. This dataset was produced in order to avoid producing statistics that would be distorted by the absence of eskers for the above reasons. Some measurements, such as the spacing between subglacial channels, are overestimated if there are gaps in eskers; conversely, the length of subglacial channels is underestimated. Thus, the 'interpolated' dataset indicates where the major channels which formed the eskers were generated. Esker fragments were joined conservatively (13,314 'gaps' were connected, of which 94% were < 10 km long) and we are confident that they connect eskers which are genetically related (see Figure 4.1). We refer to the two datasets as *mapped* and *interpolated* eskers, respectively.

4.2.2 Length (l_e)

Esker length (here given the notation l_e) is the distance covered by the crestline of an esker, (Figure 4.3A) and is related to the length of the conduit in which it is formed. Esker crestline lengths were extracted from the *mapped* eskers dataset. In addition, length was also extracted from the *interpolated* eskers data, to allow an estimation of the fragmentation (induced by gaps) of eskers and also to provide an approximate measurement of the esker-forming conduit. Where

two or more eskers coalesced, the longest ridge was systematically used to determine length (see Figure 4.3A).

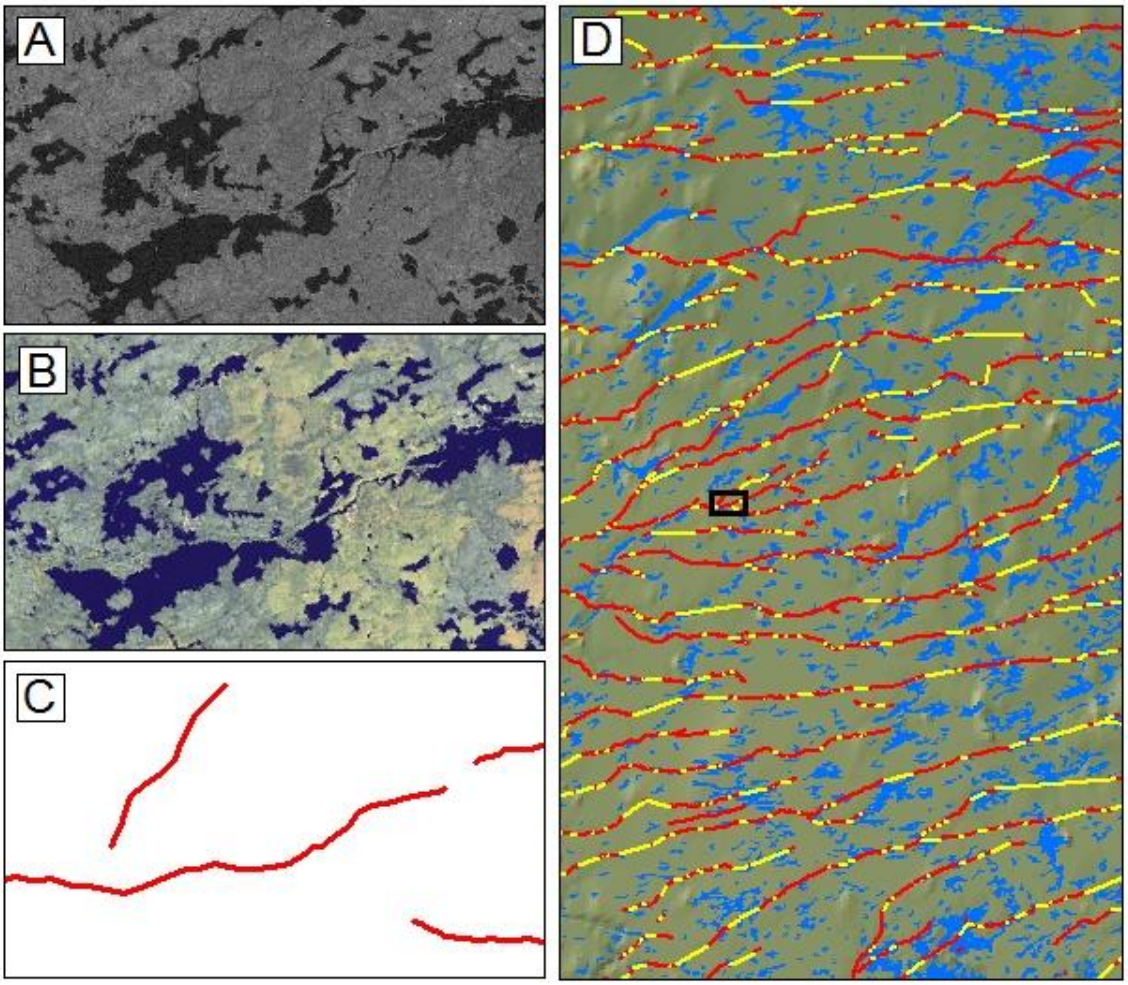

Figure 4.1. A) Eskers in band 8 Landsat image (15 m resolution); B) Eskers in 7,5,2 (R,G,B) Landsat image (30 m resolution); C) Eskers digitised from A) and B). Note fragmentary nature of esker ridges, mostly due to lakes. D) DEM and lakes (blue) with digitised esker ridges (red) and 'interpolated' eskers (yellow), which join breaks in esker ridges. Location of A, B and C is shown by the black box.

4.2.3 Sinuosity (*S*)

Sinuosity was calculated for both *mapped* and *interpolated* eskers by dividing l_e by the length of a straight line (l_s) between the co-ordinates of the esker start (x_{start} and y_{start}) and end (x_{end} and y_{end}) points:

$$l_s = \sqrt{(x_{end} - x_{start})^2 + (y_{end} - y_{start})^2} \qquad (4.1)$$

Measurements of esker sinuosity are typically dependent on the length of the esker. Very short eskers tend to have very low sinuosity values (the lowest possible value being 1) because they often make up short, straight segments of a larger, more sinuous system (see Figure 4.4A).

Thus, because the *mapped* eskers represent a fragmented view of the channels in which they formed, it is likely that the sinuosity values calculated from them are an underestimate of the sinuosity of the original channels in which they formed.

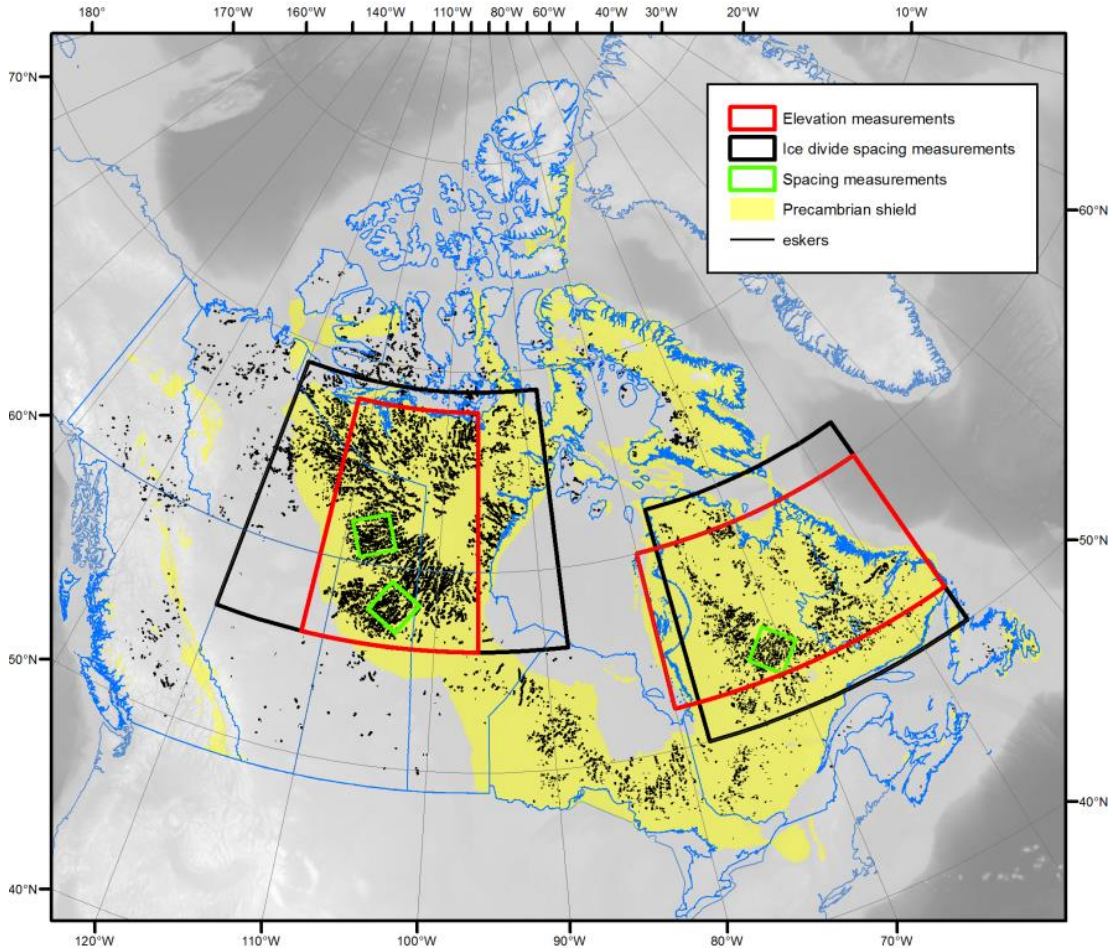

Figure 4.2. Eskers mapped from Landsat imagery of Canada. Also shown are the areas used to calculate spacing and frequency around the final locations of the Keewatin (west) and Ungava (east) ice divides, the areas used to calculate esker spacing in high density locations (see section 4.2.4), and the area used to measure elevation changes. The Precambrian Shield is shown in yellow (from Wheeler *et al.*, 1996).

In order to explore this potential bias, we conducted a sensitivity analysis, whereby the *mapped* eskers were used to test the extent to which calculations of sinuosity are distorted by the length of the esker fragment. We split the *mapped* eskers into smaller ridges of different lengths (in 0.5 km increments from 0.5 km to 20 km; see Figure 4.4 for details) and measured the sinuosity of all the smaller ridges in each case (Figure 4.4). As expected, this demonstrates that longer fragments of eskers tend to have higher sinuosity values. The relationship is well represented by a power law ($S = l_e^{0.0152}$ for median sinuosity [$R^2 = 0.9944$]; $S = l_e^{0.0161}$ for mean sinuosity [$R^2 = 0.9971$]). The mean and median sinuosity values of the *mapped* esker dataset lie within the upper and lower values obtained from this analysis (dashed lines in Figure 4.4C) and give us

confidence that although they are likely underestimates, the magnitude of this error is on the order of ~0.05, which is relatively small.

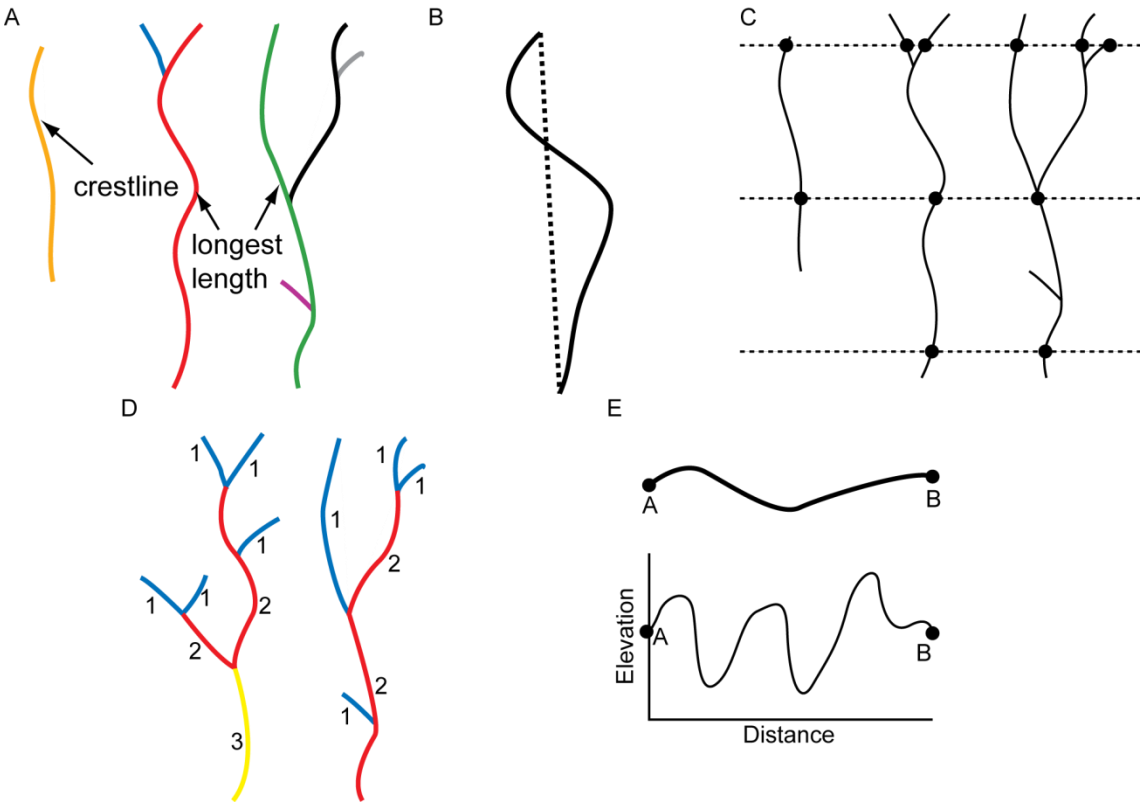

Figure 4.3. The different methods used to calculate the six parameters in this chapter. A) Length: each shaded colour represents possible length measurements. Where tributaries coalesce, the longest measurement was extracted. B) Sinuosity: the length of the esker ridge was divided by the length of a straight line between the start and end points. C) Lateral spacing: Points were calculated where eskers intersect equidistant transects and lateral spacing was calculated from the distance between these points. D) Stream ordering: the Strahler number for each esker was calculated, based on the number and order of tributaries entering each esker. E) Elevation change: elevation values were extracted at the beginning and end points of each esker from a digital elevation model (CDED).

4.2.4 Lateral spacing

In order to test model predictions of esker spacing (Boulton *et al.*, 2009; Hewitt, 2011: see Chapter 6), it is necessary to measure the spacing between eskers in an area where the eskers are sufficiently dense to represent the majority of the channels in which they were formed, because the models do not generally account for the non-formation or subsequent erosion of eskers. Three large (40,000 km^2) sample areas (see Figure 4.2) were selected where eskers are numerous and appear to be well preserved, with minimal evidence of postglacial erosion. Each area was divided into 15 × 200 km transects aligned perpendicular to the dominant esker

orientation and spaced 12.5 km apart (e.g. Figure 4.5). Esker spacing was calculated along each transect, for both *mapped* and *interpolated* eskers.

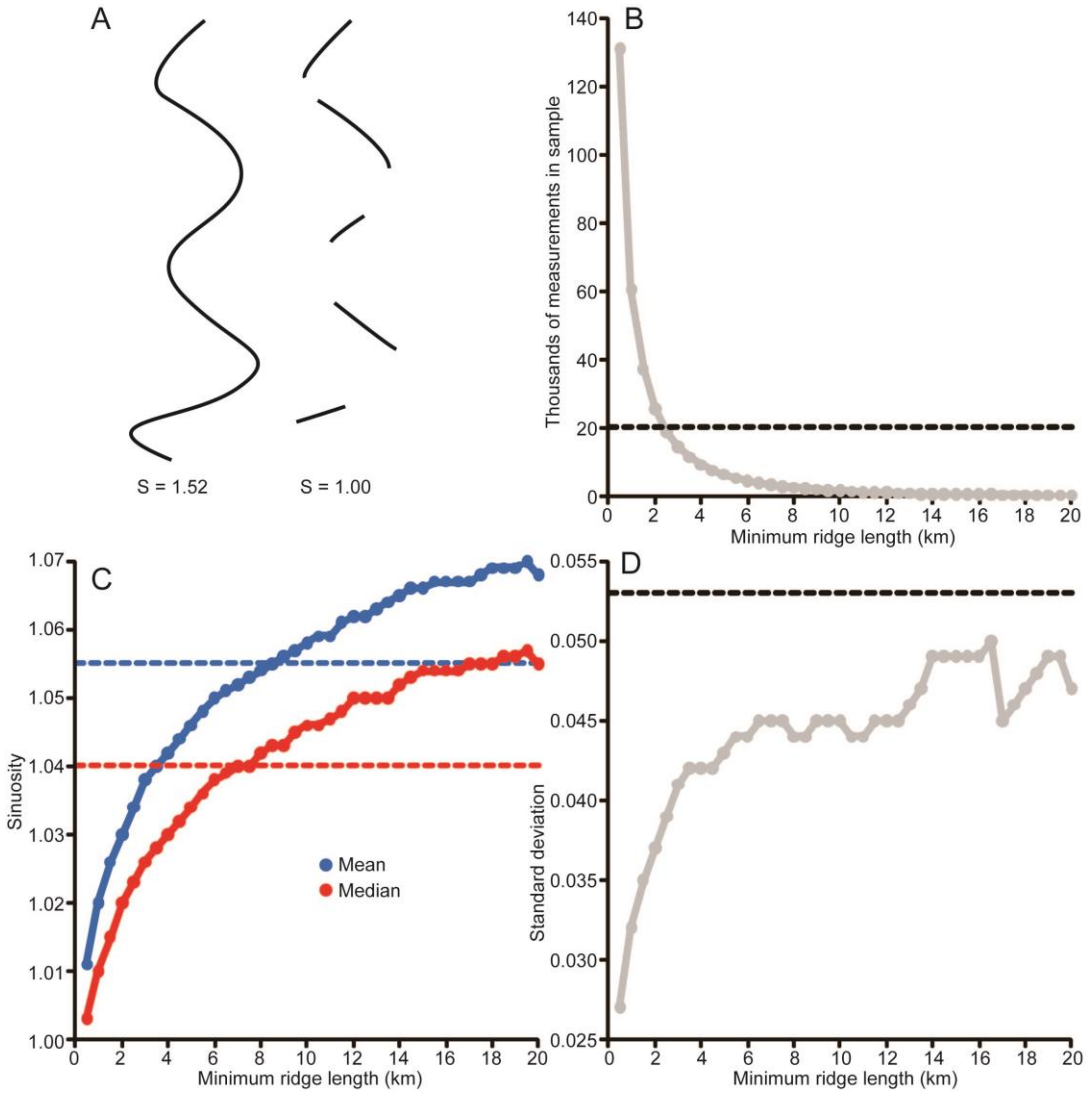

Figure 4.4. The effect of esker length on sinuosity measurements. A) Illustration of how fragmenting an esker can result in a smaller overall sinuosity (S in the second diagram represents the mean of the five smaller ridges). B) Number of measurements sampled for each minimum esker length. C) Mean and median sinuosity for each length. D) Standard deviation. Dashed lines indicate the value calculated from the whole *mapped* eskers dataset.

4.2.5 Tributary ordering

Tributaries were identified by intersecting both the *mapped* and interpolated eskers. Tributary order was calculated using the Strahler method (see Figure 4.3) for each esker.

4.2.6 Elevation change

The difference in elevation between the start and end points was calculated for 11,560 *mapped* eskers around the final locations of the Keewatin and Ungava ice divides (Figure 4.2). The locations selected for the analysis contain a large sample of eskers within an area in which we are confident of the flow direction, which radiated outwards from the final locations of the ice divides (Shilts *et al.*, 1987; Aylsworth & Shilts, 1989a; Clark *et al.*, 2000). We refrain from analysing the entire dataset because esker orientation is not known in some cases where they are more sporadic away from the ice divides. Elevations were taken from the Canadian Digital Elevation Database (CDED), which has a horizontal resolution of ~17 m and vertical resolution of 1 m in the areas studied. Elevation changes were determined by subtracting the elevation at the end point of each esker from the elevation at the start point, meaning that negative values denote a decrease in elevation down-ice and positive values denote an increase in elevation down-ice.

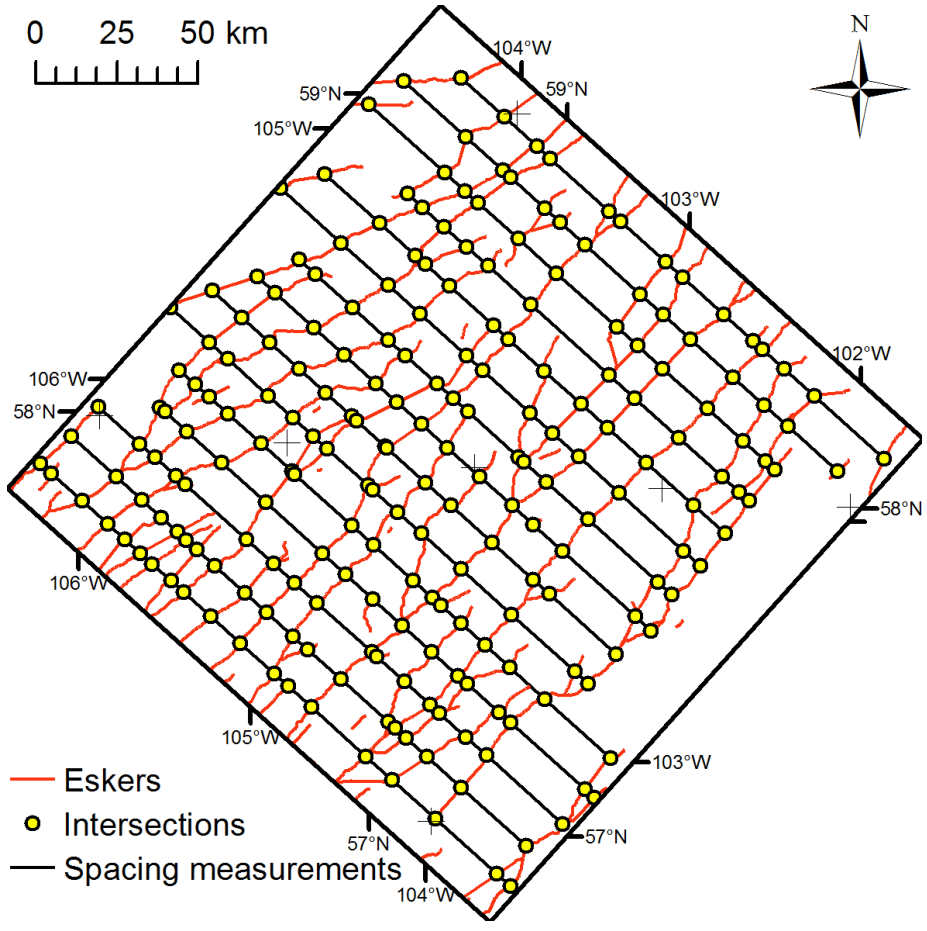

Figure 4.5. Example of the transects used for calculation of *interpolated* esker spacing in the Saskatchewan study area (lower left green box in Figure 4.2).

4.3 Results

4.3.1 Pattern and distribution

A total of 20,186 large esker ridges were mapped (see appendix; Chapter 3; Storrar *et al.*, 2013) and, most obviously, the majority of large esker systems are concentrated on the Canadian Shield, as noted by Clark & Walder (1994). Nevertheless, eskers are also present in other areas, where potentially more deformable substrates, rather than resistant shield rocks, predominate, indicating that channelized drainage can occur over softer sedimentary beds. This is discussed further in Chapter 6.

At the largest scale, eskers are seen to radiate away from the final locations of the major ice divides in Ungava and Keewatin (see appendix; Dyke & Prest, 1987; Aylsworth & Shilts, 1989a; Aylsworth & Shilts, 1989b; Boulton & Clark, 1990), beneath which they are noticeably absent: esker-free areas are roughly 100-150 km wide in both Keewatin and Ungava and are approximately 93,000 and 174,000 km^2 respectively (see map in appendix and Chapter 5 for further discussion). Radiating away from the final locations of the major ice divides, regularly spaced channels appear to correspond to an integrated system of eskers with multiple tributaries (Figure 4.6A). Outside of these systems, esker patterns are more chaotic, with some branching esker systems, but with many discrete single eskers or areas of eskers which are not obviously aligned with each other (Figure 4.6B and C).

4.3.2 Length and fragmentation

The length of *mapped* esker ridges follows a log-normal distribution (Figure 4.7), with a skewness of 4.57 and excess kurtosis of 40.94. Individual esker ridges extend up to 97.5 km, with a mean of 3.5 km and median of 2.1 km. 56 % of esker ridges are 1-5 km long and 70 % are 1-10 km long.

When gaps are taken into account, *interpolated* eskers extend for up to 760 km and have a mean length of 15.6 km and median of 4.1 km. Assuming that the gaps have been correctly identified (we are confident that they have: see Figure 4.1), this shows that eskers are highly fragmented: gaps represent 34.9% of the total length of the esker systems mapped. The distribution is also approximately log-normal, with skewness of 6.57 and excess kurtosis of 71.61. The longest esker systems radiate outwards from the final location of the Keewatin Ice Divide, though there are also esker systems up to 290 km long in Quebec (see Figure 4.8).

4.3.3 Sinuosity

Mapped esker sinuosity follows a distribution similar to log-normal, though it is more positively skewed (skewness = 3.41) towards lower values: 87% of eskers have a sinuosity value between

1.0 and 1.1 and 98% have a sinuosity value of between 1.0 and 1.2. The mean value is 1.055 and the median is 1.042. *Interpolated* esker sinuosity has a similar distribution but values tend to be slightly higher, with a mean of 1.075 and median of 1.058 (Figure 4.9).

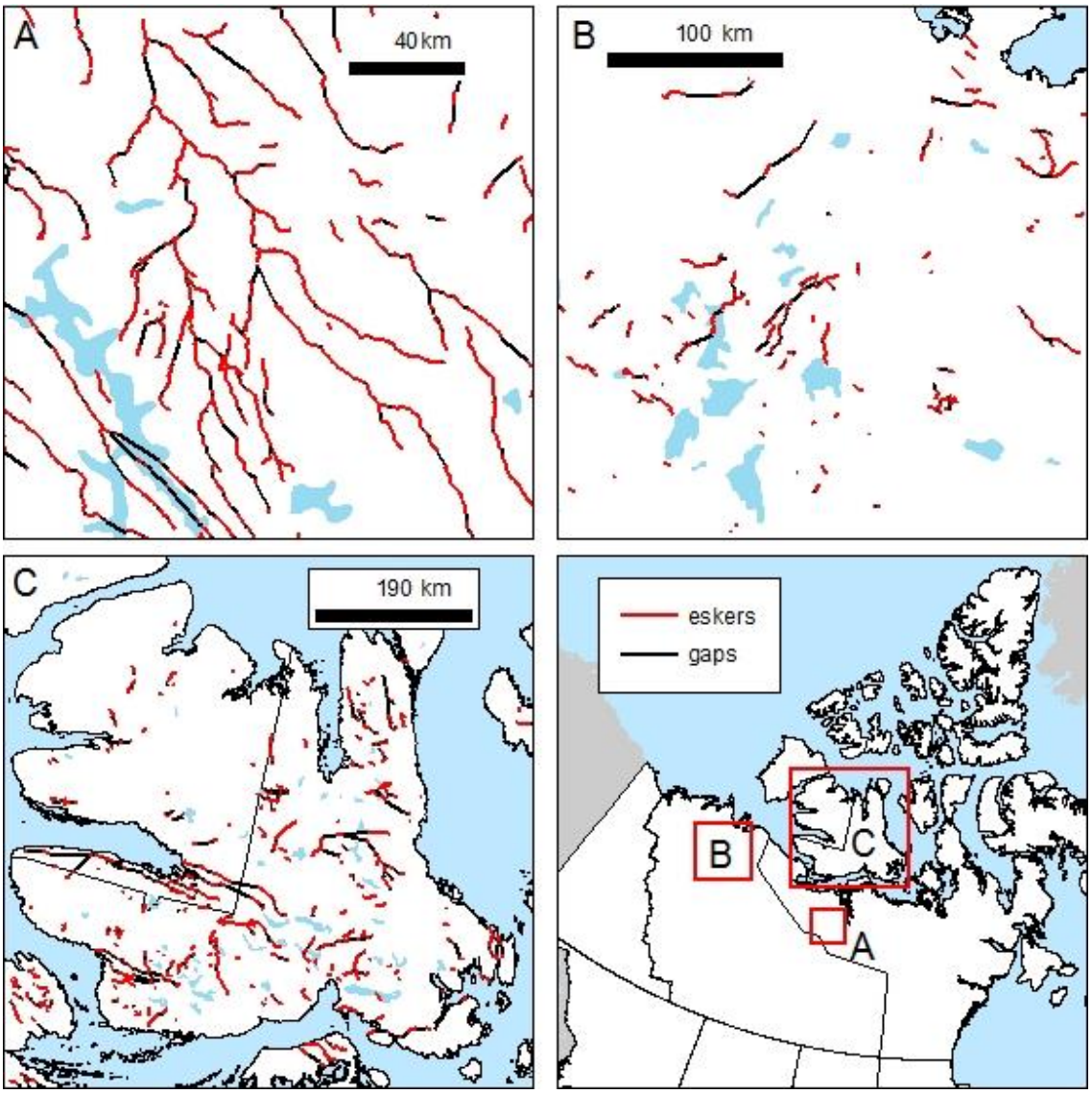

Figure 4.6. Esker patterns. A) Integrated dendritic network with multiple tributaries, typical of the eskers around the final location of the Keewatin Ice Divide. B) and C) Chaotically arranged eskers typical of the Canadian Arctic and far north-west.

4.3.4 Lateral spacing

Measurements of esker spacing in three sample areas indicate that the distribution of spacing data follow an approximately normal distribution (Figure 4.10). *Mapped* eskers have a higher mean spacing than *interpolated* eskers (18.8 km compared with 12.3 km), as would be expected, because fewer *mapped* esker ridges intersect the transects, compared with the more contiguous *interpolated* eskers. Likewise, standard deviation values of esker spacing are higher for the

mapped eskers than the *interpolated* eskers. The three sample areas, when treated individually, produce broadly similar results for esker spacing (see Table 4.1). The *mapped* esker data values span a range of 3.7 km and the *interpolated* esker data values have a range of just 0.3 km. Mean esker spacing in the three areas when combined is 18.8 km (standard deviation is 14.0 km) for *mapped* eskers and 12.3 km (standard deviation is 6.6 km) for *interpolated* eskers. The relatively low standard deviations, compared with the means, suggest that esker spacing is approximately regular, particularly in the case of the *interpolated* eskers.

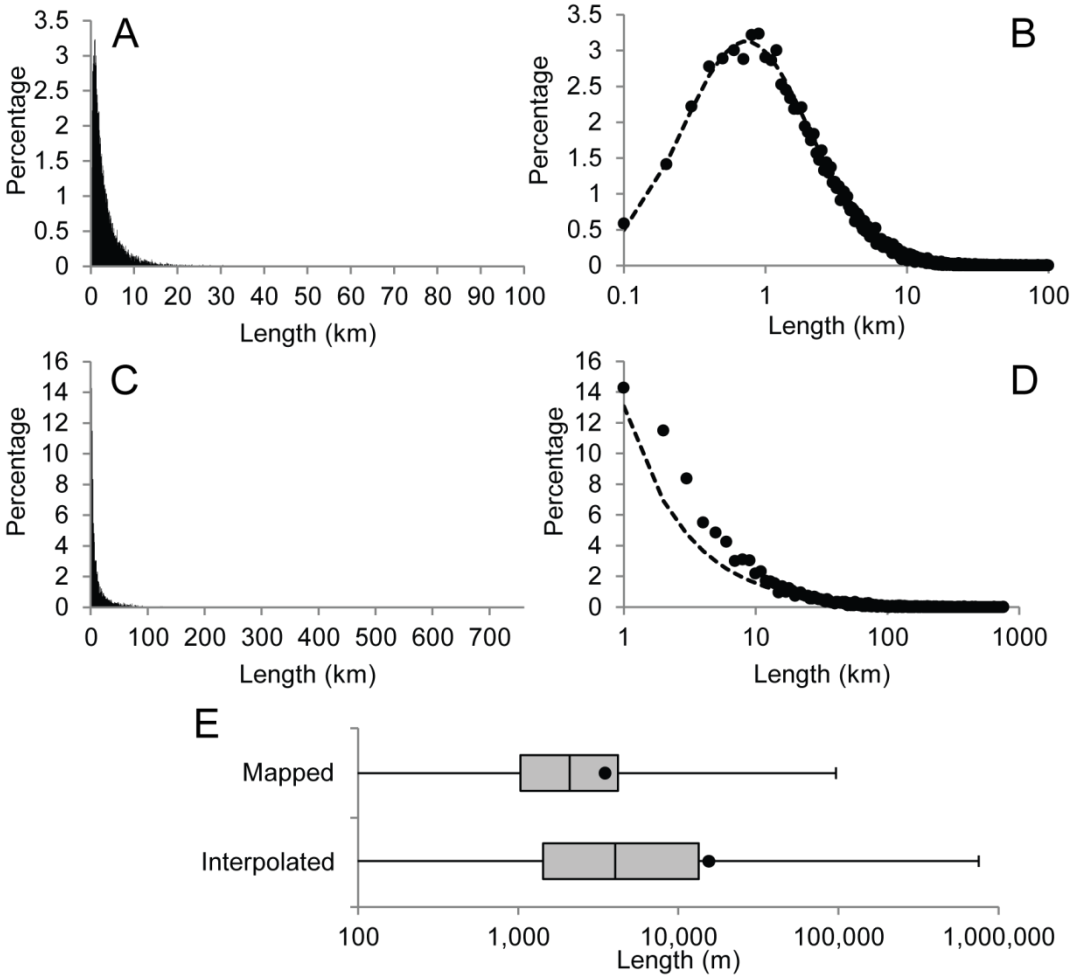

Figure 4.7. Esker length statistics. A) Histogram of *mapped* esker length (n = 20,186, 1 km bins). B) *Mapped* esker length plotted on $\log_{10}$ x-axis (1 km bins). Log-normal distribution with the same mean and standard deviation shown by dashed line. C) Histogram of *interpolated* esker length (n = 5,932, 1 km bins)). D) *Interpolated* esker length plotted on $\log_{10}$ x-axis (1 km bins). Log-normal distribution with the same mean and standard deviation shown by dashed line. E) Box and whisker plot comparing *mapped* and *interpolated* esker length measurements. Whiskers denote the range of values, points denote means and the boxes span the range of the 25 – 75% percentiles, with the median as a vertical bar. Note $\log_{10}$ x-axis.

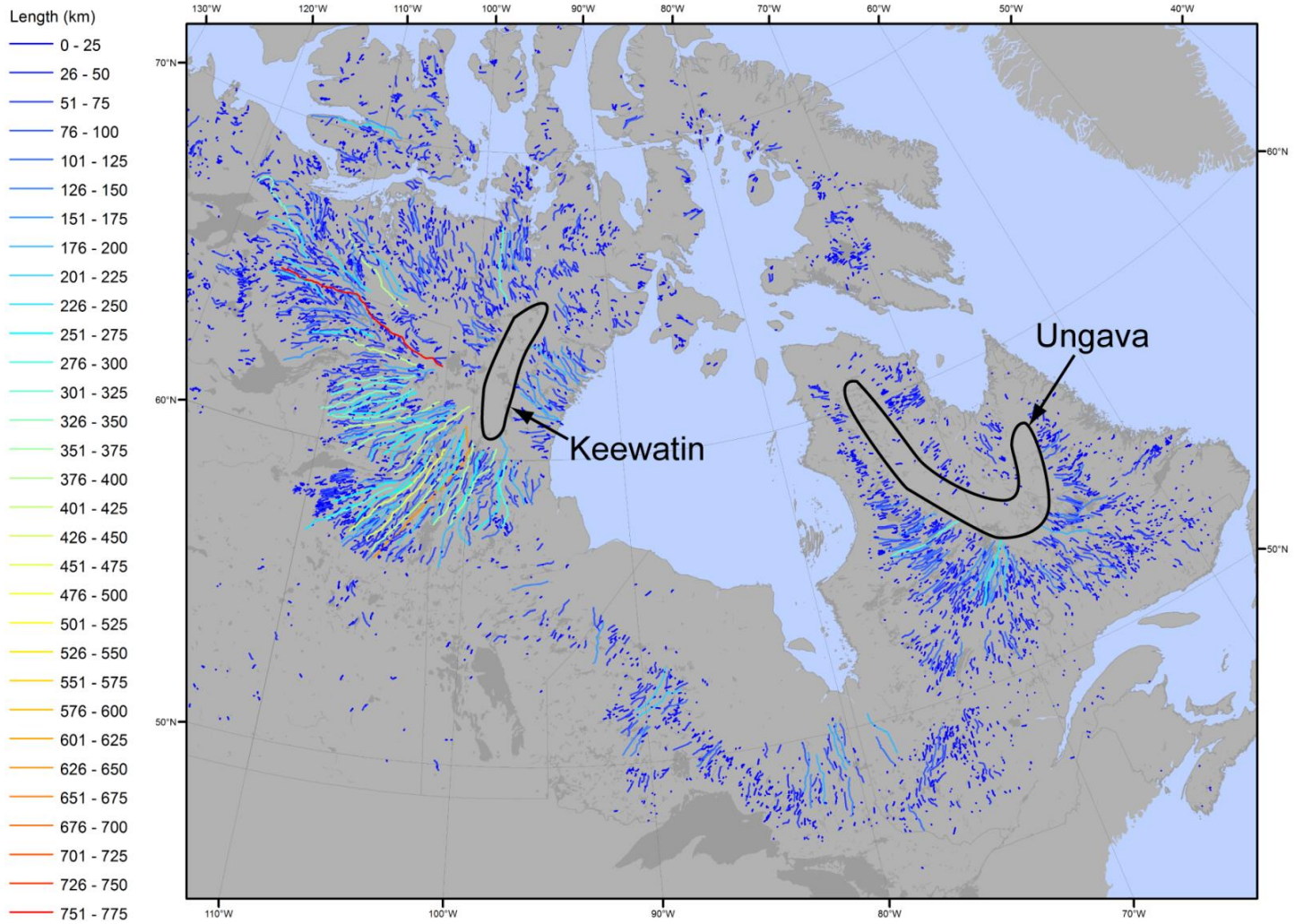

Figure 4.8. Map of *interpolated* eskers classified by length. Note the radial pattern of long esker systems radiating from the final locations of the Keewatin and Ungava Ice Divides and the relatively even spacing of the largest eskers.

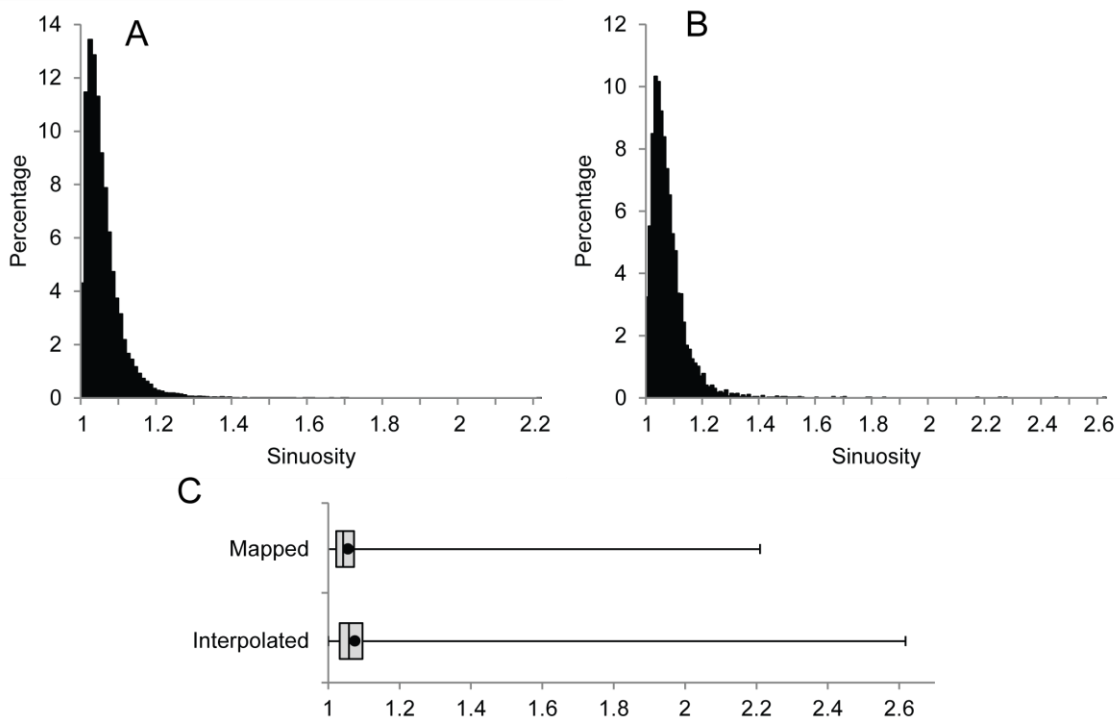

Figure 4.9. Histograms of esker sinuosity for (A) *mapped* eskers (n = 20,186, 0.01 bins) and (B) *interpolated* eskers (n = 5,932, 0.01 bins). C) Box and whisker plot comparing the two distributions. Whiskers denote the range of values, points denote means and the boxes span the range of the 25 – 75% percentiles, with the median as a vertical bar.

4.3.5 Tributary ordering

The extensive fragmentation of the *mapped* eskers resulted in the identification of few tributaries. Thus, the majority (96.5%) of eskers were found to be first-order, with 3.5% second-order tributaries and only two third-order (Table 4.2). Analysis of tributary ordering using *interpolated* eskers reveals, unsurprisingly, a much more integrated pattern: *interpolated* esker systems possess more tributaries, especially around the final location of the Keewatin Ice Divide (Figure 4.11). Fourth-order tributaries are noted in two locations and second- to fourth-order tributaries account for approximately 25% of all the *interpolated* eskers (Table 4.2). Around the final location of the Ungava ice divide, there are just two third-order tributaries, with the majority being first- to second-order. Elsewhere, third-order tributaries are rare, the systems being dominated by first- to second-order eskers.

Table 4.1. Spacing statistics for each study area. Figures in italics indicate data calculated for eskers with interpolated gaps – note the lower associated standard deviation in each case.

Location	Area	No. of spacing measurements	Mean spacing	Standard deviation
1. Northwest Territories	40,000 km^2	138	17.0 km	12.6 km
		224	*12.1 km*	*6.4 km*
2. Northern Saskatchewan	40,000 km^2	113	19.5 km	14.9 km
		209	*12.4 km*	*6.9 km*
3. Québec	40,000 km^2	96	20.7 km	14.7 km
		200	*12.4 km*	*6.6 km*
1,2 and 3 combined	120,000 km^2	347	18.8 km	14.0 km
		632	*12.3 km*	*6.6 km*

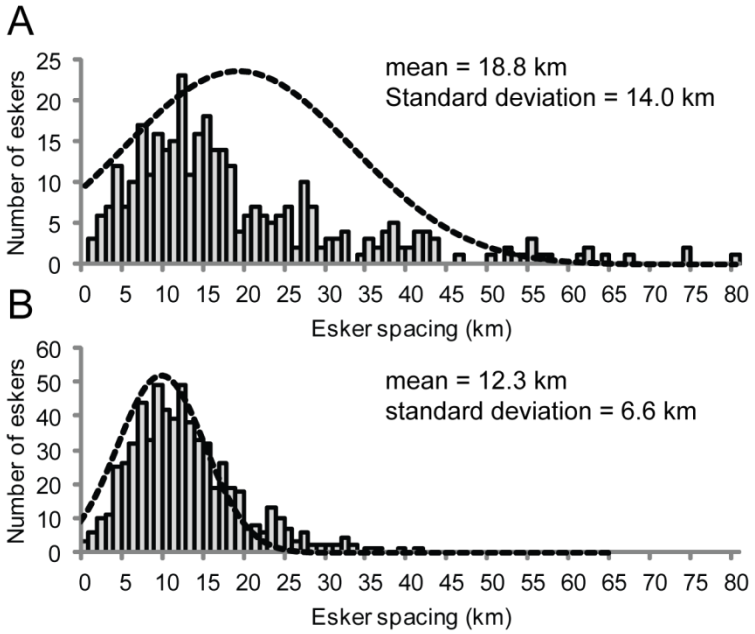

Figure 4.10. Histograms of esker spacing (1 km bins) for the three test areas (see Figure 4.2). Dashed lines are normal distributions with the same mean and standard deviation as the data. A) *Mapped* eskers (n = 347). B) *Interpolated* eskers (n = 632).

Table 4.2. Total length of first- to fourth-order tributary eskers.

Strahler number	Total length (km) *mapped*	Percentage of total *mapped*	Total length (km) *interpolated*	Percentage of total *interpolated*
1	68,785	96.472	824,268	74.999
2	2,512	3.524	232,848	21.187
3	3	0.004	41,823	3.805
4	N/A	N/A	98	0.009

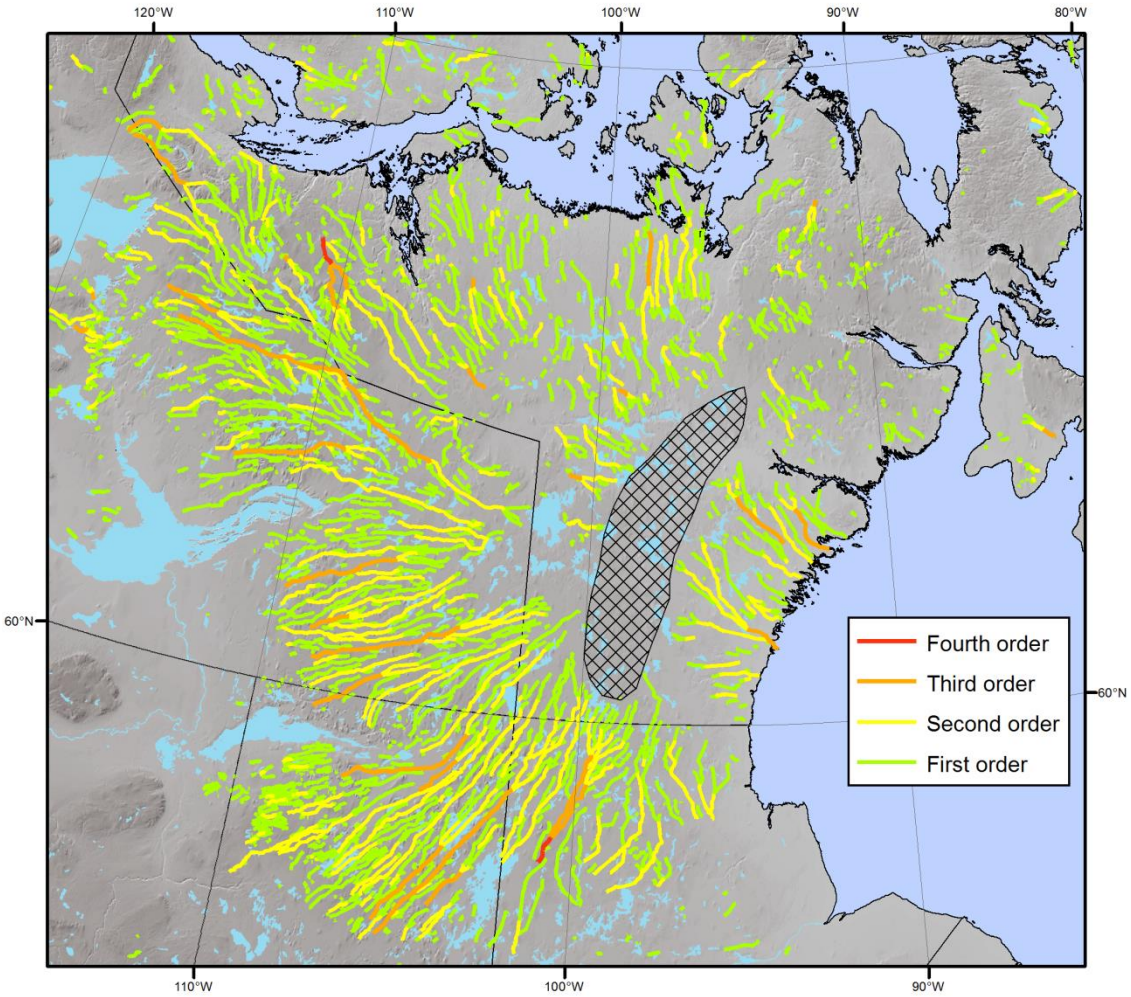

Figure 4.11. Strahler numbers calculated for *interpolated* eskers around the final location of the Keewatin (shaded). Note that fourth-order tributaries are developed in two locations.

4.3.6 Elevation change

Mapped eskers exhibit small changes in elevation along their length (Figure 4.12). The mean elevation change for 11,560 eskers is 1.07 m (a small increase in elevation down-ice) and the

median is 0 m. The standard deviation is 15.13 m. 73% of the eskers change in elevation by no more than ± 10 m. The values are normally distributed about 0 m, indicating that there is no clear uphill or downhill trend to esker profiles, though the largest elevation change is in the downslope direction (-160 m). 4,634 (40%) eskers trend downhill, 1,864 (16%) exhibit no change in elevation and 5,062 (44%) trend uphill (by up to 143 m). It is important to note that the elevation values presented here are not corrected for glacio-isostatic adjustment, which may skew the results where long eskers stretch from areas of pronounced uplift (especially near to the final location of the Keewatin ice divide) to areas of more subdued uplift (see Peltier, 2004; Dyke *et al.*, 2005).

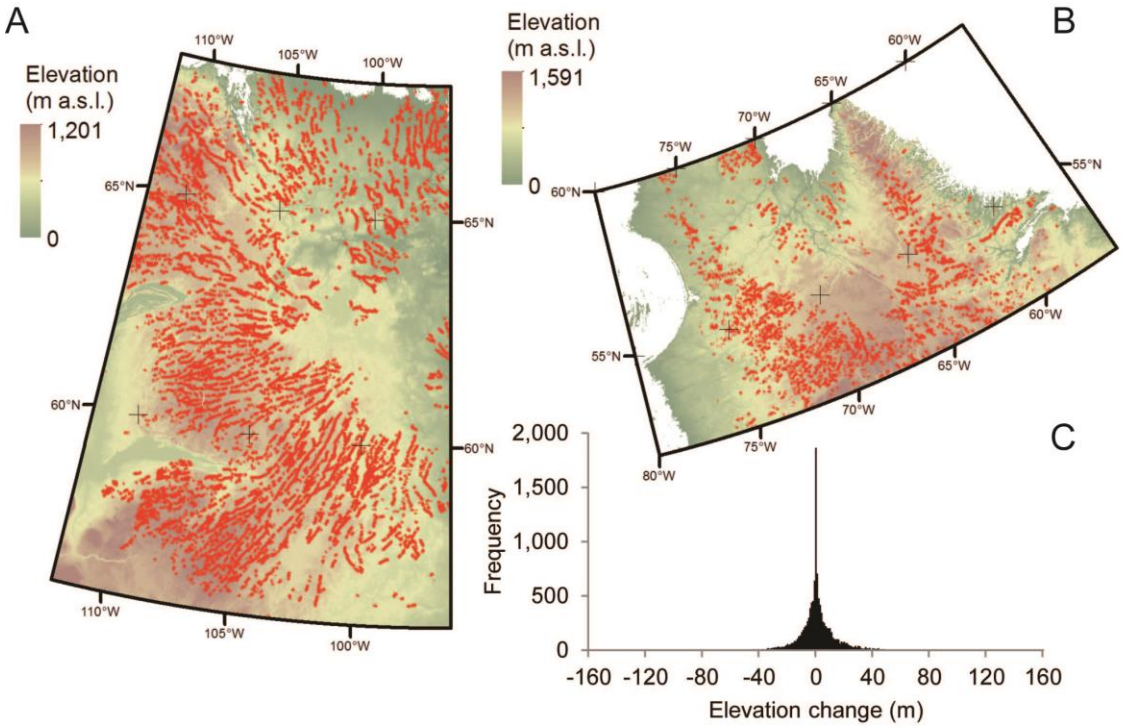

Figure 4.12. A) Topography and esker distribution in the Keewatin study area (n = 6,671). B) Topography and esker distribution in the Ungava study area (n = 4,889). C) Histogram of elevation change values (1 m bins) for eskers in both areas (n = 11,560). Positive values denote eskers trending uphill and negative values indicate a downhill trend.

4.4 Discussion

4.4.1 Pattern and distribution

Outside the areas formerly occupied by major ice divides, eskers are arranged in integrated radial networks of up to fourth-order tributaries, reflecting the network of conduits in which the eskers formed and supporting the similar observations of Shilts *et al.* (1987). The continuous retreat with minimal readvances of the ice sheet in these areas (Dyke *et al.*, 2003; Figure 4.13) made it possible for this integrated pattern of conduits to be preserved. In other locations,

notably western Northwest Territories and Victoria Island, eskers are distributed more chaotically, in marked contrast to the eskers emanating from the final locations of the ice divides (see Figure 4.8). It is likely that this reflects the deposition of eskers during different phases of the complex ice dynamics which operated in these areas as ice streams switched on and off (Kleman & Glasser, 2007; Stokes *et al.*, 2009; Brown *et al.*, 2011).

The abundance of eskers on the Canadian Shield is likely a result of three interrelated factors: (1) This is the location where deglaciation took place (Figure 4.13); (2) Resistant Shield rocks are more conducive to esker formation than areas of more deformable sediment (Clark & Walder, 1994); and (3) Topographically, the Shield provides little impediment to the formation of long, regularly spaced eskers, in contrast with the Cordilleran Ice Sheet, for example, where high relief precluded the development of regularly spaced and very long (100s of km) eskers.

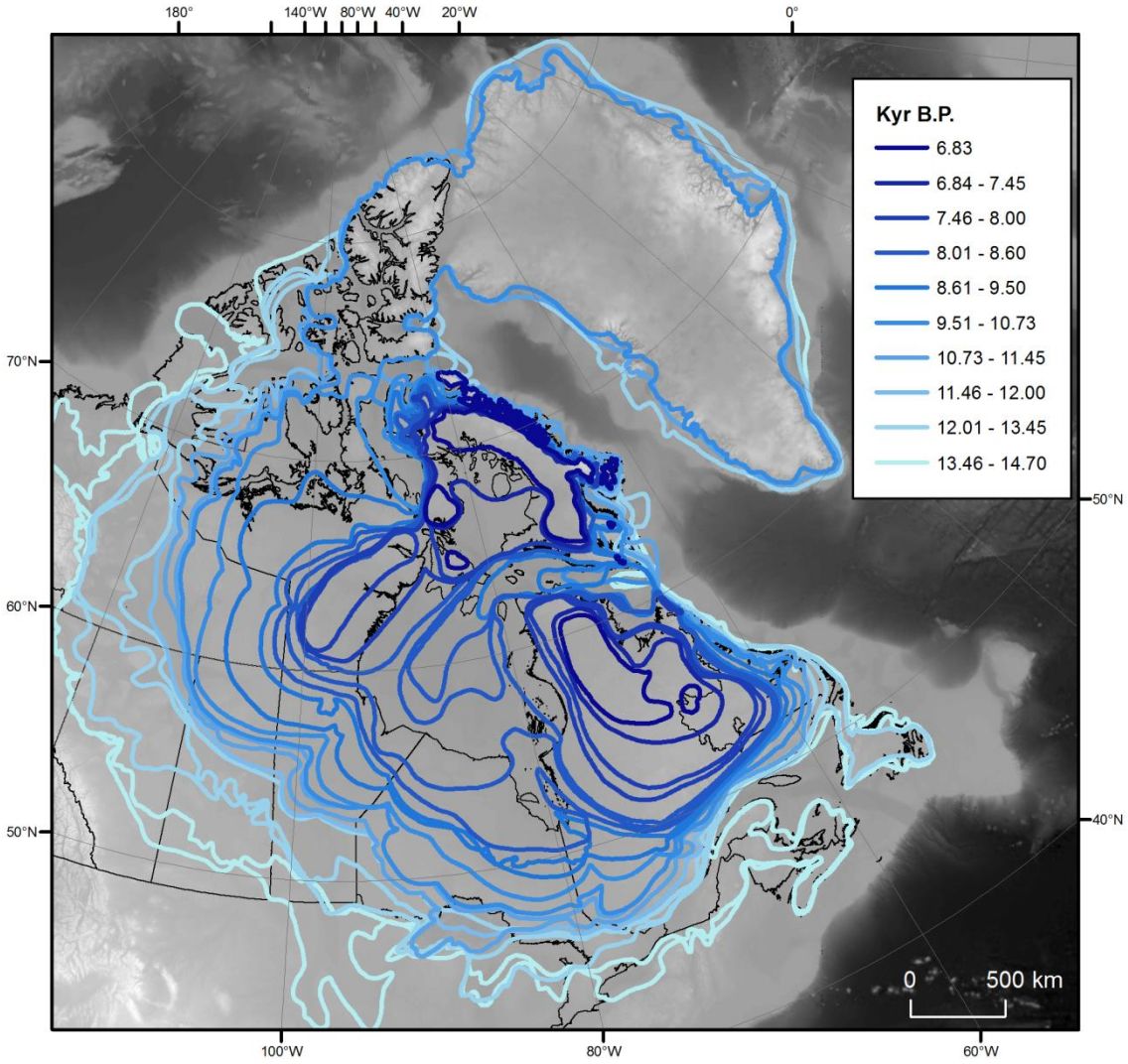

Figure 4.13. Deglaciation of the Laurentide Ice Sheet (smaller ice caps not contiguous with the Laurentide Ice Sheet not shown) from 14.70 to 6.83 kyr B.P. (after Dyke *et al.*, 2003).

No instances of cross-cutting eskers were found in the mapping, which contrasts markedly with the abundance of cross-cutting lineations found on the LIS bed (e.g. Boulton & Clark, 1990; Stokes *et al.*, 2009; Brown *et al.*, 2011). This suggests either that eskers have a low potential for preservation beneath dynamic ice sheets, or that they form exclusively during deglaciation (or both). Elsewhere, eskers have been shown to survive entire glaciations beneath frozen beds (Lagerbäck & Robertsson, 1988; Kleman, 1994) and frozen beds have been inferred beneath parts of the LIS (Kleman & Glasser, 2007), though the subglacial thermal regime changes through time (e.g. Marshall & Clark, 2002) and it is unlikely that eskers in Canada would have been preserved for an entire glacial cycle. Moreover, eskers require a significant input of meltwater in order to form, meaning that this is more likely to occur during deglaciation, when surface melting is a significant process (Carlson *et al.*, 2009) and the probability of preservation at this time is also largest, since there is then no more ice to erode them. It is for these reasons that eskers are frequently interpreted as deglacial landforms and are often used to reconstruct deglaciation (e.g. Dyke & Prest, 1987; Dyke *et al.*, 2003; Stokes *et al.*, 2009; Margold *et al.*, 2011; Margold *et al.*, 2013). Nevertheless, it is possible that some small areas may contain eskers that are related a prior flow phase and not final deglaciation (see Kleman & Hättestrand, 1999). The locations hypothesised to be relict landscapes in the Keewatin and Ungava areas by Kleman & Hättestrand (1999) are very small compared with the overall size of the ice sheet and the total population of eskers. Thus, we are confident that any eskers that are relict features will not significantly impact the results.

4.4.2 Length and sinuosity

Mean esker length (3.5 km) is comparable to data from the UK and the Kola Peninsula (Figure 2.13 & Figure 2.14), though the maximum length of Canadian eskers is much larger, as would be expected given the size of the respective ice sheets and larger sample size of Canadian eskers. Esker length, like that of other glacial landforms (e.g. Clark *et al.*, 2009; Hillier *et al.*, 2013; Stokes *et al.*, 2013), follows a log-normal distribution. Unlike other landforms, however, this likely reflects the fact that long systems of eskers are frequently broken into many shorter fragments, rather than different eskers 'growing' to different lengths, as has been suggested for drumlins (e.g. Clark *et al.*, 2009; Spagnolo *et al.*, 2012). Eskers are typically less than 10 km long but the gaps between them are shorter (typically 2 km long). The reason for this fragmentation is either non-detection of esker ridges, a cessation in sedimentation, or post-depositional erosion (Banerjee & McDonald, 1975). Erosion may arise from dissection by subsequent meltwater flow or contemporary rivers, or inundation by lakes formed either during deglaciation, or by later thermokarst processes (e.g. Smith *et al.*, 2005; Smith *et al.*, 2007; Jones *et al.*, 2011). The presence of gaps in esker systems and the extensive resultant fragmentation (34.9%) is difficult to account for if synchronous esker formation is invoked, because if this is

the case, eskers should form in a continuous conduit. Rather, this provides support for time-transgressive esker formation, whereby gaps may represent hiatuses in sedimentation during different stages of retreat of the ice sheet, with sedimentation recurring as deglaciation progresses.

It is possible that some gaps may reflect over-interpolation of the data when producing the *interpolated* eskers, though this is unlikely to be the case for the majority of gaps (Figure 4.1D). Once these gaps are accounted for, eskers may be traced for up to 760 km, indicating that the conduits in which they formed were either stable through time (e.g. Banerjee & McDonald, 1975; Gorrell & Shaw, 1991; Boulton *et al.*, 2009), or esker deposition took place rapidly across the length of very long conduits (e.g. Brennand & Shaw, 1994;1996). Whilst plausible for shorter eskers, it is unlikely that the longest eskers formed synchronously in (up to) 760 km long conduits. This raises difficult questions about (1) how such a large quantity of sediment could abruptly enter the drainage system, (2) whether it would be likely to be preserved throughout deglaciation, (3) where subsequent channels would drain (would this result in a palimpsest drainage network, where one esker forms over another as another sedimentation 'episode' is established?), and (4) what would control such short-lived and extensive deposition? Rather, we favour the parsimonious explanation which is that the very long eskers were built time-transgressively at a retreating ice margin, which would not require an abrupt and large sediment supply, extensive preservation beneath a large ice sheet, or problems arising from palimpsest drainage networks. Nevertheless, though we favour a time-transgressive explanation for the longest eskers, we do not rule out the suggestion that shorter eskers can form synchronously because there is good evidence for this happening in different settings (Brennand, 1994; Brennand & Shaw, 1996; Brennand, 2000; Burke *et al.*, 2008; Burke *et al.*, 2009; Burke *et al.*, 2010) and the questions arising above become less significant for shorter systems.

Esker sinuosity is very small: mean sinuosity is 1.055 and few values attain more than 1.2. Mean sinuosity is in accordance with data from other areas (e.g. Figure 2.15; Clark *et al.*, 2004; Hättestrand & Clark, 2006; Burke *et al.*, 2012), but maximum sinuosity is higher, likely due to the large sample size. Sinuosity is significant because it is a parameter not usually incorporated into dye-tracing experiments or numerical models of subglacial channels, but which could profoundly influence the outcome of such experiments because it has implications for the length of a channel between two points and consequently the discharge, volume, pressure and velocity of the contained water. For example, one attempt to incorporate estimates of sinuosity into a model of tracer velocity through a subglacial channel (Schuler & Fischer, 2009), suggests a sinuosity value of 1.6 as being the most realistic for an R-channel under Unteraargletscher, Switzerland. Whilst this applies to an alpine glacier, our data suggest that R-channels are significantly straighter under ice sheets. Thus, we suggest that models of subglacial channels at the ice sheet scale should assume sinuosity values on the order of 1.055 to achieve the most realistic results.

4.4.3 Lateral spacing

Numerical models which predict the spacing of eskers (Boulton *et al.*, 2007; Boulton *et al.*, 2009; Hewitt, 2011) do not account for fragmentation, which has important implications for comparing model results with measured spacing. Instead, models predict the spacing of entire channels, in which eskers form in fragments. Thus, the spacing of *mapped* eskers is useful as a geomorphological observation, whilst *interpolated* esker spacing is better suited to be used for data-model comparisons.

Measurements of *interpolated* esker spacing in three sample areas, where esker density is high, indicate that eskers are very regularly spaced. Mean spacing is 12.3 km with a standard deviation of 6.6 km, in good agreement with figures from the literature (Figure 2.22; Figure 4.14). The three areas selected are ideal for testing numerical models because the *interpolated* esker dataset has few gaps, laterally or longitudinally. Thus, models (which assume that eskers are preserved evenly across the whole bed) can be directly compared with observations. In this regard, preliminary results are encouraging: Boulton's (2009) model produced spacing values of 8-25 km in Fennoscandia and Hewitt's (2011) model produced an estimated spacing of 5-30 km. According to Boulton's (2009) model, esker spacing is primarily controlled by the transmissivity of the substrate and the basal melt rate of the ice sheet. Increasing the transmissivity or decreasing the basal melt rate results in more widely spaced eskers. In Hewitt's (2011) model, eskers become more widely spaced when the potential gradient is smaller or the permeability of the distributed system is larger. The similarity of these two models is that both suggest that the hydraulic properties of the substrate are critical in controlling esker spacing. This is discussed further in Chapters 6, 7 and 8.

4.4.4 Elevation change

Until now, few reports of elevation changes in more than a handful of eskers have been published (see Section 2.5.2). Theory suggests that eskers form in accordance with ice surface topography, which is related to bed topography, indicating that eskers should have a preference (if any) to trend down-slope (Shreve, 1972;1985a;b). Syverson *et al.* (1994), however, noted that this may not always be the case and that sometimes eskers trend across contours, when ice surface slope is a more dominant control and opposes bed topography. The data presented in Section 4.3.6 indicate that eskers show no preference to trend up- or down-slope, with a roughly even proportion trending either way. This suggests that the slope of the bed is not the primary control on esker location. The data may support Syverson *et al.*'s (1994) premise that ice surface slope may be dominant when the ice is sufficiently thick (they suggest >50 m) and that topography may predominate under thinner ice. That the majority of eskers exhibit almost no change in elevation between each end, suggests that eskers may form preferentially on flat terrain.

4.5 Conclusions

The subglacial meltwater drainage systems of ice sheets are an important but difficult environment to observe. This paper presents the first analysis of a large sample (over 20,000) of eskers in Canada, which is used to provide key insights into the properties of the subglacial drainage systems of the Laurentide Ice Sheet. Canadian eskers exhibit several patterns at different scales. They radiate away from the final locations of the two main ice divides, beneath which they are absent in areas of 93,000 and 174,000 km^2 in Keewatin and Ungava, respectively. The esker free areas are 100-150 km wide in both locations. Within the radial esker systems, they form integrated dendritic networks of up to fourth order tributaries. Elsewhere eskers are more chaotic, reflecting complex ice dynamics likely related to ice streaming.

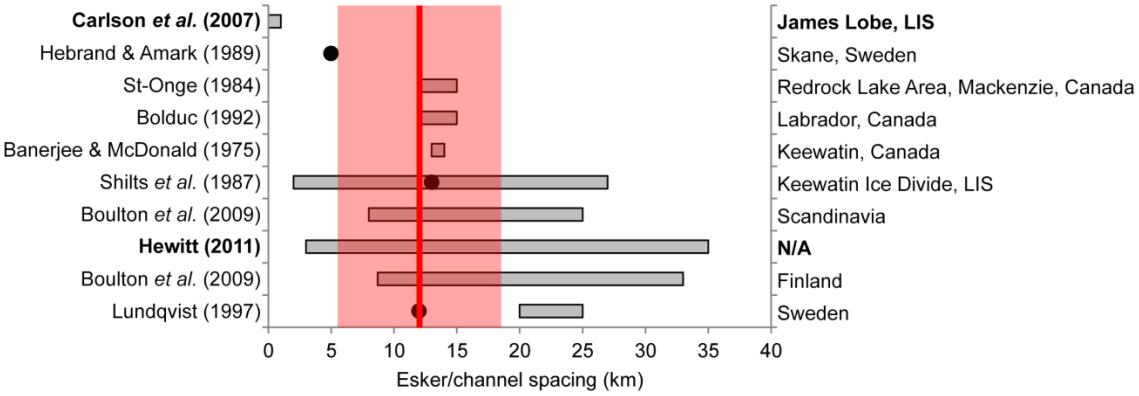

Figure 4.14. Mean (red line) *interpolated* esker spacing with standard deviation indicated by the shaded area, compared with spacing values obtained from the literature (see caption of Figure 2.22 for further details).

Eskers provide information about the conduits in which they formed. Measurements of eskers can thus provide an insight into the dimensions and spatial characteristics of these conduits. The longest esker is 97.5 km and most eskers are up to 10 km long. Gaps between eskers are numerous (mostly due to lake infilling) but when they are conservatively interpolated over distances of just a few kilometres, esker systems extend up to 760 km. This suggests that eskers either formed synchronously in channels up to 760 km long, or time-transgressively in channels that persisted in the same location for a long period of time. We favour the latter suggestion for the longest eskers because it is the explanation that requires the fewest assumptions.

Eskers are much straighter than has previously been assumed, with mean esker sinuosity at 1.055. This is an important constraint for numerical models of subglacial channels and for understanding the discharge and velocity of meltwater through channels.

Esker spacing is typically regular on the crystalline bedrock of the Canadian Shield. The spacing between esker-forming channels in three large study areas gives a mean value of 12.3 km (standard deviation 6.6 km) and this value can be used to test numerical models of subglacial channel spacing (see Chapter 6), with which it appears to roughly comply (Boulton *et al.*, 2007; Boulton *et al.*, 2009; Hewitt, 2011).

An analysis of 11,560 eskers reveals that eskers do not have a preferred up- or down-slope trend and that the majority occur on rather flat topography, indicating that eskers form preferentially on flat terrains and are unconstrained by small topographic fluctuations. Eskers trending uphill support the assertion that ice surface is an important control on esker location.

The measurements presented in this paper provide an important source of data for testing numerical models of subglacial channels, which aim to predict parameters such as esker spacing or sinuosity. These models may now be tested against a large sample of data from an entire ice sheet bed (see Chapter 6).

4.6 References

Aylsworth, J. M. & Shilts, W. W. (1989a) Bedforms of the Keewatin Ice-Sheet, Canada. *Sedimentary Geology*, 62, 407-428.

Aylsworth, J. M. & Shilts, W. W. (1989b) Glacial features around the Keewatin Ice Divide: Districts of Mackenzie and Keewatin. Geological Survey of Canada, Map 24-1987. 1:1,000,000

Banerjee, I. & McDonald, B. C. (1975) Nature of esker sedimentation. In A. V. Jopling and B. C. McDonald, *Glaciofluvial and Glacilacustrine Sedimentation*. Oklahoma, SEPM, 304-320.

Boulton, G. S. & Clark, C. D. (1990) A highly mobile Laurentide ice sheet revealed by satellite images of glacial lineations. *Nature*, 346, 813-817.

Boulton, G. S., Hagdorn, M., Maillot, P. B. & Zatsepin, S. (2009) Drainage beneath ice sheets: groundwater-channel coupling, and the origin of esker systems from former ice sheets. *Quaternary Science Reviews*, 28, 621-638.

Boulton, G. S., Lunn, R., Vidstrand, P. & Zatsepin, S. (2007) Subglacial drainage by groundwater-channel coupling, and the origin of esker systems: part II-theory and simulation of a modern system. *Quaternary Science Reviews*, 26, 1091-1105.

Brennand, T. A. (1994) Macroforms, large bedforms and rhythmic sedimentary sequences in subglacial eskers, south-central Ontario - implications for esker genesis and meltwater regime. *Sedimentary Geology*, 91, 9-55.

Brennand, T. A. (2000) Deglacial meltwater drainage and glaciodynamics: inferences from Laurentide eskers, Canada. *Geomorphology*, 32, 263-293.

Brennand, T. A. & Shaw, J. (1994) Tunnel channels and associated landforms, south-central Ontario: their implications for ice-sheet hydrology. *Canadian Journal of Earth Sciences*, 31, 505-522.

Brennand, T. A. & Shaw, J. (1996) The Harricana glaciofluvial complex, Abitibi region, Quebec: its genesis and implications for meltwater regime and ice-sheet dynamics. *Sedimentary Geology*, 102, 221-262.

Brown, V. H., Stokes, C. R. & O'Cofaigh, C. (2011) The Glacial Geomorphology of the North-West sector of the Laurentide Ice Sheet. *Journal of Maps*, 7, 409-428.

Burke, M. J., Brennand, T. A. & Perkins, A. J. (2012) Transient subglacial hydrology of a thin ice sheet: insights from the Chasm esker, British Columbia, Canada. *Quaternary Science Reviews*, 58, 30-55.

Burke, M. J., Woodward, J., Russell, A. J. & Fleisher, P. J. (2009) Structural controls on englacial esker sedimentation: Skeiðarárjökull, Iceland. *Annals of Glaciology*, 50, 85-92.

Burke, M. J., Woodward, J., Russell, A. J., Fleisher, P. J. & Bailey, P. K. (2008) Controls on the sedimentary architecture of a single event englacial esker: Skeiðarárjökull, Iceland. *Quaternary Science Reviews*, 27, 1829-1847.

Burke, M. J., Woodward, J., Russell, A. J., Fleisher, P. J. & Bailey, P. K. (2010) The sedimentary architecture of outburst flood eskers: A comparison of ground-penetrating radar data from Bering Glacier, Alaska and Skeiðarárjökull, Iceland. *Bulletin of the Geological Society of America*, 122, 1637-1645.

Carlson, A. E., Anslow, F. S., Obbink, E. A., LeGrande, A. N., Ullman, D. J. & Licciardi, J. M. (2009) Surface-melt driven Laurentide Ice Sheet retreat during the early Holocene. *Geophysical Research Letters*, L24502.

Carter, S. P., Blankenship, D. D., Young, D. A. & Holt, J. W. (2009) Using radar-sounding data to identify the distribution and sources of subglacial water: application to Dome C, East Antarctica. *Journal of Glaciology*, 55, 1025-1040.

Christoffersen, P., Piotrowski, J. A. & Larsen, N. K. (2005) Basal processes beneath an Arctic glacier and their geomorphic imprint after a surge, Elisebreen, Svalbard. *Quaternary Research*, 64, 125-137.

Clark, C. D., Evans, D. J. A., Khatwa, A., Bradwell, T., Jordan, C., Marsh, S., Mitchell, W. & Bateman, M. (2004) Map and GIS database of glacial landforms and features related to the last British Ice Sheet. *Boreas*, 33, 359-375.

Clark, C. D., Hughes, A. L. C., Greenwood, S. L., Spagnolo, M. & Ng, F. S. L. (2009) Size and shape characteristics of drumlins, derived from a large sample, and associated scaling laws. *Quaternary Science Reviews*, 28, 677-692.

Clark, C. D., Knight, J. K. & T Gray, J. (2000) Geomorphological reconstruction of the Labrador sector of the Laurentide Ice Sheet. *Quaternary Science Reviews*, 19, 1343-1366.

Clark, P. U. & Walder, J. S. (1994) Subglacial drainage, eskers, and deforming beds beneath the Laurentide and Eurasian ice sheets. *Bulletin of the Geological Society of America*, 106, 304-314.

Cowton, T., Nienow, P., Bartholomew, I., Sole, A. & Mair, D. (2012) Rapid erosion beneath the Greenland ice sheet. *Geology*, 40, 343-346.

Dunlop, P. & Clark, C. D. (2006) The morphological characteristics of ribbed moraine. *Quaternary Science Reviews*, 25, 1668-1691.

Dyke, A. S., Dredge, L. A. & Hodgson, D. A. (2005) North American deglacial marine- and lake-limit surfaces. *Géographie physique et Quaternaire*, 59, 155-185.

Dyke, A. S., Moore, A. & Robertson, L. (2003) Deglaciation of North America. *Geological Survey of Canada, Open File*, 1574.

Dyke, A. S. & Prest, V. K. (1987) Late Wisconsinan and Holocene history of the Laurentide ice sheet. *Géographie physique et Quaternaire*, 41, 237-263.

Evans, D. J. A., Nelson, C. D. & Webb, C. (2010) An assessment of fluting and "till esker" formation on the foreland of Sandfellsjokull, Iceland. *Geomorphology*, 114, 453-465.

Evans, D. J. A., Twigg, D. R., Rea, B. R. & Shand, M. (2007) Surficial geology and geomorphology of the Brúarjökull surging glacier landsystem. *Journal of Maps*, 2007, 349-367.

Flowers, G. E., Bjornsson, H. & Palsson, F. (2003) New insights into the subglacial and periglacial hydrology of Vatnajokull, Iceland, from a distributed physical model. *Journal of Glaciology*, 49, 257-270.

Fricker, H. A., Scambos, T., Bindschadler, R. & Padman, L. (2007) An active subglacial water system in West Antarctica mapped from space. *Science*, 315, 1544-1548.

Fricker, H. A., Scambos, T., Carter, S., Davis, C., Haran, T. & Joughin, I. (2010) Synthesizing multiple remote-sensing techniques for subglacial hydrologic mapping: application to a lake system beneath MacAyeal Ice Stream, West Antarctica. *Journal of Glaciology*, 56, 187-199.

Gorrell, G. & Shaw, J. (1991) Deposition in an esker, bead and fan complex, Lanark, Ontario, Canada. *Sedimentary Geology*, 72, 285-314.

Hättestrand, C. & Clark, C. D. (2006) The glacial geomorphology of Kola Peninsula and adjacent areas in the Murmansk Region, Russia. *Journal of Maps*, 30, 30-42.

Hebrand, M. & Åmark, M. (1989) Esker formation and glacier dynamics in eastern Skane and adjacent areas, southern Sweden. *Boreas*, 18, 67-81.

Hewitt, I. J. (2011) Modelling distributed and channelized subglacial drainage: the spacing of channels. *Journal of Glaciology*, 57, 302-314.

Hewitt, I. J. (2013) Seasonal changes in ice sheet motion due to melt water lubrication. *Earth and Planetary Science Letters*, 371–372, 16-25.

Hillier, J. K., Smith, M. J., Clark, C. D., Stokes, C. R. & Spagnolo, M. (2013) Subglacial bedforms reveal an exponential size-frequence distribution. *Geomorphology*, 190, 82-91.

Jones, B. M., Grosse, G., Arp, C. D., Jones, M. C., Walter Anthony, K. M. & Romanovsky, V. E. (2011) Modern thermokarst lake dynamics in the continuous permafrost zone, northern Seward Peninsula, Alaska. *Journal of Geophysical Research: Biogeosciences*, 116, n/a-n/a.

Kleman, J. (1994) Preservation of landforms under ice sheets and ice caps. *Geomorphology*, 9, 19-32.

Kleman, J. & Glasser, N. F. (2007) The subglacial thermal organisation (STO) of ice sheets. *Quaternary Science Reviews*, 26, 585-597.

Kleman, J. & Hättestrand, C. (1999) Frozen-bed Fennoscandian and Laurentide ice sheets during the Last Glacial Maximum. *Nature*, 402, 63-66.

Knudsen, Ó. (1995) Concertina eskers, Brúarjökull, Iceland: An indicator of surge-type glacier behaviour. *Quaternary Science Reviews*, 14, 487-493.

Lagerbäck, R. & Robertsson, A.-M. (1988) Kettle holes - stratigraphical archives for Weichselian geology and palaeoenvironment in northernmost Sweden. *Boreas*, 17, 439-468.

Lewis, S. M. & Smith, L. (2009) Hydrologic drainage of the Greenland Ice Sheet. *Hydrological Processes*, 23, 2004-2011.

Mäkinen, J. (2003) Time-transgressive deposits of repeated depositional sequences within interlobate glaciofluvial (esker) sediments in Koylio, SW Finland. *Sedimentology*, 50, 327-360.

Margold, M., Jansson, K., Kleman, J. & Stroeven, A. (2011) Glacial meltwater landforms of central British Columbia. *Journal of Maps*, 2011, 486-506.

Margold, M., Jansson, K. N., Kleman, J., Stroeven, A. P. & Clague, J. J. (2013) Retreat pattern of the Cordilleran Ice Sheet in central British Columbia at the end of the last glaciation reconstructed from glacial meltwater landforms. *Boreas*, n/a-n/a.

Marshall, S. J. & Clark, P. U. (2002) Basal temperature evolution of North American ice sheets and implications for the 100-kyr cycle. *Geophysical research letters*, 29, 2214.

Menzies, J. & Shilts, W. W. (1996) Subglacial environments. In J. Menzies, *Past glacial environments, sediments, forms and techniques*. Oxford, Butterworth/Heinemann. 2, 15-136.

Nienow, P., Sharp, M. & Willis, I. (1998) Seasonal changes in the morphology of the subglacial drainage system, Haut Glacier d'Arolla, Switzerland. *Earth Surface Processes and Landforms*, 23, 825-843.

Nienow, P. W., Sharp, M. & Willis, I. C. (1996) Velocity-discharge relationships derived from dye tracer experiments in glacial meltwaters: implications for subglacial flow conditions. *Hydrological Processes*, 10, 1411-1426.

Peltier, W. R. (2004) Global glacial isostacy and the surface of the ice-age Earth: the ICE-5G (VM2) model and GRACE. *Annual Review of Earth and Planetary Science*, 32, 111-149.

Prest, V. K., Grant, D. R. & Rampton, V. N. (1968) Glacial map of Canada. Geological Survey of Canada, Map 1253A. 1:5,000,000

Price, R. J. (1969) Moraines, sandar, kames and eskers near Breiðamerkurjökull , Iceland. *Transactions of the Institute of British Geographers*, 46, 17-43.

Richards, K., Sharp, M., Arnold, N., Gurnell, A., Clark, M., Tranter, M., Nienow, P., Brown, G., Willis, I. & Lawson, W. (1996) An integrated approach to modelling hydrology and water quality in glacierized catchments. *Hydrological Processes*, 10, 479-508.

Schuler, T. V. & Fischer, U. H. (2009) Modeling the diurnal variation of tracer transit velocity through a subglacial channel. *Journal of Geophysical Research*, 114, F04017.

Shilts, W. W. (1984) Esker sedimentation models, Deep Rose Lake map area, District of Keewatin. *Geological Survey of Canada, Paper*, 84-1B, 217-222.

Shilts, W. W., Aylsworth, J. M., Kaszycki, C. A. & Klassen, R. A. (1987) Canadian Shield. In W. L. Graf, *Geomorphic Systems of North America*. Boulder, Colorado, Geological Society of America, Centennial Special Volume. 2, 119-161.

Shreve, R. L. (1972) Movement of water in glaciers. *Journal of Glaciology*, 11, 205-214.

Shreve, R. L. (1985a) Esker characteristics in terms of glacier physics, Katahdin esker system, Maine. *Bulletin of the Geological Society of America*, 96, 639-646.

Shreve, R. L. (1985b) Late Wisconsin ice-surface profile calculated from esker paths and types, Katahdin esker system, Maine. *Quaternary Research*, 23, 27-37.

Smith, L. C., Sheng, Y. & MacDonald, G. M. (2007) A first pan-Arctic assessment of the influence of glaciation, permafrost, topography and peatlands on northern hemisphere lake distribution. *Permafrost and Periglacial Processes*, 18, 201-208.

Smith, L. C., Sheng, Y., MacDonald, G. M. & Hinzman, L. D. (2005) Disappearing Arctic Lakes. *Science*, 308, 1429.

Spagnolo, M., Clark, C. D. & Hughes, A. L. C. (2012) Drumlin relief. *Geomorphology*, 153–154, 179-191.

Spagnolo, M., Clark, C. D., Hughes, A. L. C. & Dunlop, P. (2011) The topography of drumlins; assessing their long profile shape. *Earth Surface Processes and Landforms*, 36, 790-804.

Spagnolo, M., Clark, C. D., Hughes, A. L. C., Dunlop, P. & Stokes, C. R. (2010) The planar shape of drumlins. *Sedimentary Geology*, 232, 119-129.

Stokes, C. R., Clark, C. D. & Storrar, R. (2009) Major changes in ice stream dynamics during deglaciation of the north-western margin of the Laurentide Ice Sheet. *Quaternary Science Reviews*, 28, 721-738.

Stokes, C. R., Spagnolo, M., Clark, C. D., O'Cofaigh, C., Lian, O. B. & Dunstone, R. B. (2013) Formation of mega-scale glacial lineations on the Dubawnt Lake Ice Stream bed: 1. size, shape and spacing from a large remote sensing dataset. *Quaternary Science Reviews*, 77, 190-209.

Storrar, R. D., Stokes, C. R. & Evans, D. J. A. (2013) A map of Canadian eskers from Landsat satellite imagery. *Journal of Maps*, 9, 456-473.

Syverson, K. M., Gaffield, S. J. & Mickelson, D. M. (1994) Comparison of esker morphology and sedimentology with former ice-surface topography, Burroughs Glacier, Alaska. *Geological Society of America Bulletin*, 106, 1130-1142.

Warren, W. P. & Ashley, G. M. (1994) Origins of the ice-contact stratified ridges (eskers) of Ireland. *Journal of Sedimentary Research*, 64, 433-499.

Wheeler, J. O., Hoffman, P. F., Card, K. D., Davidson, A., Sanford, B. V., Okulitch, A. V. & Roest, W. R. (1996) Geological map of Canada. *Geological Survey of canada, map 1860A*.

Wingham, D. J., Siegert, M. J., Shepherd, A. & Muir, A. S. (2006) Rapid discharge connects Antarctic subglacial lakes. *Nature*, 440, 1033-1036.

Chapter 5 Increased channelization of subglacial drainage during deglaciation of the Laurentide Ice Sheet

Storrar, R.D., Stokes, C.R. & Evans, D.J.A. (in press) Increased channelization of subglacial drainage during deglaciation of the Laurentide Ice Sheet. *Geology.*

Abstract

The configuration of subglacial meltwater is a critical control on ice sheet dynamics and the presence of pressurised water distributed across the bed can induce dynamic instabilities. However, this process can be offset by efficient evacuation of water within large subglacial channels, and drainage systems beneath alpine glaciers have been shown to become increasingly channelized throughout the melt season, in response to the increased production of meltwater. This seasonal evolution has recently been inferred beneath outlet glaciers of the Greenland Ice Sheet, but the extent to which this process occurs across much larger spatial and temporal scales is largely unknown, introducing considerable uncertainty about the evolution of subglacial drainage networks at the ice sheet scale and associated ice sheet dynamics. This paper uses an unprecedented dataset of over 20,000 eskers to reconstruct the evolution of channelized meltwater systems during the final deglaciation of the Laurentide Ice Sheet (13 to 7 cal ka). We demonstrate that eskers become more frequent during deglaciation and that this coincides with periods of increased rates of ice margin recession and climatic warming. Such behaviour is reminiscent of the seasonal evolution of drainage systems observed on smaller glaciers and implies that channelized drainage became increasingly important during deglaciation. An important corollary is that the area of the bed subjected to a less efficient pressurised drainage system decreased, which may have precluded dynamic instabilities, such as surging or ice streaming.

5.1 Introduction

Recent estimates have shown that mass loss from the Greenland and West Antarctic Ice Sheets is accelerating (Mernild *et al.,* 2011; Rignot *et al.,* 2011). This has been attributed to surface melt and dynamic losses caused by the acceleration, thinning and retreat of outlet glaciers (Pritchard *et al.,* 2009; van den Broeke *et al.,* 2009). These two processes are not mutually exclusive in that some workers have suggested that surface meltwater may drain to the bed and cause dynamic flow acceleration (Zwally *et al.,* 2002; Palmer *et al.,* 2011). However, others have argued that an increased melt flux may be counteracted by the evolution of the drainage

system, which responds by generating large channels that efficiently evacuate excess surface meltwater (Bartholomew *et al.*, 2010; Schoof, 2010; Sundal *et al.*, 2011), similar to the seasonal evolution inferred from beneath alpine glaciers (Hubbard & Nienow, 1997; Iken & Truffer, 1997). These potential switches in subglacial drainage introduce uncertainty when attempting to predict the future behaviour of ice sheets: could increased surface melt lead to more widespread dynamic instabilities, or will subglacial drainage systems become more efficient? Moreover, observations of subglacial drainage systems are difficult, often indirect, and generally limited to just a few years (Zwally *et al.*, 2002; van de Wal *et al.*, 2008; Bartholomew *et al.*, 2010; Palmer *et al.*, 2011; Sundal *et al.*, 2011; Cowton *et al.*, 2012). Thus, our understanding of how drainage systems might evolve over timescales of centuries to millennia, the impact this may have on ice dynamics, and our ability to model future ice sheet behaviour remains limited.

One approach to understanding the evolution of subglacial drainage systems at centennial to millennial timescales is to examine the geological record of former ice sheets that have subsequently deglaciated. In particular, evidence of channelized drainage beneath ice sheets is typically preserved in the form of eskers: elongate ridges of glaciofluvial sand and gravel deposited in glacial drainage channels (Section 2.3; Banerjee & McDonald, 1975). Here, we use eskers to investigate the evolution of channelized drainage beneath the Laurentide Ice Sheet (LIS) during 6,000 years of deglaciation from 13 to 7 cal ka. We quantify the spatial pattern of over 20,000 eskers and show that the ice sheet was progressively drained by an increased number of subglacial channels as it deglaciated. Our hypothesis is that the subglacial drainage system evolved to cope with an increasing amount of meltwater during deglaciation (Carlson *et al.*, 2008; Carlson *et al.*, 2009), in a manner that is reminiscent of the seasonal evolution of drainage under alpine glaciers, but which occurred over much longer time-scales. An important implication is that the area of the ice sheet bed subjected to a less efficient 'distributed' system would have decreased, perhaps limiting the potential for flow instabilities (surges or ice streaming) (Clarke, 1987; Clark & Walder, 1994; Zwally *et al.*, 2002). This suggests that the final demise of the ice sheet was intimately and predictably linked to its surface mass balance.

5.2 Methods

Eskers were mapped from Landsat ETM+ imagery of Canada and the data are published as a map in Storrar *et al.* (2013) and presented here in Chapter 3. They were identified using the criteria of Margold and Jansson (2012) and are conspicuous as narrow, sinuous ridges with distinct spectral signatures related to the presence of glaciofluvial sediments (see Section 3.3). Their ridge crestlines were mapped as line features directly into a Geographic Information System (GIS). Esker ridge lengths, spacing and the number of tributaries were extracted from the GIS (see Chapter 4) and we analysed their location in relation to ice margin positions during deglaciation. Specifically, we calculated the frequency of eskers that intersected dated

ice margin positions from the best available ice margin chronology, published in Dyke *et al.* (2003) and reproduced in Figure 5.1. This chronology is based on approximately 4,000 dates, most of which are from radiocarbon dating and we added intermediate margin positions to enable additional measurements in between the 'dated' margins. Where such interpolations were made, the age uncertainties are shown by error bars (e.g. Figure 5.2). It is important to note, however, that our focus is on the relative changes in eskers through time as the ice margin retreated, such that absolute ages (and their uncertainties) are less important.

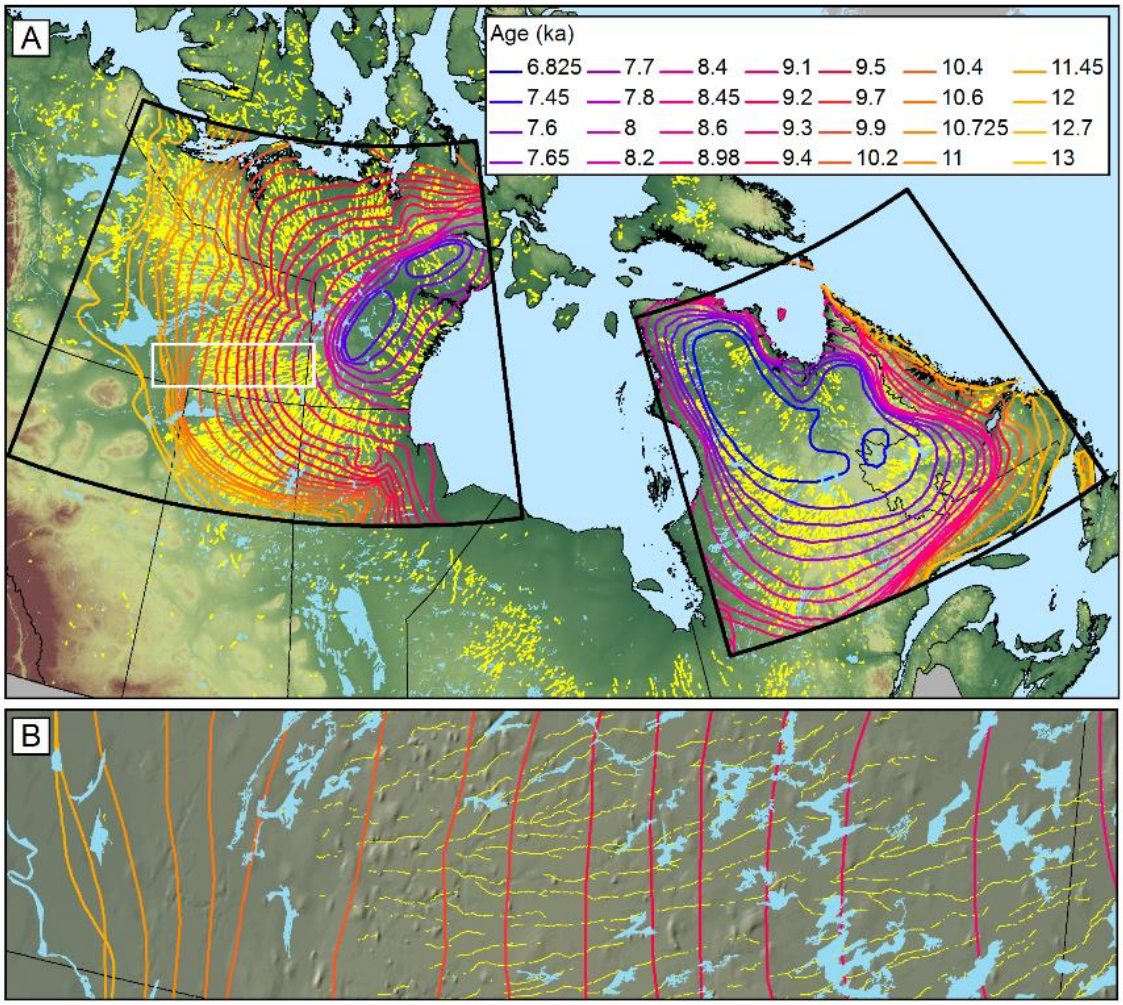

Figure 5.1. (A) Ice sheet margin positions and chronology (modified from Dyke *et al.*, 2003) are shown superimposed on mapped eskers (yellow) which reflect the configuration of meltwater channels emanating from the major ice divides in Keewatin (west of Hudson Bay) and Ungava (east of Hudson Bay). (B) shows a close-up of the white box in Keewatin.

To avoid the complexity associated with retreat from a predominantly 'soft' sedimentary bed (where eskers are rare) to the relatively 'hard' crystalline bedrock of the Canadian Shield (where eskers are far more common: Clark & Walder, 1994; Chapter 6), we focus on deglaciation across the Canadian Shield, from 13 to 7 cal ka. To account for the diminishing size of the ice

sheet (which would theoretically produce fewer eskers than a larger ice sheet), the number of eskers at the ice sheet margin was normalised per 100 km of margin length. Mean ice sheet retreat rate was calculated from 20 transects from the youngest to oldest margins in each area. Standard deviation values are given as error bars in Figure 5.2. The climate record shown in Figure 5.2 is 20 year resolution NGRIP ice core $\delta^{18}O$ data with a 100 year moving average and is described in Rasmussen *et al.* (2006) and Vinther *et al.* (2006). The numbers of tributaries in esker systems were extracted from the GIS where eskers coalesce. In order to explore whether the proportion of tributaries in esker systems changes through time, the number of tributaries per 100 km of the length of *mapped* eskers was calculated for five time slices. The time slices were based on the margin positions of Dyke *et al.* (2003).

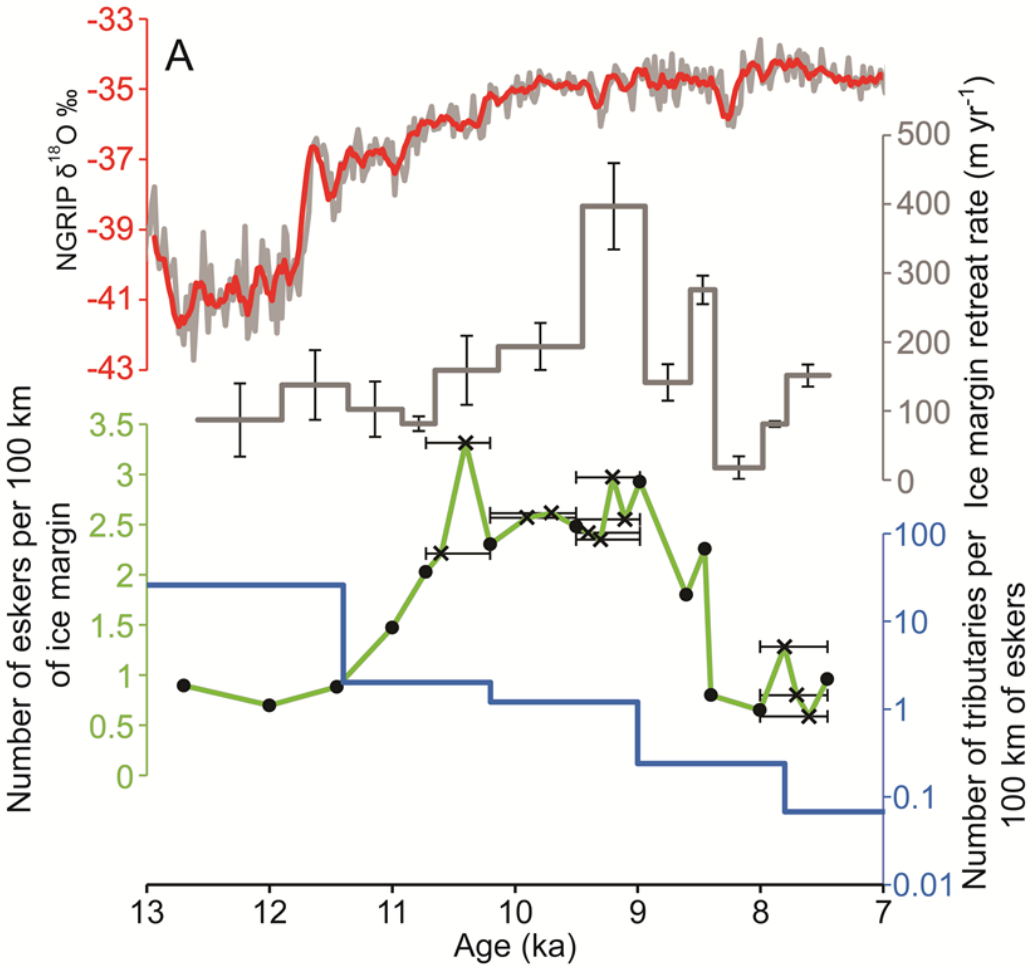

Figure 5.2. Climate and ice margin retreat rate plotted against the number of eskers and number of esker tributaries during deglaciation in Keewatin (A) and Ungava (B) (see Figure 5.1 for location). The number of eskers per 100 km at the ice margin includes error bars to indicate interpolated ice margin positions. Note $\log_{10}$ y-axis in for the number of tributaries per 100 km of eskers in (A). The NGRIP $\delta^{18}O$ record is from Rasmussen *et al.* (2006) and Vinther *et al.* (2006) and is plotted as a grey line with a 100 year moving average in red. The mean retreat rate of the Laurentide Ice Sheet includes error bars of one standard deviation of each measurement [n = 20]. Continued overleaf.

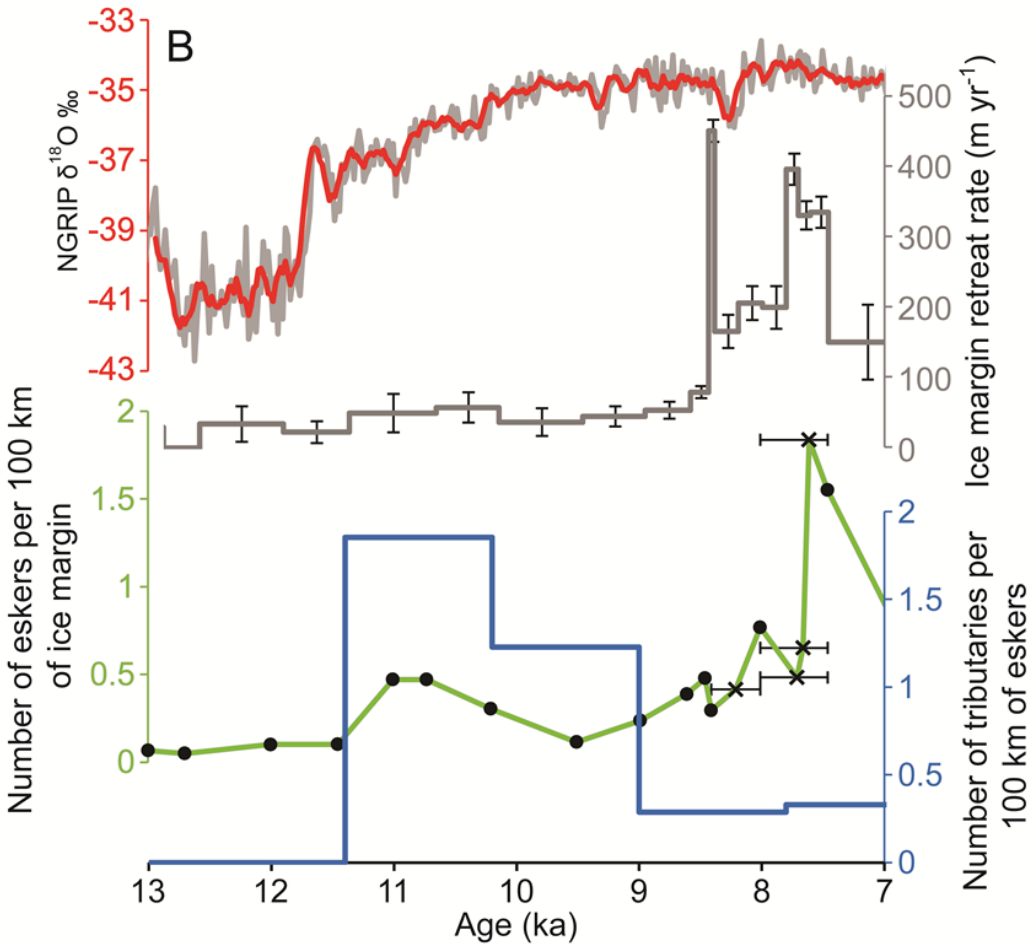

Figure 5.2 (continued).

5.3 Results

Our database includes a total of 20,186 eskers and individual ridges are up to 97.5 km in length (mean length: 3.5 km). Systems of eskers can be traced for up to 760 km, if small gaps (less than a few km) created by postglacial modification (or breaks in deposition) are taken into account. Some appear as single ridges, whereas others possess up to fourth-order tributaries (using the Strahler method). More detail on these statistics is given in Chapter 4. The mean number of eskers per 100 km of ice margin is 1.24, but this ranges from 0.05 to 3.31 (Figure 5.4). Histograms of esker frequency at each ice margin position in the Keewatin Sector of the ice sheet are given in Figure 5.3, to provide an example of the variation in esker density values. The most obvious pattern is their abundance in branching dendritic systems on the Canadian Shield, which emanate away from the positions of the major ice divides in Keewatin and Ungava (Figure 5.1). We note, however, that eskers are conspicuously absent beneath the final location of these ice divides.

In the Keewatin sector of the ice sheet (Figure 5.2A), the mean number of eskers per 100 km of ice margin is 1.24, but this ranges from 0.05 to 3.31. Retreat rates were generally between 100 and 200 m yr-1 from 13-9.5 cal ka, but increased rapidly between 9.5 and 9 cal ka, followed by

a sharp decrease to between 8.5 and 8 cal ka (see Figure 5.2A). We note that the number of eskers at the ice sheet margin broadly matches the retreat rate (Figure 5.5), increasing from 0.7 to 2.9 eskers per 100 km of ice margin between 12 and 9 cal ka, then abruptly decreasing from 2.9 to 0.8 between 9 and 8.5 cal ka, after which it decreased more gradually. In contrast, the number of tributaries per 100 km of eskers decreased steadily from 25.8 to 0.1 from 13 to 7 cal ka. To the east, the Ungava sector of the ice sheet shows a similar pattern, increasing from 0.1 to 1.8 eskers per 100 km of ice margin between 13 and 7.6 cal ka and then decreasing to 0.7 by 7 cal ka (Figure 5.2B). The retreat rate in this sector was less than 100 m yr^{-1} until ~8.4 cal ka, when it increased markedly to a peak of 450 m $yr^{-1}$and then retreated relatively rapidly thereafter. The number of tributaries per 100 km of eskers declined gradually from ~11.5 ka to 7.7 ka, with a very slight increase in the last time step (Figure 5.2B).

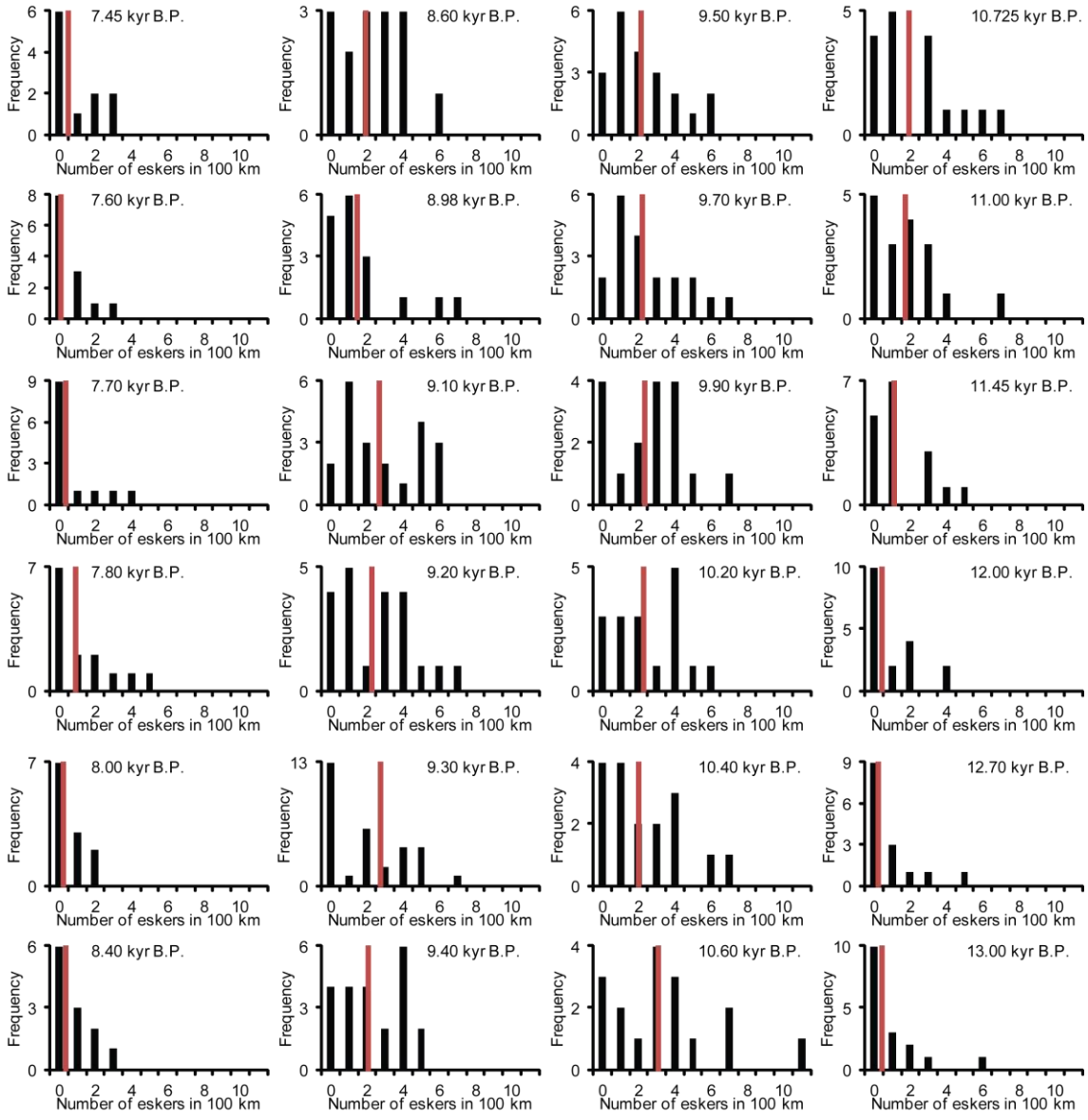

Figure 5.3. Histograms for each margin in the Keewatin sector of the ice sheet, showing the distribution of the number of eskers observed in each 100 km section (black bars) alongside the mean value (red).

5.4 Discussion

The most obvious pattern is a clear increase in esker frequency during deglaciation, which is summarised in Figure 5.6, which we now attempt to explain. Chapter 6 discusses links between esker formation and variations in sediment supply (Aylsworth & Shilts, 1989) and substrate lithological controls (Clark & Walder, 1994), but we rule these out in this case due to the relatively uniform lithology of the study area (Wheeler *et al.*, 1996). It has also been shown that esker sediments are derived primarily from the local substrate (Bolduc, 1992), with no obvious variation in lithology and sediment supply in this region that might explain the observed increase in eskers during deglaciation and their absence beneath ice divides (Figure 5.1; Figure 5.4).

Rather, we favour a simpler explanation, which is that the patterns are connected to changes in the volume of meltwater during deglaciation. Specifically, the northern hemisphere temperature record from the NGRIP ice core shows pronounced warming from 11.8 cal ka, following the Younger Dryas, and then gradual warming from 11.5 cal ka to approximately 9 cal ka (Figure 5.2). This warming would have led to a negative mass balance, with an associated increase in the production of surface meltwater (Carlson *et al.*, 2009). It may also be manifest as an increase in the rate of ice margin retreat, which does indeed occur, e.g. from 100-200 m yr^{-1} to almost 400 m yr^{-1} from 11 to 9 cal ka in Keewatin, and from 0-100 to over 400 m yr^{-1} from 8.5 to 7.5 cal ka in Ungava (Figure 5.2). Thus, we suggest that the increase in esker frequency during deglaciation is a reflection of an increased volume of surface meltwater entering the subglacial system via moulins and englacial channels, similar to that observed in the ablation zone of the Greenland Ice Sheet (Catania & Neumann, 2010). This explanation is consistent with numerical modelling experiments, which predict a decrease in esker spacing (i.e. an increase in esker frequency) with increasing meltwater supply (Boulton *et al.*, 2009; Hewitt, 2011; see also Chapter 6), though here we assume that the majority of meltwater is derived from surface, rather than basal, melting. It is important to note that limitations in the precision of the chronology preclude precise coupling between esker formation and climatic changes, and whilst the pattern of changes in esker density broadly agree with the temperature record, there are some discrepancies. For instance, temperature increases appear to lead increases in esker density by up to 1,000 years (Figure 5.2). It is not possible to discern whether this is due to uncertainty in the ice margin chronology, or whether there is genuinely a lag in the system that means that ot takes several centuries for temperature changes to register in the esker record.

We note that the increase in esker frequency in Ungava lags the Keewatin sector by approximately 1,000 years (Figure 5.2), which is consistent with the stabilisation of this sector of the ice sheet near the Gulf of St. Lawrence in the early Holocene (Hillaire-Marcel & Occhietti, 1980). Re-equilibration moraines in the St. Lawrence lowlands indicate that margin retreat paused as it switched from being marine- to land-terminating and its mass was

redistributed (Hillaire-Marcel & Occhietti, 1980). Following this switch, and the redistribution of mass, the ice margin continued its retreat. This is further supported by geomorphological evidence from Clark *et al.* (2000), who suggested that the ice sheet in this sector was strongly asymmetric, with the southern sector retreating rapidly compared with the northern sector.

In view of the above, the abrupt decrease in esker frequency after 8.5 – 9 cal ka (7.5 cal ka in Ungava) and their complete absence from the location of former ice divides requires explanation because the ice mass was still >200 km from ice divide to margin. We speculate that the LIS was sufficiently thin by this point that much of the remaining ice would have been cold and mostly cold-based (Kleman & Hättestrand, 1999; Kleman & Glasser, 2007), potentially precluding the development of subglacial meltwater channels and forcing meltwater to drain from the surface, without depositing eskers. In addition, whilst sediment supply is unlikely to explain the large-scale pattern of eskers, their absence beneath the smaller ice caps closer to final deglaciation may be related to limited sediment availability, in that low subglacial erosion rates are likely to have persisted under the ice divides. Furthermore, if a minimum length of conduit is required to erode the bed (Cowton *et al.*, 2012) and provide sufficient sediment to build eskers, this may also explain the absence of eskers toward the centre of ice dispersal.

A key implication of these results is that the final demise of the LIS may have been driven largely by surface melt. Independent support for this is found in numerical modelling of LIS mass balance, which is thought to have been strongly negative during the early Holocene, and attributed to enhanced boreal summer insolation (Carlson *et al.*, 2008; Carlson *et al.*, 2009). Dynamic mass loss (e.g. through ice streaming or surging) is typically dependent on distributed drainage of meltwater at the bed (Clarke, 1987) and so an important corollary of our findings is that dynamic mass loss may have been less significant during final deglaciation. This is supported by the relative paucity of ice streams hypothesised to have been operational at this time (Kleman & Glasser, 2007; Stokes & Tarasov, 2010), although we note that few palaeo-ice streams have been dated with any confidence.

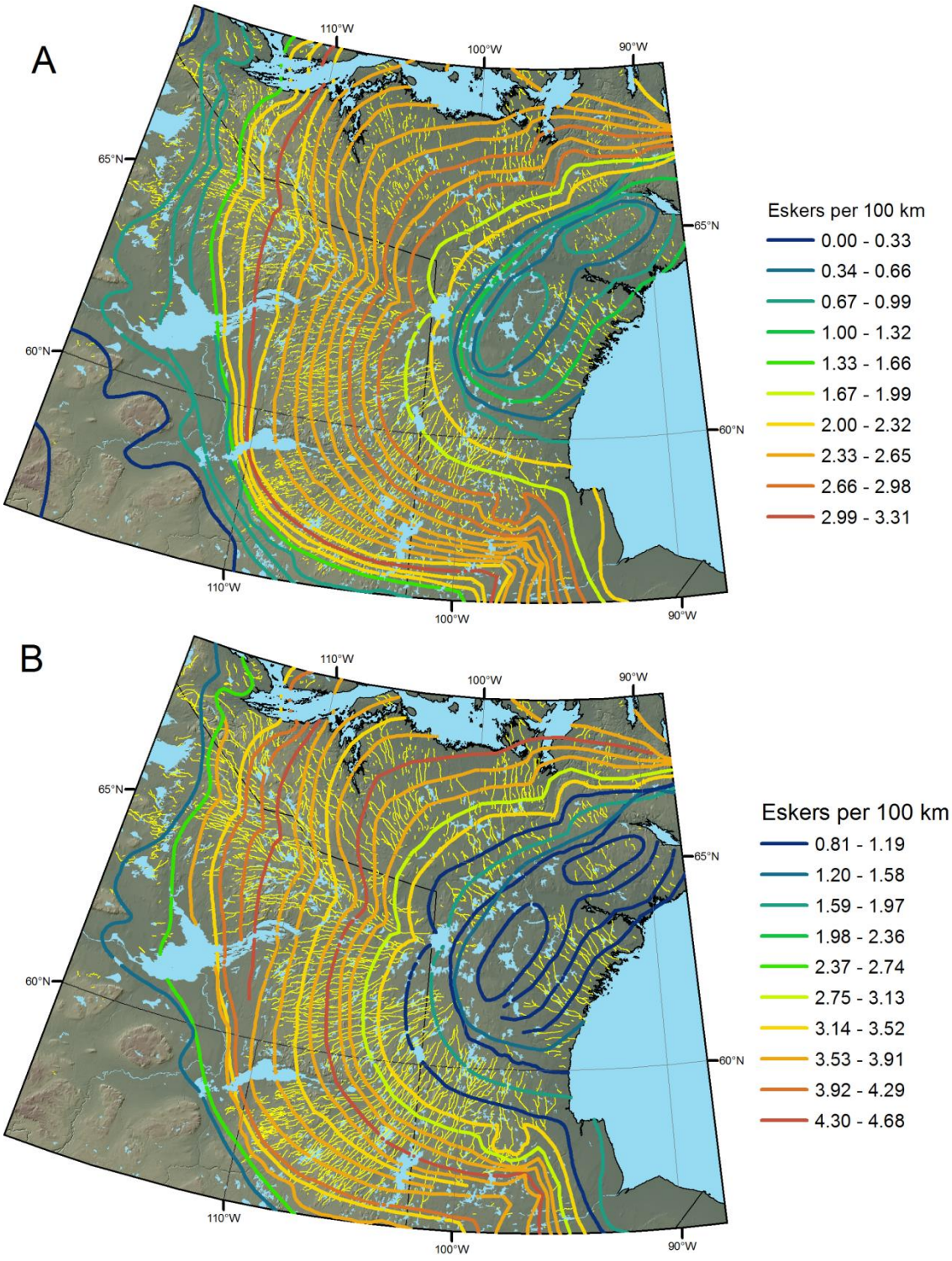

Figure 5.4. Esker frequency per 100 km of margin around the Keewatin (A and B) and Ungava (C and D) Ice Divides, derived from (A and C) *mapped* eskers; and (B and D) *interpolated eskers*. Continued overleaf.

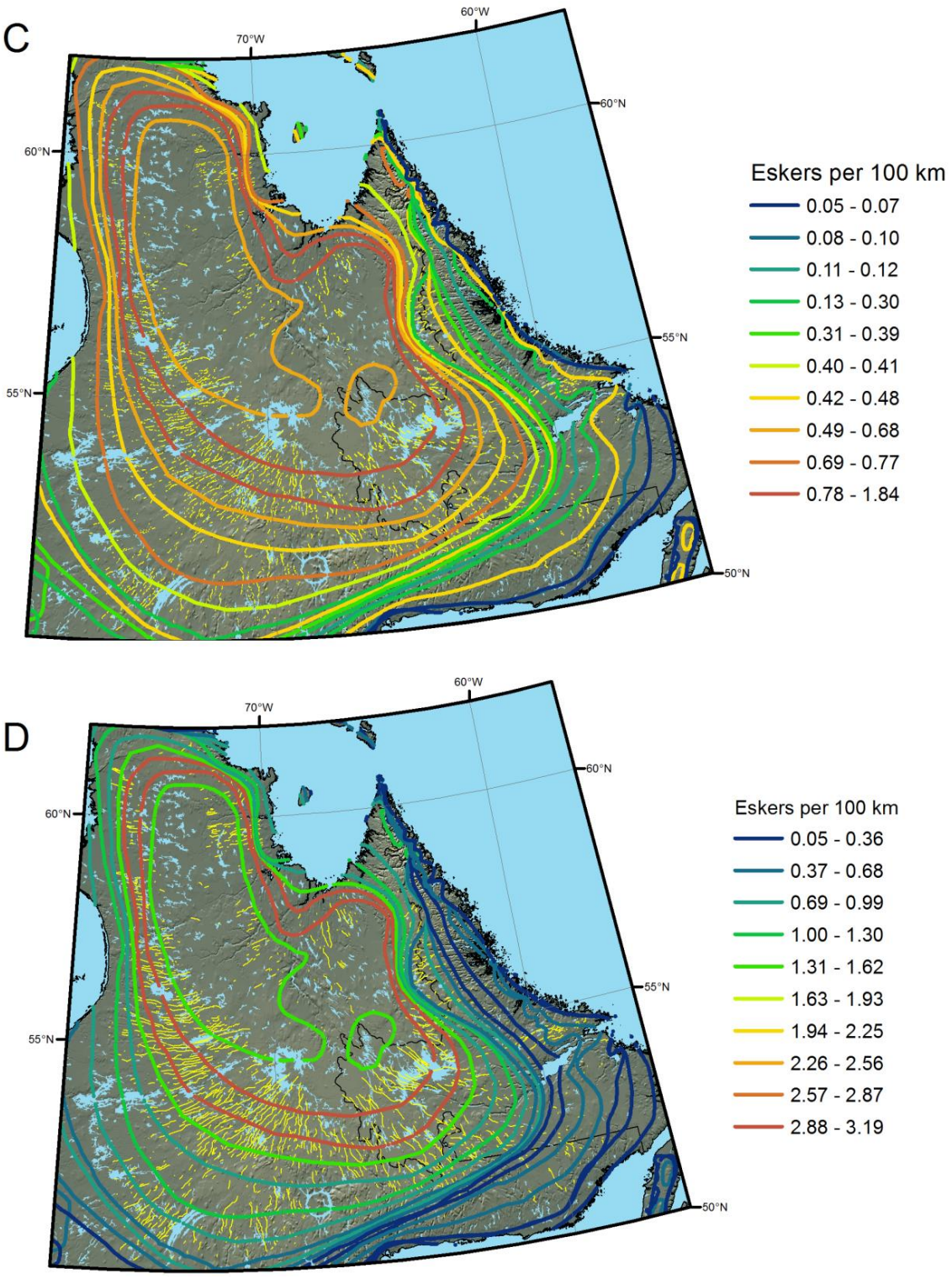

Figure 5.4 (continued).

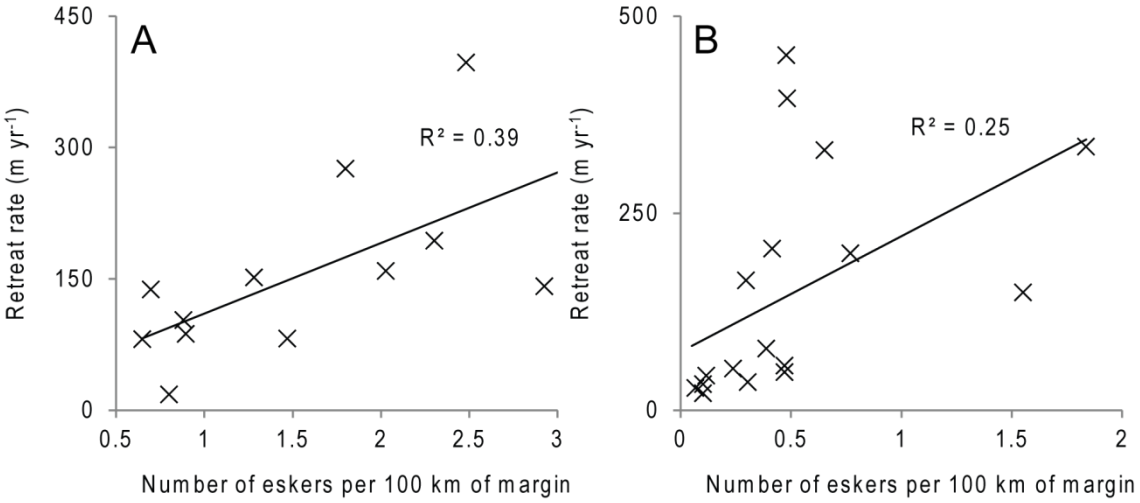

Figure 5.5. Number of eskers per 100 km of ice margin plotted against margin retreat rate for the Keewatin (A) and Ungava (B) study areas.

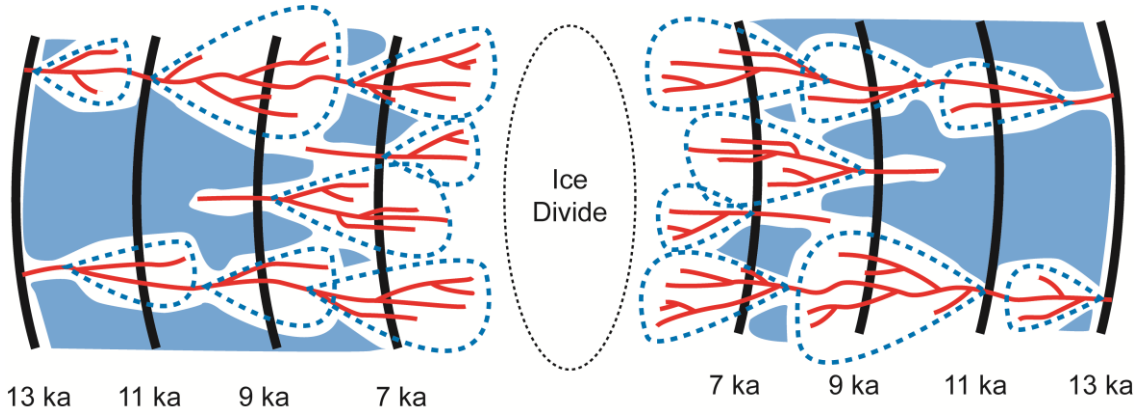

Figure 5.6. Schematic illustration of observed changes in eskers through time (not to scale). Black lines are hypothetical margin positions. Blue dashed lines indicate approximate areas of the bed drained by channels (later filled by eskers: red), which increases during deglaciation. Areas of the bed drained by distributed systems, which decrease during deglaciation, are shown as solid blue.

5.5 Conclusions

Using the pattern and spacing of >20,000 eskers formed under the Laurentide Ice Sheet, alongside an established ice margin chronology, we demonstrate that the meltwater drainage systems of ice sheets appear to evolve in response to changes in meltwater input over thousands of years, reminiscent of seasonal changes observed in valley glaciers (Hubbard & Nienow, 1997; Iken & Truffer, 1997). We suggest that increased surface melting in a warming climate following the Younger Dryas led to the formation of additional subglacial drainage channels beneath the LIS, which increased the proportion of the bed drained by efficient drainage networks. As a result, dynamic instabilities, such as ice streaming and surging, may have been less important in contributing to its eventual demise (Carlson *et al.*, 2008; Carlson *et al.*, 2009).

These findings have implications for numerical modelling of ice sheets that incorporate their basal hydrology. Ideally, they should try and account for changes in the structure of meltwater drainage systems in response to increased meltwater supply, and the associated impact on ice sheet dynamics.

5.6 References

Aylsworth, J. M. & Shilts, W. W. (1989) Bedforms of the Keewatin Ice-Sheet, Canada. *Sedimentary Geology*, 62, 407-428.

Banerjee, I. & McDonald, B. C. (1975) Nature of esker sedimentation. In A. V. Jopling and B. C. McDonald, *Glaciofluvial and Glacilacustrine Sedimentation*. Oklahoma, SEPM, 304-320.

Bartholomew, I., Nienow, P., Mair, D., Hubbard, A., King, M. A. & Sole, A. (2010) Seasonal evolution of subglacial drainage and acceleration in a Greenland outlet glacier. *Nature Geoscience*, 3, 408-411.

Bolduc, A. M. (1992) The formation of eskers based on their morphology, stratigraphy and lithologic composition, Labrador, Canada. *Unpublished Ph.D. thesis, Lehigh University*.

Boulton, G. S., Hagdorn, M., Maillot, P. B. & Zatsepin, S. (2009) Drainage beneath ice sheets: groundwater-channel coupling, and the origin of esker systems from former ice sheets. *Quaternary Science Reviews*, 28, 621-638.

Carlson, A. E., Anslow, F. S., Obbink, E. A., LeGrande, A. N., Ullman, D. J. & Licciardi, J. M. (2009) Surface-melt driven Laurentide Ice Sheet retreat during the early Holocene. *Geophysical Research Letters*, L24502.

Carlson, A. E., LeGrande, A. N., Oppo, D. W., Came, R. E., Schmidt, G. A., Anslow, F. S., Licciardi, J. M. & Obbink, E. A. (2008) Rapid early Holocene deglaciation of the Laurentide ice sheet. *Nature Geoscience*, 1, 620-624.

Catania, G. A. & Neumann, T. A. (2010) Persistent englacial drainage features in the Greenland Ice Sheet. *Geophysical Research Letters*, 37, L02501.

Clark, C. D., Knight, J. K. & T Gray, J. (2000) Geomorphological reconstruction of the Labrador sector of the Laurentide Ice Sheet. *Quaternary Science Reviews*, 19, 1343-1366.

Clark, P. U. & Walder, J. S. (1994) Subglacial drainage, eskers, and deforming beds beneath the Laurentide and Eurasian ice sheets. *Bulletin of the Geological Society of America*, 106, 304-314.

Clarke, G. K. C. (1987) Fast glacier flow: Ice streams, surging, and tidewater glaciers. *Journal of Geophysical Research: Solid Earth*, 92, 8835-8841.

Cowton, T., Nienow, P., Bartholomew, I., Sole, A. & Mair, D. (2012) Rapid erosion beneath the Greenland ice sheet. *Geology*, 40, 343-346.

Dyke, A. S., Moore, A. & Robertson, L. (2003) Deglaciation of North America. *Geological Survey of Canada, Open File*, 1574.

Hewitt, I. J. (2011) Modelling distributed and channelized subglacial drainage: the spacing of channels. *Journal of Glaciology*, 57, 302-314.

Hillaire-Marcel, C. & Occhietti, S. (1980) Chronology, paleogeography, and paleoclimatic significance of the late and postglacial events in eastern Canada. *Zeitschrift für Geomorphologie*, 24, 373-392.

Hubbard, B. & Nienow, P. (1997) Alpine subglacial hydrology. *Quaternary Science Reviews*, 16, 939-955.

Iken, A. & Truffer, M. (1997) The relationship between subglacial water pressure and velocity of Findelengletscher, Switzerland, during its advance and retreat. *Journal of Glaciology*, 43, 328-338.

Kleman, J. & Glasser, N. F. (2007) The subglacial thermal organisation (STO) of ice sheets. *Quaternary Science Reviews*, 26, 585-597.

Kleman, J. & Hättestrand, C. (1999) Frozen-bed Fennoscandian and Laurentide ice sheets during the Last Glacial Maximum. *Nature*, 402, 63-66.

Margold, M. & Jansson, K. N. (2012) Evaluation of data sources for mapping glacial meltwater features. *International Journal of Remote Sensing*, 33, 2355-2377.

Mernild, S. H., Mote, T. L. & Liston, G. E. (2011) Greenland ice sheet surface melt extent and trends: 1960 - 2010. *Journal of Glaciology*, 57, 621-628.

Palmer, S., Shepherd, A., Nienow, P. & Joughin, I. (2011) Seasonal speedup of the Greenland Ice Sheet linked to routing of surface water. *Earth and Planetary Science Letters*, 302, 423-428.

Pritchard, H. D., Arthern, R. J., Vaughan, D. G. & Edwards, L. A. (2009) Extensive dynamic thinning on the margins of the Greenland and Antarctic ice sheets. *Nature*, 461, 971-975.

Rasmussen, S. O., Andersen, K. K., Svensson, A. M., Steffensen, J. P., Vinther, B. M., Clausen, H. B., Siggaard-Andersen, M. L., Johnsen, S. J., Larsen, L. B., Dahl-Jensen, D., Bigler, M., Rothlisberger, R., Fischer, H., Goto-Azuma, K., Hansson, M. E. & Ruth, U. (2006) A new Greenland ice core chronology for the last glacial termination. *Journal of Geophysical Research-Atmospheres*, 111.

Rignot, E., Velicogna, I., van den Broeke, M. R., Monaghan, A. & Lenaerts, J. (2011) Acceleration of the contribution of the Greenland and Antarctic ice sheets to sea level rise. *Geophys. Res. Lett.*, 38, L05503.

Schoof, C. (2010) Ice-sheet acceleration driven by melt supply variability. *Nature*, 468, 803-806.

Stokes, C. R. & Tarasov, L. (2010) Ice streaming in the Laurentide Ice Sheet: A first comparison between data-calibrated numerical model output and geological evidence. *Geophysical Research Letters*, 37, L01501.

Sundal, A. V., Shepherd, A., Nienow, P., Hanna, E., Palmer, S. & Huybrechts, P. (2011) Melt-induced speed-up of Greenland ice sheet offset by efficient subglacial drainage. *Nature*, 469, 521-524.

van de Wal, R. S. W., Boot, W., van den Broeke, M. R., Smeets, C. J. P. P., Reijmer, C. H., Donker, J. J. A. & Oerlemans, J. (2008) Large and Rapid Melt-Induced Velocity Changes in the Ablation Zone of the Greenland Ice Sheet. *Science*, 321, 111-113.

van den Broeke, M., Bamber, J., Ettema, J., Rignot, E., Schrama, E., van de Berg, W. J., van Meijgaard, E., Velicogna, I. & Wouters, B. (2009) Partitioning Recent Greenland Mass Loss. *Science*, 326, 984-986.

Vinther, B. M., Clausen, H. B., Johnsen, S. J., Rasmussen, S. O., Andersen, K. K., Buchardt, S. L., Dahl-Jensen, D., Seierstad, I. K., Siggaard-Andersen, M. L., Steffensen, J. P., Svensson, A., Olsen, J. & Heinemeier, J. (2006) A synchronized dating of three Greenland ice cores throughout the Holocene. *Journal of Geophysical Research: Atmospheres*, 111, D13102.

Wheeler, J. O., Hoffman, P. F., Card, K. D., Davidson, A., Sanford, B. V., Okulitch, A. V. & Roest, W. R. (1996) Geological map of Canada. *Geological Survey of canada, map 1860A*.

Zwally, H. J., Abdalati, W., Herring, T., Larson, K., Saba, J. & Steffen, K. (2002) Surface melt-induced acceleration of Greenland ice-sheet flow. *Science*, 297, 218-222.

Chapter 6 An assessment of lithological controls on esker distribution and morphometry in Canada

Storrar, R.D., Stokes, C.R. & Evans, D.J.A. (in prep) An assessment of lithological controls on esker distribution and morphometry in Canada. *Sedimentary Geology*.

Abstract

Eskers have the potential to reveal the nature of meltwater drainage beneath ice sheets, which is otherwise difficult to observe, yet important for understanding ice dynamics. However, no consensus has yet been reached on what controls the distribution of eskers. Previous work has asserted that: (1) Eskers are located preferentially on resistant rocks, where channels are incised upwards into ice, rather than down into rock; and (2) the hydrogeological properties of the substrate control the spacing of eskers. To date, no study has previously quantified whether esker morphometry is influenced by the underlying geology. This paper therefore provides the first such study and uses a large database of eskers mapped in Canada, alongside published bedrock and surficial geological maps, to quantify the effect of substrate properties on esker distribution. We find that: (i) eskers are highly concentrated on the resistant rocks of the Precambrian Shield, as predicted by theory; (ii) there is a strong preference for eskers to form in association with till; (iii) but till thickness exerts little control on esker distribution; (iv) esker length and sinuosity are unrelated to the underlying substrate; and (v) esker spacing, contrary to theory, is relatively uniform over different rocks and surficial materials.

6.1 Introduction

Section 2.6 reviewed the different hypotheses which have been suggested to account for the distribution of eskers. Several papers have suggested that the sediment and/or bedrock underlying esker systems is a key factor in determining the distribution of eskers (e.g. Aylsworth & Shilts, 1989; Bolduc, 1992; Clark & Walder, 1994; Boulton *et al.*, 2009; Hewitt, 2011) but few of these hypotheses have been tested at the ice sheet scale. Moreover, Chapter 4 presents results of an investigation into variations in esker morphometry in Canada and, in particular, presents results which detail differences in esker length and spacing. Variations in esker length have been linked to the supply of sediment (Aylsworth & Shilts, 1989) as well as to the size of the conduit in which the esker formed (Brennand, 1994;2000) and the hydrogeological properties of the substrate are suggested to exert a central control on esker spacing (e.g. Boulton *et al.*, 2009; Hewitt, 2011). Further testing is therefore required to determine the nature of the influence of lithology on esker distribution and morphometry. Thus,

this chapter aims to use the database of eskers and esker morphometry presented in Chapters 3 and 4, alongside published geological data, to quantitatively test the influence of bedrock and sediment on the location and form of eskers. Specifically, this chapter aims to address three questions concerning the effect of substrate lithology on eskers:

- Does the distribution of eskers (and, conversely, the gaps between them) correlate with the distribution of different rock/sediment types?
- Does the morphometry of eskers vary over different substrates?
- Does the spacing of Canadian eskers agree with the groundwater hypothesis for esker tunnel spacing?

6.2 Background and methods

6.2.1 Lithological controls on esker distribution and morphometry

The nature of the bedrock and sediment beneath ice sheets has important implications for the formation and location of glacial landforms. The morphometry of drumlins and ribbed moraine at the continental scale, for example, appears not to be greatly influenced by the lithology of the substrate (Greenwood & Clark, 2010). However, the opposite has been suggested for eskers. The lithological composition of eskers has been found to be closely related to that of the local till up to a few kilometres up-ice of the esker, suggesting that esker sediments are derived from local till (Bolduc, 1992). In turn, the properties of the till are derived primarily from the bedrock lithology (Clark & Walder, 1994). Clark & Walder (1994) theorised that eskers should form preferentially over crystalline substrates because channels would be eroded upwards into ice, rather than down into the resistant till derived from crystalline rocks (see Section 2.6). Conversely, drainage over sedimentary substrates is predicted to be in wide, shallow 'canals' because channels are incised into the more deformable permeable till associated with sedimentary bedrock (Walder & Fowler, 1994). Thus, a prediction of this theory is that longer eskers will be associated with more resistant rocks. Clark & Walder (1994) categorised bedrock geology into either sedimentary or igneous/metamorphic rocks and noted the abundance of eskers on the areas of crystalline bedrock in North America and Europe to support their hypothesis. More recent work has identified eskers in locations overlying less resistant lithologies (e.g. Clark *et al.*, 2004; Storrar *et al.*, 2013: see Chapter 3), which may suggest that the controls are more complex than previously thought.

The overall length of eskers overlying each substrate type, and the length and sinuosity of each individual esker, were compared with the distribution of different bedrock types (Figure 6.1; Figure 6.2) and ages (classified by era: see Figure 6.3) and surficial geological facies (Figure 6.4), from data published in Fulton (1995) and Wheeler *et al.* (1996). First, the total length of eskers overlying each different substrate type was calculated, and then the total area of each substrate type was calculated. This facilitated the calculation of the percentage of eskers

overlying each substrate type and the percentage of the total area that each substrate type occupies. Subtracting the percentage of eskers on a particular substrate type from the percentage 'abundance' of that substrate type thus gives a value for whether eskers are over- (i.e. positive percentages) or under-represented (i.e. negative percentages) on each different substrate type. The 'gaps' between eskers (see Section 4.2.1 for an explanation of how these were derived) were also subjected to this analysis, in order to test whether gaps between esker ridges are the result of a substrate control. Length and sinuosity values were calculated for each esker (see Chapter 4) and the eskers were then split into the different substrate types, producing a length and sinuosity value for each portion of an esker that overlies a different substrate type (Figure 6.1).

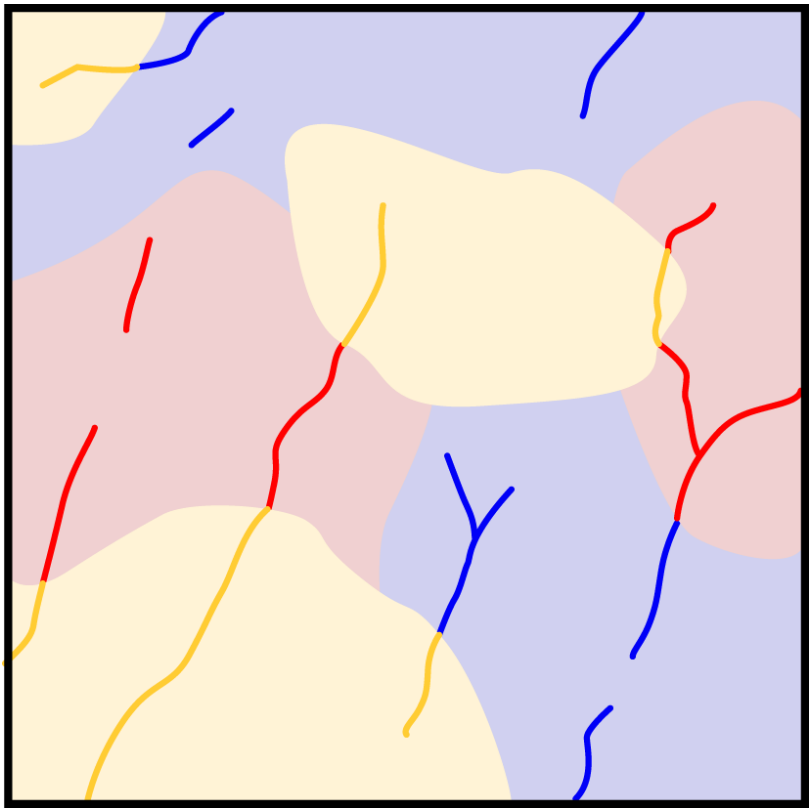

Figure 6.1. Schematic illustration of the methods used to measure esker properties on different substrates. Eskers were split and classified according to the underlying substrate, as illustrated by the different shades. Length and sinuosity values were then calculated for each ridge.

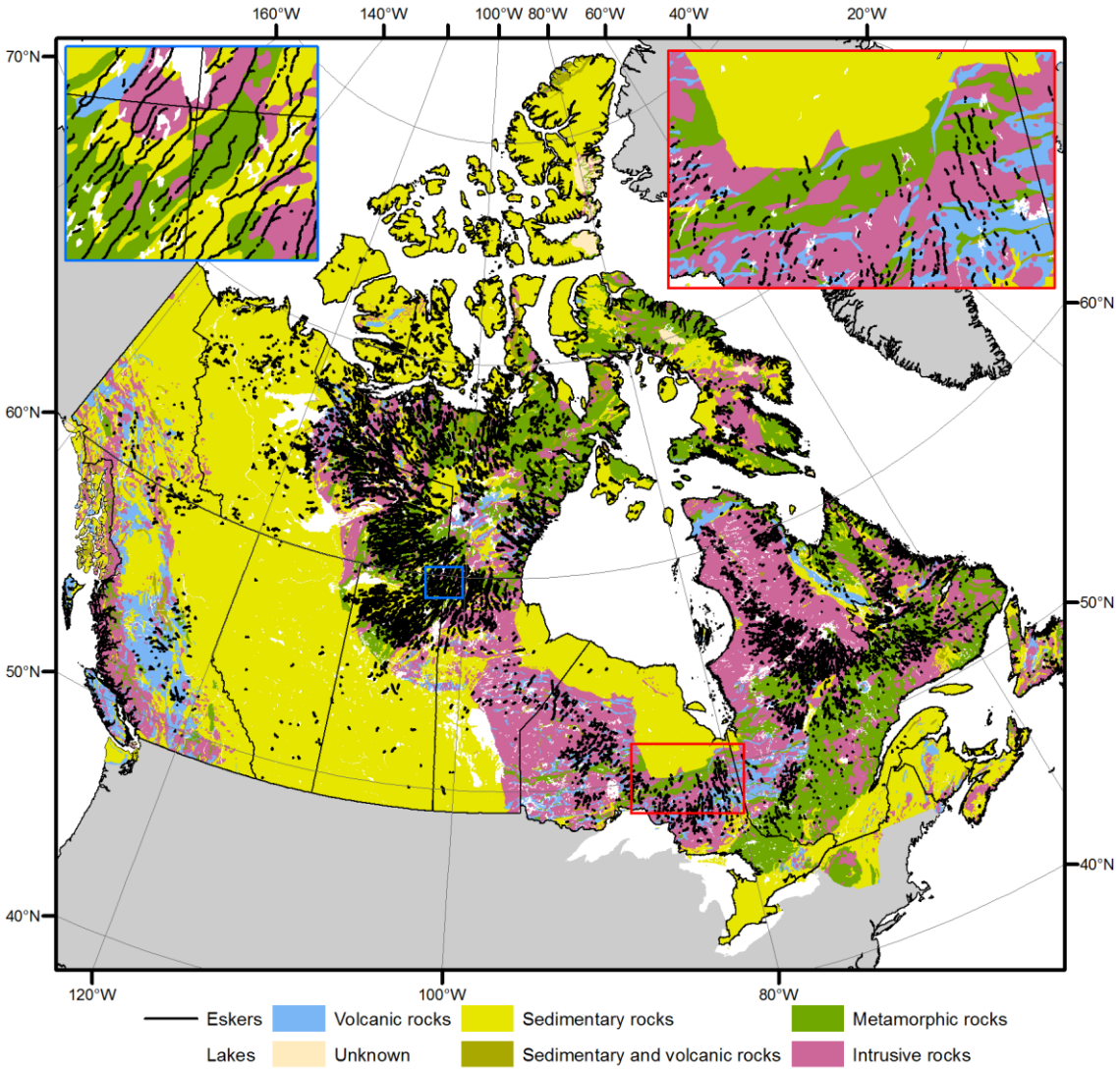

Figure 6.2. Bedrock geology classified by lithological type (after Wheeler *et al.*, 1996), overlain with mapped eskers. Inset boxes show close ups of the boxes indicated by the colours in the main map. The top left box shows eskers forming over sedimentary, metamorphic and intrusive rocks relatively evenly. In contrast, the top right box shows a strong preference for eskers to form over volcanic, intrusive and metamorphic rocks, whilst they do not form over sedimentary rocks.

As well as the type and nature of the substrate, the supply of sediment has also been proposed to be a fundamental control on esker distribution (Aylsworth & Shilts, 1989; Bolduc, 1992), with eskers expected to form in areas of abundant sediment and less likely to form in areas where sediment cover is sparse. Unfortunately, high-resolution sediment thickness data are presently not available for much of Canada. Low resolution data such as that of Laske & Masters (1997), which cover all of Canada, are unsuitable for analysing differences in esker distribution because they are too coarse in resolution (in this case 1° by 1° cells) to capture any subtle changes in esker patterns, which likely occur over relatively smaller areas. The only high-resolution data available, produced by subtracting bedrock elevation data from a digital elevation model, are available for central and southern Alberta (Atkinson & Lyster, 2011). However, this is the area

in which esker mapping from Landsat imagery is the least reliable (see Section 3.3.2). Thus, the 691 eskers included in the regional surficial geology maps produced by Shetsen (1987;1990) were used to analyse whether sediment thickness exerts any influence on esker location in central and southern Alberta (Figure 6.5). Sediment thickness was extracted from the midpoints of each esker and compared with the overall distribution of sediment thicknesses in the study area. Esker length was also calculated and compared with sediment thickness in order to test whether longer eskers are associated with higher sediment supplies.

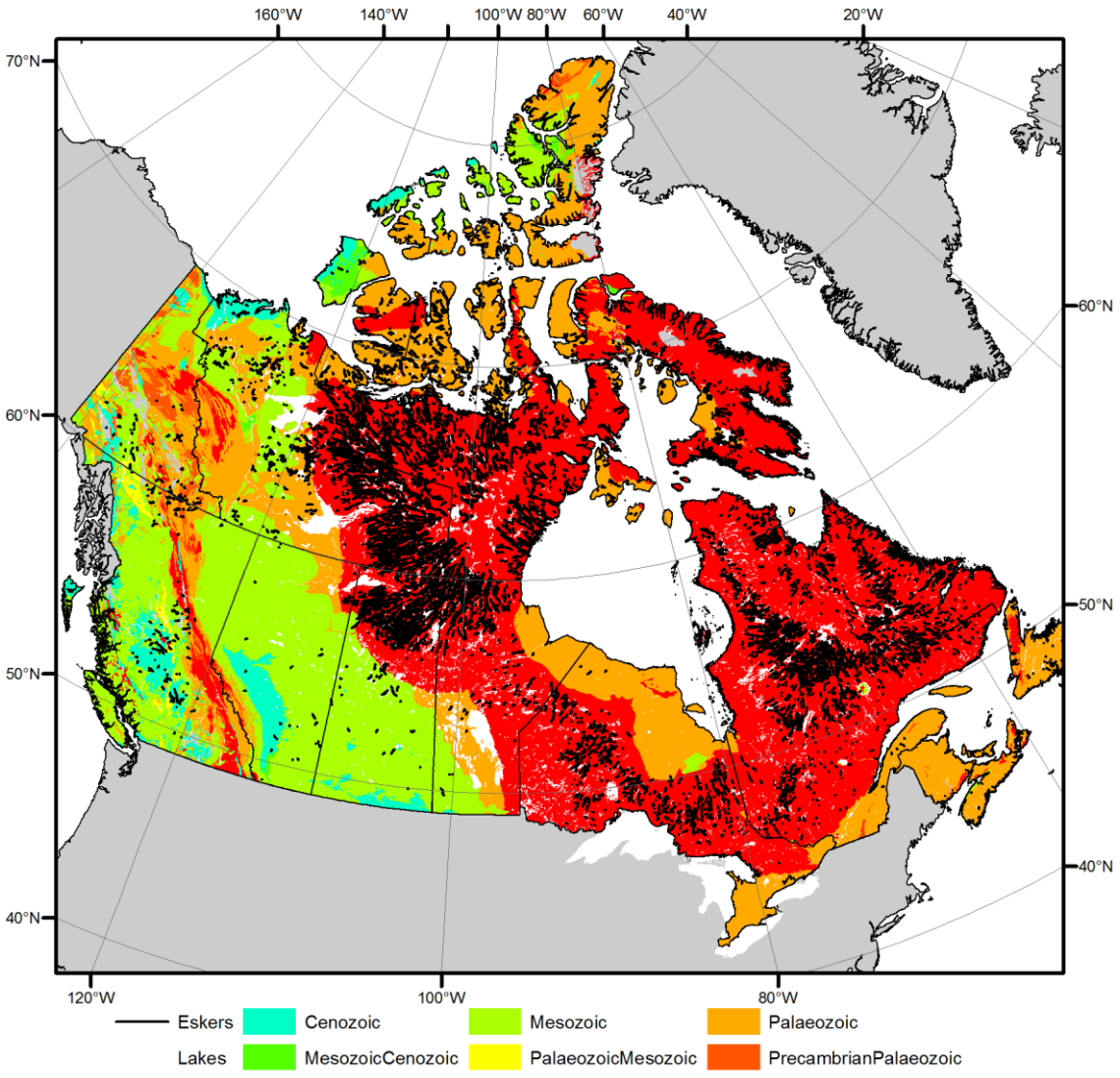

Figure 6.3. Bedrock geology classified by geological era (after Wheeler *et al.*, 1996), overlain with mapped eskers. Note the abundance of eskers on the Precambrian Shield (red).

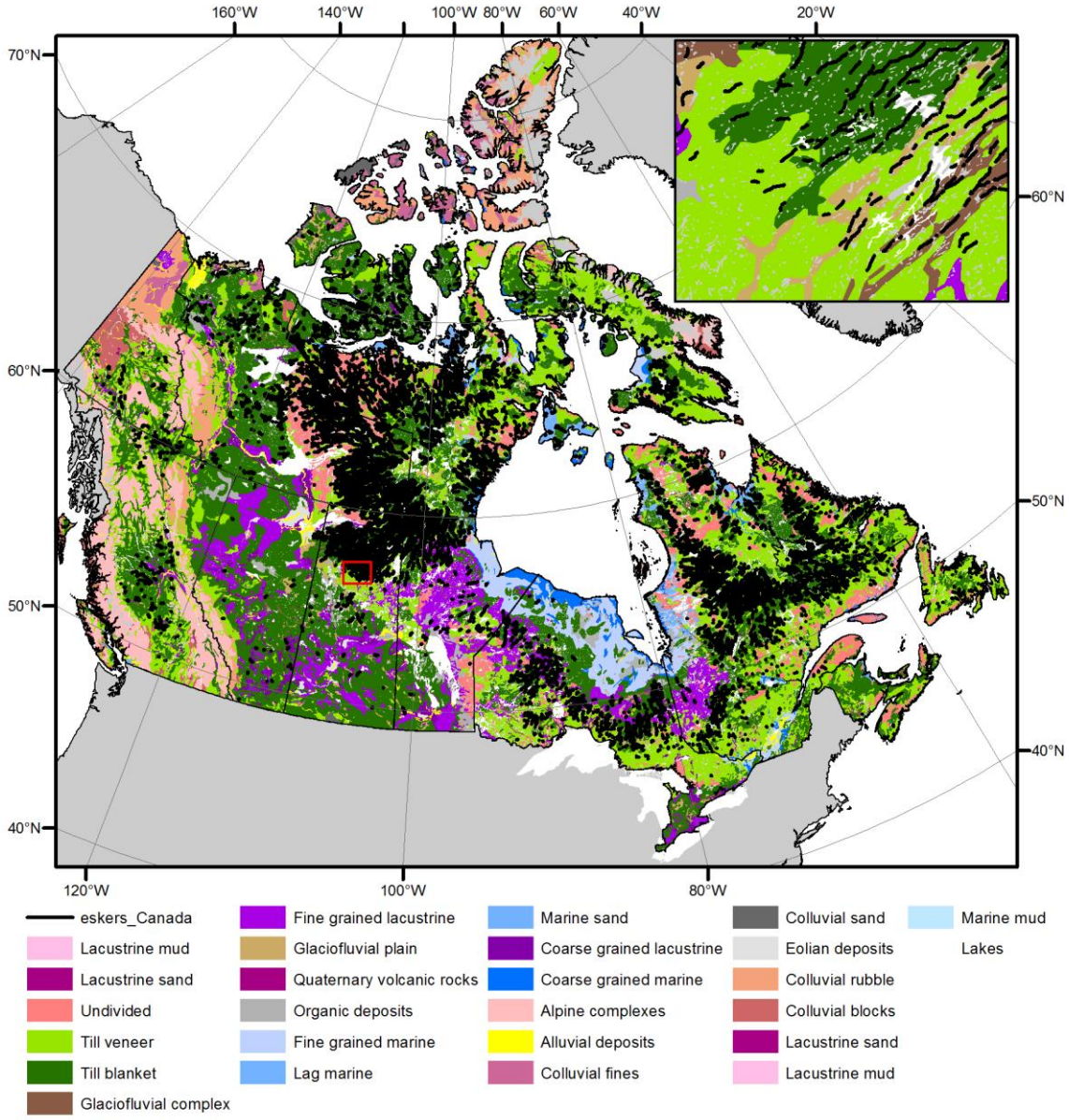

Figure 6.4. Surficial materials of Canada (after Fulton, 1995) overlain with the mapped eskers. The inset box shows eskers located preferentially over thick (typically > 2 m) till blankets (dark green) rather than thinner veneers of till (typically < 2 m) (lighter green). Also note the eskers located in the corridor of glaciofluvial material (brown).

6.2.2 Groundwater controls on esker spacing

Boulton and co-workers (Boulton *et al.*, 2001; Boulton *et al.*, 2007a;b; Boulton *et al.*, 2009; Boulton, 2010) developed a theory of groundwater controlled esker tunnel spacing (see also Section 2.6.5). The theory is predicated on the coupling of the subglacial drainage system and the local groundwater system (see Boulton *et al.*, 1993; Boulton *et al.*, 1995; Piotrowski, 1997; Piotrowski *et al.*, 1999; Piotrowski *et al.*, 2009) and predicts that the spacing between meltwater channels is a result of the scavenging of basal meltwater into groundwater systems. Boulton *et al.* (2009) used a model of the terminal 50 km of the Fennoscandian Ice Sheet to suggest that

esker spacing S (m) is related to the transmissivity T (m^2 yr^{-1}) of the substrate and the basal melt rate m (m yr^{-1}):

$$S = 77.8\left(\frac{T}{m}\right)^{1/2} \quad (6.1)$$

Boulton *et al.* (2009) assumed that tunnels form in winter, when surface meltwater input is negligible, suggesting instead that basal melt is the key supply of meltwater. Observations of esker spacing between 8 and 25 km in Finland were suggested by Boulton *et al.* (2009) to support this hypothesis, though it should be noted that esker spacing of anywhere between 2.5 and 50 km would have agreed with the prediction. The hypothesis is difficult to test empirically because the precise quantification of parameters, which vary over several orders of magnitude (for example, Boulton *et al.* suggest feasible transmissivity values which range from 80 to 25,000 m^2 yr^{-1}), is very difficult to achieve for the large areas required to be confident of esker spacing (which is typically ~12 km where eskers are well preserved: see Section 4.3.3). In this section, we therefore use a semi-quantitative, first-order approximation to test whether eskers in Canada are spaced in accordance with the groundwater theory. We measure esker spacing across Canada and estimate the transmissivity of the substrate from geological and surficial data to predict basal melt rates, which we compare with 'realistic' values.

Chapter 4 presents data on esker spacing, which we use here to provide accurate constraints on the first parameter of equation 6.1. Transmissivity (T) is difficult to estimate over large areas because it relies on knowing the thickness of the aquifer, as well as its hydraulic conductivity (K: m yr^{-1}). Hydraulic conductivity (K), however, is simpler to estimate because it depends solely on the physical properties of the rock and is not dependent on its depth (Bear, 1972). Thus, it is possible to utilise approximations of hydraulic conductivity (K) to assess the likely variations in transmissivity (T), to which it is related by the depth b (m) of the substrate:

$$T = Kb \quad (6.2)$$

Estimates of hydraulic conductivity (K) vary over several orders of magnitude between different rock and sediment types (Bear, 1972). Boulton *et al.* (2009) reported several estimates of hydraulic conductivity (K) for Shield rocks in Sweden and Finland from the literature, yielding values between 3.16×10^{-4} m yr^{-1} and 3.16×10^{1} m yr^{-1}. Variations in the depth of the permeable layer between 100 and 600 m resulted in values of transmissivity (T) from 60 m^2 yr^{-1} to 1.8×10^4 m^2 yr^{-1}. In Canada, Lemieux *et al.* (2008) assumed a transmissivity (T) value of 30 m^2 yr^{-1} for the Canadian Shield, though there are few data available to provide an indication of the variability of these numbers.

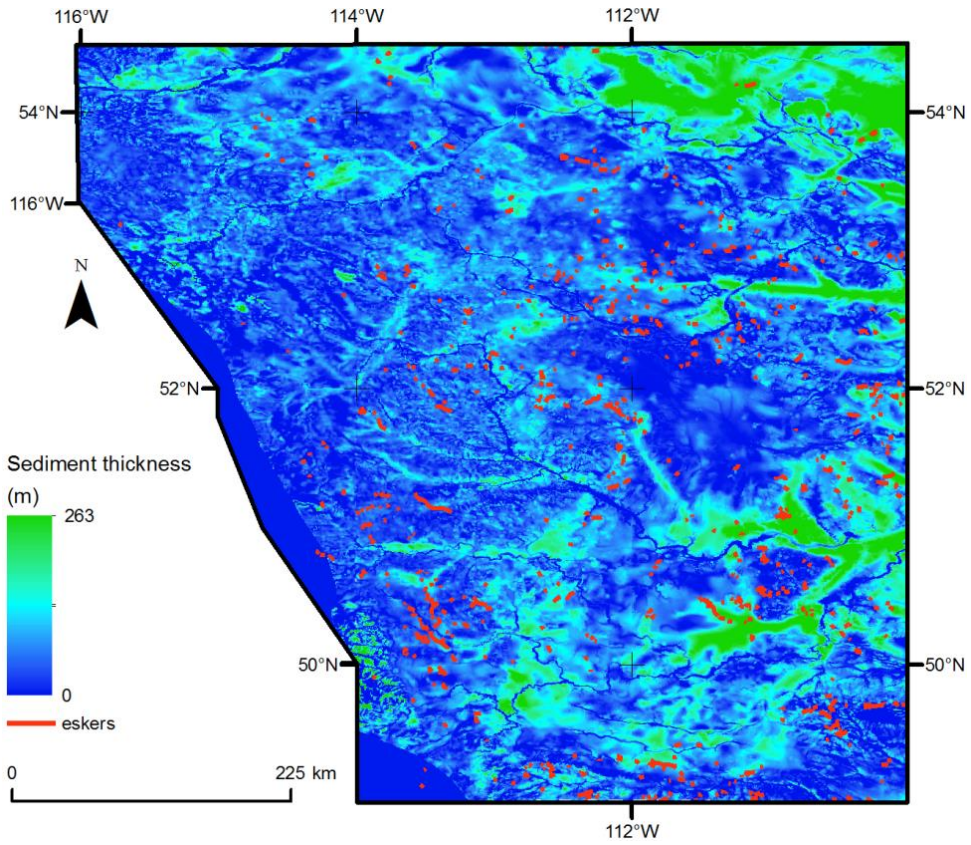

Figure 6.5. Sediment thickness and esker distribution in central and southern Alberta. Eskers are digitised from Shetsen (1987;1990) and sediment thickness is derived from Atkinson & Lyster (2011).

Clearly, with such large variations in the magnitude of hydraulic conductivity (*K*) and transmissivity (*T*), and the lack of robust constraints on the groundwater properties of large Shield areas, predictions of basal melt rate (*m*) represent a very rough approximation and rule out a purely quantitative test. Thus, a more objective way to test the hypothesis that the groundwater properties of the substrate control the spacing of eskers is to compare esker spacing in different areas with markedly different hydrogeological properties. Eskers in areas of high and low transmissivity (*T*) should, if the theory is correct, exhibit different spacing measurements, assuming that basal melt rate (*m*) is relatively uniform (see Figure 6.6).

To test this hypothesis, we use individual measurements of *interpolated* esker spacing *S* (see Section 4.3.4 for a description of *interpolated* esker spacing) and estimates of hydraulic conductivity (*K*: see Table 6.1) to produce predictions of basal melt rate (*m*), in order to establish whether a positive or negative correlation exists between esker spacing and substrate type (see Figure 6.6). Esker spacing was calculated where the space between two eskers overlies only one substrate type (e.g. Figure 6.7). We assume a uniform substrate thickness of one metre, thereby negating the term *b* in equation 6.2. Substituting hydraulic conductivity (*K*) for

transmissivity (*T*) and rearranging equation 6.1 to make basal melt rate (*m*) the subject gives the following:

$$m = K\left(\frac{S}{77.8}\right)^{-2} \tag{6.3}$$

The estimates of hydraulic conductivity (*K*) for different rock and sediment types of Bear (1972) were used to provide crude approximations of hydraulic conductivity (*K*) for each substrate type mapped by (Fulton, 1995) and Wheeler *et al.* (1996), as set out in Table 6.1. The calculated values of basal melt rate (*m*) should, if the theory is correct and the assumptions valid, be roughly consistent across different values of hydraulic conductivity (*K*) and esker spacing (*S*) (Figure 6.6B). Values of basal melt rate (*m*) which span many orders of magnitude and indicate that esker spacing does not increase with increased hydraulic conductivity (*K*) (Figure 6.6C) would suggest that the data do not support the theory.

Table 6.1. Estimates of hydraulic conductivity for different bedrock and surficial geological units, based on Bear (1972).

Substrate type	Estimated Hydraulic conductivity (m s^{-1})
Sedimentary rocks	10^{1}
Metamorphic rocks	10^{-6}
Intrusive rocks	10^{-6}
Volcanic rocks	10^{-3}
Till blanket	10^{1}
Till veneer	10^{1}
Glaciofluvial complex	10^{6}
Glaciofluvial plain	10^{6}

6.3 Results

6.3.1 Bedrock geology

Overall, eskers are located in relatively even proportions over metamorphic (26%), intrusive (33%) and sedimentary (35%) lithologies, whilst only 5% occur on volcanic lithologies (Figure 6.8A). When the distribution of eskers is compared with the relative abundance of each lithology type, a preference for esker formation over metamorphic and intrusive rocks becomes apparent, whereas they are relatively less common over volcanic and sedimentary lithologies than would be expected at random (Figure 6.8B). 85% of eskers and 90% of gaps are located on

Precambrian rocks (Figure 6.8C) and the relative abundance of eskers compared with each different era (Figure 6.8D) confirms that there is a strong preference for esker formation over Precambrian rocks. The statistics for *gaps* are similar to those for the different lithological types and eras. Esker length and sinuosity values exhibit no statistical difference at the 1σ level over different bedrock types and eras (Figure 6.9). Maximum esker length values are strongly positively correlated (R^2 = 0.87 for both rock type and era) with sample size. Maximum esker sinuosity values may also be related to sample size but the correlation coefficients are smaller (R^2 = 0.51 for rock type and 0.04 for era). The apparent absence of correlation between maximum sinuosity and rock age may be explained by the dominance of Precambrian rocks, which results in very small sample sizes for the other eras.

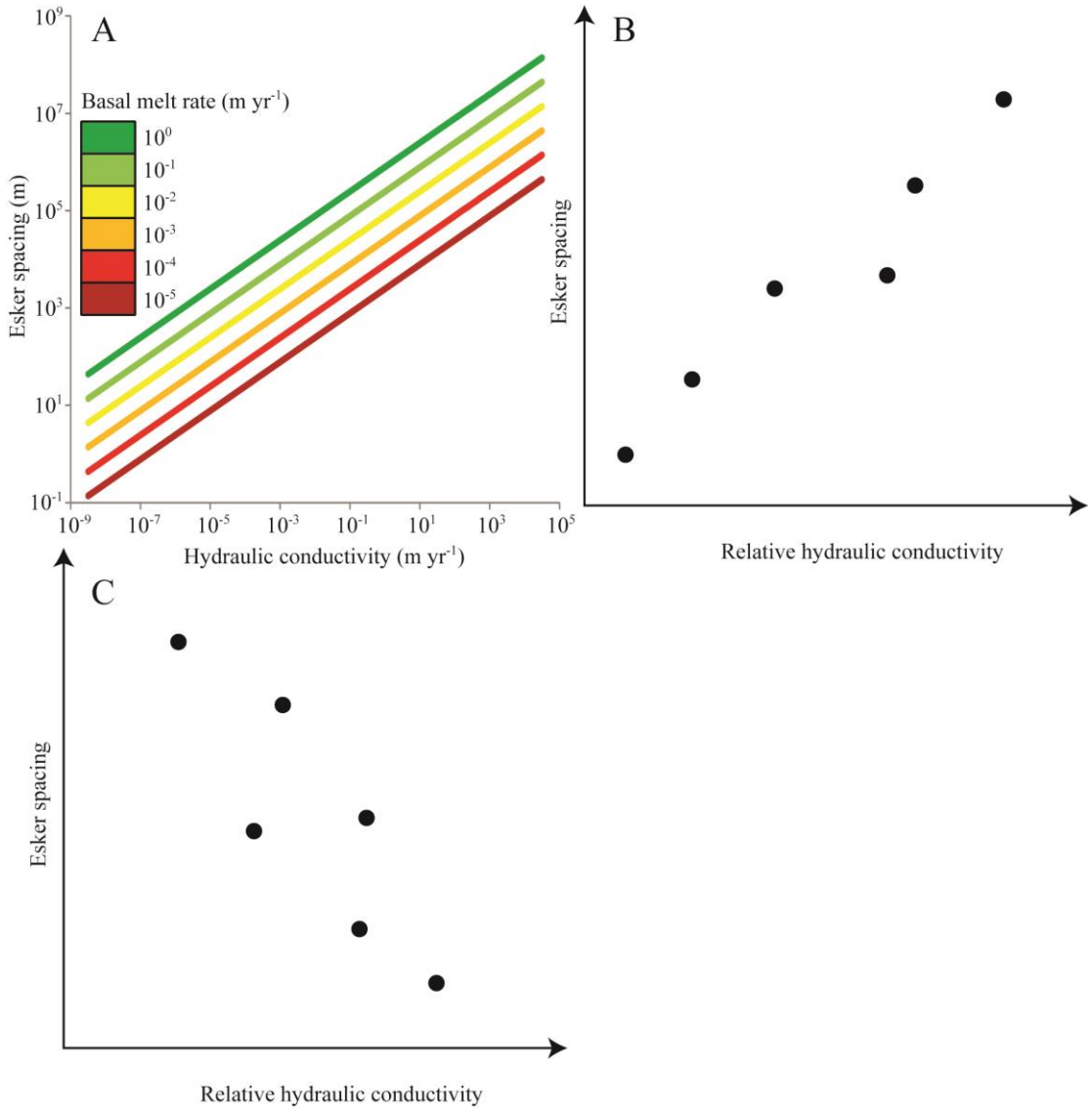

Figure 6.6. Basis for testing Boulton's (2009) hypothesis. A) Plotting hydraulic conductivity against esker spacing produces a prediction for basal melt rates, which are proportional to both parameters. Whilst hydraulic conductivity is difficult to quantify, an estimate should allow the identification of a positive (B) or negative (C) correlation. A positive correlation would support

the hypothesis because it would imply a realistic (small) range of basal melt rates. Conversely, a negative correlation would imply that the range of basal melt rates produced is unrealistic.

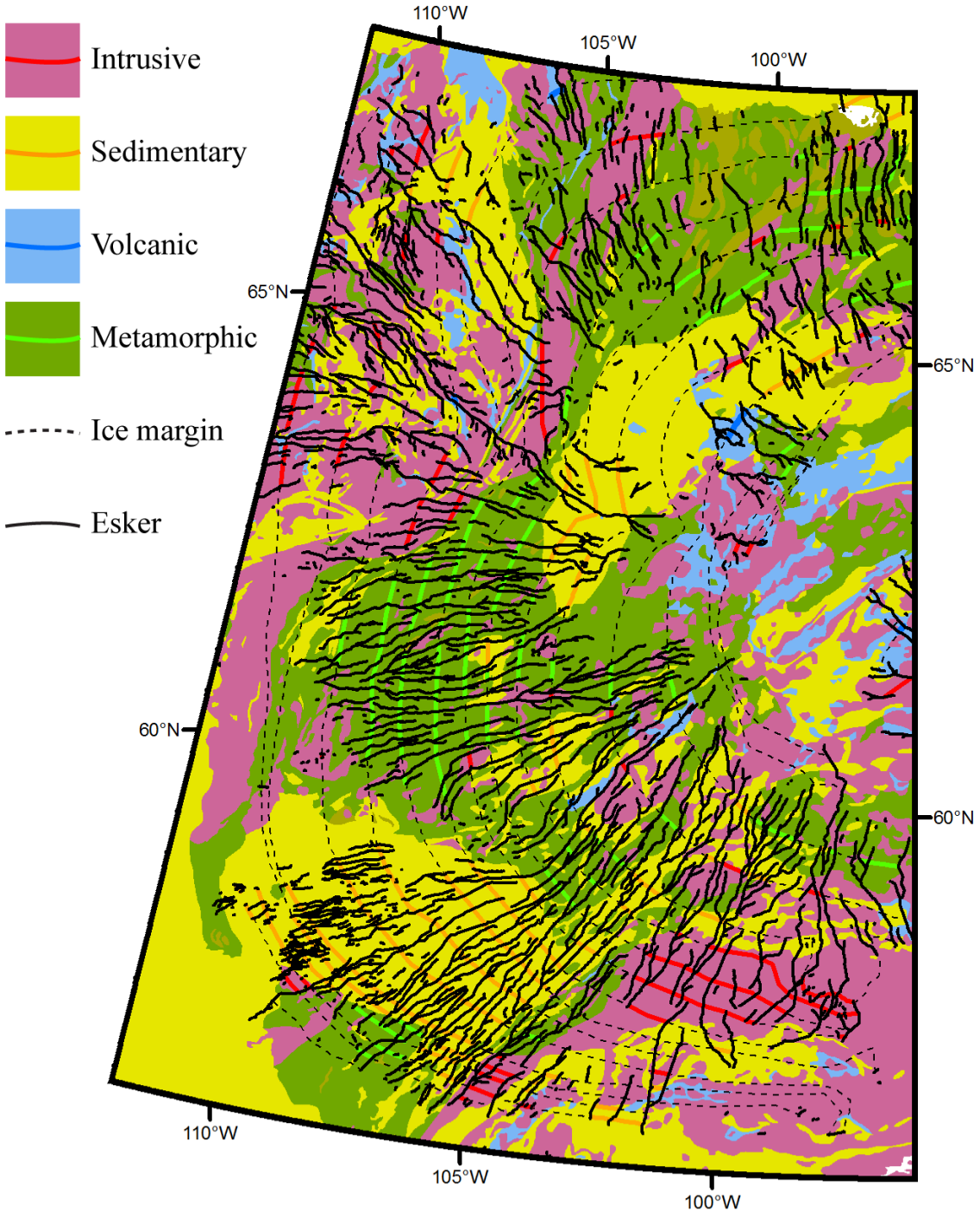

Figure 6.7. Spacing measurements taken in the Keewatin study area. Geological units are represented by the shaded areas and spacing measurements by the corresponding coloured line. Spacing measurements were taken where the ice margin crossed only one geological unit between two eskers.

6.3.2 Surficial geology

The majority (80%) of eskers are located on till, with 53% overlying thicker till blankets and 27% overlying thinner veneers of till (Figure 6.10A). Gaps follow a similar trend, 64%

occurring over till. The difference between the values of eskers and gaps forming over till may be explained by lakes. Eskers are undetectable beneath lakes, which account for 21% of gaps. When the relative abundance of each facies is taken into account, a marked preference is shown for eskers to form over till, with a small preference also registered for glaciofluvial plains and complexes. All other facies exhibit a negative anomaly value, indicating that eskers do not form preferentially on these substrates. Locally, eskers occupy narrow corridors of glaciofluvial material (St-Onge, 1984; Utting *et al.*, 2009), though few other patterns are evident. There is no statistical difference at the 1σ confidence level between length or sinuosity values over different facies (Figure 6.11). As with the bedrock data, maximum length and sinuosity values are positively correlated with sample size ($R^2 = 0.76$ for length and 0.84 for sinuosity).

6.3.3 Sediment thickness

Whilst eskers are more prevalent over till blankets than till veneers, analysis of sediment thickness beneath eskers in south and central Alberta reveals that eskers exhibit little preference for formation over sediment of a particular thickness (Figure 6.12A;B). Mean sediment thickness beneath eskers is 24.18 m and the mean sediment thickness of the area studied is 24.12 m. Median sediment thickness values are 21 m beneath eskers and 19 m for the study area. The largest bin indicates that 7.7% of eskers occur over areas with <1 m of sediment cover (Figure 6.12A), though this is 3% less than expected by the distribution of background values (Figure 6.12B). Figure 6.12C indicates that the longest eskers tend occur over sediment depths <50 m and the deepest areas of sediment tend to be overlain with shorter eskers.

6.3.4 Hydraulic conductivity

Measurements of median esker spacing range from 8.5 km to 12.9 km over different substrate types, whilst the modal values (using 1 km bins) are between 7 and 9 km for each type (Figure 6.13). Using the mean, median and modal values for esker spacing over each different substrate type, and the approximations of *K* given in Table 6.1, equation 6.3 produces a large range of basal melt rates, between 7.47×10^{-11} and 1.24×10^{-3} m yr^{-1} (Figure 6.14). Each substrate type used produces a large range of basal melt rates, whilst the spacing values do not vary considerably (Figure 6.14).

6.4 Discussion

6.4.1 Bedrock and surficial geology

Theory predicts that most eskers occur over the more resistant rocks of the Precambrian Shield (Clark & Walder, 1994) and results support this, with 85% of eskers, including the longest one

(97.5 km) occurring over Precambrian rocks (Figure 6.8). Clark and Walder (1994) suggest that the resistant bedrock gives rise to correspondingly stiff till, which then supplies the material to create the eskers. Indeed, eskers are also observed to be closely related to till, with 53% of eskers overlying till blankets and 27% overlying thinner veneers of till (Figure 6.10), which supports suggestions by Bolduc (1992) and Clark and Walder (1994) that esker material is derived primarily from the local till. Bolduc (1992) presents evidence of transport distances of esker material which is derived from till 1-27 km up-ice in northern Labrador, based on lithological composition. Despite the observation that more eskers overlie till blankets than till veneers, the thickness of the sediment appears not to influence the distribution of eskers, as indicated by the very small values in the deviation from the 'expected' percentage of sediment thickness values beneath eskers in central and southern Alberta (Figure 6.12A). Thus, it appears likely that esker location in most places is dependent on the availability of a sufficient quantity of till to form the esker, but that the depth of till is unimportant. Given that very thin sediment veneers appear to be closely related to esker occurrence, and that eskers may be up to 50 m tall (e.g. Banerjee & McDonald, 1975), this raises the question of how a sufficient quantity of sediment could become incorporated into eskers. We provide two possible explanations.

The simplest explanation is that channels receive sediment longitudinally from subglacial sources up-ice. Bolduc (1992) presents evidence of transport distances of esker material which is derived from till 1-27 km up-ice in northern Labrador, based on the lithological composition of eskers, which could conceivably provide enough sediment to build eskers. In addition, sediment may also enter channels from supraglacial or englacial sources (e.g. Shilts, 1984), which potentially includes a network of smaller tributaries which feed the main, esker-forming channel which may be in a subglacial position.

Measurements of mean esker length and sinuosity all lie within the same range of 1σ values when compared with different bedrock and surficial geological data, which indicates that esker length and sinuosity are independent of variations in the substrate. The longest individual eskers are consistently associated (R^2 values typically greater than 0.7: see Figure 6.9 and Figure 6.11) with whichever sedimentary facies, rock type or era has the largest sample size, which also suggests that the underlying substrate exerts no influence on how large an individual esker may reach.

Figure 6.12C shows sediment thickness plotted against esker length and may suggest that long eskers form preferentially over thinner sediments (no eskers longer than 7 km occur over till more than 55 m deep), however this is potentially simply an artefact of the smaller sample sizes over thicker sediments, which generally occur less frequently (Figure 6.12B). This result is surprising because, given that most eskers are associated with Precambrian rocks and till, and observations of long eskers in Shield areas (Clark & Walder, 1994), it would seem logical to suppose that the longest eskers form preferentially over these substrates. In the absence of

lithological controls on individual esker length and sinuosity, the most likely explanation is that the surface profile of the ice sheet was the primary control on these factors, because this governs the routing of meltwater (e.g. Shreve, 1972; Shilts, 1984).

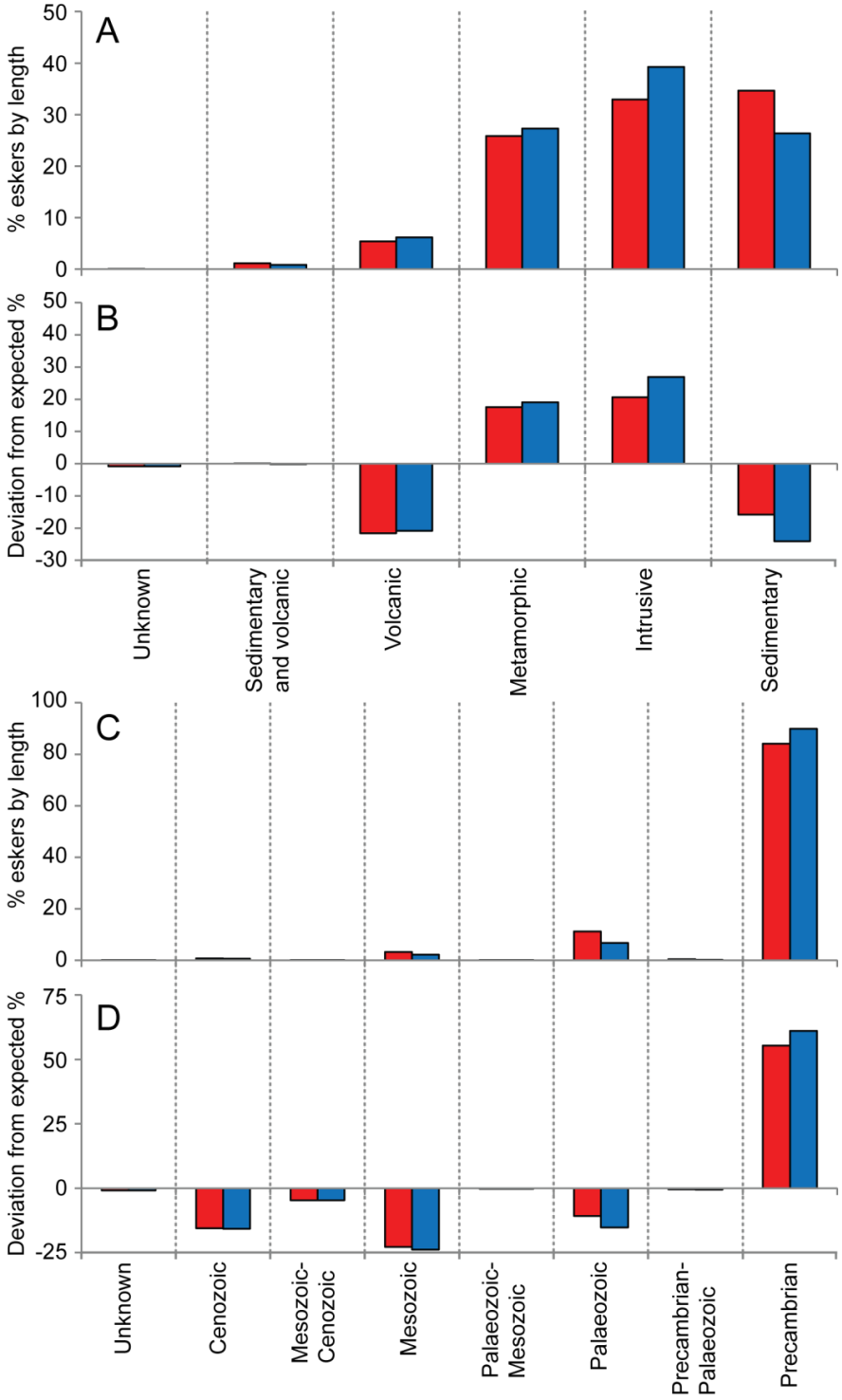

Figure 6.8. A) Percentage of total esker (blue) and gap (red) length overlying different rock types. B) Deviation of values in A from the percentage of esker length *expected* over each rock type, when weighted by area. C) Percentage of total esker length overlying rocks of different eras. D) Deviation of values in C from the percentage of esker length *expected* over each rock era, when weighted by area.

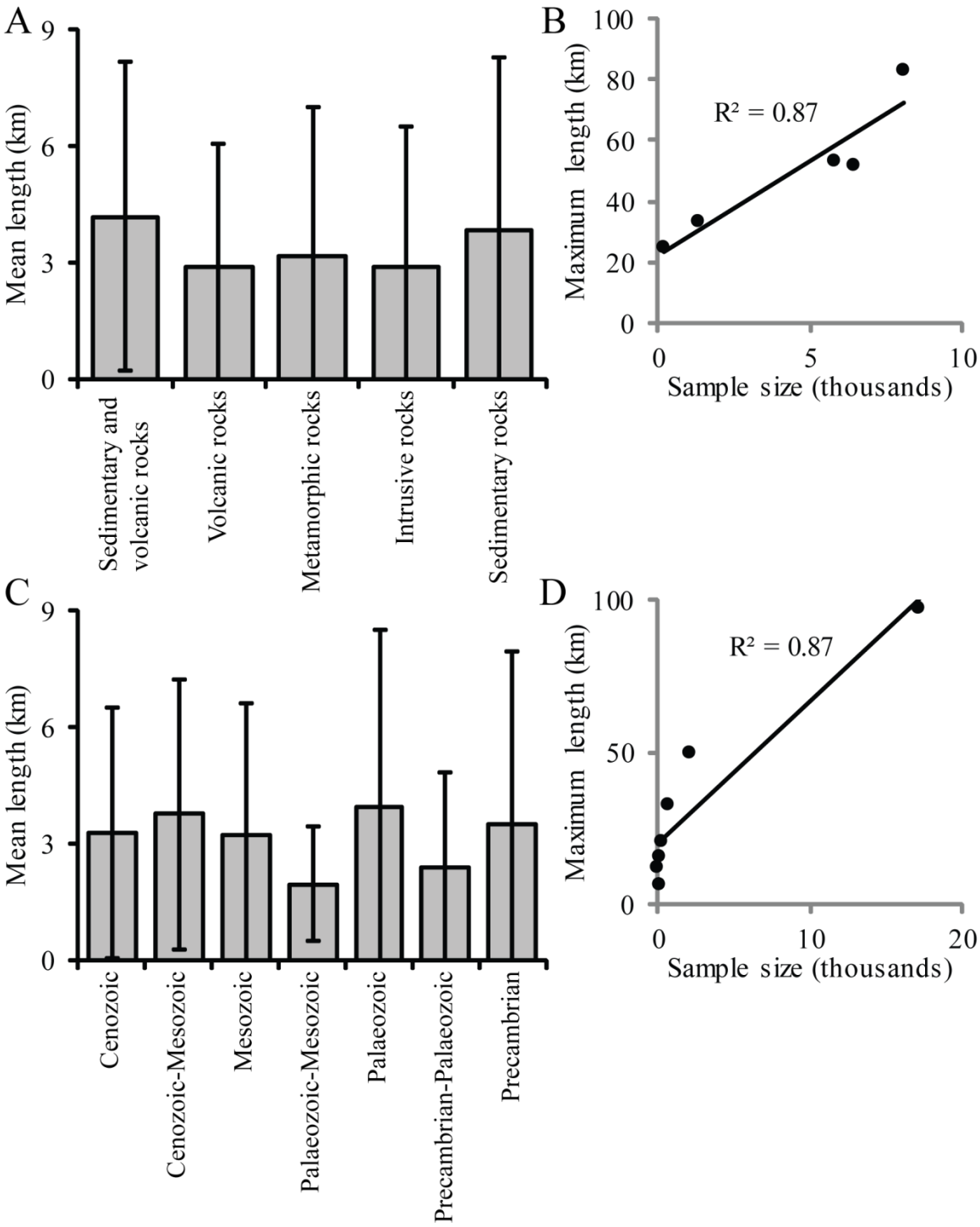

Figure 6.9. A) Mean esker length and associated 1σ error bars for each bedrock type. B) Regression plot of maximum esker length (for rock types) against sample size. C) Mean esker length and associated 1σ error bars for each bedrock era. D) Regression plot of maximum esker length (for eras) against sample size. E) Mean esker sinuosity and associated 1σ error bars for each bedrock type. F) Regression plot of maximum esker sinuosity (for rock types) against sample size. G) Mean esker sinuosity and associated 1σ error bars for each bedrock era. H) Regression plot of maximum esker sinuosity (for eras) against sample size. Continued overleaf.

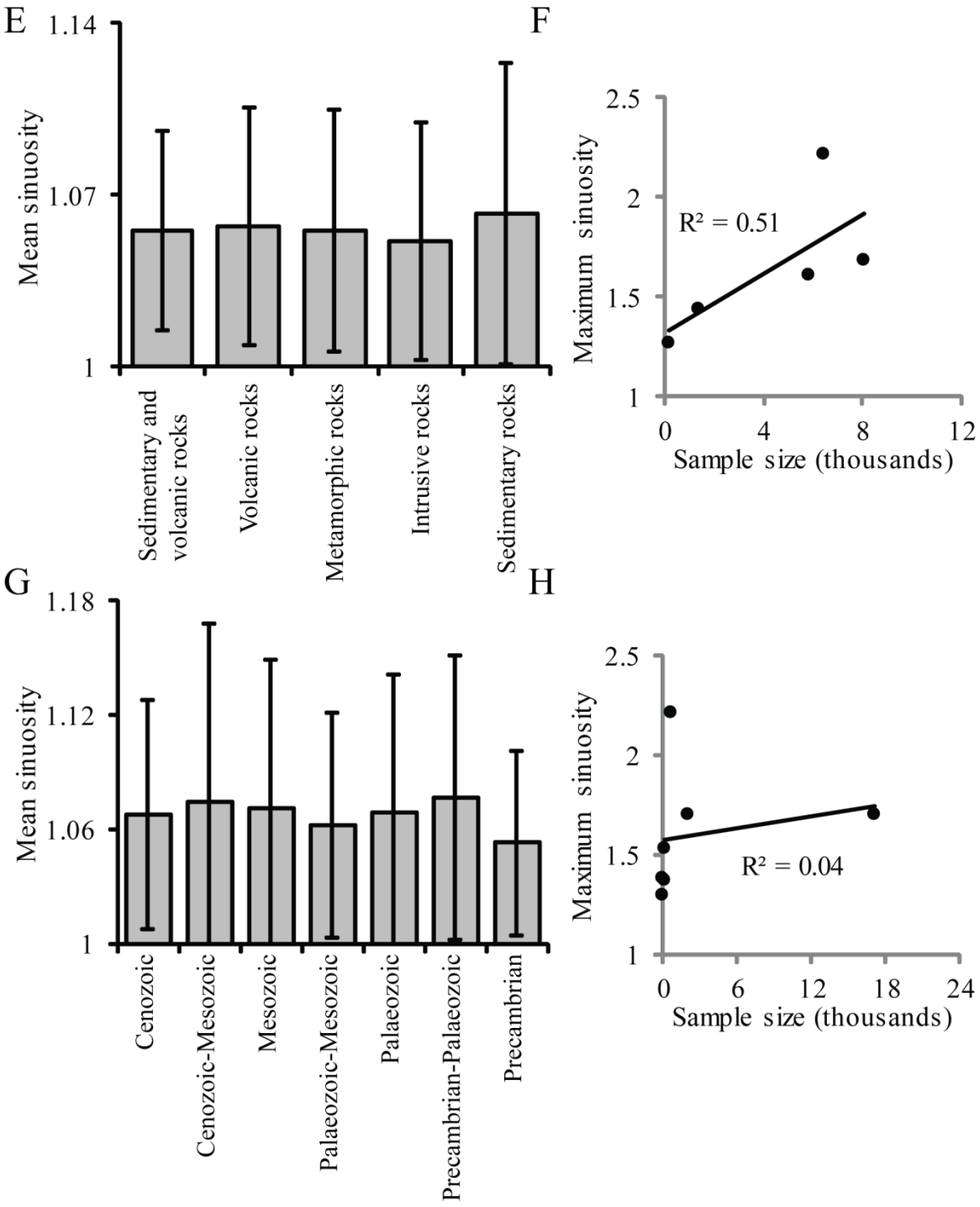

Figure 6.9 (continued).

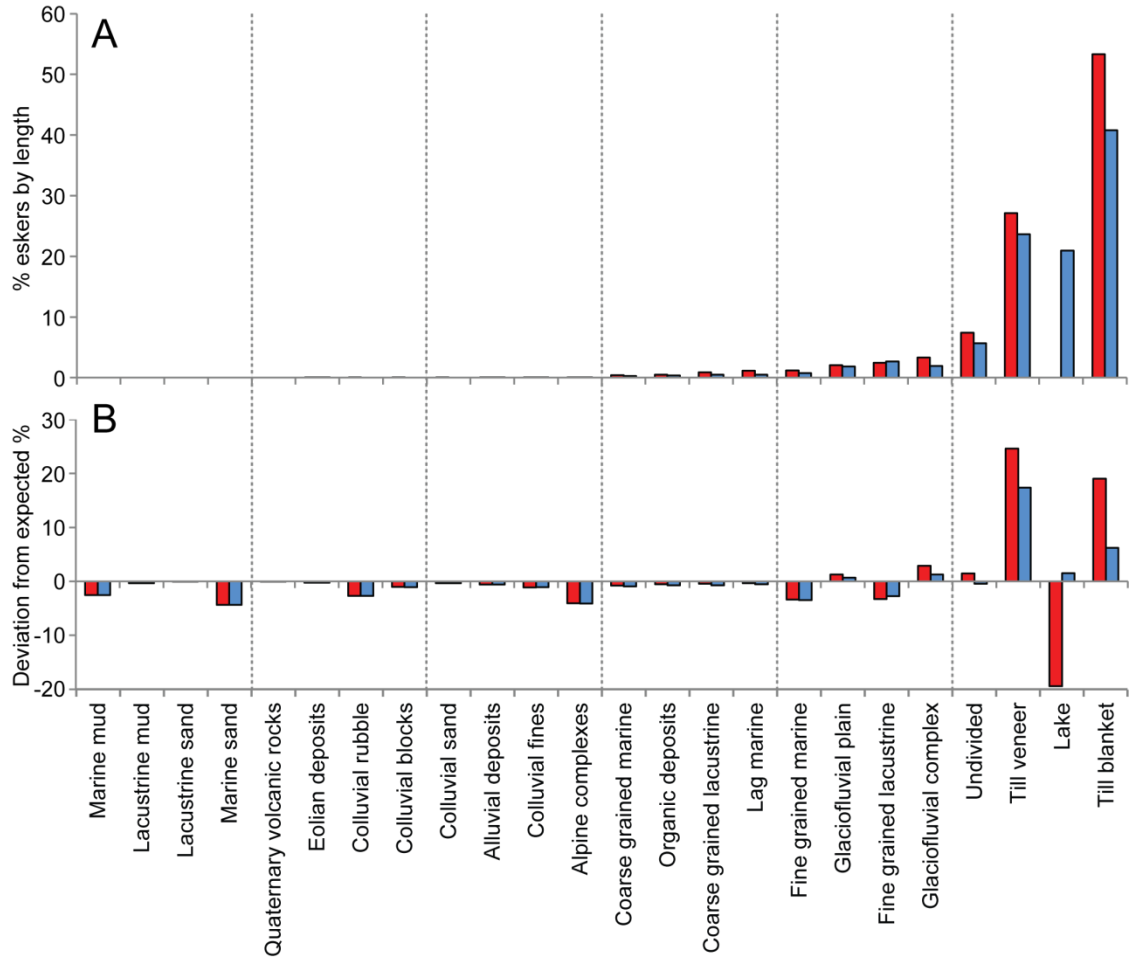

Figure 6.10. A) Percentage of total esker length overlying different surficial geological facies. B) Deviation of values in A from the percentage of esker length *expected* over each facies, when weighted by area.

Thus, the distribution of eskers predominantly over Precambrian rocks and till supports the theory of Clark and Walder (1994) and suggests that esker location is governed by two factors: (1) resistant crystalline Precambrian rocks enable channels to be incised into ice, allowing eskers to be deposited, but only when (2) there is a sufficient supply of till to form the eskers. In contrast, esker length and sinuosity are independent of substrate controls and are more likely governed by ice sheet geometry.

The similar distribution of 'gaps' and eskers overlying each bedrock and surficial geological unit (Figure 6.8; Figure 6.10) indicates that the gaps between esker ridges are not the result of a geological control. Rather than being controlled by the underlying geology, 20% of gaps in eskers are found to correspond to the locations of lakes, which provides a useful quantification of the ability of lakes to fragment eskers. Lakes may either represent a depression between eskers, where no esker was formed, or they may conceal submerged eskers which cannot then be detected in remotely sensed imagery (see Section 3.3).

The resistance of sediment to erosion is likely to be another important factor in determining whether eskers are likely to form. More resistant sediments would be more likely to support R-channels in the manner suggested by Clark & Walder (1994), since meltwater would not erode down into them as readily as more deformable sediments. Further data on till properties, including transmissivity, are therefore required in order to test the relationship between till strength, groundwater-channel coupling and esker distribution more fully.

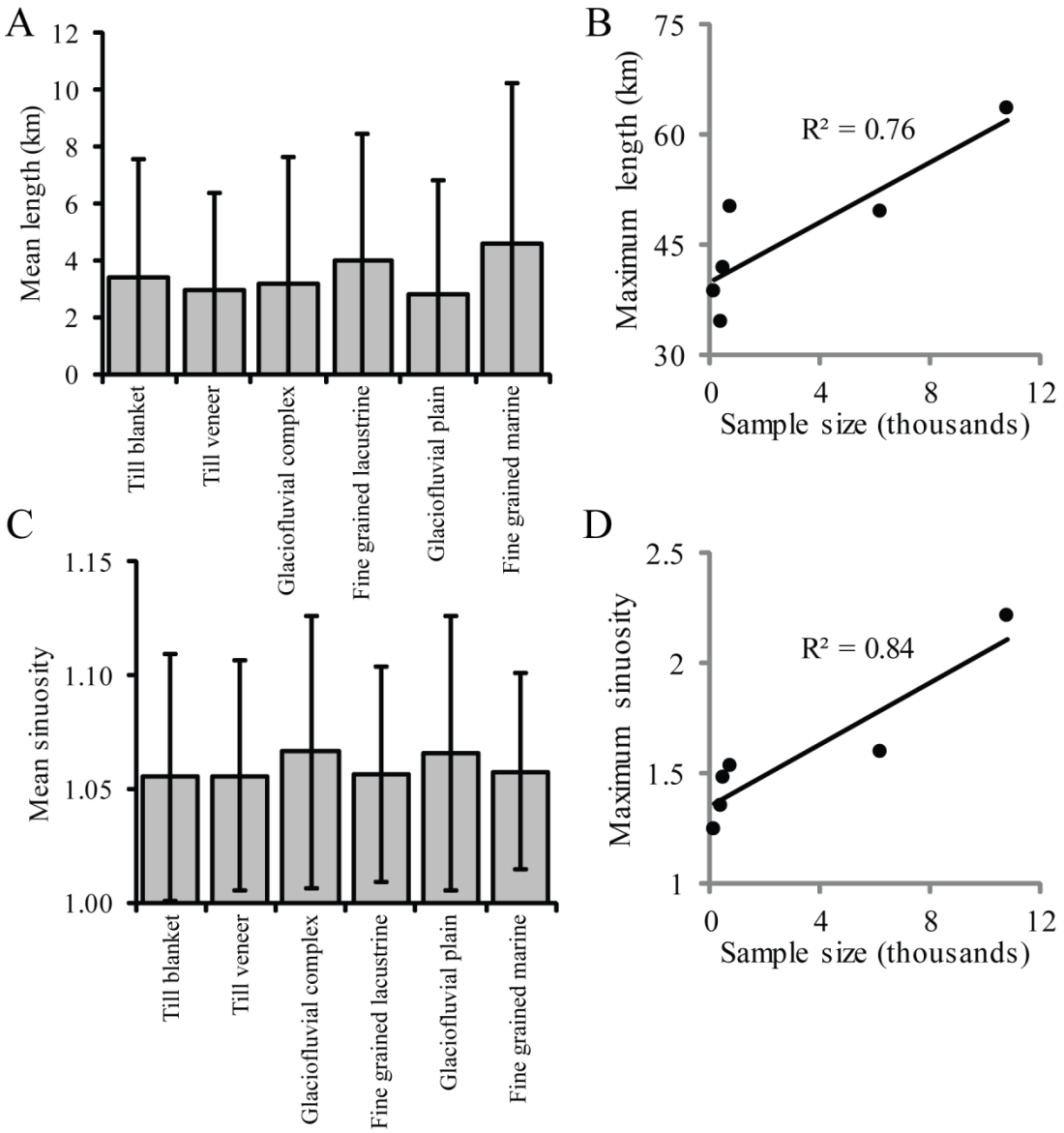

Figure 6.11. A) Mean esker length and associated 1σ error bars for each facies. B) Regression plot of maximum esker length against sample size. C) Mean esker sinuosity and associated 1σ error bars for each facies. D) Regression plot of maximum esker sinuosity against sample size.

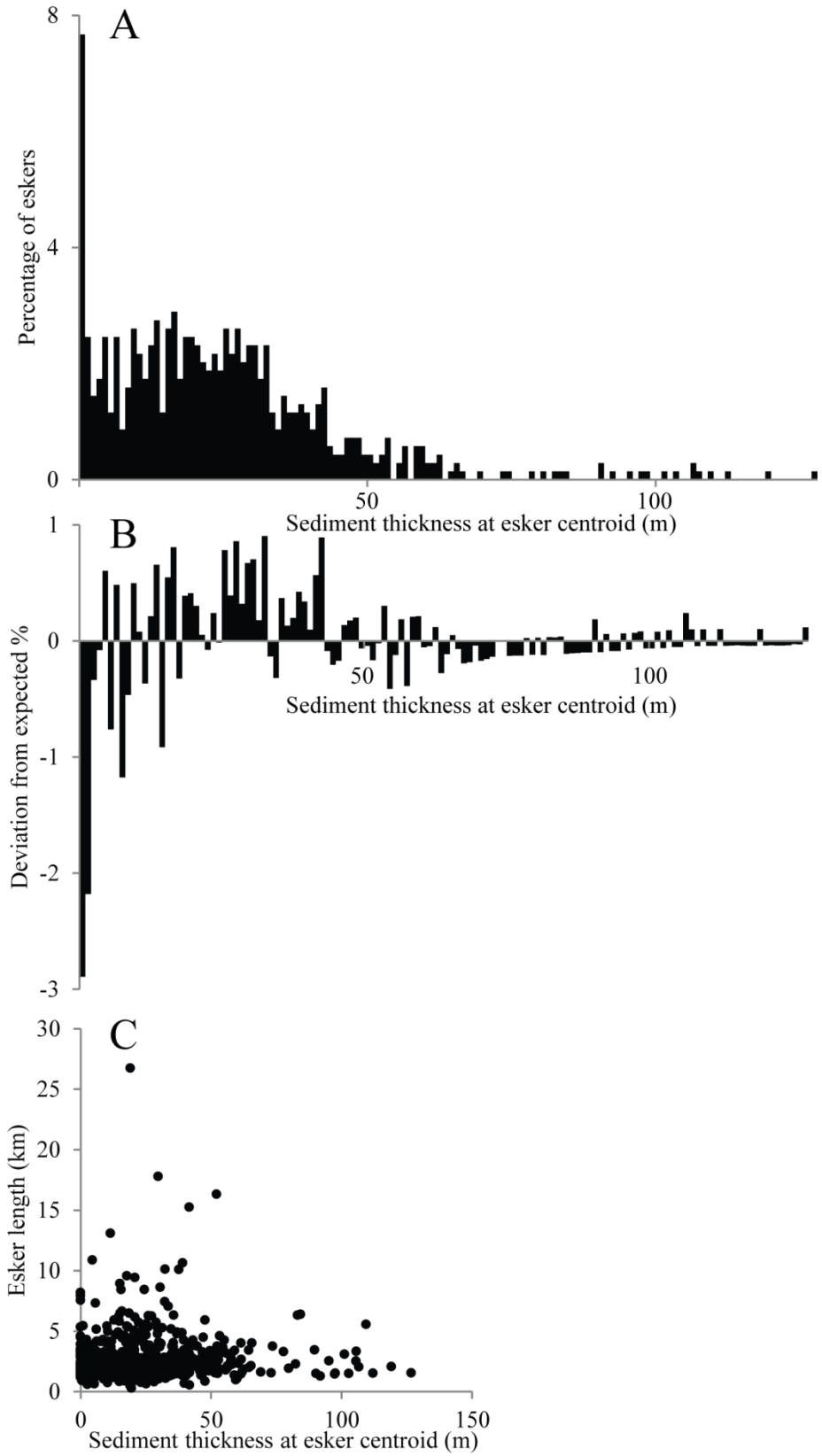

Figure 6.12. Comparison of esker distribution and length with substrate thickness in south and central Alberta. A) Distribution of eskers over different sediment thicknesses. B) The deviation from the expected percentage of eskers overlying different sediment thicknesses (1 m bins), based on the percentage of total area covered by sediment of each thickness. C) Sediment thickness at esker centroid plotted against esker length for all 691 eskers.

6.4.3 Hydraulic conductivity

Measurements of esker spacing over different substrate types do not indicate any preference for higher or lower esker spacing over different surficial or bedrock geological units (Figure 6.13). This stark similarity in the distribution of spacing values suggests that esker spacing is not primarily controlled by the nature of the substrate. Applying a first-order quantification of hydraulic conductivity to each type of substrate confirms that the observations do not conform to the predictions of Boulton *et al.'s* (2009) theory (Figure 6.14).

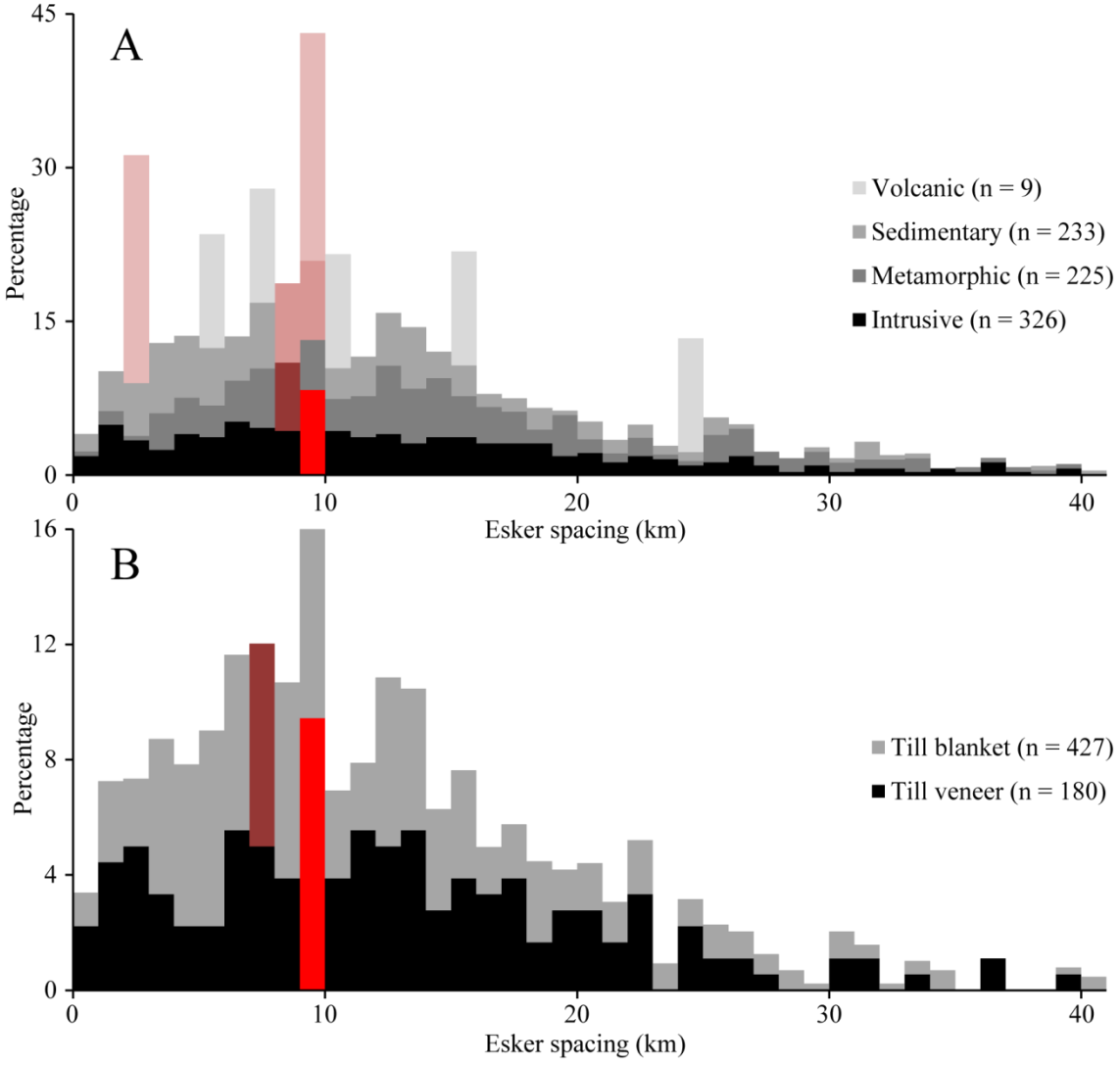

Figure 6.13. Esker spacing (1 km bins) over different (A) geological units and (B) till blankets and till veneers. Shades of red indicate the largest bin in each unit. Spacing measurements of >40 km were recorded but are not shown here for display purposes (no values in this range were >1%).

The simplistic approach to testing the groundwater hypothesis adopted here makes several important assumptions which may have influenced the results. These include the estimates for *K* (hydraulic conductivity), which carry a large range of uncertainty and are prone to local

variations (Bear, 1972; Marine, 1981; Krásný, 1993). Further, replacing *T* (transmissivity) with *K* (hydraulic conductivity) assumes that the substrate is of a uniform 1 m thickness, which is unrealistic. For example, Piotrowski *et al.* (2009) document groundwater flow up to 200 m beneath the bed of the Weichselian ice sheet in the Polish lowland and Boulton *et al.* (2009) describe a superficial zone of high *K* (hydraulic conductivity) in Sweden and Finland which is 100-600 m thick. Finally, the equation presented in Boulton *et al.* (2009) is given in the context of the terminal 50 km of the Fennoscandian Ice Sheet and may not be directly applicable to the Laurentide Ice Sheet. Nevertheless, despite these potential uncertainties, we would still expect our observations to be broadly consistent with theory (i.e. esker spacing should be larger over some rocks than others), especially given the large sample size.

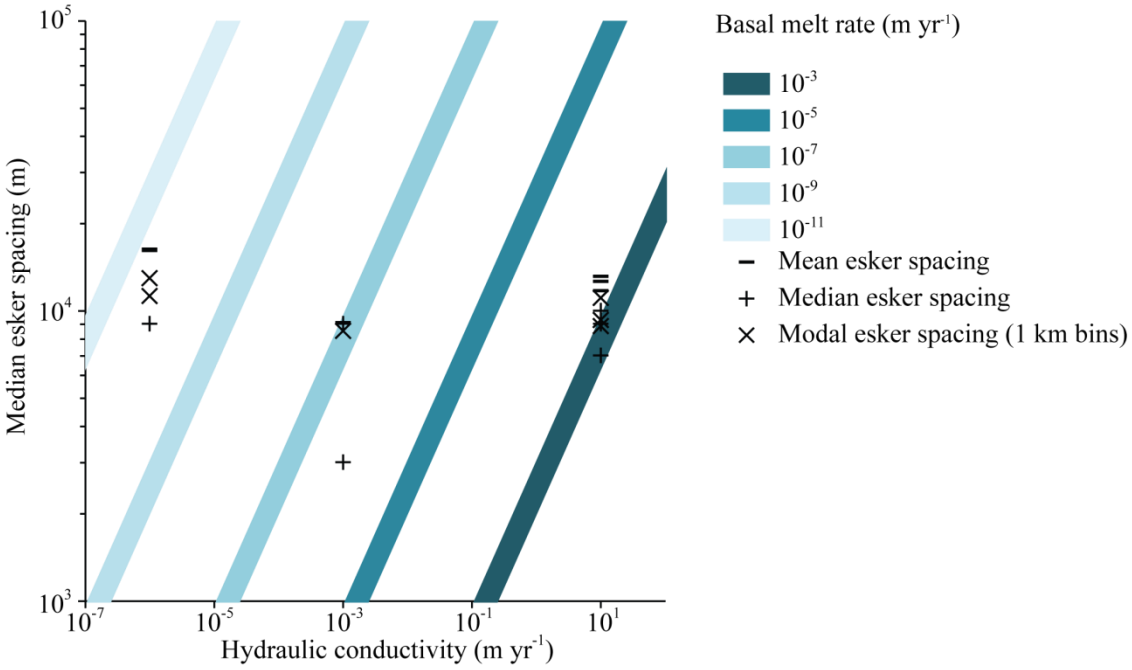

Figure 6.14. Mean, median and modal (1 km bins) esker spacing measurements plotted against estimates of hydraulic conductivity for different substrata. The coloured isolines show the basal melt rates predicted by Boulton's (2009) theory.

The results suggest that basal melt rates calculated using Boulton's (2009) theory, from esker spacing and estimates of *K* (hydraulic conductivity), produce unrealistically small values, with calculated melt rates ranging between 7.47×10^{-11} and 1.24×10^{-3} m yr^{-1} (Figure 6.14). This would appear to contradict the predictions made by Boulton *et al*'s (2009) theory, as a relatively small range of melt rate values would be expected (see Figure 6.6). Numerically modelled subglacial melt rates beneath the Laurentide Ice Sheet at the Last Glacial Maximum (LGM) range from 10^{-4} to 0.6 m yr^{-1}, with typical values over the Canadian Shield of 10^{-2} m yr^{-1} (Lemieux *et al.*, 2008; Figure 6.15). This observation matches the findings of Chapter 5 that supraglacial meltwater may be key to esker formation. Boulton *et al.*'s (2009) model does not

include supraglacial meltwater supply and this may offer one reason that the results here produce an underestimate. The increased frequency of eskers during deglaciation (Chapter 5) could then be explained by increased supraglacial meltwater supply, which modulates esker spacing alongside groundwater, which may have less of an influence than previously thought. The mapped eskers formed after the LGM, when melt rates would have been different (most likely higher), but these values serve as a useful guide as to feasible values for melt rates beneath the Laurentide Ice Sheet and support the suggestion that the values presented in Figure 6.14 are small. Rather, Figure 6.14 suggests that esker spacing is relatively consistent, regardless of the underlying substrate.

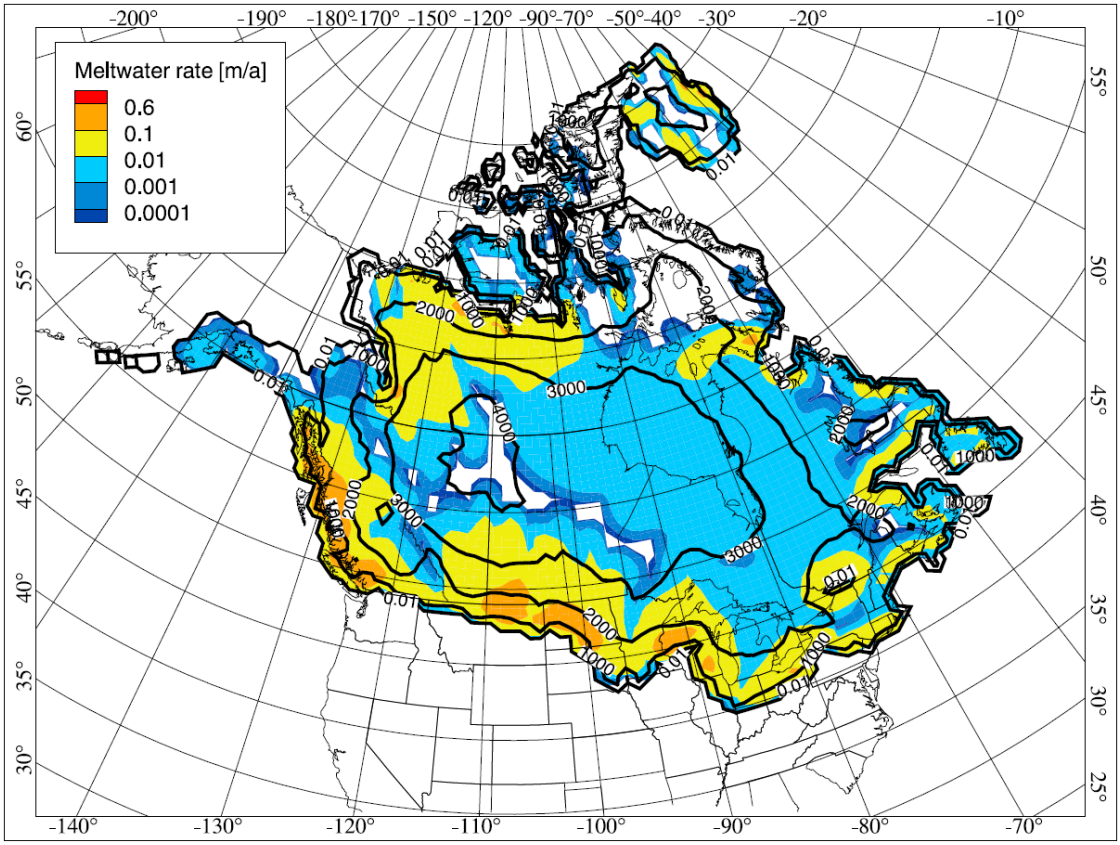

Figure 6.15. LGM subglacial melt rates beneath the north American Ice Sheet Complex (ice elevations shown by black contours) from Lemieux *et al.* (2008).

6.5 Conclusions

We use the database of Canadian eskers presented in Chapter 3 and morphometric data presented in Chapter 4 to provide the first quantification of lithological controls on esker distribution and morphometry. Eskers are found to exhibit a strong preference for formation over the more resistant rocks of the Canadian Shield, as noted by Clark and Walder (1994). Eskers also display a strong preference for formation over till, in particular over 'blankets' of

till, suggesting that the supply of sediment is important for esker formation. In contrast, the specific thickness of the sediment appears to have little influence on esker distribution.

Esker length and sinuosity appear to be unrelated to bedrock or surficial geology, which indicates that they are controlled by other factors. We suggest that ice surface slope is likely to be the primary control, because this is important for determining the position of esker forming conduits and the shape that they maintain.

Esker spacing also appears to be unrelated to bedrock and surficial geology. This is contrary to predictions made by Boulton *et al.* (2009) who suggest that bedrock transmissivity and basal melt rate dictate the spacing between the channels in which eskers form. This may indicate that the supply of meltwater and sediment exerts a stronger influence on esker spacing than the geological properties of the substrate (see Chapter 7 for further evidence of this).

6.6 References

Atkinson, N. & Lyster, S. (2011) Thickness and Distribution of Quaternary and Neogene Sediment in Alberta, Canada. *Alberta Geological Survey*, Digital Data, 2010-0036.

Aylsworth, J. M. & Shilts, W. W. (1989) Bedforms of the Keewatin Ice-Sheet, Canada. *Sedimentary Geology*, 62, 407-428.

Bear, J. (1972) *Dynamics of Fluids in Porous Media*. New York, Elsevier.

Bolduc, A. M. (1992) The formation of eskers based on their morphology, stratigraphy and lithologic composition, Labrador, Canada. *Unpublished Ph.D. thesis, Lehigh University*.

Boulton, G. S. (2010) Drainage pathways beneath ice sheets and their implications for ice sheet form and flow: the example of the British Ice Sheet during the Last Glacial Maximum. *Journal of Quaternary Science*, 25, 483-500.

Boulton, G. S., Caban, P. E. & Van Gijssel, K. (1995) Groundwater flow beneath ice sheets: part I--large scale patterns. *Quaternary Science Reviews*, 14, 545-562.

Boulton, G. S., Dobbie, K. E. & Zatsepin, S. (2001) Sediment deformation beneath glaciers and its coupling to the subglacial hydraulic system. *Quaternary International*, 86, 3-28.

Boulton, G. S., Hagdorn, M., Maillot, P. B. & Zatsepin, S. (2009) Drainage beneath ice sheets: groundwater-channel coupling, and the origin of esker systems from former ice sheets. *Quaternary Science Reviews*, 28, 621-638.

Boulton, G. S., Lunn, R., Vidstrand, P. & Zatsepin, S. (2007a) Subglacial drainage by groundwater-channel coupling, and the origin of esker systems: Part I-glaciological observations. *Quaternary Science Reviews*, 26, 1067-1090.

Boulton, G. S., Lunn, R., Vidstrand, P. & Zatsepin, S. (2007b) Subglacial drainage by groundwater-channel coupling, and the origin of esker systems: part II-theory and simulation of a modern system. *Quaternary Science Reviews*, 26, 1091-1105.

Boulton, G. S., Slot, T., Blessing, K., Glasbergen, P., Leijnse, T. & Vangijssel, K. (1993) Deep circulation of groundwater in overpressured subglacial aquifers and its geological consequences. *Quaternary Science Reviews*, 12, 739-745.

Brennand, T. A. (1994) Macroforms, large bedforms and rhythmic sedimentary sequences in subglacial eskers, south-central Ontario - implications for esker genesis and meltwater regime. *Sedimentary Geology*, 91, 9-55.

Brennand, T. A. (2000) Deglacial meltwater drainage and glaciodynamics: inferences from Laurentide eskers, Canada. *Geomorphology*, 32, 263-293.

Clark, C. D., Evans, D. J. A., Khatwa, A., Bradwell, T., Jordan, C., Marsh, S., Mitchell, W. & Bateman, M. (2004) Map and GIS database of glacial landforms and features related to the last British Ice Sheet. *Boreas*, 33, 359-375.

Clark, P. U. & Walder, J. S. (1994) Subglacial drainage, eskers, and deforming beds beneath the Laurentide and Eurasian ice sheets. *Bulletin of the Geological Society of America*, 106, 304-314.

Fulton, R. J. (1995) Surficial materials of Canada *Geological Survey of Canada, "A" Series Map 1880A*. 1:5,000,000

Greenwood, S. L. & Clark, C. D. (2010) The sensitivity of subglacial bedform size and distribution to substrate lithological control. *Sedimentary Geology*, 232, 130-144.

Hewitt, I. J. (2011) Modelling distributed and channelized subglacial drainage: the spacing of channels. *Journal of Glaciology*, 57, 302-314.

Krásný, J. (1993) Classification of transmissivity magnitude and variation. *Ground Water*, 31, 230-236.

Laske, G. & Masters, A. (1997) A global digital map of sediment thickness. *EOS Transactions of the AGU*, 78, F483.

Lemieux, J. M., Sudicky, E., Peltier, W. & Tarasov, L. (2008) Simulating the impact of glaciations on continental groundwater flow systems: 1. Relevant processes and model formulation. *Journal of Geophysical Research*, 113, F03017.

Marine, I. W. (1981) Comparison of laboratory, in situ, and rock mass measurements of the hydraulic conductivity of metamorphic rock at the Savannah River Plant near Aiken, South Carolina. *Water Resources Research*, 17, 637-640.

Piotrowski, J. A. (1997) Subglacial hydrology in north-western Germany during the last glaciation: groundwater flow, tunnel valleys and hydrological cycles. *Quaternary Science Reviews*, 16, 169-185.

Piotrowski, J. A., Geletneky, J. & Vater, R. (1999) Soft bedded subglacial meltwater channel from the Welzow Süd opencast lignite mine, Lower Lusatia, eastern Germany. *Boreas*, 28, 363-374.

Piotrowski, J. A., Hermanowski, P. & Piechota, A. M. (2009) Meltwater discharge through the subglacial bed and its land-forming consequences from numerical experiments in the

Polish lowland during the last glaciation. *Earth Surface Processes and Landforms*, 34, 481-492.

Shetsen, I. (1987) Quaternary Geology, Southern Alberta. Alberta Research Council. 1:500,000

Shetsen, I. (1990) Quaternary Geology, Central Alberta. Alberta Research Council. 1:500,000

Shilts, W. W. (1984) Esker sedimentation models, Deep Rose Lake map area, District of Keewatin. *Geological Survey of Canada, Paper*, 84-1B, 217-222.

Shreve, R. L. (1972) Movement of water in glaciers. *Journal of Glaciology*, 11, 205-214.

St-Onge, D. A. (1984) Surficial deposits of the Redrock Lake area, District of Mackenzie. *Current research: part A. Geological Survey of Canada Paper*, 84-01A, 271-278.

Storrar, R. D., Stokes, C. R. & Evans, D. J. A. (2013) A map of Canadian eskers from Landsat satellite imagery. *Journal of Maps*, 9, 456-473.

Utting, D. J., Ward, B. C. & Little, E. C. (2009) Genesis of hummocks in glaciofluvial corridors near the Keewatin Ice Divide, Canada. *Boreas*, 38, 471-481.

Walder, J. S. & Fowler, A. (1994) Channelized subglacial drainage over a deformable bed. *Journal of Glaciology*, 40, 3-15.

Wheeler, J. O., Hoffman, P. F., Card, K. D., Davidson, A., Sanford, B. V., Okulitch, A. V. & Roest, W. R. (1996) Geological map of Canada. *Geological Survey of canada, map 1860A*.

Chapter 7 Controls on the formation of complex esker systems at decadal timescales, Breiðamerkurjökull, SE Iceland

Storrar, R.D., Evans, D.J.A. & Stokes, C.R. (in review) Controls on the formation of complex esker systems at decadal timescales, Breiðamerkurjökull, SE Iceland. *Earth Surface Processes and Landforms.*

Abstract

Eskers are mapped on the Breiðamerkurjökull foreland for eight time slices between 1945 and 2007, from high resolution (~50 cm) aerial photography, permitting their long term morphological evolution to be analysed at high resolution. Eskers have increased in abundance since 1945 as the ice margin retreated, revealing a total length of 90 km of both simple and highly complex systems by 2007. By comparing the eskers at different time steps we reveal the evolution of two types of esker complex and simpler single-ridge eskers. We term the two types of esker complex *topographically constrained* and *esker fan.* The formation of esker complexes is a function of a large sediment supply and sufficiently small drainage channels, which results in the choking of tunnels and the concomitant creation of multiple distributaries. The high sediment concentrations in some ice-walled tunnels at Breiðamerkurjökull are primarily derived from large medial moraines through which englacial meltwater drainage is directed. The planform morphology of esker complexes resembles a fan shape unless they are impeded by topography. Small eskers form within a single melt season, while larger eskers may take several years to emerge. Large esker complexes may take several decades to form if they are contained within ice buried beneath outwash. These results may be used to better understand the processes surrounding esker formation in a variety of geographical settings, enabling a more detailed understanding of the operation of meltwater drainage systems in sub-marginal zones beneath glaciers and ice sheets.

7.1 Introduction

Eskers are straight-to-sinuous ridges of glaciofluvial sand and gravel, formed in ice-walled meltwater channels (Warren & Ashley, 1994). They are widely preserved on the beds of palaeo-ice sheets (Chapter 3; Clark & Walder, 1994; Clark *et al.*, 2004), reflecting the configuration of meltwater channels, and can be seen melting out of contemporary glacier termini (e.g. Lewis, 1949; Stokes, 1958; Price, 1966;1969; Gustavson & Boothroyd, 1987; Syverson *et al.*, 1994; Huddart *et al.*, 1999; Burke *et al.*, 2010). These properties make eskers an invaluable source of

information on the nature of meltwater flow within and beneath past and present glaciers and ice sheets (e.g. Chapter 1; Chapter 2; Brennand, 2000), where process observations are otherwise difficult or impossible to make. Indeed, ice dynamics are strongly influenced by the drainage structure beneath glaciers and ice sheets (e.g. Nienow *et al.*, 1998; Boulton *et al.*, 2001; Bartholomew *et al.*, 2010; Hewitt, 2013), but there remain some important gaps in our understanding. For example, observations of meltwater interactions with ice dynamics typically cover, at most, a season or just a few years, so our understanding of their long-term effects is limited. Therefore, the evolution of esker systems can provide valuable insights into meltwater and glacier dynamics over longer timescales.

Whilst links between eskers and glacial meltwater drainage systems have been the focus of previous research (e.g. Clark & Walder, 1994; Brennand, 2000; Boulton *et al.*, 2009), several problems must be addressed before observations on eskers on palaeo-ice sheet beds and valley glacier forelands can be extrapolated to make inferences about meltwater behaviour beneath both contemporary and ancient ice masses. This paper focuses on three of these problems:

What controls the morphology of simple and complex esker systems?

The varying morphology of esker systems (e.g. Sections 2.3 and 2.5; Figure 7.1) is directly related to the controls on esker formation (e.g. sediment supply, flow magnitude, topographic constraints: see Section 2.6 for a review) and is thus indicative of the conditions in which the esker formed; important information when using eskers to reconstruct former meltwater behaviour. Esker morphology is highly variable and eskers can comprise simple systems of single, long ridges which occur in relative isolation (e.g. Shilts, 1984; Aylsworth & Shilts, 1989) as well as what we term esker complexes: systems of anastomosing ridges and esker-fan complexes which contain numerous branching tributaries and distributaries (e.g. Price, 1966; Gorrell & Shaw, 1991; Plouffe, 1991; Margold *et al.*, 2011). Whilst these different systems are frequently described and often occur together, the factors which control the morphology of esker systems have received relatively little attention.

How long does it take to form eskers?

Little is known about how quickly eskers form (see Section 2.4.3.1), a subject which is fundamentally important when using eskers to understand the drainage structure of ice masses. Sedimentological observations have been used to suggest that eskers form quickly and record a snapshot of the drainage system in time, forming synchronously in large conduits (e.g. Brennand, 1994;2000; Burke *et al.*, 2010). Others have suggested that eskers predominantly form time-transgressively over a longer period, at a retreating ice margin (e.g. Banerjee & McDonald, 1975; Hebrand & Åmark, 1989). Limited observations of eskers forming at modern glacier snouts also provide support for these different explanations (Price, 1966;1969; Howarth, 1971; Huddart *et al.*, 1999; Evans & Twigg, 2002; Burke *et al.*, 2010), but more data are

required to gain a better understanding of the spatial and temporal operation of each process-form scenario.

How do esker systems evolve through time?

Eskers at the Casement Glacier, Alaska and Breiðamerkurjökull, Iceland (Price, 1966;1969; Howarth, 1971; Evans & Twigg, 2002) have been mapped from aerial photographs from different years to provide the first assessments of the temporal evolution of eskers and esker systems over several decades. Eskers are seen to melt directly out of glacier snouts and are also seen to emerge after several years from wasting outwash deposits, suggesting a more complex origin than simple subglacial tunnel infilling (e.g. Shreve, 1985). Notably, Price (1966;1969), Howarth (1971) and Evans & Twigg (2002) represent the only published observations of esker evolution over several years, highlighting the lack of contemporary examples of esker formation for palaeoglaciological reconstruction.

Few papers report on eskers in the process of formation and most eskers forming beneath present-day glaciers are relatively small, occur in isolation, and are likely controlled by drainage beneath glaciers which are heavily constrained by topography (e.g. Jewtuchowicz, 1965; Price, 1966), unlike many of the eskers preserved on palaeo-ice sheet beds. A limited number of papers have described eskers forming in larger systems, comprising two or more lobes (e.g. Gustavson & Boothroyd, 1987; Huddart *et al.*, 1999), which are more similar to former ice sheets.

This paper presents the first high resolution mapping of the evolution of simple and complex eskers systems at Breiðamerkurjökull, Iceland. We build on the legacy of esker research at Breiðamerkurjökull and utilise new mapping of eskers at high resolution using aerial photographs spanning the period 1945 – 2007, augmented by field observations. This allows detailed insights into the processes controlling the morphology, formation and evolution of simple and complex eskers at one of the few glaciers where large esker systems can be observed in the process of formation, and snout morphology is more analogous to palaeo-ice sheet settings than most previous studies (Evans & Twigg, 2002; Boulton *et al.*, 2007a).

7.2 Study area and a brief summary of previous work

Breiðamerkurjökull is a large (~13.5 km wide) composite glacier comprising four lobes, separated by three medial moraines. It drains part of the Vatnajökull ice cap, in south-east Iceland (Figure 7.2) and has a history of surging at its eastern flow unit (Björnsson *et al.*, 2003). The glacier retreated approximately 5 km from its Neoglacial maximum position in 1890 (Figure 7.2), revealing a foreland with a complex glacial geomorphology (Breiðamerkursandur), covering approximately 78.3 km^2 by 2007. The substrate comprises bedrock and unlithified sediments (Boulton, 1987, Evans & Twigg, 2002), which are at least 120 m thick in places

(Boulton *et al.*, 1982). Surficial sediments often comprise overridden outwash fans, which tend to have steep ice-contact faces and dip away from the glacier, producing inset overdeepenings (Evans & Twigg, 2002).

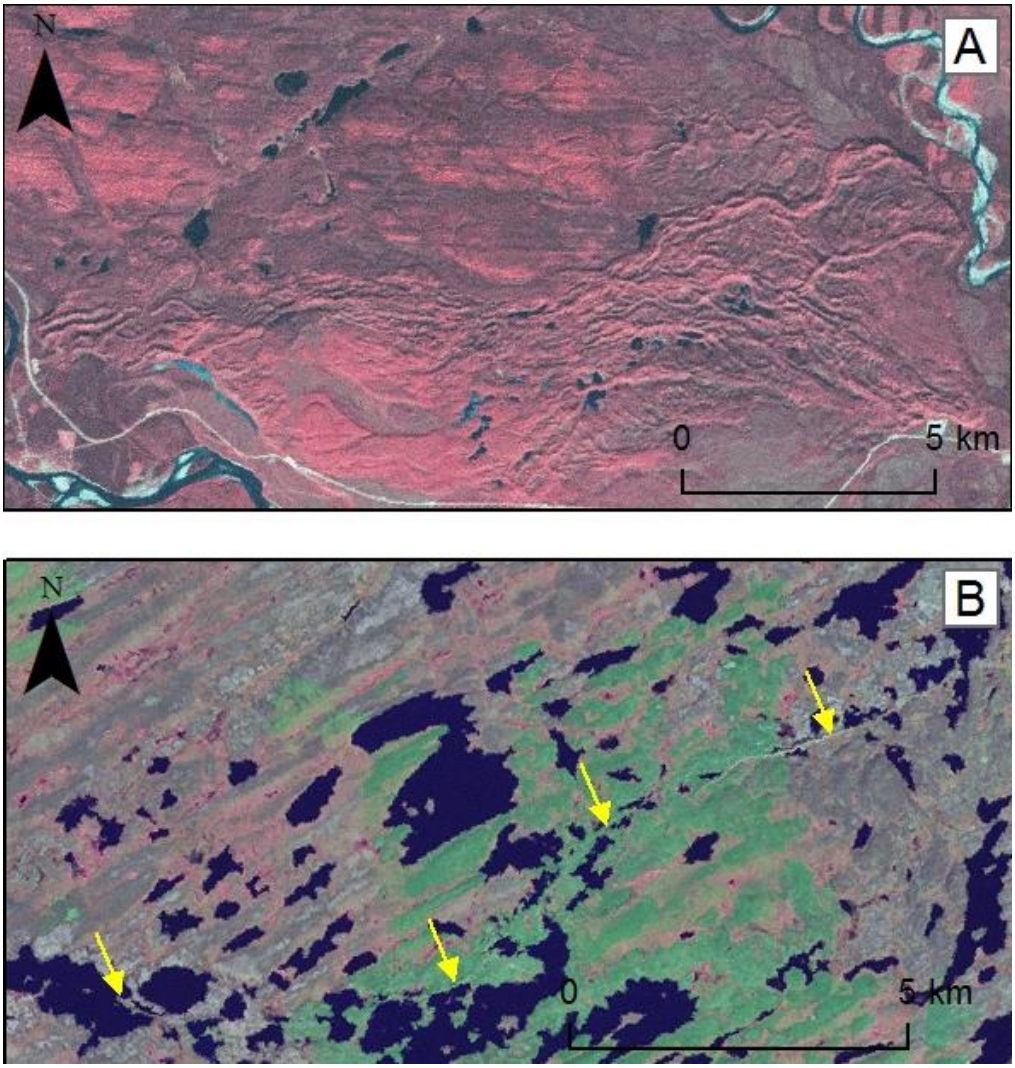

Figure 7.1 Landsat images of different esker morphologies in Canada. A) Complex esker morphology in northern British Columbia, down-ice of the Cassiar Mountains (see Margold *et al.*, 2013). B) Simple, single ridge esker morphology in Nunavut.

Maps of the glacial geomorphology at Breiðamerkurjökull, based on field observations and aerial photography, were produced at a scale of 1:30,000 for the years 1945 (Howarth & Welch, 1969a), 1965 (Howarth & Welch, 1969b) and 1998 (Evans & Twigg, 2000). Seminal papers by Price and Howarth (Howarth, 1968; Howarth & Price, 1969; Price, 1969; Price & Howarth, 1970; Howarth, 1971; Price, 1971;1982) document the evolution of complex glacial landforms using field and photogrammetric techniques, and provide measurements of the downwastage of eskers from the melting of buried ice. Evans & Twigg (2002) used aerial photographs from

1945, 1965 and 1998 as well as field observations to review the glacial geomorphology of Breiðamerkurjökull and define the active, temperate glacial landsystem. In particular, they note the historical evolution of large areas of pitted sandar, which evolved into complex esker networks by 1998 and are discussed further below. We build on and extend this work by mapping eskers in an unprecedented level of detail, which allows us to present a detailed picture of the complexities which underlie the origin of the complex esker systems at Breiðamerkurjökull and explore what controls this complexity.

Boulton & Hindmarsh (1987) detailed the subglacial deformation of till beneath Breiðamerkurjökull and, more recently, Boulton and co-workers have developed a theory of groundwater controlled hydraulic spacing of esker tunnels (Boulton *et al.*, 2001; Boulton *et al.*, 2007a;b; Boulton *et al.*, 2009). They suggest that the hydraulic properties of the substrate dictate the spacing of channels (and eskers) by scavenging meltwater into groundwater until it becomes saturated: at this point, meltwater drains in subglacial channels, which become optimally spaced to reflect the balance between substrate transmissivity and the supply of meltwater. This theory of groundwater controlled hydraulic spacing is discussed in Section 7.5.4, in light of our more detailed mapping of the esker systems.

7.3 Methods

Eight sets of aerial photographs (30 – 380 cm resolution; e.g. Figure 7.3) of the study area, covering approximately eight-yearly intervals from 1945 to 2007/9, were used to provide a detailed account of esker evolution through time (Table 1). The photographs were orthorectified and georeferenced, based on control points used in the 1998 aerial photographs and subsequent geomorphological map (Evans & Twigg, 2000;2002). Eskers, lakes, rivers and ice margins were identified from stereo pairs of the photographs using a stereoscope and were then digitised as shapefiles in ArcGIS 10. Eskers were identified as pronounced straight-to-sinuous ridges, predominantly oriented orthogonal to the ice margin (thus distinguishing them from morphologically similar push moraines in aerial photographs). In a small number of instances, eskers were oriented parallel to the ice margin and were identified by their continuation with other eskers. In places, eskers are difficult to differentiate from the ridges surrounding pits in outwash. In such cases, a rule of thumb was applied such that eskers were identified when ridges continued for longer than one edge of a depression.

The resolution, sharpness and azimuth of the photographs vary between the different sets due to different camera parameters, flying heights, weather conditions and time of the day/year. A result of this is that eskers are more easily resolved in some images than others. Table 7.1 describes the main characteristics of each set of photographs and provides an indication of which are the most useful. Most photographs provided sufficient clarity to resolve eskers in a high (and comparable) level of detail. Moreover, field observations and the highest resolution

photographs suggest that most eskers in the study area are greater than 2 m in width, within the resolvable resolution of all but the 1945 photographs. The resolution and, to a lesser extent, the sharpness of the 1945 photographs are poorer than the other photographs. However, they were still used for the analysis because they are the oldest set of photographs and are invaluable for understanding the changes in the area at a key time. Fewer eskers existed over a smaller area in 1945 and so the impacts on this study of any errors associated with identifying eskers on the 1945 photographs is likely to be small. Aerial photograph interpretation was supported by observations and ground truthing in the field, which were carried out in September 2011 and September 2012.

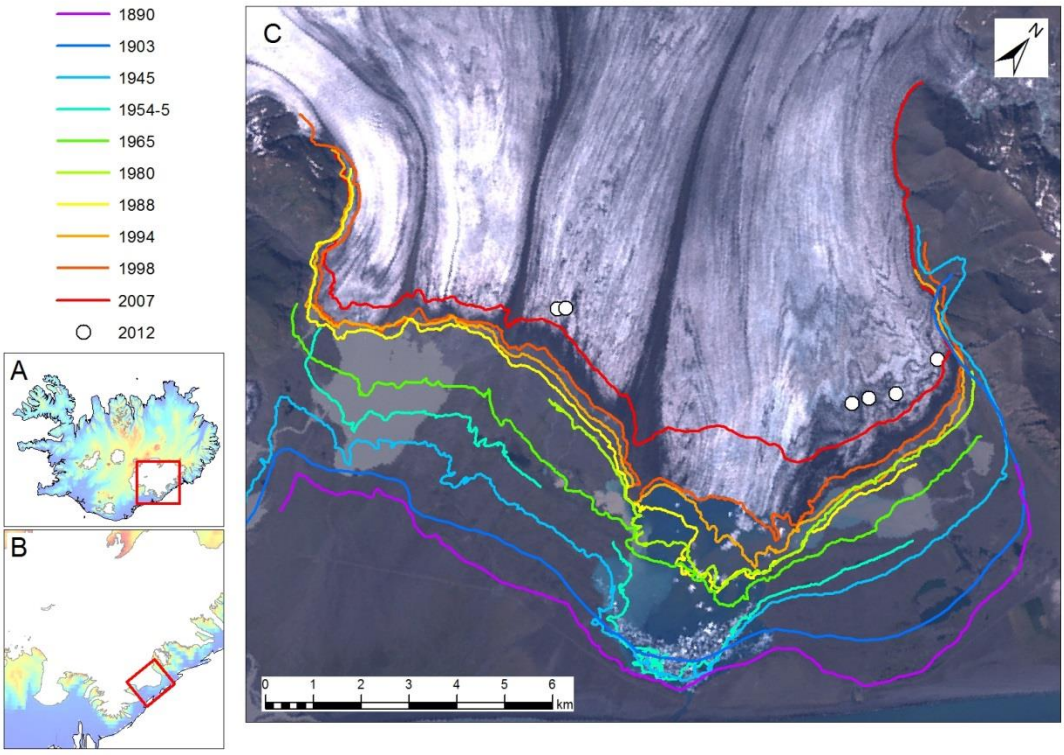

Figure 7.2. Location map. A) Location of the Vatnajökull Ice Cap in Iceland. The red box indicates the location of B. B) Location of Breiðamerkurjökull within Vatnajökull. The red box indicates the location of C. C) 1999 Landsat image of Breiðamerkurjökull with margin positions from 1890 (neoglacial maximum) to 2012. Note that some margins have gaps relating to the absence of aerial photograph coverage, and the 2012 data are points measured by handheld GPS in the field. Breiðamerkurjökull was confluent with Fjallsjökull (to the southwest) until some point between 1945 and 1954. The 1890 margin is from Price (1980) and the 1903 margin is from Price (1982).

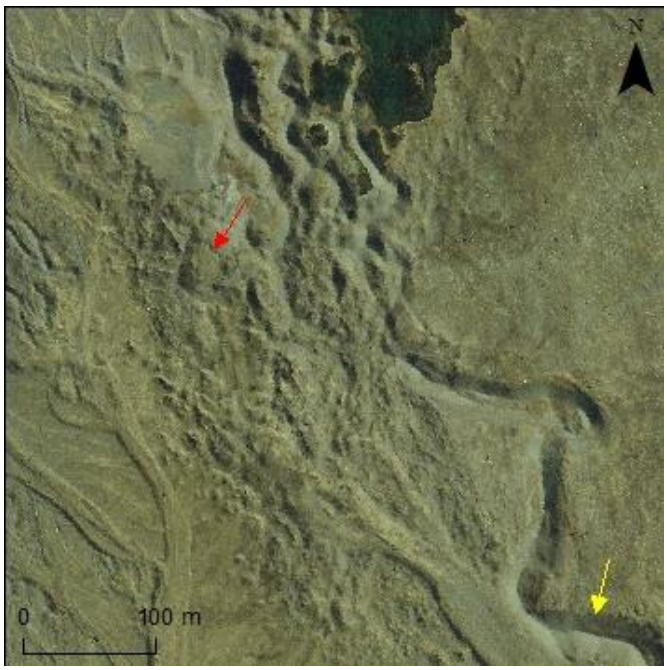

Figure 7.3. Example of the resolution of the aerial photographs from 2007, showing a main esker ridge ~30 m wide in the bottom right corner (yellow arrow) and smaller ridges, discernible at just 2 m wide (red arrow) in the centre of the image. Note the complex morphology of the eskers at this location. Copyright NERC ARSF aerial photograph 2007.

7.4 Results

7.4.1 Overview of esker systems at Breiðamerkurjökull

Mapping from eight different time slices reveals a total of 5,326 esker ridges, with a cumulative length of 324 km. Perhaps unsurprisingly, the most complex pattern of eskers is provided by the 2007/9 photographs (Figure 7.4), when 2,395 eskers (total length: 89 km) were mapped, although a handful of eskers which formed previously had since disappeared (either from submergence beneath lakes, melting of ice cores, or other erosional processes). In general, most of the eskers occupy two areas, either side of Jökulsarlon. The eskers to the west of Jökulsarlon comprise what we term 'Major Esker Systems' (MES) 1 and 2 (discussed below; see Section 7.4) and several smaller isolated suites of eskers. The largest eskers in the western sector are aligned with the medial moraine Mavabyggdarond (Figure 7.6). A smaller suite of eskers near to the south-west shore of Jökulsarlon is aligned with the largest medial moraine (Esjufjallarond). Several smaller eskers, including some melting out of the ice margin in 2007, occur in this area which do not line up with medial moraines. To the east of Jökulsarlon, MES3 is associated with the lake Stemmulon and appears to continue on the north-eastern shore of Jökulsarlon. Further south, several smaller sinuous eskers occur in narrow corridors (Figure 7.7A). Previous work (e.g. Price, 1969; Evans & Twigg, 2002) and field observations show that many eskers across the foreland trend upslope. Some smaller eskers near to MES1 terminate at, or are diverted by, large boulders.

Table 7.1. Aerial photograph properties.

Date	Coverage	Number of photographs	Approx. azimuth	Approx. resolution	Sharpness
1945	Complete	15	190	380 c m	v. grainy
15/9/1954	Partial	6	190		excellent
14/9/1955		3	210	39 cm	
24/8/1965	Complete	42	315	65 cm	excellent
18/9/1980	Partial	6	250	52 cm	v. good
28/8/1988	Complete	14	270	56 cm	grainy
9/8/1994	Complete	15	130	55 cm	v. grainy
22/8/1998	Complete	36	100	125 cm	v. good
3-4/7/2007	Complete	113	270	30 & 45 cm	excellent
9/6/2009		157	180	30 cm	

7.4.2 Major esker system 1 (MES1)

MES1 was revealed primarily during three of the time steps shown in Figure 7.5 (1903-1945, 1945-1954 and 1954-1965). MES1 occupies a trough (see Figure 7.5) which descends from the proximal part of the system, before reaching a large outwash fan approximately 15 m tall, where it abruptly terminates. A total of 639 eskers, representing a total length of 21.9 km, were mapped within MES 1 from the 2007 photographs. We now describe the eskers in each of the above time steps.

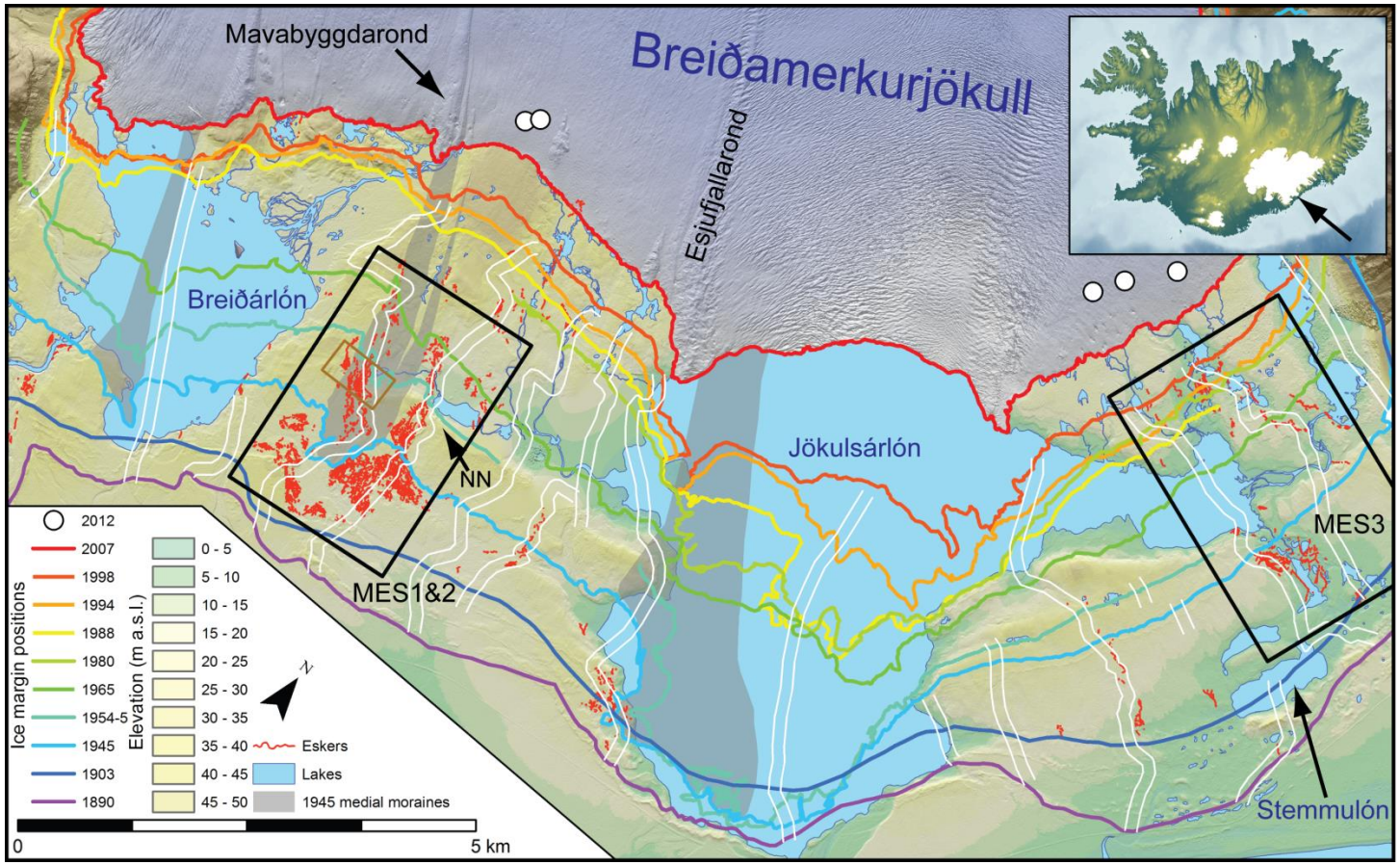

Figure 7.4. Location map showing eskers digitized from 2007/9 aerial photographs and locations mentioned in the text. Historic ice margin positions are from previous maps (Price 1980; 1982) and aerial photograph mapping and point measurements taken by GPS in 2012. Note that some margins have gaps relating to the absence of aerial photograph coverage. Breiðamerkurjökull was confluent with Fjallsjökull (to the southwest) until some point between 1945 and 1954. The parallel white lines indicate the meltwater drainage axes proposed by Boulton *et al.* (2007a). NN refers to Nygrædnakvis. Areas shown in Figure 7.5 are indicated by black boxes. The area shown in Figure 7.6 corresponds to the black box labelled MES1&2.

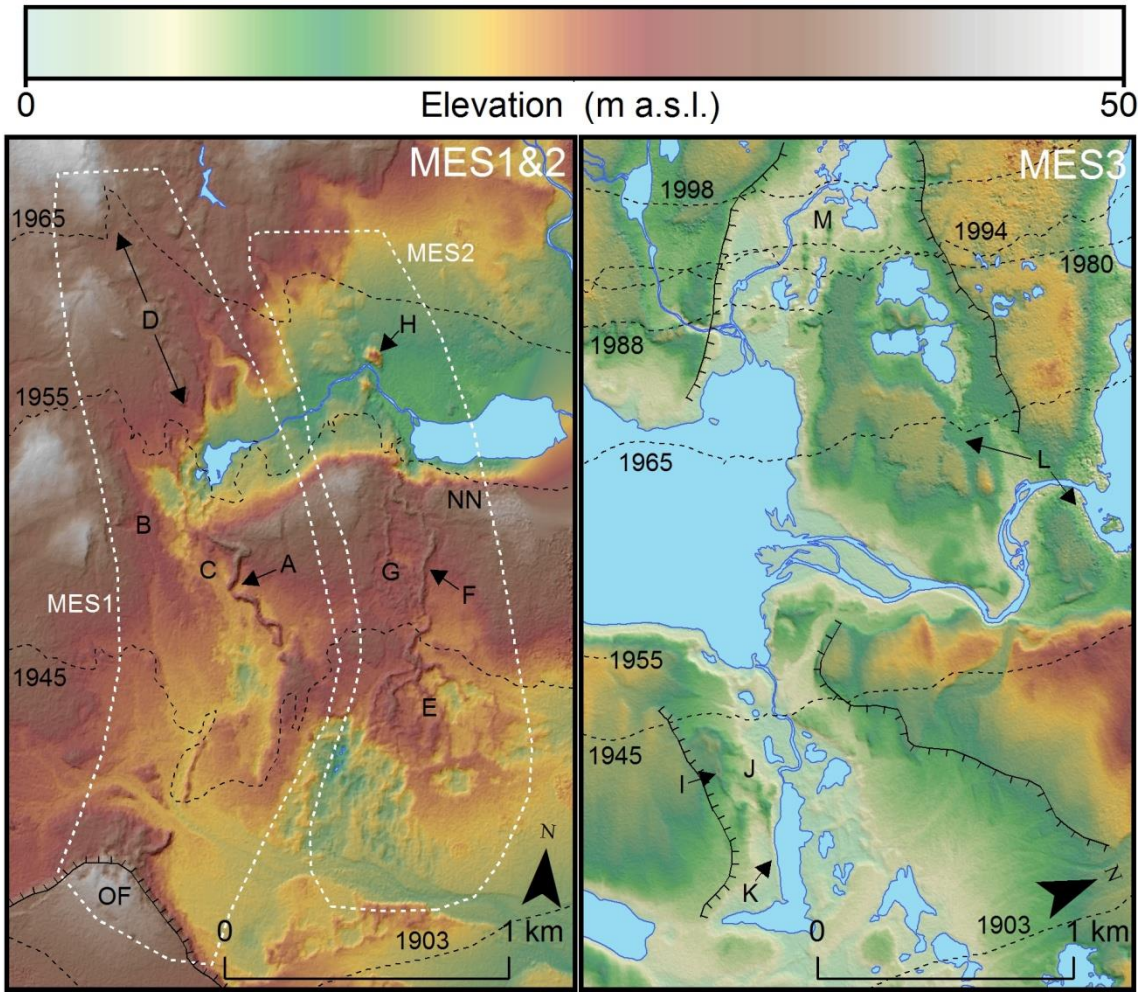

Figure 7.5. Detailed topography (in 2007) and ice margin positions (dashed lines) in MES1,2 and 3 (see Figure 7.4 for locations). Locations referred to in the text are given by letters. The location of Figure 7.3 corresponds to C.

1903 to 1945:

The distal section of MES1 emerged between 1903 and 1945. In 1945, a prominent esker (which was subsequently 20 m wide by 2007) was melting out of the medial moraine Mavabyggdarond. This esker is abruptly dissected by a large meltwater channel, which was active in 1945, and then continues for a further 180 m before terminating at a large outwash fan (OF in Figure 7.5). There are many small, complex anabranching tributary eskers to the west of the main esker but few to the east. Where the trunk esker reaches the fan, several smaller eskers diverge from the main ridge, mostly trending parallel to the edge of the outwash fan to the east and displaying an anastomosing morphology, with increasingly smaller tributaries (Figure 7.7B).

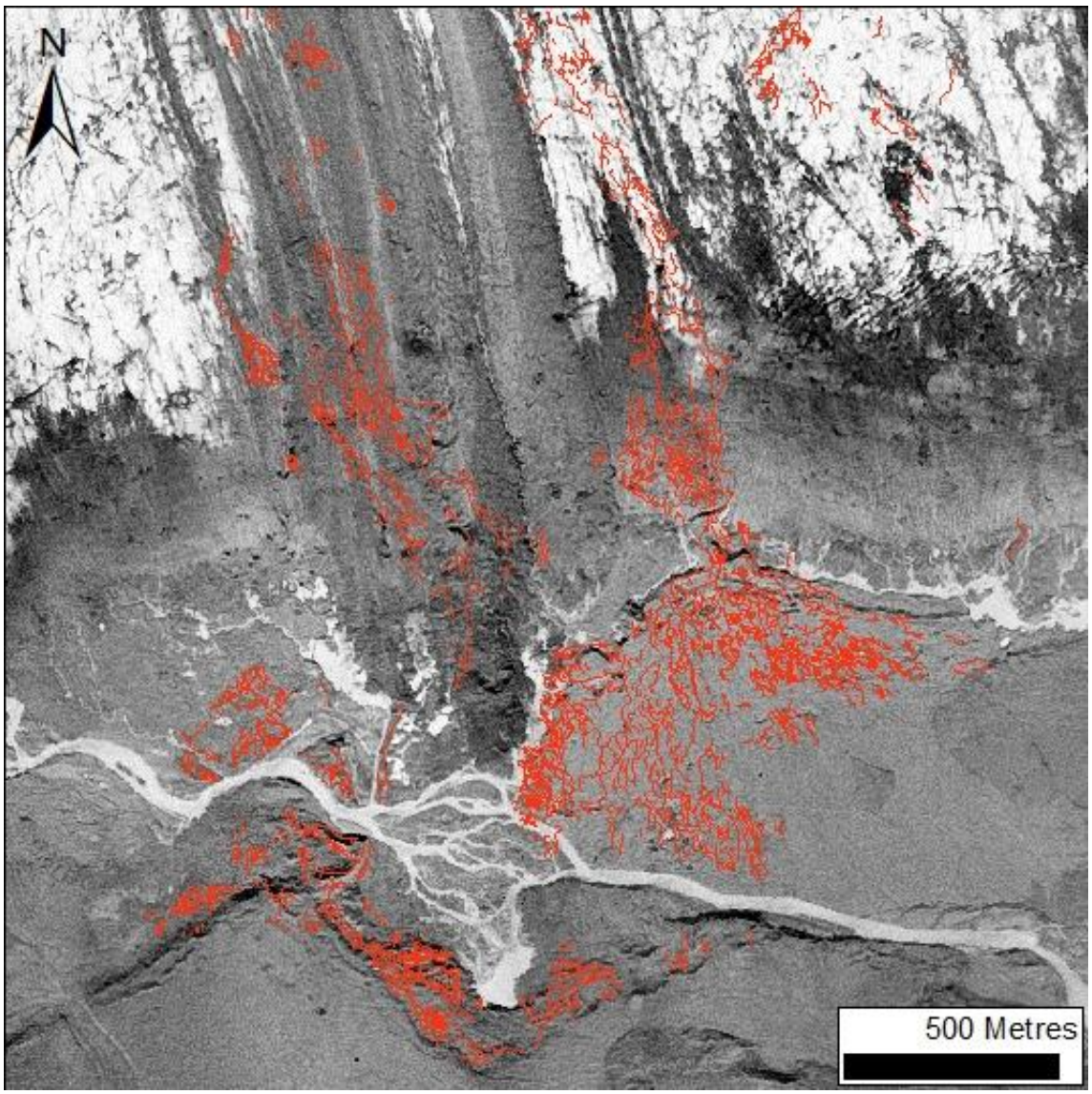

Figure 7.6. Eskers of MES1 (left) and 2 (right) digitised from 2007 photographs and overlain on 1945 photograph. Note that the esker systems appear to have originated from beneath and from either side of the medial moraine (Mavabyggdarond). See Figure 7.4 for location.

1945 to 1954:

The central section of MES1 comprises several distinct esker ridges 10 – 20 m wide. In the eastern portion of this sector, the eskers are large (~50 m wide in 1954; ~30 m wide by 2007) and evolved from being broad- to sharp-crested between 1954 and 2007 (A in Figure 7.5). To the west, eskers are smaller and display a more round-crested profile in 2007, having melted out from what was a pitted fan surface in 1954. The smaller ridges form a complex anastomosing pattern (Figure 7.3), with eskers ranging from ~1.5 to 15 m wide. There is also a downstream-branching esker network to the west of the system, where a 12 m wide esker branches down-ice into multiple smaller (1-5 m wide) distributaries (B in Figure 7.5). At its distal end, the main esker bifurcates and re-joins 90 m down flow before stopping abruptly. To the east of this esker,

several small eskers branch from and re-join the main ridge. To the west, the morphology is more complex, with many anastomosing eskers on the order of 1-6 m wide (C in Figure 7.5).

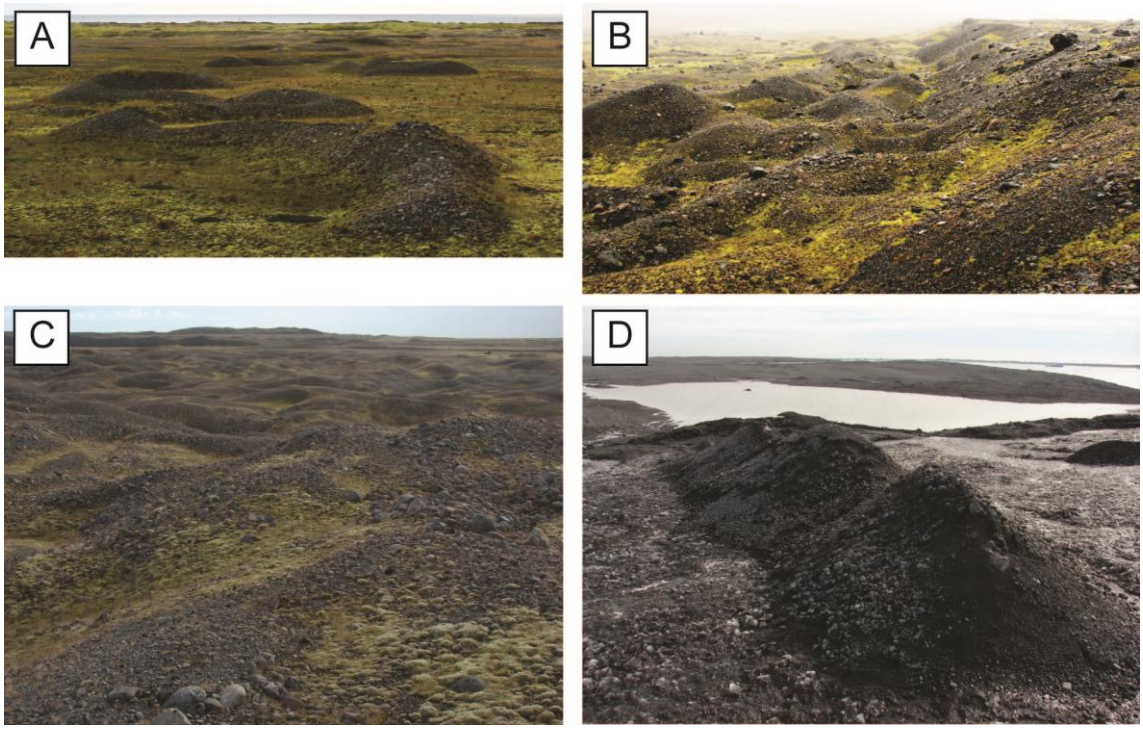

Figure 7.7. A) A 'zig-zag' esker west of Stemmulon. B) View to the south-east, of eskers at the distal end of MES1, diverted by the large outwash fan (to the right of the image). Note the preponderance of tributaries branching from the main ridge in the foreground and in the distance. C) Complex morphology of eskers in MES2. D) An esker on the glacier surface, close the eastern snout margin.

1954 to 1965:

At its proximal end, MES1 was melting out of the ice margin in 1965 (Figure 7.8) and formed a prominent ridge ~35 m wide. By 2007, the prominent esker had degenerated into a series of small, fragmentary ridges (D in Figure 7.5; Figure 7.8). Some fragmented but well defined eskers extend past the 1965 margin and were formed at some point between 1965 and 1980.

7.4.3 Major esker system 2 (MES2)

MES2 is located immediately to the east of MES1 and similarly formed primarily between the three ice margin positions 1903-1945, 1945-1954 and 1954-1965. MES2 initiates in a trough, before climbing up Nygrædnakvis (labelled NN in Figure 7.5), an overridden outwash fan (Evans & Twigg, 2002) approximately 20 m tall, and then it gradually descends to form a large, highly complex esker fan (Figure 7.5; Figure 7.7C). A total of 486 eskers, representing a total

length of 34.0 km in MES2, were mapped from the 2007 aerial photographs, and we now outline the eskers in each of the above time steps.

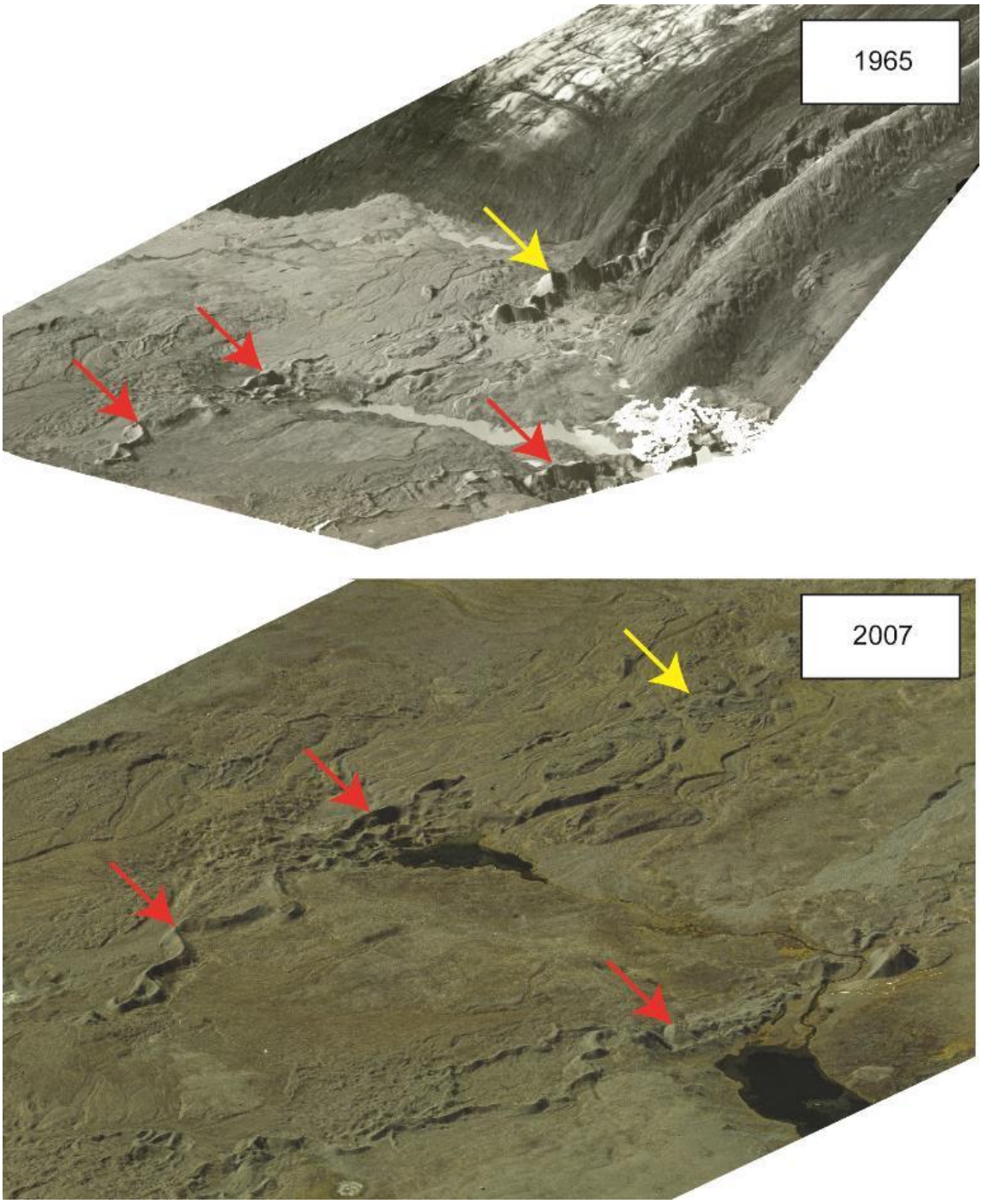

Figure 7.8. 3-D visualisation of MES1 and 2 in 1965 and 2007 (not to scale). Part of MES1 is melting out of the western section of the medial moraine Mavabyggdarond in the 1965 image (yellow arrow). Note that this esker appears to have decreased in size relative to the more distal eskers (red arrows) by 2007.

1903 to 1945:

In 1945, the ice margin was at the apex of the complex esker fan (E in Figure 7.5). Within the fan, there are subsets where eskers form either anastomosing or downstream-branching networks. The fan has undergone significant changes since 1945, evolving from a relatively flat, pitted fan surface to the complex network of eskers apparent in the 2007 images (Figure 7.9).

1945 to 1954:

Between 1945 and 1954, the ice margin retreated from the apex of the esker fan into the overdeepening north of Nygrædnakvis, forming a proglacial lake, which is evident in the 1954 photographs. The 1954 photographs show a continuous esker 18 – 30 m wide which stretches from the fan apex to Nygrædnakvis (F in Figure 7.5). To the west of this esker, a complex system of eskers was emerging from a pitted surface in 1954. By 2007 a coherent network of anastomosing and downstream-branching eskers up to 5 m wide was revealed, including a prominent esker 15 m wide, which was not visible in 1954 (G in Figure 7.5). This esker is connected at each end with the large esker to the east. A large esker up to 40 m wide was emerging from an englacial position and disappearing into the proglacial lake in 1954 and is seen to drape the ice-proximal side of Nygrædnakvis in 2007.

1954 to 1965:

As with MES1, a few small (3-5 m wide) eskers formed between 1965 and 1980 but the proximal end of the system mostly began to emerge before 1965. The most proximal eskers are relatively narrow but are continuous, forming more coherent patterns than eskers formed at a similar time in MES1. Nevertheless, some downstream-branching patterns are observed. Gradually, the eskers become larger as they approach Nygrædnakvis from the north; a conspicuously large, teardrop shaped feature, 110 m long and up to 70 m wide, appears to be a very large esker segment (H in Figure 7.5).

7.4.4 Major esker system 3 (MES3)

MES3 comprises the complex esker system around Stemmulon, with a large main esker sitting on a topographic high (I in Figure 7.5). A complex system of eskers has gradually emerged immediately to the north and east of this esker as lake levels have dropped, following the switch in the east margin drainage from the Stemmulon system to the Jökulsarlon system between 1988 and 1994. The system extends to the present day margin on the north-east side of Jökulsarlon. A total of 275 eskers, representing a total length of 13.4 km in MES3, were mapped from the 2007 aerial photographs. The changing drainage system in this sector of the foreland has also resulted in the disappearance of some eskers, which were present on a small island in Jökulsarlon in 1998 but which now lie beneath lake water level. We now describe three components of the system in detail, which emerged in three intervals, 1903-1945, 1945-1998 and post-1998.

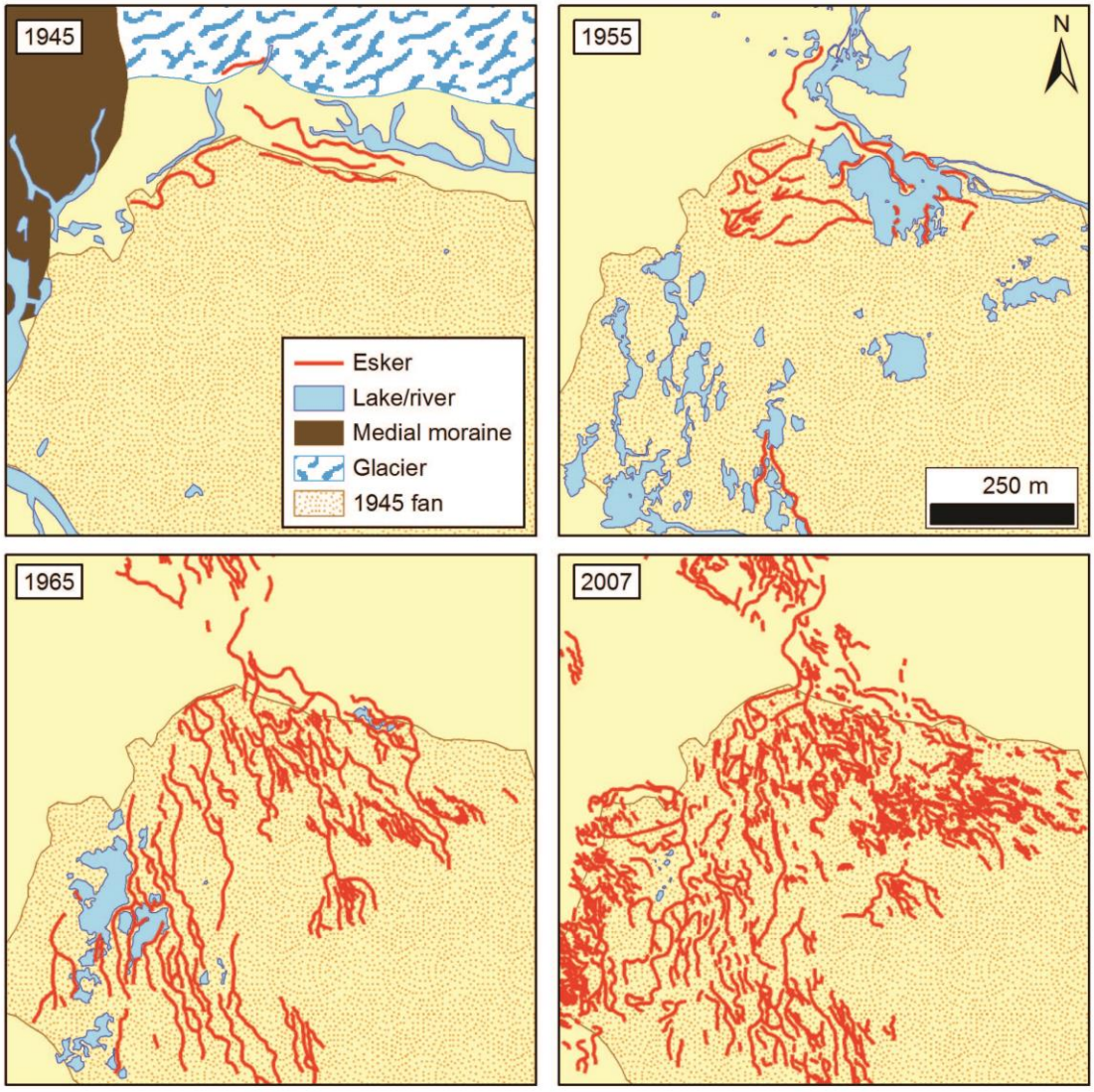

Figure 7.9. Eskers comprising the fan of MES2 mapped from aerial photographs from 1945, 1955, 1965 and 2007. Note the gradual evolution of the eskers from a flat fan with a few eskers in 1945 to a complex fan of prominent esker ridges in 2007.

1903 to 1945:

The main esker ridge (I in Figure 7.5; Howarth's (1971) 'esker 1') was exposed between 1903 and 1945. In 1945, the proximal end of MES3 was melting out of the glacier snout, as two coherent (but fragmented) sinuous ridges. By 2007, the southern part of the system was composed of a main ridge 12 – 15 m wide, with a complex system of smaller (1 – 5 m wide) eskers which branch preferentially to the north (J in Figure 7.5). The main ridge is sinuous and terminates near a large bedrock knob. Immediately in the lee of this knob, a conspicuously straight esker (K in Figure 7.5) runs for 390 m, narrowing from 30 m at its proximal end to approximately 6 m. There is a network of eskers immediately to the north of the main ridge which has a more complex history because it is associated with the Stemmulon lake system,

which drained the eastern part of Breiðamerkurjökull until some point between 1988 and 1994. The esker system gradually emerged (and is still emerging) from the lake as the levels recede.

1945 to 1998:

Between 1945 and 1965, two prominent (up to 11 m wide) zig-zag shaped eskers (L in Figure 7.5) were exposed, with relatively few tributaries. The southernmost of these two eskers continued to be exposed until approximately 1980. Between 1980 and 1988, the margin in this location underwent a readvance/surge of approximately 150 m. After 1988, the margin once again steadily retreated. Between 1980 and 1998, several anastomosing esker networks (M in Figure 7.5) were exposed, as well as a single fragmented ridge.

1998 to 2012:

After 1998, the margin in the north retreated rapidly, ranging from 0.9 to 1.5 km in 14 years. Relatively few eskers were exposed here after 1998 but during fieldwork in 2012, several small eskers were observed emerging on the surface of the glacier near the terminus (Figure 7.7D).

7.4.5 Chronology of esker emergence

Our new mapping reveals the rate of esker emergence over the last ~70 years. In total, 26 eskers were mapped from the 1945 photographs, increasing by almost two orders of magnitude to 2,395 eskers in the 2007/9 photographs. The total length of eskers increased steadily over this time from 4.7 km to 89.0 km, as the glacier retreated. This does not, however, simply indicate that more eskers were melting out of the glacier over the study period because many eskers were revealed some distance in front of the ice margin, several years after the glacier had retreated. The largest systems of eskers emerged between 1903 and 1965 and 89.7% of the total length of all the eskers mapped are located in front of the 1965 margin (i.e. just 62.5% of the overall observed recession). Eskers may be categorised as those which are exposed immediately as they are melted out of the glacier, and those which emerge gradually from the melting of buried ice. The form of eskers may change following retreat if they contain an ice core which subsequently melts out (e.g. Howarth, 1971) or are eroded by other processes.

7.5 Discussion

MES 1 and 2 contain a diverse range of esker patterns in a relatively confined area and, as such, are well suited for exploring the factors which control different esker morphologies. The abundance of eskers in this location may be explained by the availability of large volumes of sediment from the medial moraine Mavabyggdarond, as noted by others (Price, 1969; Evans & Twigg, 2002). We suggest that the availability of large volumes of sediment is also the reason that complex, rather than simple esker morphologies have developed here. Below we set out

depositional models for MES 1 and 2 and use these models to explain in more detail what controls the formation of different esker complexes. We also discuss what may have controlled the morphology of different parts of MES3, which do not align with a large medial moraine and so must have acquired substantial quantities of sediment from elsewhere.

7.5.1 A depositional model for MES1

We interpret MES1 as a *topographically constrained esker complex*. Distributary eskers branch from the main part of the system, but the overall morphology of the esker complex is dictated by the topographic constraint of the large outwash fan (Figure 7.7B). The main trunk esker that feeds the system likely formed as the fan was being prograded, i.e. when the ice margin was at its apex in the 1930s (Boulton, 1986). At this time the fan apex was located within a re-entrant in the glacier snout, where englacial drainage was emerging from an ice-walled tunnel (Figure 7.10). This drainage pattern was likely dictated by pre-existing ice-contact fans and their associated depositional overdeepenings (outwash heads; cf. Boulton, 1987; Kirkbride, 2000), whereby englacial drainage initially bypassed the overdeepening and debouched onto the fan apex in a supraglacial position (cf. Spedding & Evans, 2002; Bennett & Evans, 2012). Hence, once the glacier surface had lowered below the height of the fan apex, englacial meltwater issuing from the glacier snout was no longer able to drain over the fan surface and instead drained through lower elevation (eventually subglacial) tunnels excavated through the snout immediately towards the east (Figure 7.10). This is recorded by the large trunk esker which approaches the fan before splitting into increasingly smaller distributary ridges away from the fan apex. The formation of the complex network of distributaries is a product of high sediment concentrations derived from Mavabyggdarond. High sedimentation rates resulted in the frequent blocking of channels, which formed distributary eskers as meltwater was diverted around the part of the channel that became choked with sediment. Observations in the field indicate that a small number of distributary eskers near to the fan drape its former ice contact face, most likely indicating that they were deposited englacially, which matches observations of surface lowering relating to the melting of buried ice beneath most of MES1 (Price, 1969). Indeed, the fan that was fed by MES1 also contained a considerable amount of buried ice, leading to the formation of the present pitted fan surface (Boulton, 1986). Some eskers in MES1 indicate a subglacial origin, particularly the smaller eskers to the north-west of the fan which frequently terminate at, or diverge past, large boulders. Whilst there is evidence for both subglacial and englacial esker sedimentation in MES1, it is often difficult to discern which process predominated.

7.5.2 A deposition model for MES2

We interpret MES2 as an *esker fan complex*. Similarly to MES1, subglacial or englacial meltwater channels carried a large amount of sediment from Mavabyggdarond to the ice margin, initiating a complex morphology as the sediment overwhelmed the channels to produce multiple distributary eskers. The fan shape suggests that there was no topographic impediment and that the meltwater channels were at atmospheric pressure when they filled with sediment, indicating that they emerged englacially into a network of ice-walled supraglacial channels, similar to an alluvial fan (Figure 7.11). Following the choking of the supraglacial channels with sediment, outwash was aggraded over the snout, burying the sediment filled channels. Active recession of the glacier then followed, resulting in the gradual downwasting of the fan as the buried ice melted out, as supported by measurements of pervasive surface lowering between 1945 and 1965 (Welch & Howarth, 1968) and subsequent evolution of the fan morphology (Figure 7.9). Through time, the feature evolved from a flat fan (1945) to a pitted surface with a few eskers at the proximal end (1955) to more eskers and pitted outwash (1965) and then to a complex network of eskers resembling the shape of the fan by 2007 (Figures 7.7 and 7.9; see also Price, 1969; Evans & Twigg, 2002). This gradual emergence of eskers from ice buried beneath outwash is in concordance with observations of Gustavson & Boothroyd (1987) of some eskers at the Malaspina Glacier, Alaska.

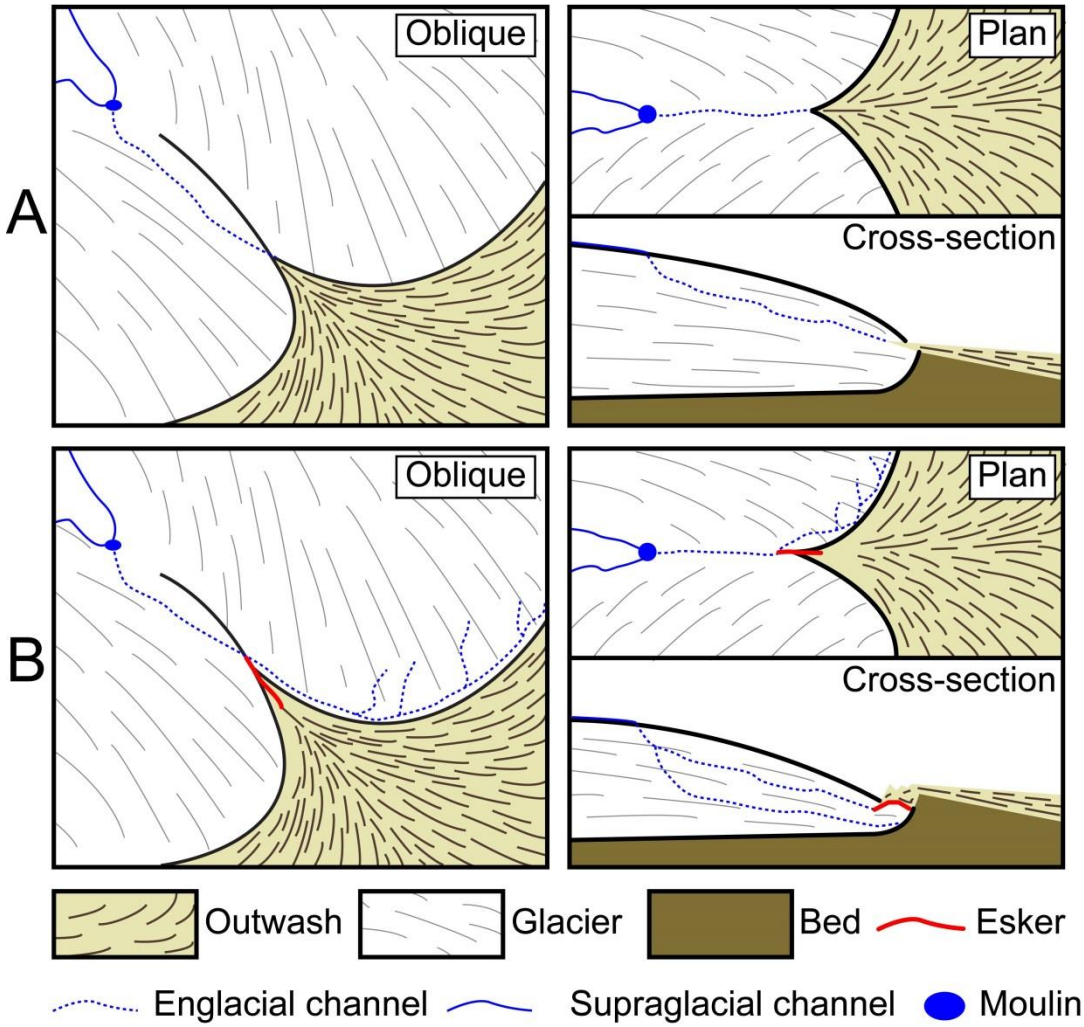

Figure 7.10. Depositional model for a *topographically constrained esker complex.* A) Englacial stream feeds the development of an ice contact fan. B) As the glacier surface lowers during retreat, drainage is impeded by the fan and meltwater is diverted along the apex of the fan. Eskers form where the channels clog with sediment. Not to scale.

7.5.3 A deposition model for MES3

We interpret MES 3 as a subdued *esker fan complex*. The complex morphology of parts of the system and absence of a topographic obstacle suggest that the eskers make up an *esker fan complex*, though it is less clear than MES2 because the occupation of much of the area by lakes over the past 60 years means that the morphology of the esker system is subdued, as parts have been lost through submergence or erosion by meltwater channels. Howarth (1971) produced the first detailed measurements of the main esker ridge in MES3 (the long esker to the south-east in Figure 5B) and noted that between 1945 and 1965 its surface lowered by up to 8 m, indicating the melting out of ice buried beneath the esker. Additionally, the northern edge of the system contained more buried ice. Howarth suggests that deposition took place subglacially but the esker was then melted out proglacially from the sandur. More recently, Evans & Twigg (2002) suggested that a surge mechanism may be responsible for the processes leading to the

development of these eskers, based on observations on their planform, which are similar to zig-zag shaped eskers produced during surges at Brúarjökull, Iceland (Knudsen, 1995; Evans & Rea, 2003), as well as the occurrence of nearby, surge-diagnostic, crevasse squeeze ridges. The eastern section of Breiðamerkurjökull has a history of surging (Björnsson *et al.*, 2003) and the occurrence of surges in the past may explain the presence of the large amount of sediment necessary to build the eskers of MES3 (Evans & Rea, 2003). Several eskers in the east display a zig-zag shape in planform (e.g. Figure 7.7A; section 7.4.4) consistent with a surge origin. The presence of the complex eskers in MES3 would otherwise be difficult to explain because there is no large medial moraine to supply the sediment, as with MES1 and 2.

7.5.4 Are the esker patterns compatible with groundwater controlled hydraulic spacing of esker tunnels?

Borehole measurements and observations of the subglacial till and aquifer beneath Breiðamerkurjökull have been used to suggest that water is drawn to perennial subglacial channels through groundwater (Section 2.6.5; Boulton *et al.*, 2007a). Boulton *et al.* (2007a) suggest that Breiðamerkurjökull is drained along 16 main axes (see Figure 7.4) dictated by a coupling between the subglacial channels and groundwater system, and that some of the major esker systems originate from these channels. Our mapping shows that some of the larger eskers do appear to be concentrated along these pathways in accordance with Boulton *et al.* (2007a). However, it is also clear that some pathways do not appear to have generated eskers and closer inspection of the more subtle esker patterns suggests a complex depositional history, e.g. a large number of eskers occupy intermediate positions and, in some places (such as MES3), eskers are densely clustered between two axes. Thus, whilst it appears that Boulton *et al.*'s (2007a) hypothesis operates at a large scale, other local factors, such as sediment supply from medial moraines, are also important for esker formation. Further, meltwater has been shown to concentrate between lobes (e.g. Thome, 1986; Mäkinen, 2003; Benn *et al.*, 2009) because of the lateral convergence of supraglacial drainage systems (Benn *et al.*, 2009). This, combined with the availability of sediment associated with medial moraines, provides an additional explanation for the location of the largest eskers at Breiðamerkurjökull and reveals that subglacial tunnel deposition, together with potential groundwater coupling, is only partly responsible for esker sedimentation.

Importantly, the results presented above, as well as previous work (e.g. Price, 1969; Howarth, 1971), have shown that many of the eskers at Breiðamerkurjökull formed in englacial or supraglacial positions, which would mean that their location could not be directly influenced by groundwater. It is likely that some sections of eskers were deposited englacially and others subglacially, but further work is required in order to demonstrate the extent of subglacial esker deposition at Breiðamerkurjökull.

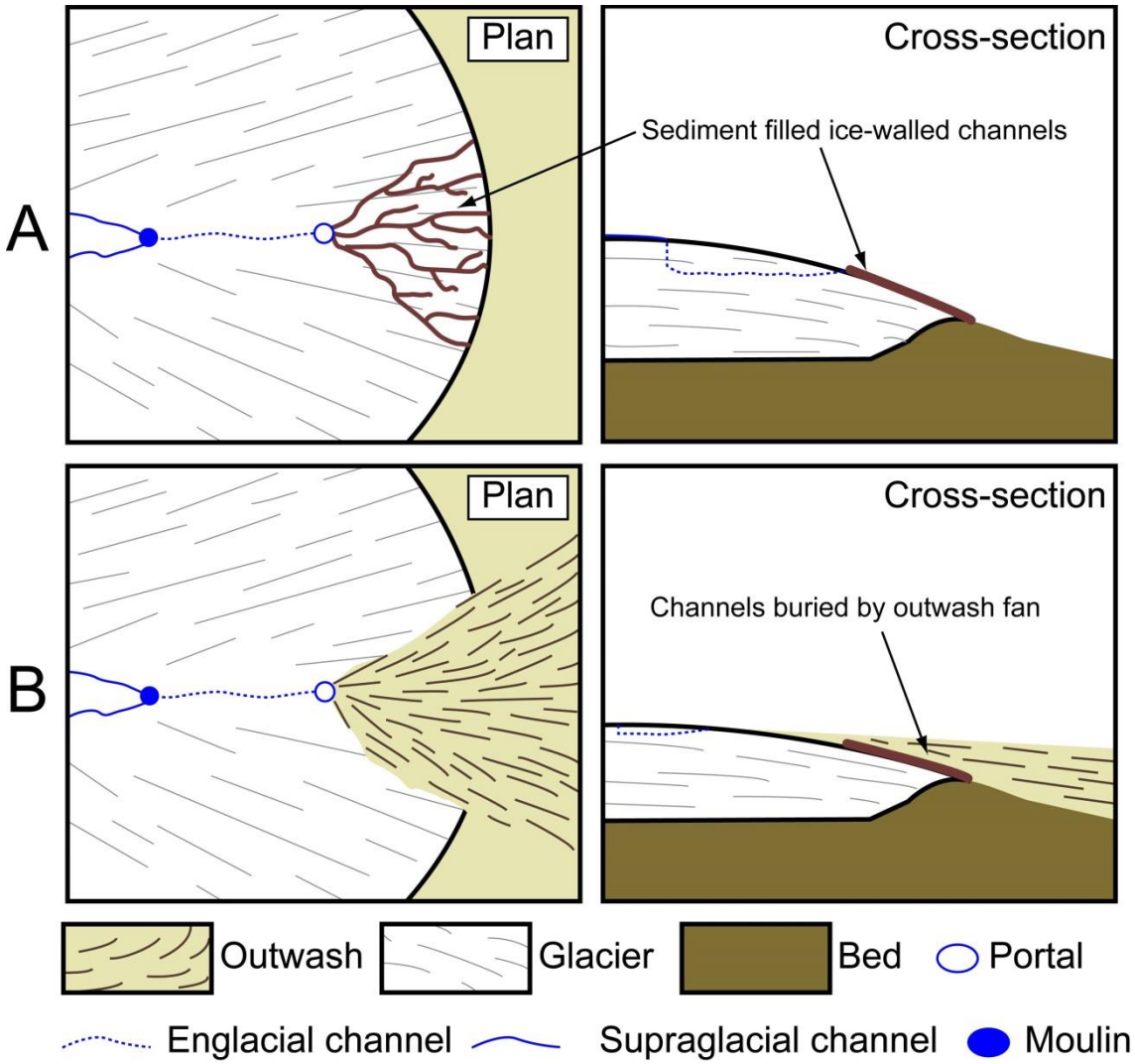

Figure 7.11. Depositional model for an *esker fan complex*. A) An englacial stream emerges on the glacier surface and water drains in supraglacial ice walled channels, which form a fan shape because they are at atmospheric pressure and unimpeded by topography. The channels then become choked with sediment. B) An outwash fan subsequently aggrades over the ice-walled channels, burying the channels and ice. The network of eskers preserved in the channel system is gradually lowered onto the bed and emerges as the ice melts out. Not to scale.

7.5.5 What controls the morphology of simple and complex esker systems?

Observations on the three major esker systems at Breiðamerkurjökull permit some conclusions to be drawn regarding the controls on the formation of simple (single ridges, separate from but often associated with complexes) and complex (multiple ridges, often in fans) esker morphologies. Based on the observed bed topography, areas of inferred increased sediment supply (by proximity to large medial moraines or, to a lesser extent, surges), and channel size (inferred from esker size), it is apparent that complex systems of eskers require certain conditions in order to form, which we summarise in Figure 7.12. They require an abundance of sediment and a sufficiently sized conduit. More complex esker morphologies, such as esker fans

and anastomosing networks are more likely to form if there is a large amount of sediment in the system and the conduits are relatively small, such that they become clogged with sediment and drainage is diverted to form new channels and new eskers. Conversely, if the conduit is sufficiently large relative to the supply of sediment, single ridge morphologies are more likely to develop. Increasing conduit size and sediment supply together promote the development of larger eskers (in terms of length, width and height) and, conversely, eskers will not form if the conduit is too small or there is insufficient sediment.

There is also evidence that these principles apply to Pleistocene eskers of North America. For example, complex esker systems are found in British Columbia and Yukon Territories, Canada (see map in appendix; Chapter 3; Armstrong & Tipper, 1948; Plouffe, 1991; Margold *et al.*, 2013) which are morphologically similar to the esker fan at Breiðamerkurjökull (Figure 7.1A). The complex Canadian eskers tend to occur down-ice from topographic obstacles which, in addition to producing a shallow depression in the ice surface down-ice of the obstacle and a location for meltwater accumulation (Margold *et al.*, 2013), would provide a significant supply of sediment with which to build complex eskers. Conversely, eskers exhibiting simpler morphologies are located on the Canadian Shield (Chapter 3; Shilts *et al.*, 1987; Storrar *et al.*, 2013) where sediment sources tended to be limited (Aylsworth & Shilts, 1989; Bolduc, 1992) and, as such, are less conducive to forming complex eskers. For example, Wilson (1939) and Aylsworth & Shilts (1989) note that where till is absent or scarce between Great Slave and Great Bear lakes, eskers are absent or poorly developed. It is also the case that eskers are more prevalent over the Canadian Shield than areas of more deformable beds (see Chapter 6), which produce fewer eskers because meltwater channels are incised into sediment rather than ice (Clark & Walder, 1994). In contrast, the substrate at Breiðamerkurjökull consists predominantly of deformable sediment, yet contains numerous eskers. This is likely due to the high concentrations of sediment and meltwater at Breiðamerkurjökull, and the formation of eskers in englacial as well as subglacial positions.

Whether complex esker networks develop into fans is related to topography. *Esker fan complexes* are likely to develop if the conditions above are met (high sediment supply, relatively small conduit) and the bed topography is fairly flat. Adverse slopes hinder the development of esker fans because drainage is diverted by the slope, giving rise to complex anastomosing networks, but not a fan morphology (*topographically constrained esker complexes*).

7.5.6 How long do eskers take to form?

In order to estimate how long it took to deposit the eskers we must first consider the seasonal changes occurring in the drainage system. Several workers have theorised that in winter months, channelized drainage systems slowly close due to ice creep and a lack of meltwater (e.g. Röthlisberger, 1972; Hewitt, 2013). If this is the case at Breiðamerkurjökull, it provides us with

a way to constrain esker formation, since eskers are deposited in active subglacial or englacial channels. Runoff has been shown to decrease markedly in the winter months at Breiðamerkurjökull (Boulton & Zatsepin, 2006), limiting supraglacial meltwater input to the drainage system, which may facilitate conduit closure and the termination of esker sedimentation. It is possible, however, that larger channels will remain open due to their size (Hewitt, 2013) and because of the high geothermal melt rate at Breiðamerkurjökull, which provides meltwater to the subglacial system even in winter (Boulton *et al.*, 2007a). Thus, the larger eskers may reflect sedimentation over several years. Nevertheless, the smaller eskers likely reflect rapid deposition, at the most over the course of a single summer, because smaller channels are less likely to be maintained through winter (they are not the dominant arteries of the drainage system). We suggest that large eskers may take longer to form, but that it is unlikely that this takes more than a few years because, given the rapid retreat of the ice margin over the last ~100 years, it seems unlikely that conduits could remain stable enough for eskers to slowly accumulate in them over periods of 10 years or more.

Eskers at Breiðamerkurjökull variously exhibit evidence of being formed in englacial, subglacial and potentially even supraglacial positions. However, given the rapid retreat of the ice margin, it is likely that the channels in which eskers formed changed over time, for example from being englacial to subglacial. This could occur as a result of surface lowering during retreat, with englacial drainage being diverted to a subglacial position. Alternatively, changes in the hydraulic gradient imparted by negative mass balance could have the effect of diverting drainage into different positions. Future work should therefore focus on identifying the sub-, en- or supraglacial origin of the eskers at Breiðamerkurjökull and, in particular, how this may evolve along the length of individual eskers.

7.5.7 How does esker morphology evolve through time?

'Simple' eskers, which melt directly out of the glacier onto the foreland, typically change less over time than more complex esker systems following deposition. Nevertheless, simple eskers can experience surface lowering if they contain an ice core which subsequently melts out (e.g. Price, 1966; Price, 1969; Howarth, 1971; Schomacker & Kjær, 2008). Later erosion of sections of eskers by meltwater streams is commonplace, especially when drainage systems change frequently, as at Breiðamerkurjökull (Price & Howarth, 1970). Eskers are frequently concealed or revealed after the glacier has retreated if, for example, they were submerged beneath a lake which subsequently drained, as with the esker complex associated with the Stemmulon system, or *vice-versa*. Other eskers may be overridden by readvances or surges and be removed or reworked beyond recognition. MES 1 and 2 provide pertinent examples of more complex esker systems, which may take several decades to emerge from ice buried beneath outwash, making a gradual but marked transition from a flat or pitted outwash surface to a complex network of

eskers once all the buried ice has melted. These observations may be used to make inferences about the conditions under which different eskers formed under palaeo-ice sheets. For example, eskers deposited beneath the Laurentide and Cordilleran Ice Sheets exhibit different morphologies (see Chapter 3), most eskers being simple in planform but some comprising complex anastomosing esker systems (e.g. Armstrong & Tipper, 1948; Aylsworth & Shilts, 1989; Margold *et al.*, 2013; Storrar *et al.*, 2013). In this case, we can infer that the simple eskers have changed little since deposition, whereas the more complex eskers may reflect deposition and gradual emergence in evolving systems, likely beneath stagnant ice and with outwash initially obscuring them. This differs dramatically from the simple supposition that eskers form from the filling of single conduits (e.g. Shreve, 1985) and means that it is important to consider esker morphology when using eskers to interpret the meltwater drainage history of a landscape; a simplistic model for esker sedimentation may suffice for some locations but will be inappropriate for other places.

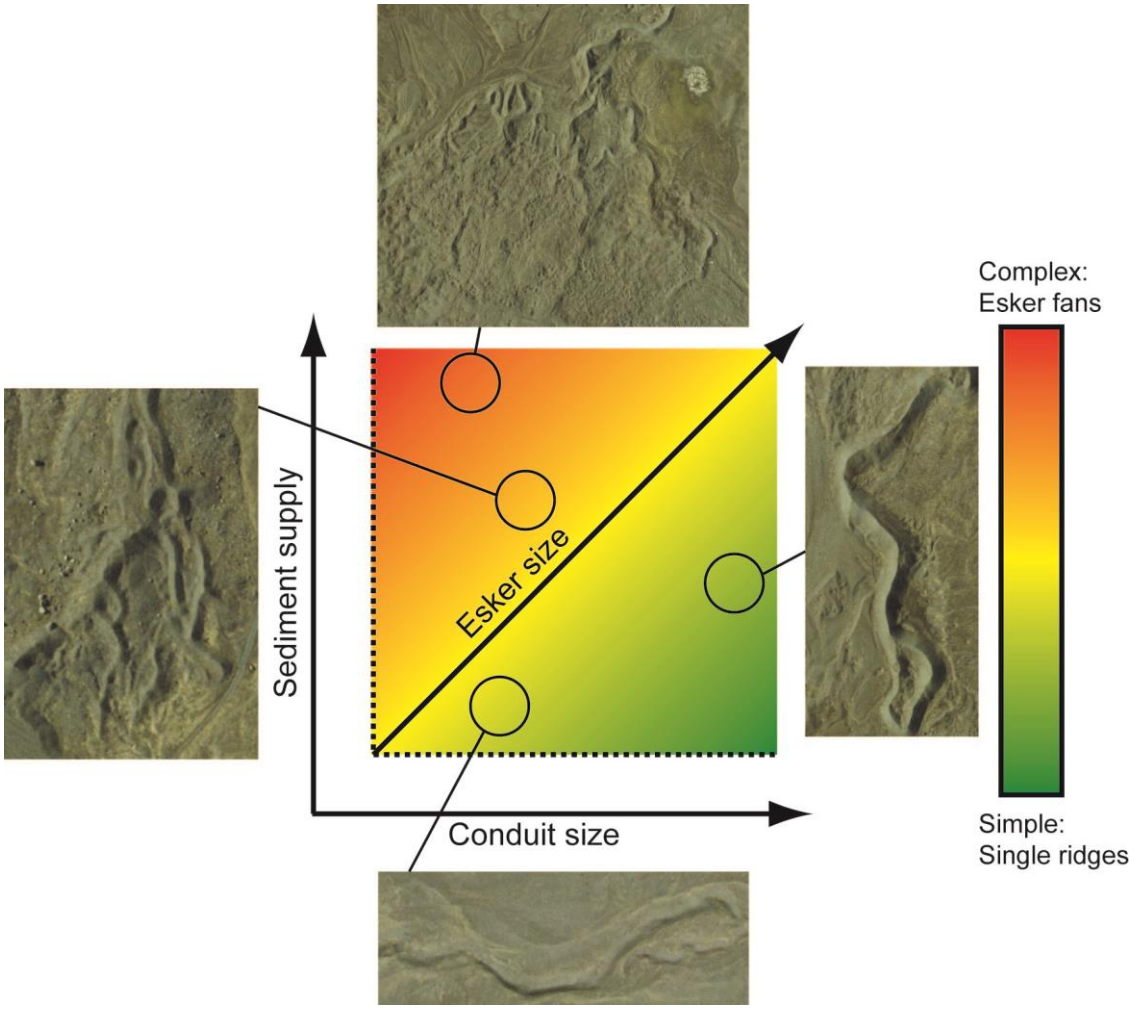

Figure 7.12. Conceptual diagram showing the effect of conduit size and sediment supply on esker size and morphology. Dashed lines indicates that eskers do not form until sufficient sediment is available in a sufficiently sized conduit. Examples of different esker morphologies are given from the 2007 photographs and their relative position in the diagram indicated.

7.6 Conclusions

Detailed mapping of over 5,000 eskers over eight different time slices from the last ~70 years at Breiðamerkurjökull reveals complex anabranching esker networks and simpler, single ridge morphologies which emerged at a mean rate of 990 m yr^{-1} and total almost 90 km by 2007. Esker location, particularly of the more complex esker systems, is primarily driven by sediment supply and meltwater concentrated along medial moraines, or more locally by crevasse infilling during surges. The spacing of eskers is broadly consistent with groundwater controlled hydraulic spacing of esker tunnels (cf. Boulton et al., 2007a, b), whereby meltwater is scavenged into the groundwater system from the subglacial channels until it becomes saturated. However, the pattern of development and subsequent emergence of eskers is also controlled by topography and sediment availability in addition to partial supraglacial sedimentation. In relation to this, depositional models are presented for two complex esker systems: *esker fan complexes*, which produce anastomosing eskers in a fan shape; and *topographically constrained esker complexes*, which are characterised by anastomosing eskers whose planform is dictated by topographic impedances and thus not able to develop into a fan shape. These complex morphologies were created by the gradual melting out of buried ice which contained eskers beneath a layer of outwash. Both of these complex esker systems require a large supply of sediment and meltwater to form; conversely, simple esker systems predominate when less sediment or meltwater is available. Small esker ridges may form almost instantaneously (likely within a year), whilst large eskers may require several years to form. Complex esker systems may take several decades to melt out of outwash and evolve into the complex patterns which we observe today.

7.7 References

Armstrong, J. E. & Tipper, H. W. (1948) Glaciation in north-central British Columbia. *American Journal of Science*, 246, 283-310.

Aylsworth, J. M. & Shilts, W. W. (1989) Bedforms of the Keewatin Ice-Sheet, Canada. *Sedimentary Geology*, 62, 407-428.

Banerjee, I. & McDonald, B. C. (1975) Nature of esker sedimentation. In A. V. Jopling and B. C. McDonald, *Glaciofluvial and Glacilacustrine Sedimentation*. Oklahoma, SEPM, 304-320.

Bartholomew, I., Nienow, P., Mair, D., Hubbard, A., King, M. A. & Sole, A. (2010) Seasonal evolution of subglacial drainage and acceleration in a Greenland outlet glacier. *Nature Geoscience*, 3, 408-411.

Benn, D. I., Kristensen, L. & Gulley, J. D. (2009) Surge propagation constrained by a persistent subglacial conduit, Bakaninbreen-Paulabreen, Svalbard. *Annals of Glaciology*, 50, 81-86.

Bennett, G. L. & Evans, D. J. A. (2012) Glacier retreat and landform production on an overdeepened glacier foreland: the debris-charged glacial landsystem at Kviárjökull, Iceland. *Earth Surface Processes and Landforms*, 37, 1584-1602.

Björnsson, H., Pálsson, F., Sigurðsson, O. & Flowers, G. E. (2003) Surges of glaciers in Iceland. *Annals of Glaciology*, 36, 82-90.

Bolduc, A. M. (1992) The formation of eskers based on their morphology, stratigraphy and lithologic composition, Labrador, Canada. *Unpublished Ph.D. thesis, Lehigh University*.

Boulton, G. S. (1986) Push-moraines and glacier-contact fans in marine and terrestrial environments. *Sedimentology*, 33, 677-698.

Boulton, G. S. (1987) A theory of drumlin formation by subglacial sediment deformation. In J. Menzies and J. Rose, *Drumlin Symposium*. Rotterdam, Balkema, 25-80.

Boulton, G. S., Dobbie, K. E. & Zatsepin, S. (2001) Sediment deformation beneath glaciers and its coupling to the subglacial hydraulic system. *Quaternary International*, 86, 3-28.

Boulton, G. S., Hagdorn, M., Maillot, P. B. & Zatsepin, S. (2009) Drainage beneath ice sheets: groundwater-channel coupling, and the origin of esker systems from former ice sheets. *Quaternary Science Reviews*, 28, 621-638.

Boulton, G. S., Harris, P. W. V. & Jarvis, J. (1982) Stratigraphy and structure of a coastal sediment wedge of glacial origin inferred from Sparker measurements in glacial lake Jokulsarlon in southeast Iceland. *Jokull*, 32, 37-47.

Boulton, G. S. & Hindmarsh, R. C. A. (1987) Sediment deformation beneath glaciers: rheology and geological consequences. *Journal of Geophysical Research*, 92, 9059-9082.

Boulton, G. S., Lunn, R., Vidstrand, P. & Zatsepin, S. (2007a) Subglacial drainage by groundwater-channel coupling, and the origin of esker systems: Part I-glaciological observations. *Quaternary Science Reviews*, 26, 1067-1090.

Boulton, G. S., Lunn, R., Vidstrand, P. & Zatsepin, S. (2007b) Subglacial drainage by groundwater-channel coupling, and the origin of esker systems: part II-theory and simulation of a modern system. *Quaternary Science Reviews*, 26, 1091-1105.

Boulton, G. S. & Zatsepin, S. (2006) Hydraulic impacts of glacier advance over a sediment bed. *Journal of Glaciology*, 52, 497-527.

Brennand, T. A. (1994) Macroforms, large bedforms and rhythmic sedimentary sequences in subglacial eskers, south-central Ontario - implications for esker genesis and meltwater regime. *Sedimentary Geology*, 91, 9-55.

Brennand, T. A. (2000) Deglacial meltwater drainage and glaciodynamics: inferences from Laurentide eskers, Canada. *Geomorphology*, 32, 263-293.

Burke, M. J., Woodward, J., Russell, A. J., Fleisher, P. J. & Bailey, P. K. (2010) The sedimentary architecture of outburst flood eskers: A comparison of ground-penetrating radar data from Bering Glacier, Alaska and Skeiðarárjökull, Iceland. *Bulletin of the Geological Society of America*, 122, 1637-1645.

Clark, C. D., Evans, D. J. A., Khatwa, A., Bradwell, T., Jordan, C., Marsh, S., Mitchell, W. & Bateman, M. (2004) Map and GIS database of glacial landforms and features related to the last British Ice Sheet. *Boreas*, 33, 359-375.

Clark, P. U. & Walder, J. S. (1994) Subglacial drainage, eskers, and deforming beds beneath the Laurentide and Eurasian ice sheets. *Bulletin of the Geological Society of America*, 106, 304-314.

Evans, D. J. A. & Rea, B. R. (2003) Surging Glacier Landsystem. In D. J. A. Evans, *Glacial Landsystems*. London, Hodder Arnold, 259-288.

Evans, D. J. A. & Twigg, D. R. (2000) Breiðamerkurjökull 1998. 1: 30,000 Scale Map. University of Glasgow and Loughborough University.

Evans, D. J. A. & Twigg, D. R. (2002) The active temperate glacial landsystem: a model based on Breiðamerkurjökull and Fjallsjökull, Iceland. *Quaternary Science Reviews*, 21, 2143-2177.

Gorrell, G. & Shaw, J. (1991) Deposition in an esker, bead and fan complex, Lanark, Ontario, Canada. *Sedimentary Geology*, 72, 285-314.

Gustavson, T. C. & Boothroyd, J. C. (1987) A depositional model for outwash, sediment sources, and hydrologic characteristics, Malaspina Glacier, Alaska: A modern analog of the southeastern margin of the Laurentide Ice Sheet. *Bulletin of the Geological Society of America*, 99, 187.

Hebrand, M. & Åmark, M. (1989) Esker formation and glacier dynamics in eastern Skane and adjacent areas, southern Sweden. *Boreas*, 18, 67-81.

Hewitt, I. J. (2013) Seasonal changes in ice sheet motion due to melt water lubrication. *Earth and Planetary Science Letters*, 371–372, 16-25.

Howarth, P. J. (1968) Geomorphological and glaciological studies, eastern Breiðamerkurjökull, Iceland. *Department of Geography*, University of Glasgow. PhD.

Howarth, P. J. (1971) Investigations of two eskers at eastern Breiðamerkurjökull, Iceland. *Arctic and Alpine Research*, 3, 305-318.

Howarth, P. J. & Price, R. J. (1969) The proglacial lakes of Breiðamerkurjökull and Fjallsjökull, Iceland. *The Geographical Journal*, 135, 573-581.

Howarth, P. J. & Welch, R. (1969a) Breiðamerkurjőkull, South-east Iceland, August 1945. 1:30,000 scale map. University of Glasgow. 1:30,000

Howarth, P. J. & Welch, R. (1969b) Breiðamerkurjőkull, South-east Iceland, August 1965. 1:30,000 scale map. University of Glasgow.

Huddart, D., Bennett, M. R. & Glasser, N. F. (1999) Morphology and sedimentology of a high-arctic esker system: Vegbreen, Svalbard. *Boreas*, 28, 253-273.

Jewtuchowicz, S. (1965) Description of eskers and kames in Gåshamnöyra and on Bengebreen, south of Hornsund, Vestspitsbergen. *Journal of Glaciology*, 5, 719-725.

Kirkbride, M. P. (2000) Ice-marginal geomorphology and Holocene expansion of debris-covered Tasman Glacier, New Zealand. In M. Nakawo, C. Raymond and A. Fountain, *Devris-Covered Glaciers*, IAHS Publication. 264, 211-218.

Knudsen, Ó. (1995) Concertina eskers, Brúarjökull, Iceland: An indicator of surge-type glacier behaviour. *Quaternary Science Reviews*, 14, 487-493.

Lewis, W. V. (1949) An esker in process of formation: Boverbreen, Jotunheimen, 1947. *Journal of Glaciology*, 1, 314-319.

Mäkinen, J. (2003) Time-transgressive deposits of repeated depositional sequences within interlobate glaciofluvial (esker) sediments in Koylio, SW Finland. *Sedimentology*, 50, 327-360.

Margold, M., Jansson, K., Kleman, J. & Stroeven, A. (2011) Glacial meltwater landforms of central British Columbia. *Journal of Maps*, 2011, 486-506.

Margold, M., Jansson, K. N., Kleman, J. & Stroeven, A. P. (2013) Lateglacial ice dynamics of the Cordilleran Ice Sheet in northern British Columbia and southern Yukon Territory: retreat pattern of the Liard Lobe reconstructed from the glacial landform record. *Journal of Quaternary Science*, 28, 180-188.

Nienow, P., Sharp, M. & Willis, I. (1998) Seasonal changes in the morphology of the subglacial drainage system, Haut Glacier d'Arolla, Switzerland. *Earth Surface Processes and Landforms*, 23, 825-843.

Plouffe, A. (1991) Preliminary study of the Quaternary geology of the northern interior of British Columbia. *Current research, Geological Survey of Canada*, 91-1A, 7-13.

Price, R. J. (1966) Eskers near the Casement glacier, Alaska. *Geografiska Annaler. Series A. Physical Geography*, 48, 111-125.

Price, R. J. (1969) Moraines, sandar, kames and eskers near Breiðamerkurjökull , Iceland. *Transactions of the Institute of British Geographers*, 46, 17-43.

Price, R. J. (1971) The Development and Destruction of a Sandur, Breiðamerkurjökull, Iceland. *Arctic and Alpine Research*, 225-237.

Price, R. J. (1980) Rates of geomorphological changes in proglacial areas. In R. A. Cullingford, D. A. Davidson and J. Lewin, *Timescales in geomorophology*. Chichester, Wiley, 79-93.

Price, R. J. (1982) Changes in the proglacial area of Breiðamerkurjökull , southeastern Iceland: 1890-1980. *Jökull*, 29-35.

Price, R. J. & Howarth, P. J. (1970) The evolution of the drainage system (1904-1965) in front of Breiðamerkurjökull *Jökull*, 20, 27-37.

Röthlisberger, H. (1972) Water pressure in intra-and subglacial channels. *Journal of Glaciology*, 11, 177-203.

Schomacker, A. & Kjær, K. H. (2008) Quantification of dead ice melting in ice cored moraines at the high Arctic glacier Holmströmbreen, Svalbard. *Boreas*, 37, 211-225.

Shilts, W. W. (1984) Esker sedimentation models, Deep Rose Lake map area, District of Keewatin. *Geological Survey of Canada, Paper*, 84-1B, 217-222.

Shilts, W. W., Aylsworth, J. M., Kaszycki, C. A. & Klassen, R. A. (1987) Canadian Shield. In W. L. Graf, *Geomorphic Systems of North America*. Boulder, Colorado, Geological Society of America, Centennial Special Volume. 2, 119-161.

Shreve, R. L. (1985) Esker characteristics in terms of glacier physics, Katahdin esker system, Maine. *Bulletin of the Geological Society of America*, 96, 639-646.

Spedding, N. & Evans, D. J. A. (2002) Sediments and landforms at Kvíárjökull, southeast Iceland: a reappraisal of the glaciated valley landsystem. *Sedimentary Geology*, 149, 21-42.

Stokes, J. C. (1958) An esker-like ridge in process of formation, Flatisen, Norway. *Journal of Glaciology*, 3, 286-289.

Storrar, R. D., Stokes, C. R. & Evans, D. J. A. (2013) A map of Canadian eskers from Landsat satellite imagery. *Journal of Maps*, 9, 456-473.

Syverson, K. M., Gaffield, S. J. & Mickelson, D. M. (1994) Comparison of esker morphology and sedimentology with former ice-surface topography, Burroughs Glacier, Alaska. *Geological Society of America Bulletin*, 106, 1130-1142.

Thome, K. N. (1986) Melt-water drainage pattern of composite glaciers. *Journal of Glaciology*, 32, 95-100.

Warren, W. P. & Ashley, G. M. (1994) Origins of the ice-contact stratified ridges (eskers) of Ireland. *Journal of Sedimentary Research*, 64, 433-499.

Welch, R. & Howarth, P. (1968) Photogrammetric measurements of glacial landforms. *The Photogrammetric Record*, 6, 75-96.

Wilson, J. (1939) Eskers north-east of Great Slave Lake. *Trans. Roy. SOC. Can*, 119-129.

Chapter 8 Discussion

This chapter synthesises the findings of Chapters 3-7 and discusses the results in the context of the research questions outlined in Section 1.2. Limitations of using eskers to reconstruct subglacial meltwater drainage are discussed and, finally, areas of future research are suggested in light of the results presented in this thesis.

8.1 What controls the pattern and morphology of eskers?

8.1.1 Length

Section 4.3.2 revealed that esker systems in Canada reach up to 760 km, when small gaps between eskers are taken into account. The enormous length of these esker systems presents a challenge for understanding how they formed. For example, if synchronous deposition is invoked, difficulties arise in explaining how sedimentation could occur rapidly over such a long distance and what controlled the initiation of such an event (see Section 4.4.2 for more detail). Alternatively, if time-transgressive deposition is preferred, the continuity of the drainage network at a retreating ice margin becomes difficult to explain, because the configuration of the ice sheet changes dramatically during deglaciation (Shilts, 1984).

One explanation for the large lengths observed is the former ice surface slope. Ice surface slope exerts an important control on the location of R-channels (Röthlisberger, 1972; Shreve, 1972) and has, in part, been used to explain the pattern of eskers around the Keewatin Ice Divide (Shilts, 1984; Shilts *et al.*, 1987; Aylsworth & Shilts, 1989). The flat profile of the LIS over the Keewatin Ice Divide is suggested to have controlled the pattern of supraglacial drainage networks, which then switched to a subglacial position in the terminal parts of the ice sheet (Shilts, 1984; Shilts *et al.*, 1987; Aylsworth & Shilts, 1989). This hypothesis is suggested to account for the integrated dendritic network of eskers, which would reflect the configuration of supraglacial meltwater channels and also the time-transgressive deposition of the resultant eskers, potentially explaining why up to fourth-order tributaries (Section 4.3.5; Shilts *et al.*, 1987) are developed. Others have argued, however, that esker forming channels were predominantly subglacial and are not related to the configuration of the supraglacial drainage system, though their locations were still likely ultimately controlled by the surface slope of the ice sheet (Shreve, 1972; Clark & Walder, 1994).

Whilst this thesis does not directly test whether esker locations in Canada are controlled by the former ice surface slope, the absence of an alternative explanation for controls on esker length (i.e. the nature of the substrate has little influence: see Chapter 6) suggests that the former ice surface may have been important. In order to form long (100s of km) esker systems, three

conditions are required: 1) a sufficient supply of meltwater must have been available in the location of the esker; 2) a sufficient supply of sediment must have been available in the location of the esker; and 3) sufficient time to build the esker must have been available. It has been demonstrated that eskers do not necessarily require a large quantity of sediment in order to form (Section 6.3.3; Bolduc, 1992), which then leaves the supply of meltwater and the time taken to construct the esker. Both of these parameters are dependent on the geometry of the ice sheet through time. If the esker was deposited time-transgressively, which is the simplest explanation for very long eskers (see Section 4.4.2), the presence of long eskers requires that the ice sheet maintained a roughly consistent geometry through deglaciation, in order to maintain a conduit in the same sector to build a continuous esker. This explanation seems to be reasonable in that the longest eskers occur around the Keewatin Ice Divide (Figure 4.9), which maintained a relatively uniform shape through deglaciation (Chapter 5; Dyke *et al.*, 2003). In contrast, the eskers around the Ungava Ice Divide, which experienced a markedly more asynchronous deglaciation (Section 5.4; Hillaire-Marcel & Occhietti, 1980; Clark *et al.*, 2000; Dyke *et al.*, 2003), tend to be shorter (see Section 4.3.1.).

8.1.2 Sinuosity

Section 4.3.3 noted that sinuosity values for eskers indicate that they are remarkably straight (98% have a sinuosity value of less than 1.1), especially in comparison with sinuosity values typically found in river systems (freely meandering river systems have a mean sinuosity of 3.14: Stølum, 1996). This raises an important question: given the fluvial nature of their formation, why are eskers so straight? Few studies have previously considered the sinuosity of subglacial drainage channels because it is very difficult to measure either directly or remotely (except in the case of eskers, as reported here). Thus, supraglacial and englacial channels may provide the most useful proxies for understanding what controls subglacial channel sinuosity. Moreover, if the hypothesis of Shilts (1984), as outlined above, is correct, the sinuosity of eskers should, to some extent, be influenced by the sinuosity of the supraglacial streams from which they originate, because the supraglacial channels define the (two-dimensional) location of the resultant subglacial channels.

As a result of the relative ease of accessibility, most previous studies into glacial channel geometry have focused on the supraglacial channels of small glaciers, which are often perennial (Ferguson, 1973). Marston (1983) showed that, based on a study of the Juneau Icefield, USA, high stream power upstream initiates meandering, which propagates down-ice. However, stream power is inversely proportional to sinuosity in a given section. Increasing ice surface slope has the effect of decreasing supraglacial channel sinuosity, which varies between 1.05 and 1.25 in the Juneau Icefield (roughly similar to esker sinuosity: see Section 4.3.3). Data obtained from Swiss valley glaciers by Ferguson (1973) revealed that maximum sinuosity is achieved in

reaches with the greatest initial power expenditure, with meanders migrating downstream until meandering is restricted by a decrease in the energy gradient associated with increased resistance from rising sinuosity values. Esker sinuosity may, therefore, be a function of stream power and ice surface slope. Unfortunately, relatively few values of sinuosity for supraglacial channels are presently available, particularly for ice sheet-scale systems. However, recent developments in remote sensing methodology (Kang & Smith, 2013) may be able to shed light on the sinuosity of supraglacial streams on modern ice sheets at a large scale, potentially providing a useful constraint on what controls supraglacial channel sinuosity and whether this subsequently has implications for the sinuosity of englacial and subglacial channels.

More recently, work has begun to focus on the geometry of englacial conduits (e.g. Vatne, 2001; Gulley & Benn, 2007; Benn *et al.*, 2009a; Benn *et al.*, 2009b; Gulley, 2009; Gulley *et al.*, 2009a; Gulley *et al.*, 2009b). Directly accessing englacial conduits allows detailed measurements and observations to be made, but also means that sample sizes are limited by logistics. It is not surprising, therefore, that observations of englacial conduit sinuosity vary markedly. For example, Vatne (2001) noted that englacial conduits beneath Austre Brøggerbreen, Svalbard, tend to meander (have high sinuosity) when they exhibit shallow slopes. Conversely, Gulley *et al.* (2009a) noted that the straightest channel observed beneath Longyearbreen, Svalbard and Khumbu Glacier, Nepal, also exhibited the lowest gradient. Gulley and Benn (2007) provided evidence for migrating meanders in englacial conduits beneath Himalayan debris-covered glaciers and Gulley *et al.* (2009a) noted a wide range of sinuosity values, from 1.17 to 6.29, far exceeding the highest esker sinuosity recorded here (see Section 4.3.3). The extent to which englacial conduits in polythermal glaciers reflect the drainage channels beneath former ice sheets is not clear. However, given the large variations in the sinuosity values noted for englacial conduits compared with the esker data given in Section 4.3.3, it seems likely that large differences exist between the two environments, likely meaning that esker sinuosity is not analogous to that of englacial channels.

In summary, if networks of eskers reflect the surface drainage pattern over ice sheets (Shilts, 1984; Shilts *et al.*, 1987; Aylsworth & Shilts, 1989), it would seem logical that their sinuosity is influenced by the sinuosity of the supraglacial streams from which they originate, suggesting that esker sinuosity is controlled, at least in part, by ice surface slope and stream power. This would likely be modified to some extent once the supraglacial streams plunge to subglacial positions close to the ice margin (Shilts, 1984), where the drainage channels would exist under different pressure regimes (see Section 2.2), but the overall pattern would remain similar because the locations of the subglacial channels are dictated by the supply of water from supraglacial channels. The closer resemblance of supraglacial stream sinuosity values, compared with englacial values, to the esker data (Section 4.3.3), support this hypothesis. However, a larger sample size of supraglacial channel sinuosity values, particularly at the ice sheet scale, is necessary to further explore this link.

8.1.3 Spacing

The spacing between eskers has been hypothesised to be controlled by the coupling of groundwater flow and meltwater drainage in subglacial channels (see Section 2.6.5.). Specifically, this theory predicts that esker spacing should decrease when the supply of meltwater to the system increases, or the transmissivity of the substrate decreases. The observations in Chapter 5 of increased esker frequency (decreased esker spacing) associated with increased meltwater supply during deglaciation of the Laurentide Ice Sheet supports the groundwater hypothesis, though we note that Boulton *et al.* (2009) assume a basal melt source, compared with the supraglacial source invoked in Chapter 5. Conversely, the observations of similar esker spacing over different substrates in Canada (Section 6.3.4; Figure 6.13) offers no support for the groundwater hypothesis, which predicts that eskers should be spaced more closely over substrates with lower transmissivity. Section 6.4.2 revealed that there is little variability between esker spacing over different substrates and that extrapolation of Boulton's (2009) equation 1 produces unrealistic values for basal melt rate, when hydraulic conductivity is estimated based on rock type (Bear, 1972). Whilst our test is, in this instance, a first-order evaluation of the hypothesis, the stark disagreement between the predictions of the theory and our results are difficult to account for, given the large sample size used to measure esker spacing. One possibility is that the influence of meltwater supply outweighs that of the hydrogeological properties of the substrate in controlling esker spacing. This would account for the observations that increased meltwater leads to decreased esker spacing but that no differences between substrate types were identified.

Section 7.5.4 revealed that eskers mapped on the foreland of Breiðamerkurjökull exhibit some tendency to be spaced in accordance with the drainage axes proposed by Boulton *et al.* (2007). However, the mapping presented (Figure 7.4) reveals that the pattern of eskers at Breiðamerkurjökull is much more complex than a simple system of regularly spaced eskers. The main esker systems at Breiðamerkurjökull are suggested in Section 7.5.5 to be primarily controlled by the abundance of sediment and meltwater associated with convergent ice lobes and medial moraines. Given these observations, it is difficult to separate groundwater controlled esker spacing from spacing resulting from other factors, especially sediment supply.

In summary, it is likely that the coupling between the subglacial and groundwater drainage systems exerts some control on the spacing of eskers. However, the theory represents a simplification of the complex factors which govern the formation of eskers. In particular, whilst the theory explains the distribution of water between channels and groundwater systems beneath ice masses relatively well, it does not account for the subsequent sedimentation that is necessary to form eskers (Boulton *et al.*, 2009). Sediment supply is strongly variable and dependent on localised conditions (for example, see Section 7.5.5) and so this is likely to influence the

location of eskers more than groundwater coupling, where sediment is abundant. Meltwater supply also appears to be a more important factor than previously assumed.

8.1.4 Sediment supply

A common theme of Chapters 5-7 is that the supply of sediment is fundamentally important to the formation of eskers, because it dictates where they may form and how large they may be. Shilts *et al.* (1987) emphasize the importance of sediment supply to the formation of eskers around the Keewatin Ice Divide, which commonly attain 30 m in height compared to their surroundings, where the till cover is usually <5 m. They also note locations where eskers are scarce or absent and relate this to the absence of till, noting that glaciological conditions may have existed that favoured esker formation but that esker formation could not take place because the raw materials required were not present. Moreover, Clark and Walder (1994) point out that where a small amount of sediment is present in a conduit, it is likely to be flushed out, rather than deposited.

Chapter 5 suggested that one reason for the absence of eskers beneath the Keewatin and Ungava Ice Divides is that insufficient sediment was available, resulting from of a lack of erosion and/or sediment transport beneath the small ice caps towards the end of deglaciation. In Chapter 6 it was demonstrated that the distribution of eskers in central and southern Alberta appear to bear little relation to the thickness of the sediment beneath them, suggesting that as long as there is *sufficient* sediment within the vicinity of the esker there does not need to be a particular thickness of till to favour esker formation. For example, Bolduc (1992) suggests that eskers derive their material from till up to several 10s of kilometres up-ice. Taken together, these interpretations suggest that there may be a threshold for esker formation based on the availability of sufficient sediment.

Sediment supply was also a key focus of Chapter 7, in which it was revealed that esker morphology (as well as just formation or non-formation) is likely governed by sediment (and meltwater) supply (Section 7.5.5). Eskers form where there is sufficient meltwater to form large channels and also, crucially, where there is sufficient sediment to fill them. *Complex* esker systems form where sediment is abundant and able to ‘clog’ channels to form multiple distributary ridges (see Figure 7.12). The alignment of complex esker systems with large medial moraines, and contrastingly smaller and simpler eskers away from medial moraines at Breiðamerkurjökull provides compelling evidence that sediment and meltwater supply is critical for esker formation. The same process can be linked to the presence of complex eskers in the Rocky Mountains (cf. Margold *et al.*, 2013), where sediment was readily provided by erosion of the high terrain by the Cordilleran Ice Sheet. The same mechanism may also explain the absence of complex eskers on the Canadian Shield, where sediment is derived from the base of a relatively flat ice sheet and so is less abundant than in other locations (Shilts *et al.*, 1987).

Clearly, sediment supply is a crucial parameter for esker formation and, whilst it is obvious that no eskers can form without sediment, its importance may be underestimated by hypotheses attempting to explain the distribution of eskers (cf. Shreve, 1985; Boulton *et al.*, 2009) and may explain why there is often a discordance between observations and predictions.

8.2 How did subglacial drainage systems evolve during ice sheet deglaciation?

Chapter 5 presented the first analysis of meltwater drainage system evolution on millennial and continental (ice sheet) scales, revealing that the drainage system beneath the LIS became more channelized as more meltwater became available. The observations of increased esker frequency during deglaciation are logical and provide a useful fit between theory and observation. However, whilst the LIS displays a clear trend in drainage system evolution during deglaciation, whether this is the case for other past ice sheets remains unknown. Eskers similar in size to those of the LIS are present in large numbers in Fennoscandia (Section 2.5) and changes in the subglacial meltwater drainage system related to fluctuations in the supply of meltwater have been suggested previously (Lundqvist, 1997; Punkari, 1997; Lundqvist, 1999). Notably, the conditions under which the Fennoscandian eskers were formed were different from the LIS. Specifically, many of the Fennoscandian eskers were formed in a glacimarine environment (Lundqvist, 1997; Lundqvist, 1999), as opposed to the LIS eskers, which typically emerged either terrestrially or in proglacial lakes (Brennand, 2000). Ice sheet dynamics were also different from those of the LIS, where ice streaming appears to have been less significant during deglaciation (Chapter 5; Kleman & Glasser, 2007; Stokes & Tarasov, 2010). In contrast, ice streaming was pervasive during the deglaciation of the Fennoscandian Ice Sheet (Punkari, 1997). Small scale observations have been used to suggest that esker sediments may contain rhythmic patterns, potentially related to the El Nino Southern Oscillation and 11 year sunspot cycles (Lundqvist, 1997; Lundqvist, 1999), however no further climatic correlations have been made.

In summary, the meltwater drainage system beneath the LIS evolved to accommodate additional meltwater, similar to alpine glaciers, but whether this is the case for other ice sheets remains to be seen.

8.3 How can eskers be used to further our understanding of subglacial hydrology?

Eskers can be used to evaluate the distribution of meltwater drainage in channels beneath ice sheets during deglaciation. Specifically, they reveal the spatial pattern of subglacial meltwater channels, as discussed in Chapter 3. By extension, understanding what controls the location of eskers (cf. Chapters 5, 6 and 7) also provides insights into what controls the location of R-channels and the transport of sediment in meltwater channels. Analysing changes in esker

morphology through time (e.g. Chapter 5) provides a novel and important way to reconstruct the evolution of meltwater drainage systems during the deglaciation of ice sheets. This relies on having a robust margin chronology but is a powerful technique to gain valuable insights into a hitherto unknown process.

Esker morphometry (see Chapter 4) can also be used to provide an important constraint on the properties of subglacial channels beneath ice sheets. Whilst subglacial channels have been identified in different settings, such as alpine glaciers (e.g. Hubbard & Nienow, 1997), outlet glaciers (e.g. Bartholomew *et al.*, 2010) and ice streams (e.g. Fricker *et al.*, 2010), their presence is often inferred from indirect observations. This means that direct observations of parameters such as channel size and continuity are rare. Thus, eskers can provide a snapshot of the dimensions of subglacial channel in an unparalleled level of detail, though some important caveats must be addressed before doing so, as discussed in Section 8.4.

8.4 Limitations

Despite the potential offered by eskers to provide analogues for contemporary subglacial drainage channels, there are several limitations that need to be accounted for. These can be categorised into 'known' limitations (i.e. eskers definitely cannot be used to reconstruct X) and 'unknown' limitations (i.e. there is uncertainty about how much eskers can be used to reconstruct Y).

'Known' limitations include the identification of distributed drainage networks. Eskers form primarily in channelized networks, where branching dendritic systems are common (Shilts *et al.*, 1987; Clark & Walder, 1994; Brennand, 2000), as opposed to distributed drainage systems, which are not conducive to esker formation because they lack the coherent channels necessary for eskers to be deposited in (Clark & Walder, 1994). Distributed drainage networks have been implied to operate beneath contemporary (e.g. Kamb, 1987; Alley, 1989) and ancient (e.g. Walder & Hallet, 1979; Eyles *et al.*, 1982; Clark & Walder, 1994; Walder & Fowler, 1994) glacier systems and may also operate alongside channelized systems (Willis *et al.*, 2012) and so are an important component of the drainage system. Clearly, eskers are unable to directly offer insights into distributed drainage networks, though the trend observed in Chapter 5 of esker frequency increasing through deglaciation may suggest that channelized meltwater drainage increased at the cost of distributed meltwater drainage (see Figure 5.5), as has been observed on a seasonal basis beneath alpine and outlet glaciers (Hubbard & Nienow, 1997; Bartholomew *et al.*, 2010). Indeed, Clark and Walder (1994) hypothesise that drainage occurs either in channelized *or* distributed systems, depending on the lithology of the bed.

Another 'known' limitation in using eskers to reconstruct ice sheet meltwater drainage systems is that most eskers formed during deglaciation (e.g. Punkari, 1980; Hättestrand, 1997;

Brennand, 2000), when meltwater was abundant (Carlson *et al.*, 2008; Carlson *et al.*, 2009). Though this is an important period of ice sheet history for understanding ice sheet-climate interactions (e.g. Carlson *et al.*, 2009), and it is very useful that eskers can be used to infer drainage characteristics during deglaciation, they are unlikely to be representative of the 'steady-state' meltwater drainage conditions prior to deglaciation, when the supply of meltwater was smaller (less surface melting) and glaciological conditions were significantly different (Tarasov *et al.*, 2012). During more stable ice sheet conditions, it is possible that geothermal flux, rather than surface melting, provided the main source of meltwater to the subglacial system (e.g. Boulton *et al.*, 2009). The configuration of subglacial drainage networks under such conditions beneath the Laurentide and other ice sheets is, at present, unknown.

'Unknown' limitations include uncertainty as to what controls the location and formation of eskers in different settings, as discussed in Section 2.6. It is important to understand the factors which control the distribution of eskers before using esker patterns to reconstruct subglacial meltwater systems. Previous work (e.g. Price, 1969; Banerjee & McDonald, 1975; Shreve, 1985; Shilts *et al.*, 1987; Hebrand & Åmark, 1989; Brennand, 1994; Clark & Walder, 1994; Syverson *et al.*, 1994; Boulton *et al.*, 2009), as well as the work presented in this thesis, have made substantial progress in addressing these unknowns, but the continued debate over competing hypotheses exemplifies the element of uncertainty in esker-based reconstructions. A corollary uncertainty is that there is also a limited understanding of why esker *don't* form under some ice sheets. For example, in contrast to the abundant esker systems of Canada and Fennoscandia (Prest *et al.*, 1968; Boulton *et al.*, 2009), relatively few eskers formed beneath other ice sheets, such as the Patagonian Ice Sheet (cf. Glasser *et al.*, 2008; Lovell *et al.*, 2011). Potential reasons include the presence of cold-based ice during deglaciation (cf. Benn & Clapperton, 2000a; Benn & Clapperton, 2000b; Lovell *et al.*, 2012), which would preclude the formation of eskers. Alternatively, the predominance of softer sediments following the deposition of outwash during repeated glaciations (Mercer, 1976; Clapperton, 1990) may have favoured a distributed drainage system rather than an esker-forming channelized system (Clark & Walder, 1994), however, further research into the deglaciation of the Patagonian Ice Sheet is necessary in order to elucidate these important uncertainties.

8.5 Future research directions

Section 2.7 proposed four areas of future research following a review of the literature on eskers. This thesis has addressed three of the suggested research areas: 'morphometry and large scale patterns of eskers' (Section 2.7.1), 'channelized and distributed drainage systems at the ice sheet scale' (Section 2.7.2) and 'using eskers to test numerical models of meltwater drainage' (Section 2.7.3). This section now presents an updated list of important areas for future research, in light of the results presented in Chapters 3-7.

8.5.1 Time-transgressive or synchronous deposition?

A key difficulty in using eskers to reconstruct subglacial meltwater drainage is the uncertainty surrounding whether the large eskers of the Canadian Shield formed time-transgressively or synchronously (see Section 2.4.3.1; Section 2.5.4; Section 4.4.2). Ground Penetrating Radar (GPR) has been used to gain insights into longitudinal variations in sedimentary architecture of eskers in Iceland, Alaska and British Columbia, Canada and has provided strong evidence for synchronous esker formation (e.g. Burke *et al.*, 2008; Burke *et al.*, 2009; Burke *et al.*, 2010; Burke *et al.*, 2012a;b) at these localities, albeit for smaller eskers than those of the Canadian Shield. Thus, GPR may be used to assess the sedimentary architecture of the large eskers on the Canadian Shield and would be a robust method for determining whether large parts of the esker systems were formed synchronously or time-transgressively. In addition, detailed mapping of landforms associated with the long eskers will provide further evidence. For example, if most large eskers formed time-transgressively, they should be punctuated by fans (Figure 8.1) and/or contain enlargements (Lindström, 1993), the identification of which would provide compelling evidence for a time-transgressive origin.

8.5.2 Channelized and distributed drainage systems at the ice sheet scale

Chapter 5 presented the first observations of increased channelized drainage of meltwater beneath a deglaciating ice sheet. As discussed above in Section 8.2, extension of the same method to eskers in Fennoscandia could yield some interesting and potentially useful results, especially given the markedly different conditions under which the Fennoscandian eskers were formed. Other landforms, such as meltwater channels or GFCs (see Section 2.2.3) could also be used in a similar way to provide an added level of detail regarding the nature and magnitude of meltwater drainage, and to assess the more subtle changes in the evolution of meltwater drainage beneath ice sheets.

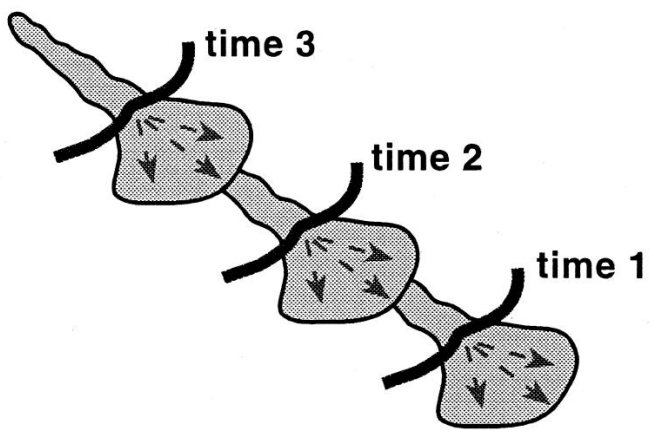

Figure 8.1. Illustration of fans punctuating a time-transgressive esker. From Brennand (2000).

8.5.3 Using eskers to test numerical models of meltwater drainage

Chapter 6 presents a large scale first-order test of Boulton *et al.'s* (2009) numerical model, which predicts the spacing between esker ridges. Future work should be directed towards testing this and other models (e.g. Hewitt, 2011) in a higher level of detail. Specifically, further work should focus on smaller areas, when and where the hydrogeological properties of the substrate (i.e. parameters such as permeability, hydraulic conductivity and aquifer thickness) are well constrained, and where eskers exhibit regular spacing. Whilst Chapter 6 explains the difficulty of applying Boulton *et al.*'s model at a large scale, it may be the case that smaller scale variations in aquifer properties exert a stronger or clearer control on esker spacing and would provide a valuable contribution to the discipline.

8.5.4 Quantification of channelized meltwater drainage beneath deglaciating ice sheets

A large amount of attention has been given to the production of meltwater during the deglaciation of the LIS and the effect that this has had on sea level and climate (e.g. Broecker *et al.*, 1989; Clark *et al.*, 2001; Teller *et al.*, 2002). Recent work focused on mass loss of the Greenland Ice Sheet has begun to partition the mass loss between surface processes and ice dynamics (van den Broeke *et al.*, 2009). A longer-scale perspective on this for the deglaciation of the LIS may be possible, by close examination of the record of glaciofluvial landforms. Building on the observations in Chapter 5, estimates of the discharge of channelized meltwater drainage may be produced, if the three-dimensional (i.e. cross-sectional) properties of eskers are known. Eskers could be used to approximate the cross-sectional area of subglacial channels, which could be extrapolated from a digital elevation model, and the discharge required to form the esker could be estimated by approximating the melt rate and drainage area of the esker (cf. Hooke & Fastook, 2007). The duration of channel occupation may be crudely approximated by interpolating between known ice margins (e.g. Dyke *et al.*, 2003). Whilst there may be a high uncertainty associated with these parameters, such a calculation would yield a potentially useful ball-park figure for meltwater flux through subglacial channels at the ice sheet scale and would be useful to compare to estimations of meltwater contributions to sea level (e.g. Carlson & Clark, 2012), for example.

Moreover, observations of eskers and moraines in Sweden have related eskers to the contribution of sediment and meltwater to proglacial lakes (Fyfe, 1990). Large proglacial lakes existed around the Laurentide throughout deglaciation (e.g. Dyke *et al.*, 2003) and could potentially be linked to the meltwater and sediment supply from subglacial channels, preserved as eskers. Lake volumes (e.g. Brown, 2012) could be compared with discharge estimates from eskers to assess the contribution to lake levels of meltwater from esker-forming channels, providing a first (albeit crude) approximation of melt partitioning of ancient ice sheets.

8.6 References

Alley, R. B. (1989) Water-pressure coupling of sliding and bed deformation. 1. Water-system. *Journal of Glaciology*, 35, 108-118.

Aylsworth, J. M. & Shilts, W. W. (1989) Bedforms of the Keewatin Ice-Sheet, Canada. *Sedimentary Geology*, 62, 407-428.

Banerjee, I. & McDonald, B. C. (1975) Nature of esker sedimentation. In A. V. Jopling and B. C. McDonald, *Glaciofluvial and Glacilacustrine Sedimentation*. Oklahoma, SEPM, 304-320.

Bartholomew, I., Nienow, P., Mair, D., Hubbard, A., King, M. A. & Sole, A. (2010) Seasonal evolution of subglacial drainage and acceleration in a Greenland outlet glacier. *Nature Geoscience*, 3, 408-411.

Bear, J. (1972) *Dynamics of Fluids in Porous Media*. New York, Elsevier.

Benn, D. I. & Clapperton, C. M. (2000a) Glacial Sediment–Landform Associations and Paleoclimate during the Last Glaciation, Strait of Magellan, Chile. *Quaternary Research*, 54, 13-23.

Benn, D. I. & Clapperton, C. M. (2000b) Pleistocene glacitectonic landforms and sediments around central Magellan Strait, southernmost Chile: evidence for fast outlet glaciers with cold-based margins. *Quaternary Science Reviews*, 19, 591-612.

Benn, D. I., Gulley, J., Luckman, A., Adamek, A. & Glowacki, P. S. (2009a) Englacial drainage systems formed by hydrologically driven crevasse propagation. *Journal of Glaciology*, 55, 513-523.

Benn, D. I., Kristensen, L. & Gulley, J. D. (2009b) Surge propagation constrained by a persistent subglacial conduit, Bakaninbreen-Paulabreen, Svalbard. *Annals of Glaciology*, 50, 81-86.

Bolduc, A. M. (1992) The formation of eskers based on their morphology, stratigraphy and lithologic composition, Labrador, Canada. *Unpublished Ph.D. thesis, Lehigh University*.

Boulton, G. S., Hagdorn, M., Maillot, P. B. & Zatsepin, S. (2009) Drainage beneath ice sheets: groundwater-channel coupling, and the origin of esker systems from former ice sheets. *Quaternary Science Reviews*, 28, 621-638.

Boulton, G. S., Lunn, R., Vidstrand, P. & Zatsepin, S. (2007) Subglacial drainage by groundwater-channel coupling, and the origin of esker systems: Part I-glaciological observations. *Quaternary Science Reviews*, 26, 1067-1090.

Brennand, T. A. (1994) Macroforms, large bedforms and rhythmic sedimentary sequences in subglacial eskers, south-central Ontario - implications for esker genesis and meltwater regime. *Sedimentary Geology*, 91, 9-55.

Brennand, T. A. (2000) Deglacial meltwater drainage and glaciodynamics: inferences from Laurentide eskers, Canada. *Geomorphology*, 32, 263-293.

Broecker, W. S., Kennett, J. P., Flower, B. P., Teller, J. T., Trumbore, S., Bonani, G. & Wolfli, W. (1989) Routing of meltwater from the Laurentide Ice-Sheet during the Younger Dryas cold episode. *Nature*, 341, 318-321.

Brown, V. H. (2012) Ice Stream Dynamics and Pro-glacial lake evolution along the north-western margin of the Laurentide Ice Sheet. *Department of Geography*, Durham University. Unpublished PhD thesis.

Burke, M. J., Brennand, T. A. & Perkins, A. J. (2012a) Evolution of the subglacial hydrologic system beneath the rapidly decaying Cordilleran Ice Sheet caused by ice-dammed lake drainage: implications for meltwater-induced ice acceleration. *Quaternary Science Reviews*, 50, 125-140.

Burke, M. J., Brennand, T. A. & Perkins, A. J. (2012b) Transient subglacial hydrology of a thin ice sheet: insights from the Chasm esker, British Columbia, Canada. *Quaternary Science Reviews*, 58, 30-55.

Burke, M. J., Woodward, J., Russell, A. J. & Fleisher, P. J. (2009) Structural controls on englacial esker sedimentation: Skeiðarárjökull, Iceland. *Annals of Glaciology*, 50, 85-92.

Burke, M. J., Woodward, J., Russell, A. J., Fleisher, P. J. & Bailey, P. K. (2008) Controls on the sedimentary architecture of a single event englacial esker: Skeiðarárjökull, Iceland. *Quaternary Science Reviews*, 27, 1829-1847.

Burke, M. J., Woodward, J., Russell, A. J., Fleisher, P. J. & Bailey, P. K. (2010) The sedimentary architecture of outburst flood eskers: A comparison of ground-penetrating radar data from Bering Glacier, Alaska and Skeiðarárjökull, Iceland. *Bulletin of the Geological Society of America*, 122, 1637-1645.

Carlson, A. E., Anslow, F. S., Obbink, E. A., LeGrande, A. N., Ullman, D. J. & Licciardi, J. M. (2009) Surface-melt driven Laurentide Ice Sheet retreat during the early Holocene. *Geophysical Research Letters*, L24502.

Carlson, A. E. & Clark, P. U. (2012) Ice sheet sources of sea level rise and freshwater discharge during the last deglaciation. *Reviews of Geophysics*, 50, RG4007.

Carlson, A. E., LeGrande, A. N., Oppo, D. W., Came, R. E., Schmidt, G. A., Anslow, F. S., Licciardi, J. M. & Obbink, E. A. (2008) Rapid early Holocene deglaciation of the Laurentide ice sheet. *Nature Geoscience*, 1, 620-624.

Clapperton, C. M. (1990) Quaternary glaciations in the southern hemisphere: An overview. *Quaternary Science Reviews*, 9, 299-304.

Clark, C. D., Knight, J. K. & T Gray, J. (2000) Geomorphological reconstruction of the Labrador sector of the Laurentide Ice Sheet. *Quaternary Science Reviews*, 19, 1343-1366.

Clark, P. U., Marshall, S. J., Clarke, G. K. C., Hostetler, S. W., Licciardi, J. M. & Teller, J. T. (2001) Freshwater forcing of abrupt climate change during the last glaciation. *Science*, 293, 283-287.

Clark, P. U. & Walder, J. S. (1994) Subglacial drainage, eskers, and deforming beds beneath the Laurentide and Eurasian ice sheets. *Bulletin of the Geological Society of America*, 106, 304-314.

Dyke, A. S., Moore, A. & Robertson, L. (2003) Deglaciation of North America. *Geological Survey of Canada, Open File*, 1574.

Eyles, N., Sladen, J. A. & Gilro, S. (1982) A depositional model for stratigraphic complexes and facies superimposition in lodgement tills. *Boreas*, 11, 317-333.

Ferguson, R. I. (1973) Sinuosity of Supraglacial Streams. *Geological Society of America Bulletin*, 84, 251-256.

Fricker, H. A., Scambos, T., Carter, S., Davis, C., Haran, T. & Joughin, I. (2010) Synthesizing multiple remote-sensing techniques for subglacial hydrologic mapping: application to a lake system beneath MacAyeal Ice Stream, West Antarctica. *Journal of Glaciology*, 56, 187-199.

Fyfe, G. J. (1990) The effect of water depth on ice-proximal glaciolacustrine sedimentation: Salpausselkä I, southern Finland. *Boreas*, 19, 147-164.

Glasser, N. F., Jansson, K. N., Harrison, S. & Kleman, J. (2008) The glacial geomorphology and Pleistocene history of South America between 38°S and 56°S. *Quaternary Science Reviews*, 27, 365-390.

Gulley, J. d. (2009) Structural control of englacial conduits in the temperate Matanuska Glacier, Alaska, USA. *Journal of Glaciology*, 55, 681-690.

Gulley, J. D. & Benn, D. I. (2007) Structural control of englacial drainage systems in Himalayan debris-covered glaciers. *Journal of Glaciology*, 53, 399-412.

Gulley, J. D., Benn, D. I., Muller, D. & Luckman, A. (2009a) A cut-and-closure origin for englacial conduits in uncrevassed regions of polythermal glaciers. *Journal of Glaciology*, 55, 66-80.

Gulley, J. D., Benn, D. I., Screaton, E. & Martin, J. (2009b) Mechanisms of englacial conduit formation and their implications for subglacial recharge. *Quaternary Science Reviews*, 28, 1984-1999.

Hättestrand, C. (1997) Ribbed moraines in Sweden — distribution pattern and palaeoglaciological implications. *Sedimentary Geology*, 111, 41-56.

Hebrand, M. & Åmark, M. (1989) Esker formation and glacier dynamics in eastern Skane and adjacent areas, southern Sweden. *Boreas*, 18, 67-81.

Hewitt, I. J. (2011) Modelling distributed and channelized subglacial drainage: the spacing of channels. *Journal of Glaciology*, 57, 302-314.

Hillaire-Marcel, C. & Occhietti, S. (1980) Chronology, paleogeography, and paleoclimatic significance of the late and postglacial events in eastern Canada. *Zeitschrift für Geomorphologie*, 24, 373-392.

Hooke, R. L. & Fastook, J. (2007) Thermal conditions at the bed of the Laurentide ice sheet in Maine during deglaciation: implications for esker formation. *Journal of Glaciology*, 53, 646-658.

Hubbard, B. & Nienow, P. (1997) Alpine subglacial hydrology. *Quaternary Science Reviews*, 16, 939-955.

Kamb, B. (1987) Glacier Surge Mechanism Based on Linked Cavity Configuration of the Basal Water Conduit System. *Journal of Geophysical Research*, 92, 9083-9100.

Kang, Y. & Smith, L. C. (2013) Supraglacial Streams on the Greenland Ice Sheet Delineated From Combined Spectral–Shape Information in High-Resolution Satellite Imagery. *Geoscience and Remote Sensing Letters, IEEE*, 10, 801-805.

Kleman, J. & Glasser, N. F. (2007) The subglacial thermal organisation (STO) of ice sheets. *Quaternary Science Reviews*, 26, 585-597.

Lindström, E. (1993) Esker enlargements in northern Sweden. *Geografiska Annaler Series A - Physical Geography*, 75, 95-110.

Lovell, H., Stokes, C. R. & Bentley, M. J. (2011) A glacial geomorphological map of the Seno Skyring-Seno Otway-Strait of Magellan region, southernmost Patagonia. *Journal of Maps*, 7, 318-339.

Lovell, H., Stokes, C. R., Bentley, M. J. & Benn, D. I. (2012) Evidence for rapid ice flow and proglacial lake evolution around the central Strait of Magellan region, southernmost Patagonia. *Journal of Quaternary Science*, 27, 625-638.

Lundqvist, J. (1999) Scandinavian eskers, global climatic relationships, and solar forcing. *Geological Quarterly*, 43, 149-152.

Lundqvist, J. A. N. (1997) Structure and rhythmic pattern of glaciofluvial deposits north of Lake Vänern, south-central Sweden. *Boreas*, 26, 127-140.

Margold, M., Jansson, K. N., Kleman, J. & Stroeven, A. P. (2013) Lateglacial ice dynamics of the Cordilleran Ice Sheet in northern British Columbia and southern Yukon Territory: retreat pattern of the Liard Lobe reconstructed from the glacial landform record. *Journal of Quaternary Science*, 28, 180-188.

Marston, R. A. (1983) Supraglacial Stream Dynamics on the Juneau Icefield. *Annals of the Association of American Geographers*, 73, 597-608.

Mercer, J. H. (1976) Glacial history of southernmost South America. *Quaternary Research*, 6, 125-166.

Prest, V. K., Grant, D. R. & Rampton, V. N. (1968) Glacial map of Canada. Geological Survey of Canada, Map 1253A. 1:5,000,000

Price, R. J. (1969) Moraines, sandar, kames and eskers near Breiðamerkurjökull , Iceland. *Transactions of the Institute of British Geographers*, 46, 17-43.

Punkari, M. (1980) The ice lobes of the Scandinavian ice sheet during the deglaciation in Finland. *Boreas*, 9, 307-310.

Punkari, M. (1997) Subglacial processes of the Scandinavian Ice Sheet in Fennoscandia inferred from flow-parallel features and lithostratigraphy. *Sedimentary Geology*, 111, 263-283.

Röthlisberger, H. (1972) Water pressure in intra-and subglacial channels. *Journal of Glaciology*, 11, 177-203.

Shilts, W. W. (1984) Esker sedimentation models, Deep Rose Lake map area, District of Keewatin. *Geological Survey of Canada, Paper*, 84-1B, 217-222.

Shilts, W. W., Aylsworth, J. M., Kaszycki, C. A. & Klassen, R. A. (1987) Canadian Shield. In W. L. Graf, *Geomorphic Systems of North America*. Boulder, Colorado, Geological Society of America, Centennial Special Volume. 2, 119-161.

Shreve, R. L. (1972) Movement of water in glaciers. *Journal of Glaciology*, 11, 205-214.

Shreve, R. L. (1985) Esker characteristics in terms of glacier physics, Katahdin esker system, Maine. *Bulletin of the Geological Society of America*, 96, 639-646.

Stokes, C. R. & Tarasov, L. (2010) Ice streaming in the Laurentide Ice Sheet: A first comparison between data-calibrated numerical model output and geological evidence. *Geophysical Research Letters*, 37, L01501.

Stølum, H. H. (1996) River meandering as a self-organization process. *Science*, 271, 1710-1713.

Syverson, K. M., Gaffield, S. J. & Mickelson, D. M. (1994) Comparison of esker morphology and sedimentology with former ice-surface topography, Burroughs Glacier, Alaska. *Geological Society of America Bulletin*, 106, 1130-1142.

Tarasov, L., Dyke, A. S., Neal, R. M. & Peltier, W. R. (2012) A data-calibrated distribution of deglacial chronologies for the North American ice complex from glaciological modeling. *Earth and Planetary Science Letters*, 315–316, 30-40.

Teller, J. T., Leverington, D. W. & Mann, J. D. (2002) Freshwater outbursts to the oceans from glacial Lake Agassiz and their role in climate change during the last deglaciation. *Quaternary Science Reviews*, 21, 879-887.

van den Broeke, M., Bamber, J., Ettema, J., Rignot, E., Schrama, E., van de Berg, W. J., van Meijgaard, E., Velicogna, I. & Wouters, B. (2009) Partitioning Recent Greenland Mass Loss. *Science*, 326, 984-986.

Vatne, G. (2001) Geometry of englacial water conduits, Austre Brøggerbreen, Svalbard. *Norsk Geografisk Tidsskrift - Norwegian Journal of Geography*, 55, 85-93.

Walder, J. & Hallet, B. (1979) Geometry of former subglacial water channels and cavities. *Journal of Glaciology*, 23, 335-346.

Walder, J. S. & Fowler, A. (1994) Channelized subglacial drainage over a deformable bed. *Journal of Glaciology*, 40, 3-15.

Willis, I. C., Fitzsimmons, C. D., Melvold, K., Andreassen, L. M. & Giesen, R. H. (2012) Structure, morphology and water flux of a subglacial drainage system, Midtdalsbreen, Norway. *Hydrological Processes*, 26, 3810-3829.

Chapter 9 Conclusions and implications

The aim of this thesis was to use the spatial and temporal variation in the form and pattern of eskers to gain insight into the subglacial meltwater dynamics which operate beneath ice masses in both modern and ancient systems. 20,186 eskers were mapped from Landsat ETM+ imagery of Canada and 5,326 eskers were mapped from aerial photographs for eight time slices at Breiðamerkurjökull, Iceland during the retreat of the glacier from 1945 to 2007.

Mapping of ancient Canadian eskers reveals several distinctive patterns. Eskers are prevalent on the Canadian Shield, where they radiate outwards from former Ice Divides, beneath which they are absent. Within the radial systems, eskers occur in long dendritic systems. In some places, eskers produce anastomosing patterns and in places of complex ice dynamics during deglaciation, such as Victoria Island and northern North West Territories, exhibit no discernible regional trend. Eskers are relatively evenly spaced in Shield areas. The modern eskers at Breiðamerkurjökull exhibit quasi-regular spacing and are typically aligned with large medial moraines.

Analysis of the morphometry of eskers in Canada reveals that individual esker ridges extend up to 97.5 km but are frequently fragmented, either during deposition or by postglacial erosion. When gaps are taken into account, eskers can be traced for up to 760 km. The extreme length of these esker systems indicates that they were likely formed time-transgressively at a retreating margin, as opposed to synchronously in one large system. Eskers are remarkably straight, 98% having a sinuosity value of less than 1.2. This has implications for models of subglacial channels, which may assume higher values of sinuosity and therefore overestimate parameters such as discharge. In areas of high esker density, eskers are relatively evenly spaced at approximately 12 km apart. Within the dendritic systems of eskers around the Keewatin Ice Divide, eskers are well connected, with fourth-order tributaries noted in two locations. Esker elevation typically changes very little (73% exhibit changes of no more than 10 m) between their beginning and end points, with no preference observed for up- or down-slope trends. These observations indicate that eskers form preferentially over flat terrain and that ice surface slope is a dominant control on esker morphometry.

Esker frequency at reconstructed ice margins shows marked changes during deglaciation and can be used to reconstruct the number of drainage channels operating at various stages. Esker frequency beneath the Laurentide Ice Sheet was found to increase during deglaciation, as more meltwater became available as a result of increased surface melting, following climatic warming at the end of the Younger Dryas. This suggests that the drainage system of the Laurentide Ice

Sheet evolved during deglaciation into an increasingly channelized system, in a manner similar to alpine and outlet glaciers, which operate on much smaller spatial and temporal scales. A corollary implication of this is that dynamic instabilities such as ice streaming are less common during deglaciation, because the distributed meltwater drainage systems necessary to facilitate them were less prevalent.

Canadian eskers occur predominantly over the metamorphic, intrusive and sedimentary rocks of the Precambrian Shield, as predicted by theory. Esker location is also strongly related to the presence of till, particularly in thicker blankets. This supports research which suggests that the lithological composition of eskers is closely related to the local till. However, sediment thickness alone does not influence esker location, which suggests that eskers do not require a large quantity of sediment to form. Esker length and sinuosity are independent of the underlying bedrock and surficial materials, suggesting that they are most likely controlled by the geometry of the ice sheet. Esker spacing also appears to be independent of bedrock control, with similar spacing values recorded over different substrates. This is in disagreement with the predictions of the groundwater theory of esker spacing put forward by Boulton *et al.* (2009), which suggests that esker spacing should increase over substrates of higher transmissivity.

In addition to simple, single ridge eskers, complex eskers exist in Canada and at Breiðamerkurjökull. Detailed mapping of the eskers at Breiðamerkurjökull reveals two distinctive types of esker complex: *topographically constrained esker complexes* and *esker fan complexes* The development of complex esker morphology is dependent on having a sufficiently high supply of sediment to clog meltwater channels and branch off to form distributaries. *Esker fan complexes* develop where there is no topographic impediment and distributaries branch outwards in a fan shape, whereas *topographically constrained esker complexes* occur where drainage is constrained by a topographic barrier, precluding the development of fan morphology.

The main implications of this work are that supraglacial meltwater drainage, ice surface slope, meltwater supply and sediment supply are the most important factors in controlling the distribution, morphometry and formation of eskers. These linkages form the basis of using eskers to reconstruct meltwater drainage beneath glaciers and ice sheets and provide the details necessary to understand the environments under which different eskers form.

Four key areas of potential future research in using the meltwater landform record to interpret the dynamics of meltwater beneath ice sheets are highlighted. These include mapping the association between long eskers on the Canadian Shield and other meltwater landforms, and using ground penetrating radar of the sedimentary architecture of the long eskers, to determine whether they formed synchronously or time-transgressively. Large scale mapping of meltwater landforms such as glaciofluvial corridors, meltwater channels and tunnel valleys will provide an increased level of detail to reconstructions of the evolution of meltwater drainage systems over

time. Advances in the quality of hydrogeological data should be used to test numerical models of esker spacing in high resolution, using the database of eskers mapped in this thesis. Finally, further analysis of eskers, such as using digital elevation models to survey their cross-sectional geometry may be used alongside the mapping presented here to gain insights into the quantities of sediment and meltwater transported by eskers, which could have implications for our understanding of proglacial lake evolution.

Appendix

A map of large Canadian eskers from Landsat satellite imagery

Robert D. Storrar, Chris R. Stokes & David J.A. Evans

Department of Geography, Durham University, UK

Eskers were digitised from Landsat ETM+ imagery.
Elevation data are derived from the GTOPO30 database.
Lakes are from the North American Atlas.
Ice cover data are from the Atlas of the Cryosphere and the Randolph Glacier Inventory.

Scale: 1:5,000,000 (when printed at A0 size)
Datum: North American Datum 1983
Projection: Canada Lambert Conformal Conic

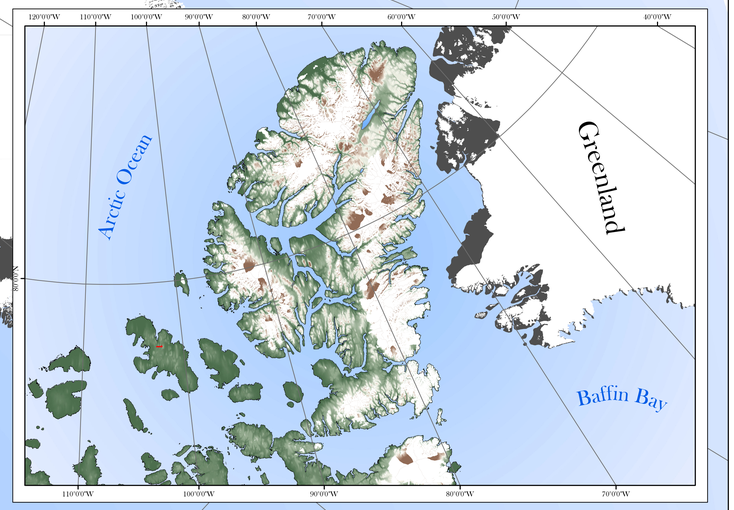

Legend

- Ice
- Eskers
- Lakes
- Other countries

Elevation (m a.s.l.)

5,800 — 1

Arctic Ocean
Greenland
Baffin Bay
Beaufort Sea
United States of America
Great Bear Lake
Great Slave Lake
Lake Athabasca
Lake Winnipeg
Hudson Bay
Labrador Sea
Gulf of St. Lawrence
Canada
Lake Superior
Lake Michigan
Lake Huron
Lake Erie
Lake Ontario
Pacific Ocean
Atlantic Ocean
United States of America

130°0'0"W 120°0'0"W 110°0'0"W 100°0'0"W 90°0'0"W 80°0'0"W 70°0'0"W
80°0'0"N 60°0'0"N 50°0'0"N